UNIVERSITY OF OKLAHOMA

GRADUATE COLLEGE

MICROBIAL ECOLOGY OF COASTAL ECOSYSTEMS: INVESTIGATIONS OF THE GENETIC POTENTIAL FOR ANAEROBIC HYDROCARBON TRANSFORMATION AND THE RESPONSE TO HYDROCARBON EXPOSURE

A DISSERTATION

SUBMITTED TO THE GRADUATE FACULTY

in partial fulfillment of the requirements of the

Degree of

DOCTOR OF PHILOSOPHY

By

JAMIE M. JOHNSON DUFFNER
Norman, Oklahoma
2017

MICROBIAL ECOLOGY OF COASTAL ECOSYSTEMS: INVESTIGATIONS OF THE GENETIC POTENTIAL FOR ANAEROBIC HYDROCARBON TRANSFORMATION AND THE RESPONSE TO HYDROCARBON EXPOSURE

A DISSERTATION APPROVED FOR THE
DEPARTMENT OF MICROBIOLOGY AND PLANT BIOLOGY

BY

_____
Dr. Amy V. Callaghan, Chair

_____
Dr. Lee R. Krumholz

_____
Dr. Michael J. McInerney

_____
Dr. Mark A. Nanny

_____
Dr. Boris Wawrik

This dissertation is dedicated to my husband, Derick, for his unwavering love and support.

Acknowledgements

I would like to thank my advisor, Dr. Amy Callaghan, for her guidance and support during my time as a graduate student, as well as for her commitment to my success as a scientist. I would also like to thank the members of my doctoral committee for their guidance over the years, particularly that of Dr. Boris Wawrik. I would like to also thank Drs. Josh Cooper, Chris Lyles, and Chris Marks for their friendship and support during my time at OU, both in and outside the lab.

Table of Contents

List of Tables

List of Figures

Appendix II

Appendix III

Abstract

Microbial-mediated hydrocarbon transformation plays a vital role in the attenuation of natural and anthropogenic-sourced petroleum contamination in the environment, particularly in marine systems. Indigenous microbial communities in marine habitats are resilient to influxes of petroleum, and it is well documented that many taxa are capable of responding and utilizing these compounds. Coastal ecosystems are often either subjected to or at risk for oil contamination and are of particular concern due to their significant environmental and economic value. The research projects presented here focused on coastal ecosystems and investigated microbial community compositions via next-generation sequencing of 16S rRNA genes, the genetic potential for anaerobic hydrocarbon biodegradation within these communities via molecular surveys of marker genes, and the response of anaerobic populations to exposure of a hydrocarbon via microcosm studies or to products of hydrocarbon transformation processes (i.e. photolysis) via sulfate reduction assays (SRAs).

Chesapeake Bay is the largest estuary in the United States, and experiences high nutrient loading and water column hypoxia due to watershed runoff, as well as petroleum contamination from urban runoff, atmospheric deposition, and spills directly into the water column. Past studies have demonstrated that aerobic hydrocarbon-degrading bacteria can be enriched from the water column and from the sediment. However, evidence for anaerobic biodegradation of hydrocarbons had not been demonstrated at the time of our

study. Given the recurring seasonal water column hypoxia and the transient exposure to hydrocarbons, we hypothesized that the potential for degradation under anaerobic conditions may exist in Chesapeake Bay sediments. Here, molecular surveys and microcosms were utilized to investigate microbial community composition and the potential for anaerobic hydrocarbon degradation among sites along a transect of the Bay. Sampling locations were chosen both within and outside areas of recurring hypoxia. Distinct geochemical gradients along the transect were revealed. Low oxygen, low sulfate, and high methane concentrations were observed in the upper Bay, as were significantly higher levels of taxa associated with anaerobic processes (e.g., sulfate reducers and methanogens). In contrast, higher oxygen, higher sulfate, and very low methane were measured in the lower Bay. Sulfate-reducers and methanogens decreased in abundance in lower Bay sediments as well. Similarly, molecular surveys showed more frequent detection of marker genes associated with the anaerobic activation of hydrocarbons via the 'fumarate addition' pathway (e.g., *assA*, *bssA*) in the upper Bay, and microcosms established under sulfate-reducing and/or methanogenic conditions suggested that the model hydrocarbon, hexadecane, was being converted to methane by indigenous sediment communities obtained from the upper Bay sites. These findings illustrate the variability of microbial communities between different locations in Chesapeake Bay as well as differences in their response to a hydrocarbon. Together, the data highlighted the significance that anaerobic processes could potentially play in the event of an oil spill in Chesapeake Bay.

The Gulf of Mexico (GoM) is one of the most environmentally and economically important coastal regions in the United States. The Deepwater Horizon (DWH) spill in the GoM was the largest accidental release of crude oil into U.S. waters. Extensive research was carried out on the response of microbial communities to the discharged oil and gas. Collectively, studies emphasized the importance of both aerobic and anaerobic hydrocarbon transformation processes and concluded that native microbial populations responded quickly to the petroleum, promoting contaminant removal from the environment. Two of the research projects presented herein aimed to (1) further study the impact that released oil, once weathered, can have on indigenous anaerobic microbial communities, and to (2) characterize microbial populations associated with weathered oil residues (i.e., sand patties) that have remained in the environment years after the spill and to determine the role these populations have in the attenuation of residual contamination.

Once introduced into the environment, oil is subjected to a number of weathering processes, including evaporation, emulsification, and photooxidation. Photooxidation of oil can lead to the incorporation of oxygen molecules into hydrocarbon constituents, which can subsequently result in enhanced bioavailability and/or increased toxicity to certain organisms. Microbial toxicity studies are typically conducted using individual aerobic taxa, as opposed to indigenous communities or anaerobic microorganisms, and little is known with regard to how photolyzed oil affects anaerobes. Experiments presented here assessed the impact that photooxidized hydrocarbons can have

on sulfate-reducing communities in coastal sediments. We hypothesized that photolyzed oil or photolyzed oil components would inhibit the sulfate-reducing communities. Three distinct GoM coastal locations were chosen for study. Sediment microbial communities were characterized via 16S rRNA gene sequencing, and the impact of irradiated crude oil or irradiated PAHs (i.e., pyrene, phenanthrene, and a phenanthrene/anthracene mixture) was tested via sulfate reduction assays (SRAs). Sulfate-reducing taxa varied in both abundance and composition across sampling sites. Overall, no impact on sulfate reduction rates was observed for any of the photolyzed compounds at any of the coastal locations investigated. Data suggested that water-soluble photogenerated products did not negatively impact sulfate-reducing communities and that these compounds could potentially be utilized by sulfate-reducing microorganisms. These findings highlight the resilience of native microbial communities in response to an influx of weathered hydrocarbons, as well as the potential of these populations to further mediate hydrocarbon transformation processes.

Weathering of oil released during the DWH spill also led to the formation of water-in-oil emulsions. Many of these emulsions washed ashore early after the onset of the spill, whereas an unknown quantity sank in nearshore environments, resulting in the formation of submerged oil mats (SOMs). Fragments of these buried mats continued to wash ashore coastal beaches and marshes years after the spill in the form of oil:sand aggregates (e.g., tar balls, sand patties, etc.). The third research project presented here aimed to use next-

generation sequencing of 16S rRNA genes to characterize microbial communities associated with individual oil:sand aggregates collected from different GoM beaches, to use metagenomic sequencing to survey for marker genes associated with hydrocarbon transformation pathways to determine the genetic capacity for biodegradation within the microbial populations, and to conduct targeted metabolomics via mass spectrometry to assess whether these communities mediate transformation of hydrocarbons *in situ* (i.e., once aggregates are deposited on the beach). Given the presumed differences in residence times and exposure to different environmental conditions, we hypothesized that sand patty microbial communities would be different between sites. Together, molecular surveys demonstrated that individual aggregates had either an anaerobic, facultative anaerobic, or aerobic signature with regard to both the taxonomic composition of communities and the metabolic potential associated with hydrocarbon degradation pathways. Several taxa with known or suspected hydrocarbon-degrading ability were detected (e.g., *Marinobacter*, *Alcanivorax*, *Mycobacterium*), and specific taxa varied among samples. Additionally, profiles of functional genes involved in aerobic and anaerobic hydrocarbon transformation pathways (e.g., *assA*, *alkB*) also varied among samples and corresponded with 16S rRNA gene profiles. Results from beach sand and seawater samples confirmed that microbial populations were distinct from those obtained from sand patties. Taxonomic profiles of core communities (i.e., taxa comprising ≥1% of libraries) identified ten shared operational taxonomic units (OTUs) between aggregates and beach sand and seven

shared OTUs between aggregates and seawater. Targeted mass spectrometry putatively identified metabolites indicative of aerobic and/or anaerobic hydrocarbon transformation processes (e.g., toluic acid, hydroxybenzoic acid, phenylpropionic acid), and showed that these compounds were not detected in beach sand. These findings provide evidence that aggregate-associated microbes are capable of hydrocarbon degradation and also highlight the potential role that microorganisms likely play in the long-term attenuation of remnant oil present in the environment years after the DWH spill.

Preface

Work presented in this dissertation is the result of collaborations with several research groups. Microbial analysis of Chesapeake Bay sediments presented in Chapter 1 was published in FEMS Microbiology Ecology (2015) 91 (2):1-14, DOI: 10.1093/femsec/fiu035 and is included here under license number 4102200770753. Sample collection aboard the R/V *Hugh R. Sharp* was conducted by Drs. Amy Callaghan (OU), Boris Wawrik (OU), and Cat Isom (OU), and by former graduate student Wilford B. Boling (OU). My contributions to this project included DNA extractions, qPCR analyses, *assA* and *bssA* clone library generation, and the establishment and monitoring of microcosms via ion and gas chromatography. Additionally, I prepared the 16S rRNA gene libraries and analyzed sequence data with support from Dr. Boris Wawrik. Preparation of the manuscript was conducted in conjunction with Drs. Amy Callaghan and Boris Wawrik.

The Gulf of Mexico photochemistry and toxicity experiments outlined in Chapter 2 were part of a collaborative effort among several institutions. Transport to Gulf of Mexico sampling locations was provided by Captain William McDonnel (Dominator Fishing Charters, Biloxi, MS). I collected samples with the help of Dr. Boris Wawrik, Brian Harriman (OU), and Dustin Kountz (University of New Orleans). Aqueous extracts of photolyzed hydrocarbons used in sulfate reduction assays (SRA) experiments were generated by Dustin Kountz during his tenure in the laboratory of Dr. Matthew Tarr at the University of New Orleans. SRA techniques were initially demonstrated by Dr. Irene

Davidova (OU) and Brian Harriman in the laboratory of Dr. Joseph Suflita (OU). My contributions to this project included DNA extractions, preparation of 16S rRNA gene libraries, analysis of resulting sequence data with support from Dr. Boris Wawrik, and SRA experiments. I also composed the text and generated figures presented in this dissertation.

The Gulf of Mexico sand patty samples used in the preliminary analyses described in Chapter 3 were collected by Drs. Joseph Sulfita, Christoph Aeppli (Bigelow Laboratory for Ocean Sciences), and by Brian Harriman. For these samples, my responsibilities included DNA extractions and sequence analysis with support from Drs. Amy Callaghan and Boris Wawrik. The central focus of the data presented in Chapter 3 is from samples collected on a separate trip. Here, my responsibilities included sample collection, DNA extractions, generation of 16S rRNA gene and metagenomic libraries, analysis of sequences in conjunction with Drs. Amy Callaghan and Boris Wawrik, along with text and figure generation. Oil extraction, characterization, and subsequent data analyses were carried out by Dr. Christoph Aeppli. Sand patty and beach sand extractions, in preparation for mass spectrometry, were conducted by myself, with support from Dr. Egemen Aydin (OU). Mass spectrometry and data analyses were performed by Drs. Egemen Aydin and Vincent Bonifay (OU) with support from Dr. Jan Sunner (OU).

Chapter 1. Interrogation of Chesapeake Bay Sediment Microbial Communities for Intrinsic Alkane-Utilizing Potential Under Anaerobic Conditions

ABSTRACT

Based on the transient exposure of Chesapeake Bay sediments to hydrocarbons and the metabolic versatility of known anaerobic alkane-degrading microorganisms, it was hypothesized that distinct Bay sediment communities, governed by geochemical gradients, would have intrinsic alkane-utilizing potential under sulfate-reducing and/or methanogenic conditions. Sediment cores were collected along a transect of the Bay. Community DNA was interrogated via pyrosequencing of 16S rRNA genes, PCR of anaerobic hydrocarbon activation genes, and qPCR of 16S rRNA genes and genes involved in sulfate reduction/methanogenesis. Site sediments were used to establish microcosms amended with *n*-hexadecane under sulfate-reducing and methanogenic conditions. Sequencing of 16S rRNA genes indicated that sediments associated with hypoxic water columns contained significantly greater proportions of Bacteria and Archaea consistent with syntrophic degradation of organic matter and methanogenesis compared to less reduced sediments. Microbial taxa frequently associated with hydrocarbon-degrading communities were found throughout the Bay, and the genetic potential for hydrocarbon metabolism was demonstrated via the detection of benzyl- (*bssA*) and alkylsuccinate synthase (*assA*) genes. Although microcosm studies did not indicate sulfidogenic alkane degradation, the data suggested that methanogenic conversion of alkanes was occurring. These findings highlight the potential role

that anaerobic microorganisms could play in the bioremediation of hydrocarbons in the Bay.

INTRODUCTION

Petroleum hydrocarbons are frequently released into marine environments via natural seeps, as well as anthropogenic activities including crude oil extraction, transport, storage, and refining processes (NRC, 2003). An estimated 1.3×10^6 metric tonnes of petroleum enter marine systems each year, of which approximately 55% are attributable to anthropogenic sources (NRC, 2003). The scales of different pollution events can vary dramatically, resulting in variable impacts on marine ecosystems. This was well illustrated in the Gulf of Mexico by the blowout of the Macondo 252 well and the subsequent sinking of the Deepwater Horizon, which resulted in an unprecedented amount of crude oil being released (~4.1 to 4.4 million barrels) (Crone & Tolstoy, 2010, OSAT, 2010). Although a significant proportion of the Macondo 252 oil was removed through human intervention or physical processes (78%), the remainder had a fate classified as 'other,' suggesting that some of the oil and gas may have been removed via microbially mediated processes (Ramseur, 2010). Subsequent studies investigating microbial communities in the Gulf of Mexico water column, deep-sea sediments, and coastal sediments have provided overwhelming evidence that the microbial community played an important role in the removal of the oil (for review, see Joye *et al.*, 2014, Kimes *et al.*, 2014, King *et al*, 2015). These events and the initial devastation of the

Deepwater Horizon spill prompted immediate discussion about oil spill assessment and preparedness, especially for delicate and economically important ecosystems, such as the Chesapeake Bay (Behn, 2010).

The Chesapeake Bay is the largest estuary in the United States, with a watershed encompassing 165,000 km^2 of forest and woodland (64%), agricultural land (24%), and urban areas (8%) (Paolisso *et al.*, 2015). More than 100,000 rivers and streams drain into the Chesapeake Bay (Chesapeake Bay Program, 2014a). The Bay has a larger land-to-water ratio than any other coastal body in the world (Chesapeake Bay Program, 2014a). This, along with the extensive dendritic shoreline (18,800 km) (Kemp *et al.*, 2005) and low flushing rates (i.e., flushing time is approximately 200 days) (Fisher *et al.*, 1988), makes the Bay vulnerable to high nutrient loading and other types of contamination. As a result of nitrogen (N) and phosphorous (P) loading, the Bay has suffered from increased phytoplankton abundance, declining water clarity, depletion of bottom-water oxygen, redox changes in sediment biogeochemistry, decreases in benthic microalgal primary production and loss of benthic macroinfauna, loss of oyster beds and benthic filtration, major shifts in fish populations, loss of seagrasses and other submersed vascular plants, and loss of tidal marshes as nutrient buffers (for review, see Kemp *et al.*, 2005). The Bay has also suffered from pollution with metals, polychlorinated biphenyls (PCBs), and hydrocarbons (Chesapeake Bay Program, 2014b). From both an ecological and economic perspective, the Chesapeake Bay is of significant value. Beyond commercial fishing, it was estimated in 2001 that for persons living in parts of

Virginia, Maryland, and the District of Columbia, the annual benefits of the Bay ranged from $357.9 million to $1.8 billion based on (1) recreation (fishing, boating, and swimming); (2) health; (3) property values; (4) regional economic impacts; and (5) non-use value (Morgan & Owens, 2001). Despite restoration and mitigation efforts, the Bay is still at a continual risk for hydrocarbon contamination (and other types of pollution) via commercial shipping, recreational boating activity, and urban inputs.

Typically, the major hydrocarbon inputs to the Bay are urban runoff (Foster *et al.*, 2000) and atmospheric deposition (Webber, 1983). Concern about a large hydrocarbon spill event emerged in the 1970s due to the proposed construction of superports for oil tankers. This prompted several investigations of the Bay's microbial potential for degradation of petroleum and petroleum compounds (Walker & Colwell, 1973, Walker *et al.*, 1976a, Walker *et al.*, 1976b, Okpokwasili *et al.*, 1984, West *et al.*, 1984). By the 1990s, the importance of this research was self-evident. There were 3,651 oil spill events (each spill >75 gallons) in Chesapeake Bay between 1985 and 1994, which led to an estimated release of more than 1.3×10^6 gallons of oil (Balch, 1997). In 2000, the Bay suffered one of its worst oil spills when 140,000 gallons of oil were spilt into the Patuxent River as a result of a ruptured underground pipeline (Michel *et al.*, 2009). Due to the transient, but continual, exposure to hydrocarbons over several decades, hydrocarbons are measureable in Bay bulk water and the aquatic surface microlayer (e.g., alkane concentrations ranging from 3.16 ± 0.77 to > 200 μg L^{-1}) (Hardy *et al.*, 1990), as well as

sediments (Walker *et al.*, 1975a, Walker *et al.*, 1975b, Arzayus *et al.*, 2001). Accordingly, microbial studies have demonstrated the enrichment of petroleum hydrocarbon and PAH-degrading bacteria from Chesapeake Bay water and sediment (Walker *et al.*, 1976a, West *et al.*, 1984), the impact of different refined fuels and crude oils on the growth of microbial populations enriched from Chesapeake Bay water (Walker *et al.*, 1976b), and the effect that prior oil exposure has on the number of cultivable petroleum-degrading microorganisms enriched from Chesapeake Bay water and sediment (Walker & Colwell, 1973). All of these prior studies, however, were conducted under aerobic conditions, given that anaerobic degradation of hydrocarbons was not well described or understood at the time. However, research during the last 25 years has unveiled novel microbial strategies for the anaerobic activation and degradation of hydrocarbons (for review, see Heider & Schühle, 2013), which are particularly important in sediments impacted by petroleum compounds where oxygen can be rapidly depleted. Among these strategies is the addition of aliphatic and aromatic hydrocarbons to the double bond of fumarate (i.e., 'fumarate addition'), which is catalyzed by the glycyl radical enzymes alkylsuccinate synthase (ASS)/methylalkylsuccinate synthase (MAS) (Callaghan *et al.*, 2008, Grundmann *et al.*, 2008) and benzylsuccinate synthase (BSS) (Leuthner *et al.*, 1998), respectively. As such, genes encoding the catalytic subunits of BSS and ASS (*bssA* and *assA*) serve as potential biomarkers for 'fumarate addition' in anaerobic hydrocarbon-impacted environments (Callaghan *et al.*, 2010, Agrawal & Gieg, 2013, Callaghan, 2013).

To our knowledge, the intrinsic capacity of Bay sediment microbial communities to mediate *anaerobic* hydrocarbon transformation has not been investigated. In the event of an oil spill, the shallow depth of the Chesapeake Bay would likely play an important role in the transport of hydrocarbons to Bay sediments. Therefore, in the wake of the Deepwater Horizon oil spill, we took advantage of a cruise of opportunity to assess the potential for anaerobic hydrocarbon degradation in Chesapeake Bay sediments via next generation sequencing of 16S ribosomal RNA genes, molecular surveys of functional genes for anaerobic degradation pathways, and microcosm experiments. Specifically, we focused on the anaerobic conversion of *n*-hexadecane due to the relevance of alkanes as crude oil pollutants. Based on the transient exposure of Chesapeake Bay sediments to hydrocarbons and the metabolic versatility of known anaerobic alkane-degrading microorganisms, it was hypothesized that distinct Bay sediment communities, governed by geochemical gradients, would have the potential for alkane-degrading activity under sulfate-reducing and/or methanogenic conditions.

MATERIALS & METHODS

Sampling Sites and Sample Collection. Samples were collected aboard the R/V *Hugh R. Sharp* during a transect cruise of Chesapeake Bay in August 2010. Bay oxygen concentration data for 2009 were obtained from the Chesapeake Bay Program (CBP) Water Quality Database and used as an *a*

priori guide for site selection. Four sites were then chosen based on the presence or absence of bottom anoxia during the 2010 sampling (Table S1 and Figures S1, S2, and S3). Water column oxygen concentrations during our cruise were monitored using the onboard CTD device (Note: cruise track and CTD data are available via the Biological & Chemical Oceanography Data Management Office via dataset number: HRS100808BW). Sediments were obtained by gravity coring, and core liners were immediately sectioned (1-ft intervals), capped, and moved to the on-board lab. Each 1-ft section is referred to as a 'horizon' hereafter. A piece of the core liner was removed from the middle of each horizon, and core material was immediately sampled for enrichment studies, pore water analysis, and DNA extraction.

Sediment Pore Water Analysis. Sediment pore water from each station horizon was obtained using a titanium pore water squeeze cell (GEOTEK, Daventry, UK) in a 5-ton manual hydraulic press. Several cubic centimeters of core material were removed from the center of horizon core for this analysis. A total of 5 mL of pore water was collected from each station horizon, placed in cryovials, immediately frozen in liquid nitrogen, and stored at -80°C. Sulfate concentrations were determined in triplicate using a Dionex ICS-1000 ion chromatograph equipped with an IonPac AS4A-SC anion exchange column and a conductivity detector (Dionex, Sunnydale, CA, USA). Samples were pre-filtered through a 0.22 µm membrane disk filter to remove particulate matter and diluted 10-fold in deionized water prior to analysis. The eluent contained 1.8 mM Na_2CO_3 and 1.7 mM $NaHCO_3$, and the flow rate was 2 mL min^{-1}.

For methane analysis, triplicate sediment samples (ca. 3 cm^3) were collected from each station horizon and immediately placed into 10-mL serum bottles containing 6 mL of 3.7% filter-sterilized formaldehyde to halt microbial activity. Bottles were immediately capped with butyl rubber stoppers and stored at 4°C for transport back to the laboratory. Methane was analyzed using a Varian 3300 gas chromatograph equipped with a Poropak Q 80/100 column and a flame ionization detector using helium as the carrier at a flow rate of 20 mL min^{-1}. The injector, column, and detector temperatures were held at 100°C, 100°C, and 125°C, respectively. Methane concentrations were determined using the ideal gas law equation ($PV = nRT$) and measuring the amount of methane in the headspace, the culture volume, the headspace volume, and the headspace pressure.

DNA Extraction. Triplicate sediment samples (ca. 1 cm^3) were collected from each station horizon, placed into MO BIO Powersoil® Bead Tubes (MO BIO, Carlsbad, CA, USA), frozen in liquid nitrogen, and stored at -80°C until extraction. Total genomic DNA was extracted using the MO BIO Powersoil® Kit (MO BIO, Carlsbad, CA, USA) according to the manufacturer's instructions, and DNA concentrations were quantified using a Qubit 2.0 Fluorometer and Quant-iT dsDNA BR Assay Kit (Life Technologies, Carlsbad, CA, USA).

Quantitative PCR. The numbers of bacterial and archaeal 16S ribosomal RNA gene copies per gram of wet sediment were quantified in triplicate via SYBR Green-based quantitative PCR (qPCR). Bacterial primers 27F (5'-AGAGTTTGATCMTGGCTCAG-3') (Nakatsu & Marsh, 2007) and 519R

(5’-GWATTACCGCGGCKGCTG-3’) (Turner *et al.*, 1999) and archaeal primers A344F (5’-ACGGGGIGCAGCAGGCGCGA-3’) (Nakatsu & Marsh, 2007) and A533R (5’-ATTACCGCGGCTGCTGG-3’) (Weisburg *et al.*, 1991) were used for amplification. Reactions were performed in 30-µL volumes containing 15 µL of 2X Power SYBR Green PCR Master Mix (Life Technologies, Carlsbad, CA, USA), 125 nM of each primer, and 2 µL of template DNA (1:15 dilution). Thermocycler conditions were as follows: 50°C for 2 min, 95°C for 10 min, followed by 40 cycles of 95°C for 30 s, 55°C for 1 min, and 72°C for 1 min. Reactions were carried out in a 7300 Real Time PCR Machine (Life Technologies, Carlsbad, CA, USA). DNA from *Desulfococcus oleovorans* strain Hxd3 and *Methanospirillum hungatei* strain JF-1 served as standards.

The abundances of sulfate-reducing microorganisms and methanogens were estimated in triplicate by determining the number of gene copies per gram of wet sediment for each horizon by quantification of *dsrA* (dissimilatory sulfite reductase) and *mcrA* (methyl-coenzyme M reductase) genes, respectively. Amplification of *dsrA* genes was carried out using dsr1F (5’-ACSCACTGGAAGCACG-3’) and dsrQ2r (5’-GTTGAYACGCATGGTRTG-3’) primers (Chin *et al.*, 2008) [Note: a recent study by Müller *et al* (2014) established a publically available *dsrAB*/DsrAB database and a set of recommended primers for ecological investigations]. Amplification of *mcrA* genes was conducted using forward primers ME3MFe’ (5’-ATGTCNGGTGGHGTMGGSTTYAC-3’) and ME3MFe’ (5’-ATGAGCGGTGGTGTCGGTTTCAC-3’) and reverse primer Me2r’ (5’-

TCATBGCRTAGTTDGGRTAGT-3') as described by Nunoura *et al* (2008). Reaction volumes were 30 µL and contained 15 µL of 2X Power SYBR Green PCR Master Mix (Applied Biosystems, Carlsbad, CA, USA), 250 nM of each primer, and 2 µl of template DNA (1:15 dilution). Thermocycler conditions were as follows: 50°C for 2 min, 95°C for 10 min, followed by 40 cycles of 95°C for 30 s, 52°C for 1 min, and 72°C for 1 min. Reactions were carried out in a 7300 Real Time PCR Machine (Life Technologies, Carlsbad, CA. USA). Plasmid DNA obtained from Chesapeake Bay *dsrA* and *mcrA* clone libraries was used to generate standards in qPCR reactions. These clones were generated from respective *dsrA* and *mcrA* PCR products using the TOPO TA Cloning Kit with pCR®4 TOPO vector (Life Technologies, Carlsbad, CA, USA) as recommended by the manufacturer. Inserts were sequenced to confirm their identities.

Detection of *assA/bssA* genes. Community DNA from the surface horizons and horizon 6 at station 908 was surveyed via PCR for the presence of genes encoding the catalytic subunits of glycyl radical enzymes associated with the anaerobic activation of alkanes (*assA*) (Callaghan *et al.*, 2008, Grundmann *et al.*, 2008) and aromatic hydrocarbons (*bssA*) (Leuthner *et al.*, 1998). Surface horizons were chosen for this analysis based on the hypothesis that the microbial communities in surface sediments would serve as the sediment's 'first responders' in the event of an oil spill. Horizon 6 at station 908 was selected for further investigation due to its high methane concentration. Nine primer pairs were employed as previously described (Callaghan *et al.*, 2010) (Table S2) (Note: these primers primarily target *assA* and have a more limited capacity to

detect *bssA* or *nmsA* homologs). A touchdown PCR protocol was conducted for 50-µL reaction volumes containing 25 µL of 2X DreamTaq Master Mix (Thermo Fisher Scientific, Waltham, MA, USA), 400 nM of each primer, 5 µL of betaine (5M), and 2 µL of template DNA (1:15 dilution). Thermocycler conditions were as follows: 95°C for 4 min followed by 2 cycles at each annealing temperature (i.e., 95°C for 1 min, 63 to 54°C for 1 min, 72°C for 2 min), 19 cycles at the plateau annealing temperature (53°C), and a final extension step at 72°C for 10 min. For samples that did not yield amplification via the touchdown method, the PCR protocol was conducted under less stringent parameters via gradient PCR (annealing temperatures ranging from 55 to 65°C). Reactions were performed in volumes of 50 µL containing 25 µL of 2X DreamTaq Master Mix (Thermo Fisher Scientific, Waltham, MA, USA), 2 µM of the forward and reverse primer, 1 µL (5 units μL^{-1}) of DreamTaq polymerase (Thermo Fisher Scientific, Waltham, MA, USA), and 2 µL of template (1:15 dilution, 1:5 dilution for station 818). PCR products were cleaned with a QIAquick PCR Purification Kit (Qiagen, Valencia, CA, USA) and cloned into the pCR™-II vector using a Dual Promoter TA Cloning Kit (Life Technologies, Carlsbad, CA, USA) following the manufacturer's instructions, and inserts of the expected size were sequenced. Reads were assembled into OTUs at 97% similarity, and nearest matches for each OTU were determined using BlastX of the NCBI NR database. Resulting OTUs and their closest NCBI matches were translated into protein sequences and aligned with representative AssA and BssA sequences from several well-described strains using Megalign Software (DNASTAR Inc., Madison, WI, USA)

and the ClustalW alignment method. Neighbor-joining trees were constructed with pairwise deletion and performing 10,000 bootstrap replicates. Pyruvate formate-lyase (*pfl*) served as the outgroup for phylogenetic analysis.

Microbial Community Analysis. The surface horizons for each of the stations and horizon 6 at station 908 were chosen for further analysis for the reasons stated above. The diversity of 16S rRNA genes was assayed in triplicate for each of the selected horizons via pyrosequencing of multiplexed PCR products. Bacterial 16S rRNA genes were amplified using the forward primer 27F (see above) and the reverse primer 338R (5'-TGCTGCCTCCCGTAGGAGT-3') (Nakatsu & Marsh, 2007), producing a 311 bp amplicon. The PCR primers contained 5' Titanium Fusion adapter sequences (forward primer A-tag: CCATCTCATCCCTGCGTGTCTCCGACTCAG; reverse primer B-tag: CCTATCCCCTGTGTGCCTTGGCAGTCTCAG), as well as a unique 8-nucleotide barcode tag in the reverse primer (Hamady *et al.*, 2008) to allow direct 454 sequencing. Reactions were performed in 50-µL volumes. Reaction mixtures included 0.2 µM of the 'tagged' forward primer, 0.25 µM of the reverse primer, 0.25 µL of DreamTaq (5 units μL^{-1}) (Thermo Fisher Scientific, Waltham, MA, USA), PCR Supermix (Life Technologies, Carlsbad, CA, USA), and 2 µL of template DNA (1:15 dilution). Thermocycler conditions for bacterial 16S rRNA genes were as follows: 95°C for 7 min and 30 cycles of 95°C for 20 s, 55°C for 20 s, and 72°C for 40 s. Archaeal amplification conditions were identical except that the extension step at 55°C lasted for 60 s. Archaeal 16S rRNA genes were initially amplified using primers A8F (5'-

TCCGGTTGATCCTGCC-3') and A344R (5'-TCGCGCCTGCTGCICCCCGT-3') to produce a 336 bp amplicon that was tagged with Titanium adaptors described above (Nakatsu & Marsh, 2007). However, due to inefficient amplification, the protocol was modified, and the archaeal 16S rRNA genes were amplified using A8F and A344R primers without the adaptors and then 'tagged' via a six-cycle secondary PCR reaction as previously described (Wawrik *et al.*, 2012). PCR products were purified using a QIAquick PCR Purification Kit (Qiagen, Valencia, CA, USA), and concentrations were quantified using a Qubit 2.0 and Quant-iT dsDNA BR Assay Kit (Life Technologies, Carlsbad, CA, USA). Equimolar amounts of bacterial and archaeal PCR products were combined and sequenced using 454 GS FLX Titanium sequencing.

Sequence Analysis. Reads were denoised to remove sequence errors via the denoise_wrapper.py script in QIIME (Version 1.8.0), and primer/adapter sequences were trimmed. Chimeric sequences were detected via the reference-based chimera detection algorithm, USEARCH, in QIIME and removed (Caporaso *et al.*, 2010a). No primer mismatches were allowed, and the remaining high-quality sequence reads were grouped into OTUs at 97% similarity for both Archaea and Bacteria. Sequences were aligned to the SILVA reference alignment database (Pruesse *et al.*, 2007) using PYNAST (Caporaso *et al.*, 2010b). Taxa that accounted for ≥1% reads in any of the 15 libraries (i.e., five sediment locations sequenced in triplicate) were defined as 'core taxa', which were further analyzed to assess similarities among sites using PC-ORD

(Version 6, MjM Software). To test for similarities and/or differences among sites, taxa frequency data were arcsine-square-root transformed, and a multi-response permutational procedure (MRPP) and a one-way permutational multivariate analysis of variance (PerMANOVA) (McCune *et al.*, 2002) were performed using a Bray-Curtis distance measure and 5000 permutations. Non-metric multidimensional scaling (NMDS) was used to visualize grouping patterns of the community in each pyrosequenced library. A scree plot was first conducted in order to determine the appropriate number of dimensions for ordination, and both archaeal and bacterial data sets were analyzed several times using identical parameters to ensure that consistent results were obtained. Parameters for NMDS included: Bray-Curtis distance measure, 1000 runs with real data, 1000 runs of Monte Carlo test with randomized versions of the data, plotted using two axes and rotated with orthogonal principal axes, and starting configurations were chosen randomly. In addition, community richness, diversity (Shannon and Simpson indices), and evenness were assessed using PC-ORD (Version 6, MjM Software).

Microcosm Experiments. Sediment samples (ca. 2 cm^3) were collected from each horizon and immediately placed into sterile serum bottles under N_2 while aboard the R/V *Hugh R. Sharp*. Bottles were sealed with butyl rubber stoppers and flushed with syringe-filtered N_2 gas to maintain anaerobic conditions. Bottles were stored at 4°C during transport and during laboratory storage until microcosms were established.

The surface horizons for each of the stations, as well as horizon 6 at station 908, which had a very high concentration of methane in the pore water, were chosen for microcosm experiments for the same reasons stated above for *assA*/*bssA* gene surveys and pyrosequencing. Microcosms were established under sulfate-reducing and methanogenic conditions using basal mineral medium (NaCl, 20 g L^{-1}; $MgCl_2 \cdot 6H_2O$, 3 g L^{-1}; $CaCl_2 \cdot 2H_2O$, 0.15 g L^{-1}; NH_4Cl, 0.25 g L^{-1}; KH_2PO_4, 0.2 g L^{-1}; and KCl, 0.5 g L^{-1}) (pH 7.2) (Widdel & Bak, 1992) and strictly anaerobic technique. Sodium sulfate (25 mM) was included in media for sulfate-reducing cultures. Mineral medium was supplemented with trace elements (10 mL L^{-1}) (Tanner, 1997) and 0.1 mL of resazurin (1 g L^{-1} stock). Media was degassed for 45 minutes under a stream of N_2:CO_2, and aliquots (45.5 mL) were distributed into 160-mL serum bottles using anaerobic technique, sealed with butyl rubber stoppers, and secured with aluminum crimp seals. After sterilization, each bottle was supplemented with 0.5 mL of filter-sterilized RST vitamins (Tanner, 1997) modified to include 50 mg L^{-1} nicotinamide, 5 mg L^{-1} pyridoxine·HCl, 5 mg L^{-1} thiamine·HCl, 5 mg L^{-1} riboflavin, 5 mg L^{-1} vitamin B_{12}, 5 mg L^{-1} biotin, 5 mg L^{-1} folic acid, 5 mg L^{-1} calcium pantothenate, 5 mg L^{-1} thioctic acid, 5 mg L^{-1} *p*-aminobenzoic acid, 0.4 mL cysteine-sulfide (12.5 g L^{-1} of each), and 1.5 mL $NaHCO_3$ from a 10% stock (w/v). Mercaptoethanesulfonic acid (MESA) was included in the vitamin solution at a concentration of 5 mg L^{-1} for methanogenic incubations. Filter-sterilized hexadecane (0.1 mL) (Sigma, St. Louis, MO) was added as an overlay to appropriate bottles.

Sediment inoculation was performed in an anaerobic chamber under N_2:H_2 (95:5). A sediment slurry was established with 2 g of core sediment and 50 mL of sulfate-free basal mineral medium. From the sediment slurry, 2 mL were syringe-injected into the appropriate treatment bottles. The amount of the sediment inoculum was selected to introduce sufficient biomass and to minimize the amount of endogenous carbon, which would make it more difficult to discern sulfate loss and/or methane production over background levels. Bottles were removed from the anaerobic chamber, and the headspace was flushed three times with filter-sterilized N_2:CO_2 (80:20). Five treatment conditions were established in triplicate for each horizon tested (Table S3) and included active cultures (amended with an overlay of hexadecane and the sediment inoculum), abiotic controls (amended with hexadecane but no sediment inoculum), background controls (sediment inoculum with no hexadecane), sterile controls (amended with hexadecane and sediment, autoclaved on three consecutive days), and positive controls [amended with an overlay of hexadecane, sediment inoculum, and a 10% (v/v) inoculum of *Desulfatibacillum alkenivorans* strain AK-01 (approximately 10^5 cells)]. *Desulfatibacillum alkenivorans* strain AK-01 is a known alkane-utilizing sulfate reducer originally isolated from the Arthur Kill waterway (So & Young, 1999). AK-01 was used as a positive control because this organism can utilize a range of alkanes (C13-C18) under sulfate-reducing conditions. Additionally, AK-01 has been shown to utilize *n*-hexadecane syntrophically with the methanogen *M. hungatei* strain JF-1 in the absence of sulfate (Callaghan *et al.*, 2012). AK-01

therefore served as a *potential* positive control under methanogenic conditions (i.e., methane production in these incubations above background levels would indicate that the sediments contained methanogenic archaea with the ability to couple with a known hexadecane utilizer, whereas absence of methane in these incubations would suggest that AK-01 could not couple syntrophically with the indigenous methanogens). Microcosms were incubated at room temperature (~ 24-25°C) (*in situ* water temperatures above sediment averaged 27.5°C; see Table S1) in the dark for 672 days. Microcosm activity was monitored via sulfate loss on a Dionex ICS-1100 (Dionex, Sunnydale, CA, USA) equipped with an IonPac AG23 anion exchange column using eluent of 4.5 mM Na_2CO_3 and 0.8 mM $NaHCO_3$ at a flow rate of 1 mL min^{-1}. Methane production was monitored as described above.

Accession Numbers. Sequences of *assA* and *bssA* were deposited in GenBank under the following accession numbers: KM096832-KM096849. The 16S rRNA gene sequence data were deposited in NCBI's Short Read Archive under the following accession number: SRP044028.

RESULTS

August 2010 cruise CTD data confirmed hypoxic conditions in near bottom waters of the upper Bay (stations 908 and 858) as observed in 2009 (Figure S2) and 2010 (Figure S3). Sediment gravity cores were therefore collected at four sites along the salinity gradient that spanned hypoxic and oxic

zones (Figure S1 and Table S1). The upper Bay cores (stations 908 and 858) collected within the area of seasonal hypoxia were dominated by silty clay that appeared sulfidogenic. Lower Bay sites (stations 818 and 707) yielded gray sandy cores that contained carbonate shell debris. Qualitatively, these cores appeared to contain less organic matter than upper Bay sediments.

Sediment Pore Water Analysis. Overall, pore water sulfate concentrations in cores collected from the upper Bay were ca. two orders of magnitude lower than in cores from the lower Bay stations (stations 818 and 707) (Figure 1A), and concentrations in the upper Bay declined rapidly with depth (i.e., < 0.1 mM). Methane was detected in all sampled horizons in the upper Bay, but concentrations were negligible in lower Bay sediments (Figure 1B). Pore water methane concentrations in the upper Bay increased with depth, ranging from 0.47 ± 0.02 to 2.07 ± 0.32 mM at station 908 and between 0.25 ± 0.03 to 0.54 ± 0.05 mM at station 858. Alternative terminal electron acceptors, such as nitrite and nitrate, were below the limits of detection via ion chromatography at all stations and depths (data not shown).

Microbial Community Analysis. A total of 57,633 bacterial and 17,901 archaeal sequence reads were obtained via 454-sequencing. Proteobacteria contributed to the largest proportion of the bacterial communities at each of the locations, ranging from 24-51% of the 16S rRNA reads. Proteobacteria were significantly more abundant in upper Bay sediments (averaging stations 908 and 858) compared to lower Bay sediments (averaging stations 818 and 707) ($p = 1.32E-04$). Delta- and Gammaproteobacteria made up the largest proportions

of the Proteobacteria, accounting for 67-90%, and 5-22% of proteobacterial reads, respectively (Figure 2A). Both Delta- and Gammaproteobacteria accounted for significantly greater proportions of libraries in upper Bay sediments compared to lower Bay sediments ($p = 1.62E-03$ and $p = 5.61E-05$, respectively). Detected gammaproteobacterial lineages included the Chromatiales, Thiohalophilus, Xanthomonadales, Sedimenticola, Oceanospirillales, Legionellales, Methylococcales, and Alteromonadales (Table S4). Dominant within the Gammaproteobacteria were unclassified lineages (55-79% of reads), as well as the Chromatiales, which accounted for 5-30% of gammaproteobacterial reads. Among the Deltaproteobacteria, the Desulfobacterales (8-20% of all reads) and the Syntrophobacterales (2-13% of all reads) were the most prominent orders, with both being significantly more abundant in upper Bay sediments than lower Bay sediments ($p = 0.03$ and $p = 7.90E-04$, respectively). Chloroflexi were detected in high proportional abundances at all sites, accounting for 10-38% of bacterial 16S rRNA reads and making up a significantly greater proportion of the community in the lower Bay ($p = 6.94E-05$). The majority of the Chloroflexi-like sequences were classified within the class Dehalococcoidetes (7-37% of all reads) and the genus *Dehalogenimonas* (7-33% of all reads), with both taxonomic groups being more abundant in lower Bay sediments ($p = 1.33E-04$ and $p = 6.60E-05$, respectively). With respect to depth, Dehalococcoidetes were proportionally more abundant in horizon 6 compared to the surface horizon at station 908 ($p = 1.74E-05$), whereas Deltaproteobacteria were less abundant with depth at this

station (p = 8.90E-04). Also detected in Bay sediments were a diverse group of Firmicutes, accounting for 5-14% of all sequences. A large proportion of these reads were attributed to the Clostridia (55-88% of Firmicute reads). Both the Firmicutes (phylum) as well as the Clostridia (class within the Firmicutes) were proportionally more prevalent in upper Bay sediments compared to lower Bay sediments (p = 5.71E-03 and p = 0.04, respectively). At the family level, Firmicute lineages in Bay sediments included several Bacillales, including the Bacillaceae, Paenibacillaceae, Staphylococcaceae, Thermoactinomycetaceae, Enterococcaceae, Lactobacillaceae, and Streptococcaceae. Detected, classifiable Clostridia families included Clostridiaceae, Eubacteriaceae, Peptococcaceae, Peptostreptococcaceae, Veillonellaceae, Natranaerobiaceae, and Thermoanaerobacteraceae (Table S4). None of the Firmicute OTUs assigned beyond the order level accounted for more than 1% of reads in any of the samples, and 42-65% of reads attributed to Firmicutes were either annotated as unclassified Clostridia or unclassified Firmicute lineages.

With respect to the archaeal communities (Figure 2B), the upper Bay stations were dominated by Euryarchaeota (81-88% of archaeal reads), whereas Crenarchaeota were significantly more prevalent at lower Bay stations (p = 1.88E-04). At the class level, the euryarchaeal sequences were primarily attributed to the Methanomicrobia, Thermoplasmata, or were unclassified Euryarchaeota. Methanomicrobia and Thermoplasmata were proportionally more abundant in upper Bay sediments (p = 1.51E-08 and p = 5.63E-05, respectively) (Table S5).

Clustering of the 16S rRNA reads produced 2,086 bacterial and 861 archaeal OTUs. 'Core taxa' within libraries were defined as taxa that occurred at ≥1% frequency in at least one of the libraries. The frequencies for these dominant (core) groups were used for ordination using NMDS. NMDS indicated that the bacterial communities in the upper Bay are distinct from those in the lower Bay (Figure S4A), whereas upper Bay archaeal communities clustered more tightly than those for the lower Bay (Figure S4B). PerMANOVA analysis indicated that replicates from each of the five horizons were more similar to each other than to other sites. Analysis of the core bacterial and archaeal communities through a one-way PerMANOVA using Bray-Curtis as a distance measure, with groups defined by site and 5000 randomizations, indicated an observed test statistic of F = 67.24 (p = 2.00E-04) for Archaea and an observed test statistic of F = 35.56 (p = 2.00E-04) for Bacteria (Table S6). The Shannon diversity index ranged from 2.48 to 2.86 for Bacteria and from 1.37 to 1.69 for Archaea (Table S7), and evenness ranged from 0.84 to 0.94 for Bacteria and 0.77 to 0.94 for Archaea (Table S7).

Quantitative PCR. Total bacterial abundances in Chesapeake Bay sediment, as determined by the quantification of rRNA genes (and assuming one 16S rRNA gene per genome), ranged between 4.30×10^6 and 5.63×10^7 per gram of wet sediment. The 16S rRNA gene abundances declined with depth in the sediment and were greater in the upper Bay compared to the lower Bay sediments (Table S8). Copy numbers of *dsrA* genes ranged between 3.78×10^4 and 2.98×10^6 per gram of wet sediment (Table S8). At stations 908 and

818, *dsrA* copy numbers decreased with depth, with relative frequencies (based on the ratio of *dsrA* copies to 16S gene copy numbers) of 5.28-0.96% and 3.47-0.23%, respectively (Figure S5A and Table S8). Station 707 exhibited the highest relative frequency of sulfate reducers at approximately 2 ft (0.6 m) below the surface. The relative frequencies of sulfate reducers were fairly constant with depth at station 858, averaging 1.65% (Figure S5A and Table S8).

The number of archaeal rRNA genes ranged from 10^7 to 10^8 per gram wet sediment for stations 908, 858, and 707, whereas abundances at station 818 were an order of magnitude lower (Table S9). Quantification of *mcrA* genes indicated at least an order of magnitude difference between stations 908 and 858 and stations 818 and 707 (10^5 to 10^6 and 10^4 to 10^5 per gram wet sediment, respectively). On average, the relative frequencies of methanogens accounted for ~4.9% of the archaeal community at stations 908 and 858, whereas they accounted for less than 1% (0.97%) of archaeal populations at stations 818 and 707 (Figure S5B). These data are consistent with greater proportions of reads classified within the Methanomicrobia in stations 908 and 858 versus 818 and 707 (see above). The estimated proportional abundances of methanogens among the Archaea, as measured via qPCR, are lower than in 16S rRNA gene sequence data, which likely reflects a limitation of the *mcrA* primers used herein to quantitatively capture the full diversity of this gene in the environment.

Detection of *assA/bssA* genes. Bay sediments were surveyed for *assA* and *bssA* genes via PCR. Using touchdown PCR, *bssA* genes were detected in surface horizons at upper Bay stations 908 and 858 with primer set no. 2 (Table S2). A gradient PCR protocol was carried out under less stringent parameters on the remaining samples, and *assA* gene PCR products were obtained with DNA from surface horizons at all four stations using primer set no. 7 and at depth at station 908 (horizon 6) using primer set no. 1. The gradient PCR protocol did not yield *bssA* gene products from the surface horizons at stations 818 or 707, or from the depth horizon at station 908. Overall, sequencing of cloned PCR products allowed the identification of one *bssA* genotype (stations 908 and 858) and seventeen *assA* genotypes in Chesapeake Bay sediments (Figure 3, Table S10). Among the observed *assA* genotypes, several were most similar to sequences previously obtained from hydrocarbon-impacted North Atlantic coastal sites (e.g., Arthur Kill NJ/NY and Gowanus Canal, NJ). Additionally, *assA* OTUs 1,2, and 15 were most closely related to *assA* genes recently reported in the draft genomes of *Smithella* sp. ME-1 *and Smithella* SCADC (Tan *et al.*, 2014), which were derived from different methanogenic alkane-degrading enrichment cultures (Tan *et al.*, 2013, Embree *et al.*, 2014). Ten out of seventeen Chesapeake Bay *assA* OTUs formed a clade with a clone obtained from Gulf of Mexico sediment potentially exposed to oil originating from the Deepwater Horizon oil spill (Kimes *et al.*, 2013). The *bssA* sequences detected here all assembled into a single OTU at 97% similarity (Figure 3) and were found to be most similar to *bssA* in *Desulfobacula toluolica* Tol2, a sulfate-

reducing bacterium originally isolated from anoxic marine sediment (Eel Pond, Woods Hole, MA) (Rabus *et al.*, 1993).

Microcosm Experiments. Sulfate-reducing and methanogenic microcosms were established using Bay sediments. For all stations, the positive controls containing sediment, hexadecane, and *D*. *alkenivorans* strain AK-01 exhibited significant sulfate loss compared to the background controls (p values ranged between 1.86E-04 and 1.58E-02) (Figure S6). The time for complete sulfate depletion in positive controls varied among stations, but was statistically significant (compared to initial concentrations) for all stations by 40 weeks of incubation. After additional sulfate amendments (~25 mM), the AK-01-amended cultures continued to demonstrate sulfate loss (Table S11). After 672 days, the active treatments and background controls at each of the stations exhibited small, but significant sulfate loss ($p < 0.05$) compared to the time-zero concentrations, but they were not statistically different from each other (Table S11).

Microcosms established under sulfate-reducing conditions from surface horizon sediments collected at stations 858 and 908 produced significantly more methane compared to the background controls after 672 days of incubation, ($p = 3.32E-03$ and $p = 8.77E-03$, respectively) (Figure 4 and Table S12). With respect to the AK-01 positive controls (under sulfate-reducing conditions), significantly more methane was observed in the surface horizons at stations 908, 858, 818, and 707 than in the background controls, whereas a significant difference was not seen in the positive control at depth at station 908

(horizon 6) ($p = 0.07$). Additionally, methane production in the AK-01 positive control was significantly higher than in active treatments only at Station 707 (Figure 4 and Table S12).

Microcosms established under methanogenic conditions for stations 908 (surface horizon and horizon 6), 858, and 707 produced significantly higher levels of methane ($p < 0.05$) than background controls after the 672-day incubation period. A small amount of methane was observed in the killed controls for station 858 as well as station 908 horizon 6, with observed quantities being significantly less than those observed in background controls ($p \leq 0.02$ to 1.10E-05) (Figure 4 and Table S12). No methane production occurred in media-only controls under sulfate-reducing or methanogenic conditions. The AK-01 positive control established under methanogenic conditions did result in significant ($p < 0.05$) methane production in comparison to the background control at the surface horizons at stations 858 and 707, as well as the depth horizon at station 908 (Figure 4). Overall, significantly more methane was produced in methanogenic microcosms established from upper Bay sediments as compared to sediments collected from lower Bay cores (all pairwise p-values $\leq$ 8.27E-05).

DISCUSSION

The Chesapeake Bay is a seasonally stratified estuary that experiences summer bottom anoxia, which has become increasingly widespread since its

initial identification in the 1930s (Newcombe *et al.*, 1939, Officer *et al.*, 1984). Anoxia initiates in the spring when increased freshwater and nutrient loading lead to halocline-dependent stratification and increased phytoplankton productivity. The anoxia is then driven by benthic decay of organic matter from sinking phytoplankton and from the previous summer's and fall's seasonal phytoplankton blooms (Taft *et al.*, 1980, Officer *et al.*, 1984, Boesch *et al.*, 2001). A hydrocarbon spill in the Chesapeake Bay therefore has the potential to impact both oxic and anoxic water masses as well as their underlying sediments. Therefore, one aim of the work presented here was to characterize and compare the microbial communities associated with sediments located in areas of frequent hypoxia with those that are less frequently affected by hypoxic waters. Cores were collected across the Bay's salinity gradient, which encompasses both hypoxic and oxic areas, to assess the potential for anaerobic alkane degradation, as a proxy for natural attenuation in the event that an oil spill should occur.

Assuming conservative mixing of seawater (~28 mM sulfate at a salinity of 35) and given the salinities at stations in the upper Bay (908 and 858; Table S1), where hypoxia was observed, it can be estimated that the overlying water could contain up to ~8-9 mM sulfate. Pore water sulfate concentrations, however, were substantially lower (< 0.3 mM), indicating consumption of terminal electron acceptors including sulfate, yielding methanogenic conditions. These data are consistent with pore water methane concentrations (Figure 1B), which indicated high levels of methane throughout upper Bay sediment cores,

reaching supersaturated levels in horizon 6 of station 908. These observations are consistent with the important role that sulfate reducers play in the conversion of organic matter in coastal ecosystems, particularly near-shore (Jørgensen, 1982). Conversely, at the lower Bay stations (stations 818 and 707), water column salinities would indicate sulfate concentrations of ca. 12 and 22 mM respectively, which are mirrored by similarly high sulfate concentrations observed in the sediment pore water (Figure 1A). High sulfate concentrations in lower Bay sediments may reflect less intense input of organic matter via sedimentation and/or input of organic matter that is at a later stage of decomposition and more refractory to oxidation, resulting in the incomplete depletion of terminal electron acceptors (Jørgensen, 1982). Alternatively, given the apparent higher porosities of core materials (based on visual inspection) at stations 818 and 707, sufficient pore water exchange with overlaying water might allow for continuous replenishment of sulfate, at least to the depths sampled in this study. Despite the large differences in sulfate concentrations between the upper and lower Bay sediments, no clear trend was observed with respect to differences in the abundance of sulfate-reducing organisms among the different stations (based on qPCR of *dsrA* and the primers used herein) (Figure S5A). Conversely, methanogenic archaea accounted for a 2- to 8-fold greater proportion of the archaeal populations in upper Bay sediments (Figure S5B), consistent with overall trends in pore water methane concentrations and the notion that sediment communities associated with the Bay's hypoxic zone are predominantly methanogenic.

High methane concentrations in upper Bay sediments coincided with a greater abundance of sequences classified within the deltaproteobacterial order Syntrophobacterales. Syntrophobacterales, specifically *Syntrophus* and *Smithella* spp., are common in methanogenic hydrocarbon-degrading communities, including methanogenic oil sands tailings, oil sands tailings enrichment cultures, hydrocarbon-contaminated sediments and aquifers, methanogenic hexadecane-degrading consortia, oil field production water, methanogenic coal seam groundwater, and coal-impacted wetlands (see Gray *et al.*, 2011 and references therein, Siddique *et al.*, 2011, Wawrik *et al.*, 2012, Cheng *et al.*, 2013, Tan *et al.*, 2013). Furthermore, a greater proportion of Firmicutes were detected in the upper Bay sediments. These bacteria are well known for their ability to process and ferment complex organic matter and are often detected in hydrocarbon-amended enrichment cultures and hydrocarbon-impacted environments (Gieg *et al.*, 2008, Penner *et al.*, 2010, Wawrik *et al.*, 2012). More recently it has also been reported that some members of the Firmicutes, such as Clostridiales, may play an important role in the activation of hydrocarbons under methanogenic conditions (Fowler *et al.*, 2012). Among the archaeal communities, upper Bay sediment libraries contained large proportions of Euryarchaeota, particularly the methanogenic class Methanomicrobia, consistent with both the measured pore water methane concentrations and *mcrA* data (Figure 1B and Figure S5B). Methanomicrobia are often detected in methanogenic hydrocarbon-amended enrichment cultures and hydrocarbon contaminated systems, and it has been hypothesized this group of

methanogens plays a key role in the conversion of hydrocarbons via coupling with the requisite syntrophs (for review, see Gray *et al.*, 2010).

Compared to the upper Bay, the lower Bay sediment 16S rRNA libraries contained proportionally fewer sequences within groups traditionally associated with organic matter fermentation and methanogenesis. Specifically, significantly greater proportions of sequences classified as Dehalococcoidetes (Chloroflexi) were detected in these sediments. Dehalococcoidetes and closely related groups are known to be involved in organohalide respiration and have potential roles in bioremediation of chlorinated compounds that have been used for decades as industrial solvents (Richardson, 2013). The latter is relevant to the Bay because of a history of PCB pollution (Ashley & Baker, 1999, Walker *et al.*, 1999, Foster *et al.*, 2000, King *et al.*, 2004). Archaeal communities also included large proportions of sequences within the Thermoprotei, which have been detected in methanogenic alkane-degrading enrichment cultures, albeit at low levels (Gray *et al.*, 2011).

Given large genome variability within species and high rates of lateral gene transfer, 16S rRNA gene sequences are a poor indicator for microbial functional traits. To obtain a clearer picture of a community's potential ability to degrade specific pollutants, functional gene markers are frequently used. As previously discussed, aliphatic and aromatic hydrocarbon addition to fumarate (i.e., 'fumarate addition') is one of several mechanisms of anaerobic hydrocarbon activation (for review, see Heider and Schühle, 2013). It is catalyzed by the glycyl radical enzymes ASS/MAS (Callaghan *et al.*, 2008,

Grundmann *et al.*, 2008) and BSS (Leuthner *et al.*, 1998), respectively. The genes encoding the catalytic subunits of ASS and BSS (*assA* and *bssA*) are considered useful biomarkers in this regard (for review, see Callaghan *et al.,* 2010, Callaghan, 2013, Agrawal & Gieg, 2013). More recently, intense efforts have been focused on elucidating pathways of methanogenic conversion of hydrocarbons. To date, there have been several studies that have detected *bssA* (for review, see Callaghan, 2013) and/or *assA* in methanogenic enrichment cultures and/or methanogenic hydrocarbon-impacted environments (Davidova *et al.*, 2011, Li *et al.*, 2012, Mbadinga *et al.*, 2012, Wang *et al.*, 2012, Wawrik *et al.*, 2012, Zhou *et al.*, 2012, Aitken *et al.*, 2013, Cheng *et al.*, 2013), providing evidence that fumarate addition may play an important role in the hydrocarbon activation step. A recent study of an *n*-hexadecane-degrading methanogenic enrichment culture aimed at identifying requisite alkane-degrading bacteria, resulted in a draft genome of *Smithella* sp. ME-1 (Embree *et al.*, 2013), which was subsequently reported to contain a nearly full-length *assA* gene to which metatranscriptomic reads were mapped (Tan *et al.*, 2014). These observations are consistent with data from another methanogenic alkane-degrading enrichment culture (SCADC) (Tan *et al.*, 2013), in which a single copy of *assA* (GenBank accession KF824850) was recovered from a partial *Smithella* sp. genome (Tan *et al.*, 2014). The genus *Smithella* is a member of the family Syntrophaceae*,* and *assA* genotypes closely related to this gene from *Smithella* sp. were found in both upper Bay stations (908 and 858) and station 707 (Figure 3)*.* Genotypes of *assA* closely related to the

sulfate-reducing, alkane-degrading strains *D*. *alkenivorans* AK-01 and *Desulfoglaeba alkanexedens* ALDC were also detected at all four stations. Moreover, *assA* genotypes similar to those detected in the Gulf of Mexico sediments near the Deepwater Horizon oil spill were also detected. These data are consistent with the presence of bacteria capable of alkane utilization under methanogenic (i.e., syntrophic) and sulfate-reducing conditions throughout Chesapeake Bay in both surface sediments at depth.

In contrast, *bssA*-like sequences were only observed in the surface horizons of the upper Bay stations (Figure 3). Given the limited number of samples analyzed here, our ability to derive conclusions regarding the biogeography of *ass* and *bss* genes in the Bay is limited. However, the substrate range of BSS includes toluene, ethylbenzene, and xylene isomers (i.e., TEX) (for review, see Heider & Schühle, 2013), which are far more soluble than aliphatic compounds such as the mid- to longer-chain alkanes. It is possible that the shorter residence times of these more soluble compounds in the water column and sediments may influence the lack of enrichment and/or biogeography of TEX-degrading microorganisms in the Bay. Alternatively, primer specificity may hinder the ability to detect *bssA*-type genes at some sites. To date, PCR primers that capture the full range of known *bssA* genotypes have not been reported (Acosta-González *et al.*, 2013, von Netzer *et al.*, 2013), and it is therefore possible that bacteria potentially capable of TEX-degradation are more widely distributed in Bay sediments than observed here.

In an effort to further investigate the potential for hydrocarbon degradation by microbial communities in Chesapeake Bay sediments, microcosm experiments were conducted using hexadecane as a substrate under sulfate-reducing and methanogenic conditions. Cultures were maintained for >600 days. The long incubation time is not atypical of other studies, in which lag times associated with methanogenic degradation of long-chain alkanes have been observed to be as long as 280 days (Siddique *et al.*, 2011). Despite the lengthy incubation, these experiments resulted in several observations. First, the addition of hexadecane did not significantly stimulate sulfate loss in the absence of *D. alkenivorans* strain AK-01 as a positive control (Figure S6). This observation suggests that the detected *assA* genotypes are potentially not affiliated with the indigenous and 'strict' sulfate reducers (i.e., they may be affiliated with the indigenous syntrophs). Alternatively, the absence of sulfate reduction may simply be an issue of substrate specificity. For example, known sulfate-reducing bacteria that utilize alkanes have broad, but variable, substrate ranges: *D. alkenivorans* AK-01 can utilize C13-C18 alkanes (So & Young, 1999); *D*. *alkanexedens* ALDC utilizes C6-C12 alkanes (Davidova *et al.*, 2006); and *D*. *oleovorans* Hxd3 utilizes C12-C20 alkanes (Aeckersberg *et al.*, 1991). The second observation was the production of methane under both sulfate-reducing and methanogenic conditions. Under *sulfate-reducing* conditions, the active treatments and positive controls produced significantly more methane than the background controls for microcosms established with upper Bay *surface* sediments compared to the microcosms established with lower Bay

sediments (Figure 4). Moreover, the addition of hexadecane under *methanogenic* conditions appeared to stimulate methanogenesis at stations 908 (surface and at depth), 858, and 707. Significant methane production was not observed under sulfate-reducing or methanogenic conditions in incubations established with station 818 sediment. Together, the higher levels of methane production in hypoxia-influenced sites (i.e., upper Bay sediments) are consistent with the higher abundances of Syntrophaceae and acetoclastic and hydrogenotrophic methanogens observed in upper Bay sediments.

CONCLUSION

Research addressing the fate and transport of the oil associated with the Deepwater Horizon oil spill demonstrated that the microbial community played an important role in remediation via natural attenuation mechanisms (for review, see Joye *et al.*, 2014, Kimes *et al.*, 2014, King *et al.*, 2015). With respect to the Gulf of Mexico, the microbial community demonstrated a rapid and robust response (for review, see Joye *et al.*, 2014, Kimes *et al.*, 2014, King *et al.*, 2015). Molecular analyses of plume water and ocean and coastal sediments via microarrays, targeted gene surveys, metagenomics, and metatranscriptomics highlighted the importance of both aerobic and anaerobic hydrocarbon degradation (for review, see Joye *et al.*, 2014, Kimes *et al.*, 2014, King *et al.*, 2015). In contrast to the Gulf of Mexico, the Chesapeake Bay is a much smaller, shallower, and more dynamic ecosystem, driven by different physical and chemical processes, and the predicted response to a large oil spill would also be very different. Realistically, physical remediation would in all likelihood

be the most exploited tactic in an oil spill response for a system like the Bay. Unlike in the Deepwater Horizon oil spill, which elicited a fast, 'aerobic response' of microbial communities, the Bay's bioremediation capacity in the water column and in the sediments would likely be influenced by its periods of seasonal hypoxia. Long term, this could dictate increased dependence on the anaerobic microbial community to metabolize the residual hydrocarbons that partition to sediments. Although hydrocarbons are probably not a selective pressure on Bay sediments, past investigations have demonstrated the ability of Bay microbial communities to utilize hydrocarbons aerobically (Walker & Colwell, 1973, Walker *et al.*, 1976a, Walker *et al.*, 1976b, Okpokwasili *et al.*, 1984, West *et al.*, 1984). Here, we report that the microbial communities of Bay sediments include microbial taxa frequently associated with the anaerobic conversion of hydrocarbons. The potential for anaerobic aromatic and aliphatic hydrocarbon transformation is further supported by the detection of *bssA* and *assA* genotypes at different locations throughout the Bay and the ability to stimulate methane production in the presence of hexadecane under sulfate-reducing and methanogenic conditions. The occurrence of natural attenuation of hydrocarbons under anaerobic conditions can therefore be taken into account when considering a remediation strategy in response to a major spill in the Chesapeake Bay ecosystem.

FIGURES

Figure 1. Depth profiles of **(A)** sulfate and **(B)** methane concentrations in Chesapeake Bay sediment pore water. Methane measurements were obtained for triplicate sediment samples from each horizon via gas chromatography. Sulfate concentrations were determined by analyzing triplicate pore water samples via ion chromatography.

A.

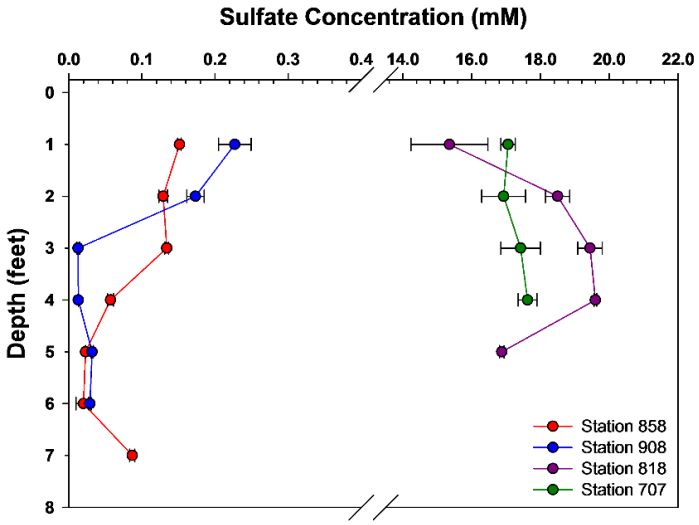

B.

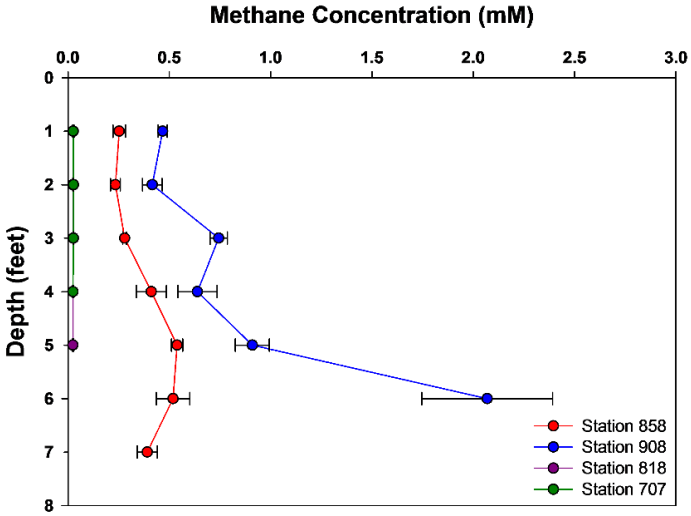

Figure 2. Microbial community composition in Chesapeake Bay sediments as determined by 454-pyrosequencing of partial 16S rRNA gene PCR products. **(A)** Bacterial and **(B)** archaeal 16S rRNA genes were amplified separately, and reads were analyzed using QIIME (Version 1.8.0) (Caporaso *et al.,* 2010a). Community composition data are shown at the class taxonomic level. Minor phylogenetic groups, which could not be visually resolved in the bar graphs, are not included in the legend.

A.

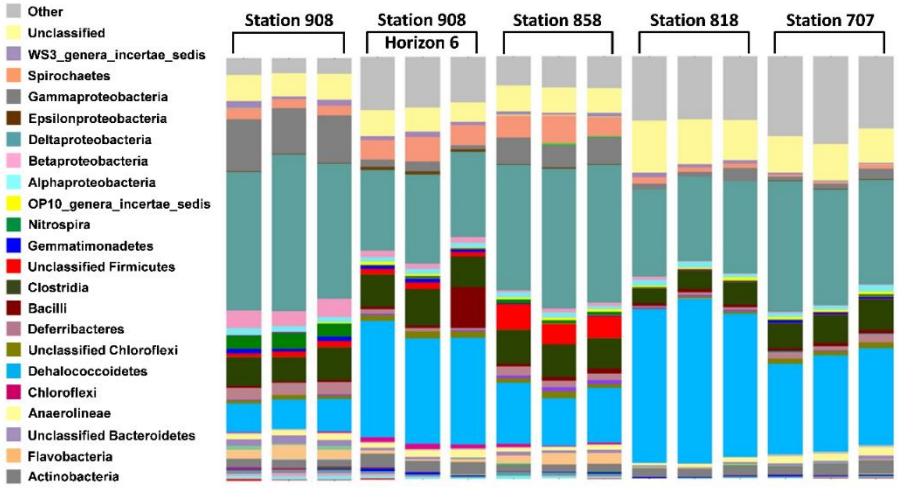

B.

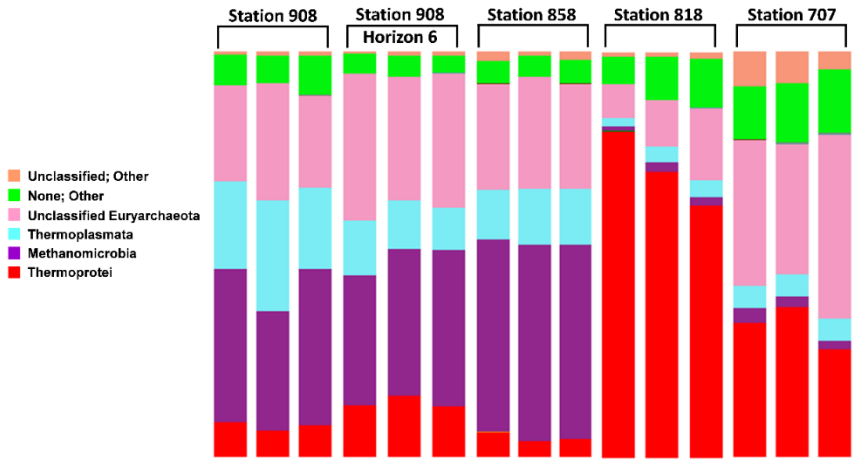

Figure 3. Neighbor-joining dendrogram of translated *assA* and *bssA* gene sequences detected in Chesapeake Bay sediments. Sequence reads were assembled into OTUs at 97% similarity, and closest matches for each OTU were determined using BlastX of the NCBI NR database. Resulting OTUs and closest matches were translated into protein sequences and aligned with representative AssA and BssA sequences from several well-described strains using Megalign Software (DNASTAR Inc., Madison, WI, USA) and the ClustalW alignment method. Neighbor-joining trees were constructed with pairwise deletion and performing 10,000 bootstrap replicates. Bootstrap values below 65 are not shown. Pyruvate formate-lyase served as the outgroup for phylogenetic analysis. Abbreviations: Ass (alkylsuccinate synthase), Mas (methylalkylsuccinate synthase), Bss (benzylsuccinate synthase), Nms (napthylmethylsuccinate synthase) and Pfl (pyruvate formate-lyase). GenBank accession numbers are indicated in parentheses. Stations where OTUs were detected are indicated on the right.

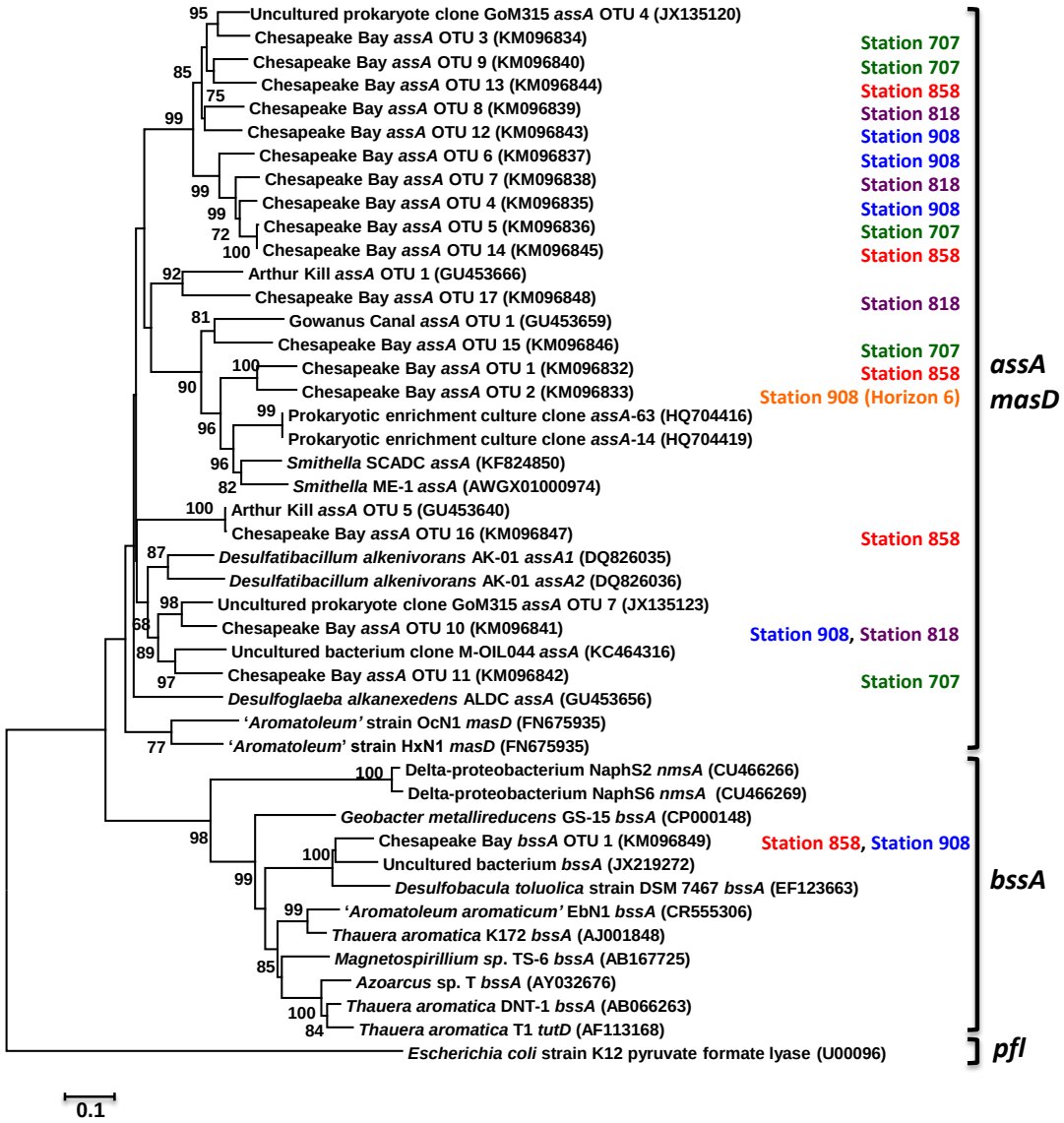
Uncultured prokaryote clone GoM315 assA OTU 4 (JX135120)
Chesapeake Bay assA OTU 3 (KM096834)
Chesapeake Bay assA OTU 9 (KM096840)
Chesapeake Bay assA OTU 13 (KM096844)
Chesapeake Bay assA OTU 8 (KM096839)
Chesapeake Bay assA OTU 12 (KM096843)
Chesapeake Bay assA OTU 6 (KM096837)
Chesapeake Bay assA OTU 7 (KM096838)
Chesapeake Bay assA OTU 4 (KM096835)
Chesapeake Bay assA OTU 5 (KM096836)
Chesapeake Bay assA OTU 14 (KM096845)
Arthur Kill assA OTU 1 (GU453666)
Chesapeake Bay assA OTU 17 (KM096848)
Gowanus Canal assA OTU 1 (GU453659)
Chesapeake Bay assA OTU 15 (KM096846)
Chesapeake Bay assA OTU 1 (KM096832)
Chesapeake Bay assA OTU 2 (KM096833)
Prokaryotic enrichment culture clone assA-63 (HQ704416)
Prokaryotic enrichment culture clone assA-14 (HQ704419)
Smithella SCADC assA (KF824850)
Smithella ME-1 assA (AWGX01000974)
Arthur Kill assA OTU 5 (GU453640)
Chesapeake Bay assA OTU 16 (KM096847)
Desulfatibacillum alkenivorans AK-01 assA1 (DQ826035)
Desulfatibacillum alkenivorans AK-01 assA2 (DQ826036)
Uncultured prokaryote clone GoM315 assA OTU 7 (JX135123)
Chesapeake Bay assA OTU 10 (KM096841)
Uncultured bacterium clone M-OIL044 assA (KC464316)
Chesapeake Bay assA OTU 11 (KM096842)
Desulfoglaeba alkanexedens ALDC assA (GU453656)
'Aromatoleum' strain OcN1 masD (FN675935)
'Aromatoleum' strain HxN1 masD (FN675935)
Delta-proteobacterium NaphS2 nmsA (CU466266)
Delta-proteobacterium NaphS6 nmsA (CU466269)
Geobacter metallireducens GS-15 bssA (CP000148)
Chesapeake Bay bssA OTU 1 (KM096849)
Uncultured bacterium bssA (JX219272)
Desulfobacula toluolica strain DSM 7467 bssA (EF123663)
'Aromatoleum aromaticum' EbN1 bssA (CR555306)
Thauera aromatica K172 bssA (AJ001848)
Magnetospirillium sp. TS-6 bssA (AB167725)
Azoarcus sp. T bssA (AY032676)
Thauera aromatica DNT-1 bssA (AB066263)
Thauera aromatica T1 tutD (AF113168)
Escherichia coli strain K12 pyruvate formate lyase (U00096)
Station 707
Station 707
Station 858
Station 818
Station 908
Station 908
Station 818
Station 908
Station 707
Station 858
Station 818
Station 707
Station 858
Station 908 (Horizon 6)
Station 858
Station 908, Station 818
Station 707
Station 858, Station 908
assA
masD
bssA
pfl
0.1

Figure 4. Methane production was monitored in microcosms established from Chesapeake Bay sediments under sulfate-reducing and methanogenic conditions. Microcosms were established with sediments from the surface horizons at each station, as well as the deepest horizon (horizon 6) at station 908. Five treatments were established in triplicate, including (active) enrichments that included media, sediment, and a hexadecane overlay; (positive) control enrichments that included media, sediment, hexadecane, and *D. alkenivorans* strain AK-01; (background) controls that contained media and sediment; (media) controls containing only medium and a hexadecane overlay; and (sterile) controls containing media, sediment, and hexadecane, which were autoclaved on three consecutive days for sterilization. An asterisk (*) indicates methane production significantly above background controls after 672 days of incubation. A (†) indicates AK-01-amended microcosms with significantly higher methane production than the active treatments.

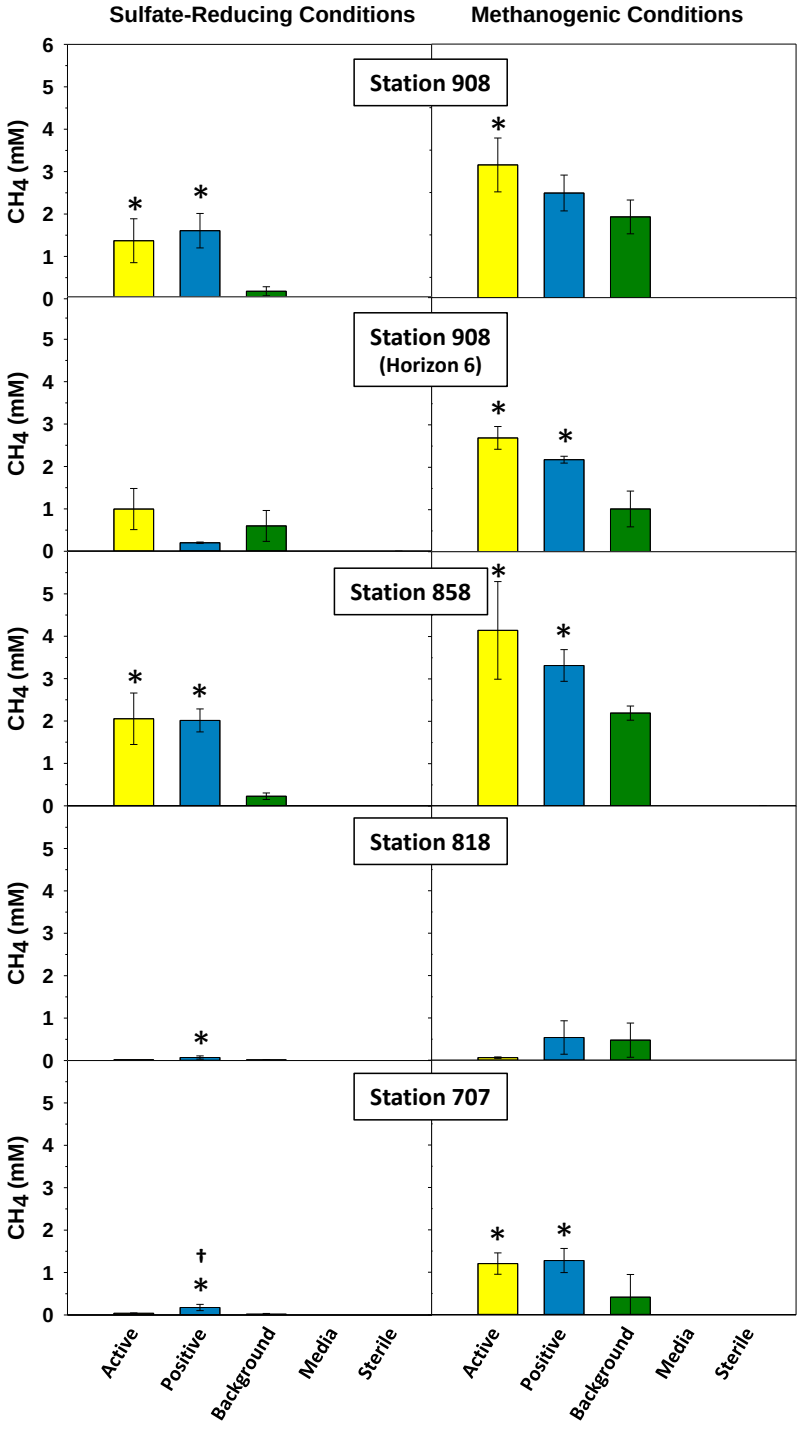
Sulfate-Reducing Conditions
Methanogenic Conditions
Station 908
Station 908
(Horizon 6)
Station 858
Station 818
Station 707
CH4 (mM)
0
1
2
3
4
5
6
*
†
Active
Positive
Background
Media
Sterile

REFERENCES

Acosta-González A, Rosselló-Móra R & Marqués S. (2013) Diversity of benzylsuccinate synthase-like (*bssA*) genes in hydrocarbon-polluted marine sediments suggests substrate-dependent clustering. *Appl Environ Microb* **79**:3667-3676.

Aeckersberg F, Bak F & Widdel F. (1991) Anaerobic oxidation of saturated hydrocarbons to CO_2 by a new type of sulfate-reducing bacterium. *Arch Microbiol* **156**:5-14.

Agrawal A & Gieg LM. (2013) In situ detection of anaerobic alkane metabolites in subsurface environments. *Front Microbiol* **4**.140.

Aitken CM, Jones DM, Maguire MJ, Gray ND, Sherry A, Bowler BFJ, Ditchfield AK, Larter SR & Head IM. (2013) Evidence that crude oil alkane activation proceeds by different mechanisms under sulfate-reducing and methanogenic conditions. *Geochim Cosmochim Acta* **109**:162-174.

Arzayus KM, Dickhut RM & Canuel EA. (2001) Fate of atmospherically deposited polycyclic aromatic hydrocarbons (PAHs) in Chesapeake Bay. *Environ Sci Technol* **35**:2178-2183.

Ashley JTF & Baker JE. (1999) Hydrophobic organic contaminants in surficial sediments of Baltimore Harbor: inventories and sources. *Environ Toxicol and Chem* **18**:838-849.

Balch BN. (1997) Oil spills in the Chesapeake Bay (1985-1994). *Int Oil Spill Conf Proc* **1997**:944-946.

Behn BN (2010) Experts question spill preparedness in Chesapeake: quick-fire response teams needed, scientists and environmentalists say. *The Baltimore Sun*, June 17, 2010.

Boesch DF, Brinsfield RB & Magnien RE. (2001) Chesapeake Bay eutrophication: sceintific understanding, ecosystem restoration, and challenges for agriculture. *J Environ Qual* **30**:303-320.

Callaghan AV, Wawrik B, Ní Chadhain SM, Young LY & Zylstra GJ. (2008) Anaerobic alkane-degrading strain AK-01 contains two alkylsuccinate synthase genes. *Biochem Biophys Res Commun* **366**:142-148.

Callaghan AV, Davidova IA, Savage-Ashlock K, Parisi VA, Gieg LM, Suflita JM, Kukor JJ & Wawrik B. (2010) Diversity of benzyl- and alkylsuccinate synthase genes in hydrocarbon-impacted environments and enrichment cultures. *Environ Sci Technol* **44**:7287-7294.

Callaghan AV, Morris BEL, Pereira IAC, McInerney MJ, Austin RN, Groves JT, Kukor JJ, Suflita JM, Young LY, Zylstra GJ & Wawrik B. (2012) The genome sequence of *Desulfatibacillum alkenivorans* AK-01: a blueprint for anaerobic alkane oxidation. *Environ Microbiol* **14**:101-113.

Callaghan AV. (2013) Metabolomic investigations of anaerobic hydrocarbon-impacted environments. *Curr Opin Biotechnol* **24**:506-515.

Caporaso JG, Kuczynski J, Stombaugh J*, et al.* (2010a) QIIME allows analysis of high-throughput community sequencing data. *Nat Methods* **7**:335-336.

Caporaso JG, Bittinger K, Bushman FD, DeSantis TZ, Andersen GL & Knight R. (2010b) PyNAST: a flexible tool for aligning sequences to a template alignment. *Bioinformatics* **26**:266-267.

Cheng L, Rui J, Li Q, Zhang H & Lu Y. (2013) Enrichment and dynamics of novel syntrophs in a methanogenic hexadecane-degrading culture from a Chinese oilfield. *FEMS Microbiol Ecol* **83**:57-766.

Chesapeake Bay Program. (2014a) *Discover the Bay - the Bay Watershed*. https://www.chesapeakebay.net/discover/baywatershed (17 June 2014, date last accessed).

Chesapeake Bay Program. (2014b) *Learn the Issues - Chemical Contaminants*. https://www.chesapeakebay.net/issues/issue/chemical_contaminants#inline (17 June 2014, data last accessed).

Chin KJ, Sharma ML, Russell LA, O'Neill KR & Lovley DR. (2008) Quantifying expression of a dissimilatory (bi)sulfite reductase gene in petroleum-contaminated marine harbor sediments. *Microbiol Ecol* **55**:489-499.

Crone TJ & Tolstoy M. (2010) Magnitude of the 2010 Gulf of Mexico Oil Leak. *Science* **330**:634-634.

Davidova IA, Callaghan AV, Duncan KE, Sunner J, Biri B & Wawrik B. (2011) Long-chain paraffin metabolism by a methanogenic bacterial consortium enriched from marine sediments. *8th International Symposium of Subsurface Microbiology* (ISSM)*.* Germany.

Davidova IA, Duncan KE, Choi OK & Suflita JM. (2006) *Desulfoglaeba alkanexedens* gen. nov., sp. nov., an n-alkane-degrading, sulfate-reducing bacterium. *Int J Syst Evol Microbiol* **56**:2737-2742.

Embree M, Nagarajan H, Movahedi N, Chitsaz H & Zengler K. (2014) Single-cell genome and metatranscriptome sequencing reveal metabolic interactions of an alkane-degrading methanogenic community. *ISME J* **8**:757-767.

Fisher TR, Harding LW, Stanley DW & Ward LG. (1988) Phytoplankton, nutrients, and turbidity in the Chesapeake, Delaware, and Hudson estuaries. *Estuar Coast Shelf Sci* **27**:61-93.

Foster GD, Roberts Jr EC, Gruessner B & Velinsky DJ. (2000) Hydrogeochemistry and transport of organic contaminants in an urban watershed of Chesapeake Bay (USA). *Appl Geochem* **15**:901-915.

Fowler SJ, Dong XL, Sensen CW, Suflita JM & Gieg LM. (2012) Methanogenic toluene metabolism: community structure and intermediates. *Environ Microbiol* **14**:754-764.

Gieg LM, Duncan KE & Suflita JM. (2008) Bioenergy production via microbial conversion of residual oil to natural gas. *Appl Environ Microbiol* **74**:3022-3029.

Gray ND, Sherry A, Hubert C, Dolfing J & Head IM. (2010) Methanogenic degradation of petroleum hydrocarbons in subsurface environments: remediation, heavy oil formation, and energy recovery. *Adv Appl Microbiol* **72**:137-161.

Gray ND, Sherry A, Grant RJ, Rowan AK, Hubert CRJ, Callbeck CM, Aitken, CM, Jones DM, Adams, JJ, Larter SR, & Head IM. (2011) The quantitative significance of *Syntrophaceae* and syntrophic partnerships in methanogenic degradation of crude oil alkanes. *Environ Microbiol* **13**:2957-2975.

Grundmann O, Behrends A, Rabus R, Amann J, Halder T, Heider J & Widdel F. (2008) Genes encoding the candidate enzyme for anaerobic activation of n-alkanes in the denitrifying bacterium, strain HxN1. *Environ Microbiol* **10**:376-385.

Hamady M, Walker JJ, Harris JK, Gold NJ & Knight R. (2008) Error-correcting barcoded primers for pyrosequencing hundreds of samples in multiplex. *Nat Methods* **5**:235-237.

Hanson RS & Hanson TE. (1996) Methanotrophic bacteria. *Microbiol Rev* **60**:439-471.

Hardy JT, Crecelius EA, Antrim LD, Kiesser SL, Broadhurst VL, Boehm PD, Steinhauer WG & Coogan TH. (1990) Aquatic surface microlayer contamination in Chesapeake Bay. *Mar Chem* **28**:333-351.

Heider J & Schühle K. (2013) Anaerobic biodegradation of hydrocarbons including methane. In: Rosenberg E, DeLong EF, Lory S, Stackebrandt E & Thompson F (eds). *The Prokaryotes.* p.605-634. Springer-Verlag, Berlin, Heidelberg.

Jørgensen BB. (1982) Mineralization of organic matter in the sea bed - the role of sulphate reduction. *Nature*. **296**:643-645.

Joye SB, Teske AP & Kostka JE. (2014) Microbial dynamics following the Macondo oil well blowout across Gulf of Mexico environments. *BioScience* **64**:766-777.

Kemp WM, Boynton WR, Adolf JE*, et al.* (2005) Eutrophication of Chesapeake Bay: historical trends and ecological interactions. *Mar Ecol Prog Ser* **303**:1-29.

Kimes NE, Callaghan AV, Aktas DF, Smith WL, Sunner J, Golding BT, Drozdowska M, Hazen TC, Suflita JM & Morris PJ. (2013) Metagenomic analysis and metabolite profiling of deep-sea sediments from the Gulf of Mexico following the Deepwater Horizon oil spill. *Front Microbiol* **4**:1-17.

Kimes NE, Callaghan AV, Suflita JM & Morris PJ. (2014) Microbial transformation of the Deepwater Horizon oil spill—past, present, and future perspectives. *Front Microbiol* **5**:603.

King GM, Kostka JE, Hazen TC & Sobecky PA. (2015) Microbial responses to the Deepwater Horizon oil spill: from coastal wetlands to the deep sea. *Annu Rev Mar Sci* **7**:377-401.

King RS, Beaman JR, Whigham DF, Hines AH, Baker ME & Weller DE. (2004) Watershed land use is strongly linked to PCBs in white perch in Chesapeake Bay subestuaries. *Environ Sci Technol* **38**:6546-6552.

Leuthner B, Leutwein C, Schulz H, Hörth P, Haehnel W, Schiltz E, Schägger H & Heider J. (1998) Biochemical and genetic characterization of benzylsuccinate synthase from Thauera aromatica: a new glycyl radical enzyme catalysing the first step in anaerobic toluene metabolism. *Mol Microbiol* **28**:615-628.

Li W, Wang LY, Duan RY, Liu JF, Gu JD & Mu BZ. (2012) Microbial community characteristics of petroleum reservoir production water amended with n-alkanes and incubated under nitrate-, sulfate-reducing and methanogenic conditions. *Int Biodeterior Biodegradation* **69**:87-96.

Mbadinga SM, Li KP, Zhou L, Wang LY, Yang SZ, Liu JF, Gu JD & Mu BZ. (2012) Analysis of alkane-dependent methanogenic community derived from production water of a high-temperature petroleum reservoir. *Appl Microbiol Biotechnol* **96**:531-542.

McCune B, Grace JB & Urban DL. (2002) *Analysis of ecological communities*. Oregon, USA: MjM Software.

Michel J, Nixon Z, Dahlin J, Betenbaugh D, White M, Burton D & Turley S. (2009) Recovery of interior brackish marshes seven years after the Chalk Point oil spill. *Marine Poll Bull* **58**:995-1006.

Morgan C & Owens N. (2001) Benefits of water quality policies: the Chesapeake Bay. *Ecol Econ* **39**:271-284.

Müller AL, Kjeldsen KU, Rattei T, Pester M & Loy A. (2014). Phylogenetic and environmental diversity of DsrAB-type dissimilatory (bi)sulfite reductases. *ISME J* **9**:1152-1165.

Nakatsu CH & Marsh TL. (2007) Analysis of microbial communities with denaturing gradient gel electrophoresis and terminal restriction fragment length polymorphism. In: *Methods for General and Molecular Microbiology*. p. 909-923. ASM Press, Washington, D.C.

National Research Council, NRC. (2003) *Oil in the sea III: inputs, fates, and effects*. National Academies Press. Washington, D.C.

Newcombe CL, Horne WA & Shepherd BB. (1939) Studies on the physics and chemistry of estuarine waters in Chesapeake Bay. No. 21. Chesapeake Biological Laboratory.

Nunoura T, Oida H, Miyazaki J, Miyashita A, Imachi H & Takai K. (2008) Quantification of *mcrA* by fluorescent PCR in methanogenic and methanotrophic microbial communities. *FEMS Microbiol Ecol* **64**:240-247.

Officer CB, Biggs RB, Taft JL, Cronin LE, Tyler MA & Boynton WR. (1984) Chesapeake Bay anoxia: origin, development, and significance. *Science* **223**:22-27.

Okpokwasili G, Somerville C, Grimes D & Colwell R. (1984) Plasmid-associated phenathrene degradation by Chesapeake Bay sediment bacteria. *Actes de Colloques* **3**:601-610.

Op den Camp HJM, Islam T, Stott MB, Harhangi HR, Hynes A, Schouten S, Jetten MSM, Birkeland NK, Pol A & Dunfield PF. (2009) Environmental, genomic and taxonomic perspectives on methanotrophic Verrucomicrobia. *Environ Microbiol Rep* **1**:293-306.

Operational Science Advisory Ream, OSAT-I. (2010) S*ummary report for sub-sea and sub-surface oil and dispersant detection: sampling and monitoring*.

http://www.dep.state.fl.us/deepwaterhorizon/files2/osat'report'17dec.pdf (1st July 2014, data last accessed).

Paolisso M, Trombley J, Hood RR & Sellner KG. (2015) Environmental models and public stakeholders in the Chesapeake Bay watershed. *Estuar Coast* **38**:97-113.

Penner TJ, Foght JM & Budwill K. (2010) Microbial diversity of western Canadian subsurface coal beds and methanogenic coal enrichment cultures. *Int J Coal Geol* **82**:81-93.

Pruesse E, Quast C, Knittel K, Fuchs BM, Ludwig W, Peplies J & Glöckner FO. (2007) SILVA: a comprehensive online resource for quality checked and aligned ribosomal RNA sequence data compatible with ARB. *Nucleic Acids Res* **35**:7188-7196.

Rabus R, Nordhaus R, Ludwig W & Widdel F. (1993) Complete oxidation of toluene under strictly anoxic conditions by a new sulfate-reducing bacterium. *Appl Environ Microbiol* **59**:1444-1451.

Ramseur JL. (2010) *Deepwater Horizon oil spill: the fate of the oil*. Congressional Research Service, Washington, D.C. Congressional Research Service Report 7-5700. fas.org/spg/crs.misc.R41531.pdf.

Richardson RE. (2013) Genomic insights into organohalide respiration. *Curr Opin Biotechnol* **24**:498-505.

Siddique T, Penner T, Semple K & Foght JM. (2011) Anaerobic biodegradation of longer-chain n-alkanes coupled to methane production in oil sands tailings. *Environ Sci Technol* **45**:5892-5899.

So CM & Young LY. (1999) Isolation and characterization of a sulfate-reducing bacterium that anaerobically degrades alkanes. *Appl Environ Microbiol* **65**:2969-2976.

Taft JL, Taylor WR, Hartwig EO & Loftus R. (1980) Seasonal oxygen depletion in Chesapeake Bay. *Estuaries* **3**:242-247.

Tan B, Dong X, Sensen CW & Foght J. (2013) Metagenomic analysis of an anaerobic alkane-degrading microbial culture: potential hydrocarbon-activating pathways and inferred roles of community members. *Genome* **56**:599-611.

Tan B, Nesbø C & Foght J. (2014) Re-analysis of omics data indicates Smithella may degrade alkanes by addition to fumarate under methanogenic conditions. *ISME J* **8**:2353-2356.

Tanner RS. (1997) Cultivation of Bacteria and Fungi. In: Hurst CJ, McInerney MJ, Stetzenbach LD, *et al*., (eds). *Manual of Environmental Microbiology*. p.69-78. Washington, DC: ASM Press.

Turner S, Pryer KM, Miao VPW & Palmer JD. (1999) Investigating deep phylogenetic relationships among cyanobacteria and plastids by small subunit rRNA sequence analysis. *J Eukaryot Microbiol* **46**:327-338.

von Netzer F, Pilloni G, Kleindienst S, Krüger M, Knittel K, Gründger F & Lueders T. (2013) Enhanced gene detection sssays for fumarate-adding enzymes allow uncovering of anaerobic hydrocarbon degraders in terrestrial and marine systems. *Appl Environ Microbiol* **79**:543-552.

Walker JD & Colwell RR. (1973) Microbial ecology of petroleum utilization in Chesapeake Bay. *Int Oil Spill Conf Proc*. Vol. 1973, 685-690.

Walker JD, Colwell RR, Hamming MC & Ford HT. (1975a) Extraction of petroleum hydrocarbons from oil-contaminated sediments. *Bull Environ Contam Toxicol* **13**:245-248.

Walker JD, Colwell RR, Hamming MC & Ford HT. (1975b) Petroleum hydrocarbons in Baltimore Harbour of Chesapeake Bay: distribution in sediment cores. *Environ Poll* **9**:231-238.

Walker JD, Colwell RR & Petrakis L. (1976a) Biodegradation of petroleum by Chesapeake Bay sediment bacteria. *Can J Microbiol* **22**:423-428.

Walker JD, Petrakis L & Colwell RR. (1976b) Comparison of the biodegradability of crude and fuel oils. *Can J Microbiol* **22**:598-602.

Walker WJ, McNutt RP & Maslanka CK. (1999) The potential contribution of urban runoff to surface sediments of the Passaic River: sources and chemical characteristics. *Chemosphere* **38**:363-377.

Wang LY, Li W, Mbadinga SM, Liu JF, Gu JD & Mu BZ. (2012) Methanogenic microbial community composition of oily sludge and its enrichment amended with alkanes incubated for over 500 days. *Geomicrobiol J* **29**:716-726.

Wawrik B, Mendivelso M, Parisi VA, Suflita JM, Davidova IA, Marks CM, Van Nostrand JD, Liang Y, Zhou J, Huizinga BJ, Strąpoć D, & Callaghan AV. (2012) Field and laboratory studies on the bioconversion of coal to methane in the San Juan Basin. *FEMS Microbiol Ecol* **81**:26-42.

Webber DB. (1983) Aerial flux of particulate hydrocarbons to the Chesapeake Bay estuary. *Mar Poll Bull* **14**:416-421.

Weisburg WG, Barns SM, Pelletier DA & Lane DJ. (1991) 16S Ribosomal DNA amplification for phylogenetic study. *J Bacteriol* **173**:697-703.

West PA, Okpokwasili GC, Brayton PR, Grimes DJ & Colwell RR. (1984) Numerical taxonomy of phenanthrene-degrading bacteria isolated from the Chesapeake Bay. *Appl Environ Microbiol* **48**:988-993.

Widdel F & Bak F. (1992) Gram-negative mesophilic sulfate-reducing bacteria. In: Balows A, Trüper HG, Dworkin M, *et al*., (eds). *The Prokaryotes: A Handbook on the Biology of Bacteria: Ecophysiology, Isolation, Identification, Applications.* p.3352-3378. Springer-Verlag, New York.

Zhou L, Li KP, Mbadinga SM, Yang SZ, Gu JD & Mu BZ. (2012) Analyses of n-alkanes degrading community dynamics of a high-temperature methanogenic consortium enriched from production water of a petroleum reservoir by a combination of molecular techniques. *Ecotoxicology* **21**:1680-1691.

Chapter 2. Impact of Photolyzed Macondo (MC252) Crude Oil and Polycyclic Aromatic Hydrocarbons (PAHs) on Indigenous Sulfate-Reducing Microorganisms in Coastal Gulf of Mexico Sediments.

ABSTRACT

Photooxidation is an important process contributing to the fate of crude oil in marine systems and can have a significant impact on the bioavailability of crude oil components to indigenous microbial communities. Sulfate-reducing bacteria (SRB) play an important role in carbon mineralization in the marine environment and are known to mediate hydrocarbon transformation processes. Determining the impact of photolyzed oil-derived compounds on SRB is important with regard to predicting the fate of crude oil in marine ecosystems. It was hypothesized that water-soluble products generated from the photolysis of Macondo (MC252) crude oil, as well as individual oil components, would inhibit the activity of indigenous Gulf of Mexico (GoM) sulfate-reducing microorganisms. Sediments were collected from three GoM locations on the coast of Biloxi, Mississippi. The impact of aqueous extracts of photolyzed source oil and individual polycyclic aromatic hydrocarbons (PAHs) was assessed via $^{35}SO_4$-reduction assays (SRAs) in sediment slurries amended with varying concentrations of extracts (0.1 - 50%, v/v). Sediment microbial communities were investigated via DNA extraction and 16S rRNA gene sequencing, which revealed that Deltaproteobacteria populations at each location were distinct. Individual SRA experiments exhibited significant increases, significant decreases, or no significant differences in sulfate

reduction rates (SRRs) of populations exposed to photooxidized hydrocarbons compared to baseline SRRs. No clear trend was observed of an effect from exposure to photogenerated products with regard to site, substrate, or irradiation treatment. These data suggest that photolyzed oil is not likely to have an overall negative impact on sulfate-reducing microbial communities in coastal GoM sediments.

INTRODUCTION

The explosion of the Deepwater Horizon (DWH) rig, blowout of the Macondo well, and subsequent discharge from the wellhead released an estimated 4.9 million barrels (McNutt *et al.*, 2011, McNutt *et al.*, 2012) of Mississippi Canyon Block 252 (MC252) crude oil into the GoM. Once introduced into the environment, crude oil is transformed via weathering through processes such as evaporation, dissolution, emulsification, and photooxidation. Photooxidation is one of the main processes affecting crude oil in marine environments (Payne & Phillips, 1985, Nicodem *et al.*, 1997, Tarr *et al.*, 2016). Numerous studies have shown that photochemical transformation of petroleum results in increased molecular oxygen content, and common photogenerated products include acids, alcohols, phenols, ketones, and esters (Hansen, 1975, Barth, 1984, Maki *et al.*, 2001, Lee, 2003). An increase in oxygen content in oil constituents was observed with oil released during the DWH event. Ray *et al* (2014) demonstrated that photochemical transformation of MC252 crude oil led

to increased oxygenation of parent compounds and an increase in water solubility of the photogenerated products. Additionally, Aeppli *et al* (2012) concluded that oxygenation of DWH hydrocarbon residues occurred in the environment and that the generated 'oxyhydrocarbons' represented a substantial portion of the mass of weathered oil. This finding has been further documented in a number of studies focusing on DWH-related oil (Hall *et al.*, 2013, Radović *et al.*, 2014, Ruddy *et al.*, 2014). Several studies have characterized weathered MC252 oil samples and have identified a number of oxygenated-derivatives of oil constituents, such as carboxylic acids, ketones, and alcohols (Aeppli *et al.,* 2012, Ray *et al.*, 2014, Ruddy *et al.*, 2014).

PAHs comprised only a small fraction of released MC252 oil (<2%; (Reddy *et al.*, 2012)), but these compounds pose an environmental and health risk due to their toxic and carcinogenic properties. Photochemical transformation of PAHs can result in increased solubility and therefore, higher levels of toxicity compared to parent compounds. Oxygenated PAH-derivatives are often identified as photoproducts of PAH photooxidation, including pyrenequinones (Sigman *et al.*, 1998) and phenanthrenequinone, which has been shown to be toxic to bacteria and aquatic plants (McConkey *et al.*, 1997). Additionally, photooxidation of anthracene has been shown to produce a variety of different types of photoproducts, including phenols, benzoic acids, anthraquinones, and benzaldehydes (Mallakin *et al.*, 2000).

Past studies have demonstrated increased toxicity of photooxidized crude oil and of photooxidized PAHs to a range of organisms. These studies

have been carried out using microbes, aquatic plants, as well as invertebrates and vertebrates, including bivalves, mysid shrimp, copepods, and a variety of fish species (Oris & Giesy, 1985, Gala & Giesy, 1992, Arfsten *et al.*, 1996, McConkey *et al.*, 1997, Pelletier *et al.*, 1997, Duesterloh *et al.*, 2002). Due to the severity of the DWH spill, extensive research was carried out on the effects of crude and weathered MC252 oil (Barron, 2012, de Soysa, 2012, Finch *et al.*, 2012, Lin & Mendelssohn, 2012, Whitehead *et al.*, 2012, Dubansky *et al.*, 2013, Incardona *et al.*, 2014, Alloy *et al.*, 2016, Beyer *et al.*, 2016, Esbaugh *et al.*, 2016, Langdon *et al.*, 2016, Pasparakis *et al.*, 2016, Stefansson *et al.*, 2016). Many of these studies were focused on higher trophic level organisms, and overall, concluded that negative impacts of crude and weathered MC252 oil occurred in a number of species. Studies on lower trophic level organisms have also found that irradiation of MC252 crude oil or a MC252 surrogate oil can increase toxic effects on zooplankton (Almeda *et al.*, 2013), phytoplankton (Paul *et al.*, 2013), and pure cultures of aerobic bacteria (i.e., *Vibrio fischeri* via Microtox® assays) (King *et al.*, 2011, Paul *et al.*, 2013, King *et al.*, 2014). However, little is known about how indigenous microbial communities are affected by photogenerated products.

Anaerobic microorganisms, particularly SRB, play a crucial role in marine carbon cycling (Jørgensen, 1982), and these microorganisms can function as key players in hydrocarbon transformation processes (Coates *et al.*, 1997, Heider *et al.*, 1998, Kniemeyer *et al.*, 2007, Musat *et al.*, 2009). Many sulfate-reducers have a wide substrate range, not only capable of utilizing a variety of

hydrocarbons, including PAHs (Coates *et al.*, 1997, Galushko *et al.*, 1999, Meckenstock *et al.*, 2016), but also other types of compounds, such as organic acids and alcohols (Rabus *et al.*, 2006). It is unclear what, if any, effect weathered oil has on indigenous sulfate-reducing populations in GoM ecosystems. However, given the significant role that SRB have in petroleum biodegradation and transformation in the environment, as well as the potential for increased toxicity of photooxidized compounds, the impact of these photogenerated products on SRB populations warrants further study. An understanding of how indigenous anaerobic microbial communities respond to weathered oil is needed in order to fully recognize the ultimate fate of residual oil along the Gulf Coast. Therefore, the aim of this study was to investigate the impact that photolyzed oil and PAHs have on native sulfate-reducing populations in GoM coastal regions. It was hypothesized that water-soluble compounds generated from irradiation of MC252 crude oil and individual PAHs would inhibit activity of indigenous sulfate-reducing microorganisms in GoM sediments.

MATERIALS & METHODS

Sample Collection. Three locations were sampled on the coast of Biloxi, Mississippi in August 2013 (Table S1). These sites had no visible oil contamination. Surface water, defined here as water collected just offshore while aboard the sampling vessel, was collected via pumping seawater through

Tygon® tubing into 10-L acid-washed, sterile carboys (Bel-Art, Wayne, NJ, USA) for on-site analyses. Additional samples of surface water and water overlying sediments, defined here as water collected onshore that overlaid sediments, were collected and immediately placed on dry ice for subsequent laboratory analyses. Onshore sediment samples (i.e., time-zero, T-0) at each site were collected at depths of approximately 12-17 cm below the surface using an ethanol-sterilized hand shovel. Two 2-L-polypropylene wide mouth bottles (VWR®, Radnor, PA, USA) were filled with sediment and overlying water (denoted as Jars A and B) at each site. Sediment and seawater collection containers were transported on ice and subsequently stored at 4°C in the laboratory until use. Four replicates of sediment were collected at each location (ca. 1 cm^3), placed in MO BIO PowerSoil® Bead Tubes (MO BIO, Carlsbad, CA, USA) on-site, immediately stored on dry ice for transport, and stored at -80°C in the laboratory until extraction.

Water Analysis. Redox potential, pH, and temperature of surface waters were measured on-site using an OAKTON pH 11 series meter (OAKTON Instruments, Vernon Hills, IL, USA). Surface water salinity (ppt, parts per thousand) was also measured on-site using a salt refractometer (Sper Scientific Ltd, Scottsdale, AZ, USA). Four replicate samples of surface water and water overlying onshore sediments collected from each site were filtered with a 0.2 µm PTFE-membrane syringe filter (VWR®, Radnor, PA, USA) to remove particulates and diluted fifty-fold in deionized water prior to ion chromatography. Chloride, nitrate, nitrite, and sulfate were measured via anion exchange

chromatography using a Dionex ICS-1100 (Dionex, Sunnydale, CA, USA) equipped with an IonPac AS23 column, an eluent of 4.5 mM Na_2CO_3 and 0.8 mM $NaHCO_3$, and a flow rate of 1 mL min^{-1}.

A colorimetric assay was also used to measure nitrate and nitrite concentrations in collected water samples (Miranda *et al.*, 2001). Sodium nitrate ($NaNO_3$) and sodium nitrite ($NaNO_2$) standards (1-1000 µM) were established in duplicate. All samples and standards were incubated for 25 minutes before absorbance was measured at 535 nm using a Unico® 1000 spectrophotometer (UNICO, Dayton, NJ, USA). Phosphate concentrations in water samples were measured colorimetrically (Zimmermann & Keefe, 1997). Sodium phosphate ($NaPO_4$) standards (1-1000 µM) were prepared in duplicate, and orthophosphate concentrations were measured at 880 nm on a Unico 1000 spectrophotometer (UNICO, Dayton, NJ, USA).

DNA Extraction. Community genomic DNA from sediments collected on-site was extracted using a MO BIO PowerSoil® DNA Isolation Kit (MO BIO, Carlsbad, CA, USA) according to manufacturer's instructions, and DNA was quantified using a Qubit® 2.0 Fluorometer and Qubit® dsDNA BR Assay Kit (Life Technologies, Grand Island, NY, USA). SRA sediment samples collected at the time of each SRA set up (see "*Assessment via SRAs*") were extracted and quantified using the same methods described for field samples.

Microbial Community Analysis. Genomic DNA extracted from sediments was used for sequencing to survey indigenous microbial populations. Partial bacterial and archaeal 16S rRNA genes were amplified using a 5' M13

tag on a universal 519F primer (5'-GTA AAA CGA CGG CCA GCA CMG CCC C-3') and with a universal Bac-785R reverse primer (5'-TAC NVG GGT ATC TAA TCC-3') as previously described (Wawrik *et al.*, 2012, Klindworth *et al.*, 2013). Amplification of 16S rRNA genes was first performed using 'untagged' forward and reverse primers. Total reaction volumes were 50 µl and contained 1 µl (100 µM stock) of forward and reverse 'untagged' primers, 25 µl of 2X PCR Master Mix (Life Technologies, Grand Island, NY, USA), and 2 µl of template (1:5 dilution). Thermocycler parameters were as follows: 95°C for 2 min, 30 cycles of 95°C for 30 s, 55°C for 1 min, and 72°C for 1.5 min, and a final 72°C extension step for 10 min. PCR products were purified using QIAGEN QIAquick PCR Purification Kit (Qiagen, Valencia, CA, USA) according to the manufacturer's protocol. Subsequently, PCR products were 'tagged' by addition of Illumina barcode sequences. Reactions were performed in 30-µl volumes and contained 15 µl of 2X PCR Master Mix (Life Technologies, Grand Island, NY, USA), 0.15 µl (100 µM stock) of 'untagged' 785R primer, 1 µl (10 µM stock) of 'tagged' forward primer, and 2 µl of cleaned PCR product. Thermocycler conditions were performed as described above for six cycles. Both 'tagged' and 'untagged' products were visualized via gel electrophoresis to ensure efficient amplification reactions. Equal volumes of barcoded PCR products were combined and cleaned as described above in preparation for sequencing. Samples were sequenced via Illumina MiSeq 300v2 at Oklahoma Medical Research Foundation (Oklahoma City, OK, USA). Samples collected in the field

nd samples collected at the time of SRA set-up were identically prepared and sequenced during two separate MiSeq runs.

Sequence Analysis. Sequencing reads were analyzed with QIIME (Version 1.9.0) (Caporaso *et al.*, 2010a). Each of the separate Illumina MiSeq runs, hereafter referred to as T-0 or SRA, were analyzed using identical methods. Individual sample libraries were demultiplexed via barcodes, and a similarity cut-off of 97% was used to group reads into operational taxonomic units (OTUs). Sequences were aligned using the SILVA reference database (Pruesse *et al.*, 2007) and PYNAST (Caporaso *et al.*, 2010b). Taxa frequency data were arcsine-square root transformed prior to statistical analyses and comparisons. T-tests were used to determine significant differences between samples using a two-tailed distribution and equal sample variance. Deltaproteobacterial taxa were further analyzed to compare populations among sites. Non-metric multidimensional scaling (NMDS) was utilized to assess community grouping patterns among sampling locations using a Bray-Curtis distance measure, 1000 runs with actual data, 1000 runs with randomized versions of the data, two ordination axes, and orthogonal principal axis rotation. NMDS analysis was repeated multiple times with identical parameters to ensure that the lowest stress value (i.e., the best fit of the data) was achieved and that consistent results were obtained. A multi-response permutational procedure (MRPP) was also conducted using a Bray-Curtis distance measure (McCune *et al.*, 2002), and diversity (e.g., Shannon and Simpson indices), richness, and

evenness were calculated. NMDS, MRPP, and descriptive statistics were all conducted using PC-ORD (Version 6, MjM Software).

Photolysis. Photolysis was carried out by layering the compound(s) on water (see below) in a jacketed beaker, covering with quartz glass to prevent evaporation, and irradiating at 27°C for 12 hours using an Atlas CPS+ solar simulator. The solar simulator was operated at 1.3 times solar noon intensity, at which 12 hours is equivalent to approximately three days of sunlight in the northern GoM. Irradiation treatments were set up in triplicate. A total of 750 mL of water was subsequently separated from the hydrocarbon layer, filtered (0.45 µm), and frozen until use in SRA experiments. Dark (non-photolyzed) treatments were generated using the same method without exposure to the solar simulator. Whole oil and PAH photolysis experiments were conducted as follows. For source oil, 307 µl of MC252 source oil was placed on the surface of filtered (0.2 µm) GoM seawater. Pyrene extracts were generated by mixing 1 mL of a 48 µM pyrene stock in a toluene/tetradecane carrier phase with 5 mL of hexane and allowing toluene/hexane to evaporate, resulting in a hydrocarbon film of approximately 750 µl on the surface of deionized water. Anthracene and anthracene/phenanthrene mix treatments were generated in the same manner, with 1 mL of 74 µM anthracene in a toluene/tetradecane carrier and with 1 mL of 63 µM anthracene/255 µm phenanthrene in a toluene/tetradecane carrier, respectively.

Assessment via Sulfate Reduction Assays (SRAs). Previous studies focused on microbial toxicity of weathered oil have been conducted using

Microtox® assays. Here, SRAs using a ^{35}S-radiotracer were conducted to determine the effects of photolyzed and non-photolyzed compounds on endogenous rates of sulfate reduction in coastal sediments collected from the three sites. Incubations were established in 120 mL serum bottles in an anaerobic chamber under N_2:H_2 (95:5) with 10 g sediment and a total volume of 10 mL, which included seawater and the different concentrations of irradiated or non-irradiated aqueous extracts. Sediment was first homogenized in an attempt to control variability between bottles by placing it in a sterile beaker and continuously stirring in the anaerobic chamber during set-up (with the exception of Site 1 source oil incubations). Bottles were sealed with butyl rubber stoppers, closed with aluminum crimp seals, and the headspace aseptically flushed three times with N_2:CO_2 (80:20) after removal from the chamber. Experimental controls were established in triplicate and included an endogenous incubation containing sediment and seawater (i.e., baseline), a positive control with a lactate amendment (2 mM), and a sterile control of autoclaved sediment and seawater. Based on preliminary experiments, amendments of 1%, 2%, and 5% (v/v) of photolyzed or non-photolyzed aqueous extracts were initially added to incubations. Subsequently, experiments were conducted using a wider range of amendment concentrations, including 0.1%, 1%, 2%, 5%, 10%, and 50% (v/v). In the case of MC252 source oil incubations, 100% treatments were also set up. This concentration was not tested with individual PAHs as these compounds were photolyzed using deionized water, and no sulfate was present. All experimental SRAs were set up in triplicate. Amendments containing source oil

and pyrene were established using sediments from Jar A at each of the three sites, whereas anthracene and anthracene/phenanthrene mix incubations were established using sediments from Jar B. Sediment and water were collected at the time of each SRA set-up and stored at -20°C until further analysis. For sediment, four replicates (ca. 1 cm^3) were placed in MO BIO PowerSoil® tubes (MO BIO, Carlsbad, CA, USA) for DNA extraction and subsequent 16S rRNA gene sequencing to assess microbial communities shifts during storage (i.e., sediment was kept at 4°C for several months as different SRAs were established) (see "*Microbial Community Analysis*"). As mentioned above, the overlying water was analyzed for sulfate via ion chromatography (see "*Water Analysis*"). These sulfate concentrations were used in SRR calculations.

SRAs were performed as described by Ulrich *et al* (1997) with modifications described here. Additions of ^{35}S-radiotracer were amended to each bottle in 100 µl volumes, and incubations were stored at room temperature in the dark for six to seven days. Sulfide traps were placed in bottles after the approximate week-long incubation period as follows: serum bottles were placed in an anaerobic chamber, un-stoppered, and a 12x75 mm borosilicate glass test tube was added. Anoxic zinc acetate (4% solution) was added to each test tube (2 mL) to precipitate any ^{35}S by-products generated through sulfate reduction. Bottles were then stoppered, sealed, and removed from the chamber. Anoxic Cr(II)-HCl (4 mL) and anoxic 12 N HCl (4 mL) were syringe-injected into each bottle, and bottles were placed on a rotary shaker (~60 rpm) for three days. Sulfide traps were subsequently removed, and the zinc acetate solution

homogenized using a combination of pipetting and sonication. Half of the homogenized solution (1 mL) was removed, placed in a scintillation vial, and mixed with 5 mL of Ultima Gold LSC-scintillation fluid (PerkinElmer, Waltham, MA, USA). Decomposition per minute (dpm) was recorded using a Hidex Triathler liquid scintillation counter (Hidex Oy, Turku, Finland). Rates of sulfate reduction were calculated by measuring the amount of radiolabel counted in zinc acetate traps, the total radiolabel initially added to bottles, and the amount of non-labeled sulfate that was present in the incubations. Rates are reported as averages of triplicates and are presented as a percent increase or decrease compared to endogenous (i.e., baseline) rates.

RESULTS

Water Analysis. Measurements of salinity, as well as sulfate concentrations, indicated that Site 1 and Site 3 were similar to each other and more typical of a brackish coastal environment. Salinities were 13 ppt and 10 ppt (Table S2) for Site 1 and Site 3, respectively. Sulfate ranged from 7.83 ± 0.04 mM to 9.42 ± 0.04 mM for these locations (Table S3). In contrast, Site 2 had a higher salinity of 26 ppt (Table S2) and higher sulfate, ranging from 16.58 ± 0.05 mM to 19.47 ± 0.06 mM (Table S3). Nitrate and nitrite were below detection limits in all samples via ion chromatography. Nitrate was detected colorimetrically in only one sample at a concentration of 0.01 ± 0.009 mM in surface water at Site 1 (Table S3). No nitrite was detected in any of the tested

samples. Phosphate concentrations ranged from 0.018 ± 0.01 mM to 0.07 ± 0.002 mM across the three sites (Table S3).

Microbial Community Analysis. Genomic DNA was extracted from time-zero (T-0) sediment samples, and partial 16S rRNA genes were sequenced to compare phylogenetic compositions of communities among sites. Of particular interest were the Deltaproteobacteria, as this taxa contains many sulfate-reducing genera. Relative abundances of Deltaproteobacteria varied among sites (Table S4). Sediment from Site 1 (Jar A: 7.31% ± 0.17%, Jar B: 4.43% ± 0.18%) and Site 3 (Jar A: 12.24% ± 0.49%, Jar B: 7.82% ± 2.55%) had significantly higher relative abundances than Site 2 sediment (Jar A: 2.54% ± 0.22%, Jar B: 2.40% ± 0.12%) ($p \leq 0.03$). The Deltaproteobacteria communities also varied in overall composition among sites (Figure 1, Tables S5, S6, S7, S8, and S9), but multiple taxa were consistently present and relatively abundant among all locations/jars, including *Desulfonauticus*, Desulfobacteraceae Sva0081 sediment group, and uncharacterized Sh765B-TzT-29 (Tables S7, S8, and S9).

Additional sediment samples were collected (ca. 1 cm^3, four replicates) at the time that each SRA was established to monitor whether community shifts occurred during sediment storage. At Site 1, the relative abundance of Deltaproteobacteria did not show significant changes in Jar A (Table S10), whereas there was a significant increase in Jar B, as abundances increased from 4.43% ± 0.18% of the total population in the T-0 sample to 5.42% ± 0.15% in anthracene/phenanthrene mix SRA samples ($p = 3.01E-04$) (Table S10). In

contrast, Site 2 Jar A sediment significantly decreased at the time pyrene incubations were established from 2.54% ± 0.22% to 1.33% ± 0.22% (p = 5.49E-04) (Table S10). Anthracene/phenanthrene mix SRA samples for Site 2 had significantly higher Deltaproteobacteria, increasing from a total of 2.40% ± 0.12% in the T-0 sample to 5.81% ± 0.77% at the time of SRA set-up (p = 1.31E-03) (Table S10). Deltaproteobacteria in Jar A sediment from Site 3 showed a general decrease in relative abundance with time, significantly decreasing to 10.05% ± 0.62% (p = 8.13E-03) for the 50% oil SRA samples and to 8.49% ± 1.99% (p = 0.04) for pyrene SRA samples (Table S10). Similarly as in Jar B from Sites 1 and 2, an increase in the abundance of Deltaproteobacteria was observed in Site 3 Jar B, increasing from 7.82% ± 2.55% in the T-0 sample to 11.42% ± 0.90% (p = 0.08) in the anthracene SRA samples and to 12.07% ± 0.69% (p = 0.04) in the anthracene/phenanthrene mix SRA samples (Table S10).

The relative abundances of Deltaproteobacteria were not consistently significantly different between T-0 and SRA samples in all cases, although shifts in microbial communities were observed within deltaproteobacterial taxa among all sites (Figure S1). These shifts occurred to varying degrees, and the deltaproteobacterial taxa present differed among individual samples (Figures S2, S3, and S4, Table S11). *Desulfonauticus* was present in all T-0 sediment samples ranging from 4.54% ± 0.64% to 15.17% ± 0.36% of total Deltaproteobacteria (Figures S2, S3, and S4, Tables S7, S8, S9). However, this group was not abundant in any of the SRA samples among any of the three

locations (Figures S2, S3, and S4, Table S11). Nitrospinaceae abundance generally increased during storage (e.g., Site 1, Jar B) (Figures S2, S3, and S4, Table S11), as did environmental groups such as Sh765B-TzT-29 (e.g., Site 2, Jar A), Desulfobacteraceae Sva0081 sediment group (e.g., Site 3, Jar B), and Desulfobacteraceae SEEP-SRB1 (e.g., Site 1, Jar A) (Figures S2, S3, and S4, Table S11). *Desulfopila*, *Desulfobacula*, and *Desulfofaba* also typically increased in relative abundance within SRA samples (e.g., Site 2, Jar B) (Figure S3, Table S11). NMDS ordination confirmed that shifts occurred among overall Deltaproteobacteria populations (Figure S1). However, grouping patterns indicated that within-site communities were generally similar to T-0 samples even as shifts occurred, and that Site 2 sediment appeared to have the largest changes in deltaproteobacterial community composition (Figure S1). Non-deltaproteobacterial sulfate-reducing lineages (e.g., *Archaeoglobus*, *Desulfotomacalum*, *Desulfosporosinus*) (Muyzer & Stams, 2008) were not abundant in T-0 or SRA sediment samples (data not shown).

Sulfate Reduction Assays (SRAs). Sulfate reduction assays using a ^{35}S radiotracer were used to assess potential impacts of photolyzed compounds on endogenous sulfate reduction rates. SRAs were established using dark (non-photolyzed) versus irradiated (photolyzed) MC252 source oil, pyrene, anthracene, and an anthracene/phenanthrene mix. Individual treatments showed significant increases, significant decreases, or had no significant differences compared to baseline rates (Figure 2, Tables S12, S13, and S14). For Site 1, incubations amended with source oil exhibited a significant increase

in the 5% irradiated treatment compared to the endogenous SRR ($p = 0.04$), whereas a significant decrease was seen in the 0.1% irradiation treatment ($p = 0.05$) (Figure 2A, Table S12). For other tested compounds at Site 1, both increases and decreases in SRRs occurred, although no clear trend was observed with regard to significant differences compared to baseline controls (Figure 2, Table S12). Overall, the source oil SRAs for Site 2 and Site 3 did not demonstrate significant differences for dark or irradiated treatments across the range of tested concentrations, with the exception of the 100% dark treatment at Site 2, which showed a decrease compared to baseline rates ($p = 0.04$) (Figure 2A, Table S13), and the 100% amendment at Site 3, which was significantly higher relative to the endogenous rate ($p = 0.02$) (Figure 2A, Table S14). Incubations using dark or photolyzed pyrene, as well as anthracene assays, again indicated that there were increases or decreases among individual treatments, but no significant trend was seen (Figure 2, Tables S12, S13, and S14). It should be noted that in some treatments, the positive control amended with lactate did not show a significant increase (e.g., Site 1 with anthracene; Site 2 with pyrene; Site 2 with anthracene) (Figure 2, Tables S12 and S13).

DISCUSSION

Photooxidation and biodegradation are major processes that govern the fate of oil in marine environments. Photooxidation alters the chemical

composition of oil, leading to generation of oxygenated compounds (Nicodem *et al.*, 1997, Tarr *et al.*, 2016). This can result in an increase in bioavailability and allow for greater biodegradation, but can also lead to enhanced toxicity of specific oil constituents (e.g., PAHs). As microbial-mediated transformation of hydrocarbons is central to the removal of petroleum from contaminated environments, it is crucial to understand the impact that photolyzed hydrocarbons have on native microbial communities. Anaerobic processes are of particular importance in coastal marshes, and, as SRB are key mediators in hydrocarbon remediation in anoxic systems (Aeckersberg *et al.*, 1991, Rueter *et al.*, 1994, Coates *et al.*, 1996, Coates *et al.*, 1997, Widdel & Rabus, 2001, Meckenstock *et al.*, 2004, Widdel *et al.*, 2010, Mbadinga *et al.*, 2011, Kleindienst *et al.*, 2014, Lueders, 2016), an understanding of the effect that photolyzed MC252 crude oil and PAHs have on indigenous sulfate-reducing communities in the GoM is needed to fully appreciate the impact the DWH spill had on the ecosystem. Therefore, the aim of this study was to determine whether irradiation of MC252 crude oil and PAHs would affect the indigenous sulfate-reducing communities in coastal GoM sediments. Sulfate reduction assays were used to evaluate the effects of these compounds by comparing baseline SRRs to rates in the presence of irradiated (photolyzed) or dark (non-photolyzed) compounds.

Microbial Community Analysis. Sulfate-reducing bacteria play a crucial role in marine environments due to their involvement in carbon cycling (Jørgensen, 1982), and their role in the natural attenuation of petroleum

contamination (Heider *et al.*, 1998, Kniemeyer *et al.*, 2007, Widdel *et al.*, 2010). Here, partial 16S rRNA genes were sequenced to inventory the sulfate-reducing communities present at each of the three sites and to monitor whether these communities shifted over the course of the experiment as sediment was stored. Deltaproteobacterial abundances in T-0 sediment samples were significantly higher at Site 1 and Site 3 than at Site 2 (Table S4), and the differences in overall Deltaproteobacteria abundance between sites likely explain the observed variations in baseline SRRs among the different sites (see "*SRA Assessments*" below) (Figure 2, Tables S12, S13, and S14). In addition to overall abundances, deltaproteobacterial taxa varied among sites, as indicated by the separate NMDS grouping patterns (Figure 1), and populations also varied somewhat between replicates from Jar A and Jar B, specifically at Site 1 (Figure 1). A number of taxa classified within the Desulfarculaceae, Desulfobacteraceae, and Desulfobulbaceae families were observed, as well as several environmental groups (e.g., Sh765B-TzT-29, Desulfobacteraceae Sva0081 sediment group, Desulfobacteraceae SEEP-SRB1) (Figures S2, S3, and S4, Table S11). These data are consistent with other studies, wherein members of these taxa, as well as the uncharacterized environmental groups, have been detected in a variety of marine and brackish environments (Knittel *et al.*, 2003, Li *et al.*, 2009, Siegert *et al.*, 2011, Sun *et al.*, 2013, Kleindienst *et al.*, 2014, Kuever *et al.*, 2015a, Kuever *et al.*, 2015b).

Given the number of treatments, controls, and replicates, all of the SRAs could not be established and monitored simultaneously, thus requiring that

sediment be stored until each SRA experiment was carried out. In order to determine that site sediment contained sulfate-reducing taxa at the time of each assay, sediment samples were collected each time an SRA experiment was set up, and partial 16S rRNA genes were sequenced to monitor potential community shifts. Changes in the relative abundances of Deltaproteobacteria were observed, as were shifts in the specific deltaproteobacterial taxa present (Figures S1, S2, S3, and S4, Table S11). Several trends were observed with regard to shifts in Deltaproteobacteria in the SRA sediment communities. Initial populations (i.e., T-0) at each of the three locations contained *Desulfonauticus* (Figures S2, S3, and S4, Tables S7, S8, and S9). However, this taxon was not abundant in any SRA sample (Figures S2, S3, and S4, Table S11). In contrast, several environmental taxa, including Sh765B-TzT-29, Desulfobacteraceae Sva0081 sediment group, and Desulfobacteraceae SEEP-SRB1 commonly increased in abundance in the SRA 16S rRNA gene libraries (Figures S2, S3, and S4, Table S11). Sva0081 and SEEP-SRB1 are classified as members of the Desulfobacteraceae family, a metabolically diverse group of sulfate-reducers with taxa capable of utilizing a wide range of substrates, including alcohols, organic acids, dicarboxylic acids, and hydrocarbons (Kuever, 2014). Previous research on Sva0081 has suggested that this group may play an important role in the oxidation of hydrogen and acetate in marine sediments (Dyksma, 2016), as it is widespread among different sediment environments (Ravenschlag *et al.*, 2000, Kleindienst, 2012, Wang *et al.*, 2013, Dyksma, 2016), whereas SEEP-SRB1 sequences are often detected at hydrocarbon

seeps (Kleindienst, 2012, Kleindienst *et al.*, 2014), where this taxa may be involved in anaerobic methane oxidation (Schreiber *et al.*, 2010) or also potentially in biodegradation of other types of hydrocarbons (Kleindienst, 2012). Changes in Deltaproteobacteria were further evident through NMDS ordination of T-0 and SRA populations, which revealed that shifts did occur, most notably within Site 2 communities (Figure S1), in which relatively large increases in Sh765B-TzT-29 (Jar A), *Desulfopila* (Jars A & B), *Desulfofaba* (Jars A & B), and *Desulfobacula* (Jar B) occurred (Figure S3). It should also be noted that changes to the native communities could explain the lack of stimulation in some of the positive lactate controls in SRA experiments (see "*SRA Assessments*" below) (Figure 2, Tables S12 and S13). However, decreases in overall metabolic activity of SRB cannot be ruled out, as several species within the detected genera are capable of utilizing lactate (Suzuki *et al.*, 2007, Gittel *et al.*, 2010, Kuever *et al.*, 2015c).

Sulfate Reduction Assay (SRA) Assessments. SRAs were utilized to monitor changes in SRRs to determine whether exposure to photogenerated products would have toxic effects (i.e., inhibition of SRR) or whether these compounds could potentially be utilized by sulfate-reducers (i.e., stimulation of SRR). Individual treatments showed inhibition, defined here as a significant decrease in SRR compared to baseline, stimulation, defined here as a significant increase in SRR, or no significant impact (Figure 2, Tables S12, S13, and S14). This holds true for each of the three sites sampled, each of the substrates tested, and for irradiation treatment. Although inhibition and

stimulation were seen in individual treatments, variability among all incubations led to the conclusion that the water-soluble photogenerated compounds did not have an overall significant impact on the activity of sulfate-reducing populations. Collectively, data presented here is in contrast to findings of other toxicity studies which have concluded that weathered MC252 oil products are toxic to a range of organisms (for review, see Barron, 2012, Beyer *et al.*, 2016). Many of these studies focused on higher trophic levels which could explain the discrepancy, although toxic effects of photooxidized MC252 oil have also been reported with microorganisms (King *et al.*, 2011, Paul *et al.*, 2013, King *et al.*, 2014).

The apparent lack of toxicity to microorganisms in these experiments compared to previous reports could potentially be due to differences in experimental approach. Previous studies on microbial toxicity of photolyzed MC252 oil have typically used Microtox® assays (King *et al.*, 2011, Paul *et al.*, 2013, King *et al.*, 2014), which measure changes to the luminescence of a single, aerobic species (i.e., *V*. *fischeri*) as a proxy for toxicity. In contrast, SRAs in this study were conducted with sediment slurries of anaerobic communities. It is possible that photogenerated products are toxic to individual sulfate-reducing species, whereas effects may not be observed at the community level as was assessed here. As many SRB are metabolically diverse (Rabus *et al.*, 2006), there is also the potential that some taxa can utilize photogenerated products, which could explain the stimulation seen among various treatments (Figure 2, Tables S12, S13, and S14). Information about the specific photogenerated

products present in the aqueous extracts used in these SRAs is needed in order to confirm what types of compounds were present and whether these compounds could be potentially used by SRB. This characterization was not conducted herein. However, Ray *et al* (2014) reported on the formation of oxygenated oil-derived compounds of MC252 crude oil after exposure to simulated sunlight using similar experimental parameters. Photoproducts were characterized via chemical functionalities, and were considered to be largely carboxylic acids, although other compound classes likely also formed from photooxidation, including ketone, aldehyde, alcohol, ether, and ester derivatives of parent compounds. These results suggest that these types of compounds were likely present within the aqueous extracts used in our SRA experiments.

The lack of toxicity could also be a result of limited bioavailability of the photogenerated compounds (e.g., due to either binding with sediment humic materials or as a result of the overall small volume of aqueous extracts amended to SRAs (amendments ranged from 5 µl to 5 mL)). The presence of dissolved humic materials has been shown to reduce PAH phototoxicity in fish and crustaceans (Oris *et al.*, 1990, Weinstein & Oris, 1999). Decreases were attributed largely to a lower availability of the compounds for uptake and bioaccumulation, and to a lesser extent, by attenuation of solar radiation (Oris *et al.*, 1990, Weinstein & Oris, 1999). However, these studies exposed the organisms to the parent PAH prior to irradiation, whereas microorganisms in this study were exposed directly to photogenerated products. It is therefore unclear what effect the presence of sediment may have had in these

incubations. Additionally, the lack of toxicity could potentially also be a result of the amount of photoproducts added to the incubations. Total organic carbon (TOC) measurements were not conducted herein. However, an increase in TOC was observed in aqueous extracts of irradiated MC252 oil generated using similar experimental parameters (Ray *et al.*, 2014).

CONCLUSION

The Deepwater Horizon spill was the largest accidental discharge of crude oil into a U.S. marine environment. Researchers responded rapidly, allowing this catastrophic spill to be studied in great detail with regard to the response of microbial communities and to the fate of the oil (for review, see Joye *et al.*, 2014, Kimes *et al.*, 2014, King *et al.*, 2015). Much of this work was focused on aerobic microbial communities in the water column, beaches, and coastal marshes (for review, see Joye *et al.*, 2014, Kimes *et al.*, 2014, King *et al.*, 2015). Little work has focused on how weathered Macondo oil would affect anaerobic microbial communities. Anaerobes, particularly sulfate-reducing bacteria, are critical to long-term hydrocarbon remediation in the environment. This study investigated the impact of photolyzed oil and PAHs on sulfate-reducing communities in coastal GoM sediments. Overall, significant inhibition of sulfate reduction activity was not observed as a result of exposure to photogenerated products, suggesting that the activity of indigenous anaerobic communities is not negatively impacted by deposition of weathered Macondo oil at coastal marshes or beaches. Stimulation of sulfate reduction in several individual incubations suggests that the water-soluble oil-derived photoproducts

could potentially be utilized by members of native communities. Use of these oil-derived compounds suggests that the anaerobic microbial populations in the GoM may function, not only in hydrocarbon remediation, but also potentially in degradation of weathered, oil-derived compounds. These findings highlight the metabolic resiliency of native microbes and provide further evidence that indigenous microorganisms play critical roles in transformation of contaminants and in the ultimate recovery of the GoM ecosystem.

FIGURES

Figure 1. Non-metric multidimensional scaling (NMDS) ordination of Deltaproteobacteria within field (i.e., T-0) sediment communities. NMDS plot was constructed in PC-ORD (Version 6, MjM Software) using a Bray-Curtis distance measure, rotated with orthogonal principal axes, and analyzed with 1000 permutations. Samples are labeled according to site and jar.

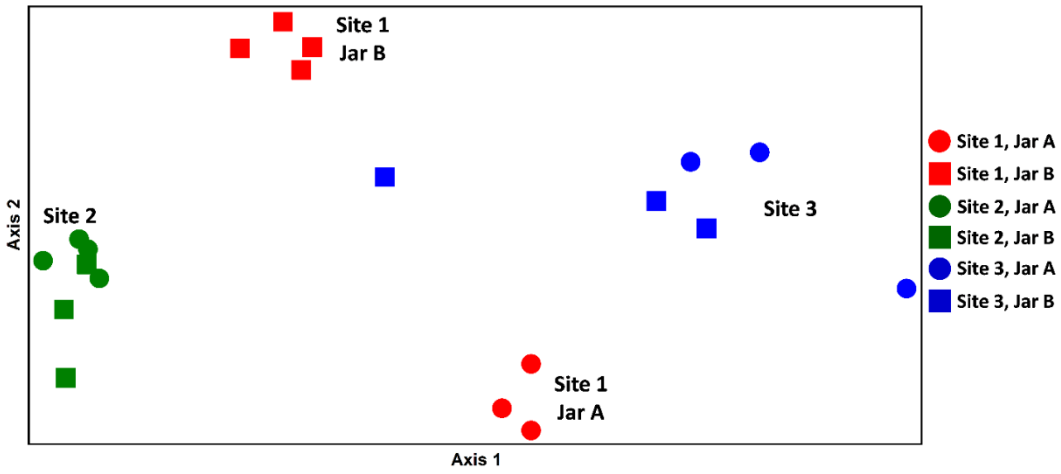

Figure 2. Sulfate reduction rates (SRRs) measured from SRA incubations with irradiated and non-irradiated (dark) **(A)** source oil, **(B)** pyrene, **(C)** anthracene and an **(D)** anthracene/phenanthrene mix. Each condition was set up in triplicate. In some cases, additional amendments were tested after initial incubations. In these instances, baseline controls were re-established each time a SRA was repeated. An asterisk (*) indicates a significant difference between endogenous sulfate reduction rates and an amendment, with a black asterisk (*) indicating a significant increase in SRR compared to baseline, and a red asterisk (*) signifying a significant decrease in SRR compared to baseline.

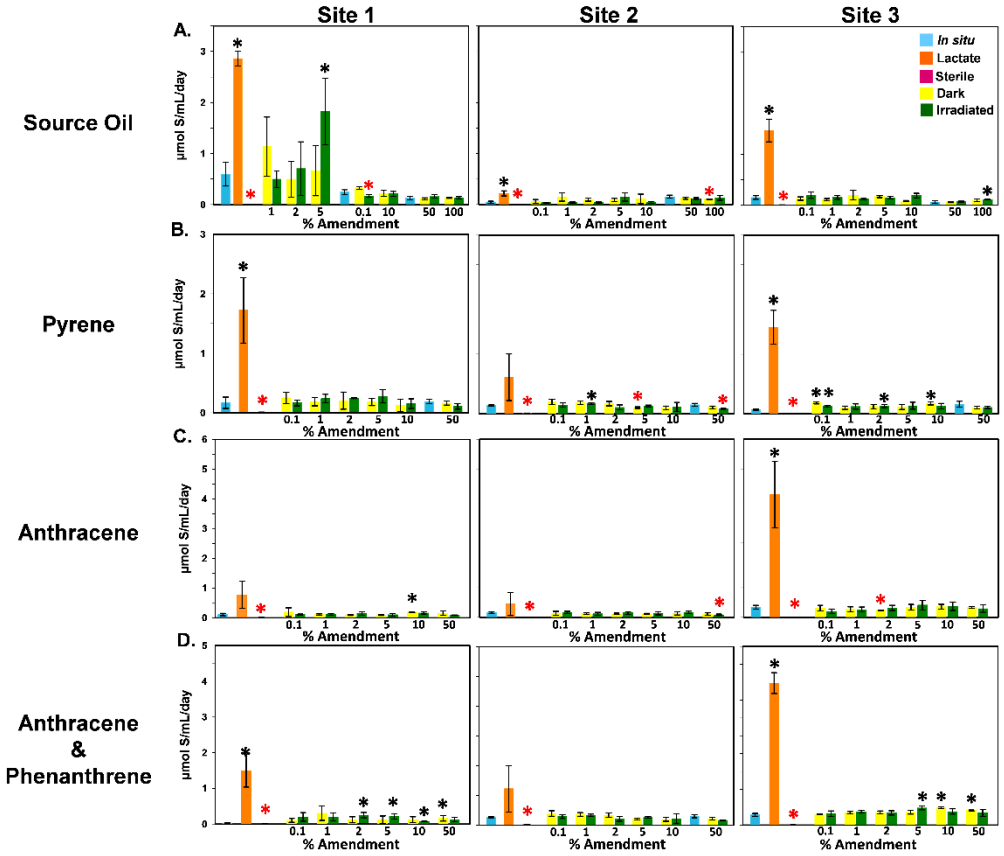

REFERENCES

Aeckersberg F, Bak F & Widdel F. (1991) Anaerobic oxidation of saturated hydrocarbons to CO_2 by a new type of sulfate-reducing bacterium. *Arch Microbiol* **156**:5-14.

Aeppli C, Carmichael CA, Nelson RK, Lemkau KL, Graham WM, Redmond MC, Valentine DL & Reddy CM. (2012) Oil weathering after the Deepwater Horizon disaster led to the formation of oxygenated residues. *Environ Sci Technol* **46**:8799-8807.

Alloy M, Garner TR, Bridges K, Mansfield C, Carney M, Forth H, Krasnec M, Lay C, Takeshita R, Morris J, Bonnot S, Oris J, & Roberts A. (2016) Co-exposure to sunlight enhances the toxicity of naturally weathered Deepwater Horizon oil to early lifestage red drum (Sciaenops ocellatus) and speckled seatrout (Cynoscion nebulosus). *Environ Toxicol Chem* **36**:780-785.

Almeda R, Wambaugh Z, Wang Z, Hyatt C, Liu Z & Buskey EJ. (2013) Interactions between zooplankton and crude oil: toxic effects and bioaccumulation of polycyclic aromatic hydrocarbons. *PLoS ONE* **8**(6):e67212.

Arfsten DP, Schaeffer DJ & Mulveny DC. (1996) The effects of near ultraviolet radiation on the toxic effects of polycyclic aromatic hydrocarbons in animals and plants: a review. *Ecotoxicol Environ Saf* **33**:1-24.

Barron MG. (2012) Ecological impacts of the Deepwater Horizon oil spill: implications for immunotoxicity. *Toxicol Pathol* **40**:315-320.

Barth T. (1984) Weathering of crude oil in natural marine environments: the concentration of polar degradation products in water under oil as measured in several field studies. *Chemosphere* **13**:67-86.

Beyer J, Trannum HC, Bakke T, Hodson PV & Collier TK. (2016) Environmental effects of the Deepwater Horizon oil spill: a review. *Marine Poll Bull* **110**:28-51.

Caporaso JG, Kuczynski J, Stombaugh J*, et al.* (2010a) QIIME allows analysis of high-throughput community sequencing data. *Nat Meth* **7**:335-336.

Caporaso JG, Bittinger K, Bushman FD, DeSantis TZ, Andersen GL & Knight R. (2010b) PyNAST: a flexible tool for aligning sequences to a template alignment. *Bioinformatics* **26**:266-267.

Coates JD, Anderson RT & Lovley DR. (1996) Oxidation of polycyclic aromatic hydrocarbons under sulfate-reducing conditions. *Appl Environ Microbiol* **62**:1099-1101.

Coates JD, Woodward J, Allen J, Philp P & Lovley DR. (1997) Anaerobic degradation of polycyclic aromatic hydrocarbons and alkanes in petroleum-contaminated marine harbor sediments. *Appl Environ Microbiol* **63**:3589-3593.

de Soysa TY, Ulrich A, Friedrich T, Pite D, Compton SL, Ok D, Bernardos RL, Downes GB, Hsieh S, Stein R, Lagdameo MC, Halvorsen K, Kesich LR, & Barresi MJF. (2012) Macondo crude oil from the Deepwater Horizon oil spill disrupts specific developmental processes during zebrafish embryogenesis. *BMC Biology* **10**:40.

Dubansky B, Whitehead A, Miller JT, Rice CD & Galvez F. (2013) Multitissue molecular, genomic, and developmental effects of the Deepwater Horizon oil spill on resident gulf killifish (Fundulus grandis). *Environ Sci Technol* **47**:5074-5082.

Duesterloh S, Short JW & Barron MG. (2002) Photoenhanced toxicity of weathered Alaska North Slope crude oil to the calanoid copepods Calanus marshallae and Metridia okhotensis. *Environ Sci Technol* **36**:3953-3959.

Dyksma S. (2016) Identification and activity of bacteria consuming key intermediates of the carbon and sulfur cycling in coastal sands. Thesis, University of Bremen, Bremen, Germany.

Esbaugh AJ, Mager EM, Stieglitz JD, Hoenig R, Brown TL, French BL, Linbo TL, Lay C, Forth H, Scholz NL, Incardona JP, Morris JM, Benetti DD, & Grosell M. (2016) The effects of weathering and chemical dispersion on Deepwater Horizon crude oil toxicity to mahi-mahi (Coryphaena hippurus) early life stages. *Sci Total Environ* **543, Part A**:644-651.

Finch BE, Wooten KJ, Faust DR & Smith PN. (2012) Embryotoxicity of mixtures of weathered crude oil collected from the Gulf of Mexico and Corexit 9500 in mallard ducks (Anas platyrhynchos). *Sci Total Environ* **426**:155-159.

Gala W & Giesy J. (1992) Photo-induced toxicity of anthracene to the green alga, Selenastrum capricornutum. *Arch Environ Contam Toxicol* **23**:316-323.

Galushko A, Minz D, Schink B & Widdel F. (1999) Anaerobic degradation of naphthalene by a pure culture of a novel type of marine sulphate-reducing bacterium. *Environ Microbiol* **1**:415-420.

Gittel A, Seidel M, Kuever J, Galushko AS, Cypionka H & Könneke M. (2010) Desulfopila inferna sp. nov., a sulfate-reducing bacterium isolated from the subsurface of a tidal sand-flat. *Int J Syst Evol Microbiol* **60**:1626-1630.

Hall GJ, Frysinger GS, Aeppli C, Carmichael CA, Gros J, Lemkau KL, Nelson RK & Reddy CM. (2013) Oxygenated weathering products of Deepwater Horizon oil come from surprising precursors. *Marine Poll Bull* **75**:140-149.

Hansen HP. (1975) Photochemical degradation of petroleum hydrocarbon surface films on seawater. *Mar Chem* **3**:183-195.

Heider J, Spormann AM, Beller HR & Widdel F. (1998) Anaerobic bacterial metabolism of hydrocarbons. *FEMS Microbiol Rev* **22**:459-473.

Incardona JP, Gardner LD, Linbo TL*, et al.* (2014) Deepwater Horizon crude oil impacts the developing hearts of large predatory pelagic fish. *Pro Natl Acad Sci* **111**:E1510-E1518.

Jørgensen BB. (1982) Mineralization of organic matter in the sea bed - the role of sulphate reduction. *Nature* **296**: 643-645.

Joye SB, Teske AP & Kostka JE. (2014) Microbial dynamics following the Macondo oil well blowout across Gulf of Mexico environments. *BioScience* **64**:766-777.

Kimes NE, Callaghan AV, Suflita JM & Morris PJ. (2014) Microbial transformation of the Deepwater Horizon oil spill – past, present, and future perspectives. *Front Microbiol* **5**:603.

King SM, Leaf PA & Tarr MA. (2011) Photochemistry of Deepwater Horizon oil. In: Benvenuto MA, Roberts-Kirchhoff ES, Murray MN, *et al* (eds). *It's All in the Water: Studies of Materials and Conditions in Fresh and Salt Water Bodies,* p. 81-95. ACS Press, Washington, D.C.

King SM, Leaf PA, Olson AC, Ray PZ & Tarr MA. (2014) Photolytic and photocatalytic degradation of surface oil from the Deepwater Horizon spill. *Chemosphere* **95**:415-422.

King GM, Kostka JE, Hazen TC & Sobecky PA. (2015) Microbial responses to the Deepwater Horizon oil spill: from coastal wetlands to the deep sea. *Ann Rev Mar Sci* **7**:377-401.

Kleindienst S. (2012) Hydrocarbon-degrading sulfate-reducing bacteria in marine hydrocarbon seep sediments. Thesis, University of Bremen, Bremen, Germany.

Kleindienst S, Herbst FA, Stagars M,von Netzer F, von Bergen M, Seifert J, Peplies J, Amann R, Musat, F, Leuders T, & Knittel K. (2014) Diverse sulfate-reducing bacteria of the Desulfosarcina/Desulfococcus clade are the key alkane degraders at marine seeps. *ISME J* **8**:2029-2044.

Klindworth A, Pruesse E, Schweer T, Peplies J, Quast C, Horn M & Glöckner FO. (2013) Evaluation of general 16S ribosomal RNA gene PCR primers for classical and next-generation sequencing-based diversity studies. *Nucleic Acids Res* **41**:e1.

Kniemeyer O, Musat F, Sievert SM, Knittel K, Wilkes H, Blumenberg, M, Michaelis W, Classen A, Bolm C, Joye SB, & Widdel F. (2007) Anaerobic oxidation of short-chain hydrocarbons by marine sulphate-reducing bacteria. *Nature* **449**:898-901.

Knittel K, Boetius A, Lemke A, Eilers H, Lochte K, Pfannkuche O, Linke P & Amann R. (2003) Activity, distribution, and diversity of sulfate reducers and other bacteria in sediments above Gas Hydrate (Cascadia Margin, Oregon). *Geomicrobiol J* **20**:269-294.

Kuever J. (2014) The Family Desulfobacteraceae. In: Rosenberg E, DeLong EF, Lory S, Stackebrandt E & Thompson F (eds.). *The Prokaryotes - Deltaproteobacteria and Epsilonproteobacteria*. p.45-73. Springer-Verlag, Berlin, Heidelberg.

Kuever J, Rainey FA & Widdel F. (2015a) Desulfobacteraceae fam. nov. In: Whitman WB, *et al.* (eds.). *Bergey's Manual of Systematics of Archaea and Bacteria*. p.1-3. John Wiley & Sons, Inc.

Kuever J, Rainey FA & Widdel F. (2015b) Desulfobulbaceae fam. nov. In: Whitman WB, *et al. Bergey's Manual of Systematics of Archaea and Bacteria*. p.1-3. John Wiley & Sons, Inc.

Kuever J, Rainey FA & Widdel F. (2015c) Desulfofaba. In: Whitman WB, *et al. Bergey's Manual of Systematics of Archaea and Bacteria*. p.1-3. John Wiley & Sons, Inc.

Langdon CJ, Stefansson ES, Pargee SM, Blunt SM, Gage SJ & Stubblefield WA. (2016) Chronic effects of non-weathered and weathered crude oil and dispersant associated with the Deepwater Horizon incident on development of larvae of the eastern oyster, Crassostrea virginica. *Environ Toxicol Chem* **35**:2029-2040.

Lee RF. (2003) Photo-oxidation and photo-toxicity of crude and refined oils. *Spill Sci Technol B* **8**:157-162.

Li H, Yu Y, Luo W, Zeng Y & Chen B. (2009) Bacterial diversity in surface sediments from the Pacific Arctic Ocean. *Extremophiles* **13**:233-246.

Lin Q & Mendelssohn IA. (2012) Impacts and recovery of the Deepwater Horizon oil spill on vegetation structure and function of coastal salt marshes in the northern Gulf of Mexico. *Environ Sci Technol* **46**:3737-3743.

Lueders T. (2016) The ecology of anaerobic degraders of BTEX hydrocarbons in aquifers. *FEMS Microbiol Ecol* **93**:fiw220.

Maki H, Sasaki T & Harayama S. (2001) Photo-oxidation of biodegraded crude oil and toxicity of the photo-oxidized products. *Chemosphere* **44**:1145-1151.

Mallakin A, George Dixon D & Greenberg BM. (2000) Pathway of anthracene modification under simulated solar radiation. *Chemosphere* **40**:1435-1441.

Mbadinga SM, Wang LY, Zhou L, Liu J-F, Gu JD & Mu BZ. (2011) Microbial communities involved in anaerobic degradation of alkanes. *Int Biodeterior Biodegradation* **65**:1-13.

McConkey BJ, Duxbury CL, Dixon DG & Greenberg BM. (1997) Toxicity of a PAH photooxidation product to the bacteria Photobacterium phosphoreum and the duckweed Lemna gibba: effects of phenanthrene and its primary photoproduct, phenanthrenequinone. *Environ Toxicol Chem* **16**:892-899.

McCune B, Grace JB & Urban DL. (2002) *Analysis of ecological communities*. Oregon, USA: MjM Software.

McNutt MK, Camilli R, Guthrie GD, Hsieh PA, Labson VF, Lehr WJ, Maclay D, Ratzel AC & Sogge MK. (2011) *Assessment of flow rate estimates for the Deepwater Horizon/Macondo well oil spill*. US Department of the Interior.

McNutt MK, Camilli R, Crone TJ, Guthrie GD, Hsieh PA, Ryerson TB, Savas O & Shaffer F. (2012) Review of flow rate estimates of the Deepwater Horizon oil spill. *Proc Natl Acad Sci* **109**:20260-20267.

Meckenstock RU, Boll M, Mouttaki H, Koelschbach JS, Cunha Tarouco P, Weyrauch P, Dong X & Himmelberg AM. (2016) Anaerobic degradation of benzene and polycyclic aromatic hydrocarbons. *J Mol Microbiol Biotechnol* **26**:92-118.

Miranda KM, Espey MG & Wink DA. (2001) A rapid, simple spectrophotometric method for simultaneous detection of nitrate and nitrite. *Nitric Oxide* **5**:62-71.

Musat F, Galushko A, Jacob J, Widdel F, Kube M, Reinhardt R, Wilkes H, Schink B & Rabus R. (2009) Anaerobic degradation of naphthalene and 2-methylnaphthalene by strains of marine sulfate-reducing bacteria. *Environ Microbiol* **11**:209-219.

Muyzer G & Stams AJM. (2008) The ecology and biotechnology of sulphate-reducing bacteria. *Nat Rev Micro* **6**:441-454.

Nicodem D, Guedes CB, Correa R & Fernandes MC. (1997) Photochemical processes and the environmental impact of petroleum spills. *Biogeochemistry* **39**: 121-138.

Oris JT & Giesy JP. (1985) The photoenhanced toxicity of anthracene to juvenile sunfish (Lepomis spp.). *Aquat Toxicol* **6**:133-146.

Oris JT, Hall AT & Tylka JD. (1990) Humic acids reduce the photo-induced toxicity of anthracene to fish and daphnia. *Environ Toxicol Chem* **9**:575-583.

Pasparakis C, Mager EM, Stieglitz JD, Benetti D & Grosell M. (2016) Effects of Deepwater Horizon crude oil exposure, temperature and developmental stage on oxygen consumption of embryonic and larval mahi-mahi (Coryphaena hippurus). *Aquat Toxicol* **181**:113-123.

Paul JH, Hollander D, Coble P, Daly KL, Murasko S, English D, Basso J, Delaney J, McDaniel L & Kovach CW. (2013) Toxicity and mutagenicity of Gulf of Mexico waters during and after the Deepwater Horizon oil spill. *Environ Sci Technol* **47**:9651-9659.

Payne JR & Phillips CR. (1985) Photochemistry of petroleum in water. *Environ Sci Technol* **19**:569-579.

Pelletier MC, Burgess RM, Ho KT, Kuhn A, McKinney RA & Ryba SA. (1997) Phototoxicity of individual polycyclic aromatic hydrocarbons and petroleum to marine invertebrate larvae and juveniles. *Environ Toxicol Chem* **16**:2190-2199.

Pruesse E, Quast C, Knittel K, Fuchs BM, Ludwig W, Peplies J & Glöckner FO. (2007) SILVA: a comprehensive online resource for quality checked and aligned ribosomal RNA sequence data compatible with ARB. *Nucleic Acids Res* **35**:7188-7196.

Rabus, R, Hansen TA, & Widdel F. (2006). Dissimilatory sulfate- and sulfur-reducing prokaryotes. In: Dworkin M, Falkow S, Rosenberg E, Schleifer KH, & Stackebrandt E (eds.)
Prokaryotes: Ecophysiology and Biochemistry. p.659-768. Springer-Verlag, New York.

Radović JR, Aeppli C, Nelson RK, Jimenez N, Reddy CM, Bayona JM & Albaigés J. (2014) Assessment of photochemical processes in marine oil spill fingerprinting. *Marine Poll Bull* **79**: 268-277.

Ravenschlag K, Sahm K, Knoblauch C, Jørgensen BB & Amann R. (2000) Community structure, cellular rRNA content, and activity of sulfate-reducing bacteria in marine Arctic sediments. *Appl Environ Microbiol* **66**:3592-3602.

Ray PZ, Chen H, Podgorski DC, McKenna AM & Tarr MA. (2014) Sunlight creates oxygenated species in water-soluble fractions of Deepwater Horizon oil. *J Hazard Mater* **280**:636-643.

Reddy CM, Arey JS, Seewald JS, Sylva SP, Lemkau KL, Nelson RK, Carmichael CA, McIntrye CP, Fenwick J, Ventura GT, Van Mooy BAS, & Camilli R. (2012) Composition and fate of gas and oil released to the water column during the Deepwater Horizon oil spill. *Proc Natl Acad Sci* **109**:20229-20234.

Ruddy BM, Huettel M, Kostka JE, Lobodin VV, Bythell BJ, McKenna AM, Aeppli C, Reddy CM, Nelson RK, Marshall AG, & Rodgers RP. (2014) Targeted petroleomics: analytical investigation of Macondo well oil oxidation products from Pensacola Beach. *Energy Fuels* **28**:4043-4050.

Rueter P, Rabus R, Wilkest H, Aeckersberg F, Rainey FA, Jannasch HW & Widdel F. (1994) Anaerobic oxidation of hydrocarbons in crude oil by new types of sulphate-reducing bacteria. *Nature* **372**:455-458.

Schreiber L, Holler T, Knittel K, Meyerdierks A & Amann R. (2010) Identification of the dominant sulfate-reducing bacterial partner of anaerobic methanotrophs of the ANME-2 clade. *Environ Microbiol* **12**:2327-2340.

Siegert M, Krüger M, Teichert B, Wiedicke M & Schippers A (2011) Anaerobic Oxidation of Methane at a Marine Methane Seep in a Forearc Sediment Basin off Sumatra, Indian Ocean. *Front Microbiol* **2**:249.

Sigman ME, Schuler PF, Ghosh MM & Dabestani RT. (1998) Mechanism of pyrene photochemical oxidation in aqueous and surfactant solutions. *Environ Sci Technol* **32**:3980-3985.

Stefansson ES, Langdon CJ, Pargee SM, Blunt SM, Gage SJ & Stubblefield WA. (2016) Acute effects of non-weathered and weathered crude oil and dispersant associated with the Deepwater Horizon incident on the development of marine bivalve and echinoderm larvae. *Environ Toxicol Chem* **35**:2016-2028.

Sun MY, Dafforn KA, Johnston EL & Brown MV. (2013) Core sediment bacteria drive community response to anthropogenic contamination over multiple environmental gradients. *Environ Microbiol* **15**:2517-2531.

Suzuki D, Ueki A, Amaishi A & Ueki K. (2007) Desulfopila aestuarii gen. nov., sp. nov., a Gram-negative, rod-like, sulfate-reducing bacterium isolated from an estuarine sediment in Japan. *Int J Syst Evol Microbiol* **57**:520-526.

Tarr M, Zito P, Overton EB, Olson GM, Adhikari PL & Reddy CM. (2016) Weathering of oil spilled in the marine environment. *Oceanography*. **29**:126-135.

Ulrich GA, Krumholz LR & Suflita JM. (1997) A rapid and simple method for estimating sulfate reduction activity and quantifying inorganic sulfides. *Appl Environ Microbiol* **63**:1627-1630.

Wang L, Liu L, Zheng B, Zhu Y & Wang .X (2013) Analysis of the bacterial community in the two typical intertidal sediments of Bohai Bay, China by pyrosequencing. *Marine Poll Bull* **72**:181-187.

Wawrik B, Mendivelso M, Parisi VA, Suflita JM, Davidova IA, Marks CM, Van Nostrand JD, Liang Y, Zhou J, Huizinga BJ, Strąpoć D, & Callaghan AV. (2012) Field and laboratory studies on the bioconversion of coal to methane in the San Juan Basin. *FEMS Microbiol Ecol* **81**:26-42.

Weinstein JE & Oris JT. (1999) Humic acids reduce the bioaccumulation and photoinduced toxicity of fluoranthene to fish. *Environ Toxicol Chem* **18**:2087-2094.

Whitehead A, Dubansky B, Bodinier C, Garcia TI, Miles S, Pilley C, Raghunathan V, Roach JL, Walker N, Walter RB, Rice CD, & Galvez F. (2012) Genomic and physiological footprint of the Deepwater Horizon oil spill on resident marsh fishes. *Proc Natl Acad Sci* **109**:20298-20302.

Widdel F & Rabus R. (2001) Anaerobic biodegradation of saturated and aromatic hydrocarbons. *Curr Opin Biotechnol* **12**:259-276.

Widdel F, Knittel K & Galushko A. (2010) Anaerobic hydrocarbon-degrading microorganisms: an overview. In: Timmis KD, McGenity TJ, van der Meer JR, & de Lorenzo V (eds.). *Handbook of Hydrocarbon and Lipid Microbiology*. p.1997-2021. Springer-Verlag, Berlin, Heidelberg.

Zimmermann CF & Keefe CW. (1997) Method 365.5: determination of orthophosphate in estuarine and coastal waters by automated colorimetric analysis. United States Environmental Protection Agency. Washington, D.C. EPA/600/R-15/011.

Chapter 3. Meta-Omics Analysis of Tar Balls: Remnants of the Deepwater Horizon Oil Spill

ABSTRACT

Residual oil from the Deepwater Horizon (DWH) spill has continued to wash ashore Gulf of Mexico (GoM) beaches in the form of oil:sand aggregates (e.g., tar balls, sand patties). Previous studies investigating these aggregates have mainly focused on chemical characterization and weathering patterns of the entrained oil. Little is known about the microbial ecology associated with aggregates and whether the microbial communities carry out biodegradation of residual hydrocarbons *in situ*. Aggregate, beach sand, and seawater samples were collected from three locations along the coast of Alabama to investigate the indigenous microbial communities associated with these residues, to determine whether associated microorganisms are capable of hydrocarbon biodegradation, and to assess whether hydrocarbon transformation processes occur *in situ*. Characterization of oil extracted from aggregates revealed that the samples were highly weathered and were substantially depleted in constituents originally present in the Macondo Mississippi Canyon Block 252 (MC252) crude oil. Genomic DNA extracted from aggregates and subsequent sequencing of 16S rRNA genes demonstrated that distinct populations were associated with sand patties collected at different locations. Known taxa capable of utilizing hydrocarbon substrates were detected, although specific taxa varied among samples. It was determined that beach sand and seawater communities were distinct from those detected among sand patties, as only ten core operational

taxonomic units (OTUs) were shared between aggregates and beach sand and only seven core OTUs were shared between aggregates and seawater. The metabolic potential of these communities was assessed via metagenomic sequencing. The genetic potential for both aerobic and anaerobic hydrocarbon degradation was detected, but the functional gene profiles varied among samples. Metabolites indicative of aerobic and/or anaerobic hydrocarbon transformation processes (e.g., toluic acid, benzylsuccinic acid) were putatively identified via QTOF mass spectrometry but could not be confirmed. Overall, data reveal that the microbial communities associated with oil:sand aggregates are capable of utilizing hydrocarbons and may play a role in the long-term attenuation of residual oil from the DWH spill.

INTRODUCTION

The blowout of the DWH drilling platform led to the accidental discharge of an estimated 4.9 million barrels of crude oil into the GoM (McNutt *et al.*, 2011, McNutt *et al.*, 2012). Efforts were made to remove the oil through the use of booms, skimmers, *in situ* burning, and chemical dispersants (Ramseur, 2010) in an attempt to prevent oil from reaching the environmentally and economically sensitive coastal beaches and marshes. Despite these efforts, oil reached the coast, and over 2,000 km of GoM shoreline were eventually impacted by petroleum (Michel *et al.*, 2013, Nixon *et al.*, 2016).

Once introduced into the environment, oil undergoes weathering processes that change its physical properties and chemical composition (NRC, 2003, Tarr *et al.*, 2016). Weathering of the MC252 oil resulted in viscous water-in-oil emulsions (Michel *et al.*, 2013) that eventually washed ashore or mixed with sand and seawater particulates in nearshore environments. Subsequent sinking of these emulsions lead to the formation of submerged oil mats (SOMs) in the intertidal and subtidal zones (OSAT-II, 2011, OSAT-III, 2013), and masses of buried weathered oil were reported in a number of coastal locations (OSAT-II, 2011, OSAT-III, 2013). Over time, SOMs can fragment as a result of wave and tidal action, leading to the formation of smaller aggregates, referred to as oil:sand aggregates, oil-soaked sands, sand patties, tar balls, or surface residue balls (Clement *et al.*, 2011, Michel *et al.*, 2013, OSAT-III, 2013). Aggregates identified in the early years following the spill were quite large, and the term ‘patty’ was used to describe material ranging from ten centimeters to one meter in diameter, whereas residues less than ten centimeters in diameter were referred to as ‘surface residue balls’ (OSAT-III, 2013). However, the above-mentioned terms are often used interchangeably. These residues have been consistently documented along GoM beaches since the DWH spill (Clement *et al.*, 2011, Hayworth *et al.*, 2011, Aeppli *et al.*, 2012, Clement *et al.*, 2012, Hall *et al.*, 2013, Mulabagal *et al.*, 2013, Urbano *et al.*, 2013, Horel *et al.*, 2014, Simister *et al.*, 2015, White *et al.*, 2016). The formation of these residues is not unique to the DWH spill (Warnock *et al.*, 2015). However, previous studies have indicated that the nature of aggregates varies with a given source

oil as well as the prevailing environmental conditions during formation (Warnock *et al.*, 2015). The DWH aggregates are unique in a number of ways. Tar balls formed in the GoM from natural seeps are firm, dark masses with little, if any, petroleum odor (OSAT-III, 2013). In contrast, tar balls originating from the DWH spill are fragile oil:sand aggregates consisting of 80% to 96% sand, often with a noticeable petroleum odor (Hayworth *et al.*, 2011, Aeppli *et al.*, 2012, Mulabagal *et al.*, 2013, OSAT-III, 2013, White *et al.*, 2016).

Clement *et al* (2011) analyzed fragments of SOMs and found that the entrained oil had matching polycyclic aromatic hydrocarbon (PAH) fingerprints with emulsified oil that washed ashore early after the DWH spill, indicating that the PAHs within buried mats were not highly weathered. Later studies confirmed that oil buried in nearshore environments was not undergoing extensive weathering within the submerged mats (Clement *et al.*, 2012, Mulabagal *et al.*, 2013). However, chemical analyses of the smaller oil:sand aggregates that washed ashore indicated that a greater degree of weathering occurred in these types of samples. A study by Elango *et al* (2014) found distinctive weathering patterns of oil collected from different locations on the beach, and specifically, more extensive weathering was observed in beached samples than that were observed in SOMs (Elango *et al.*, 2014). Analysis of multiple oil types, including surface slicks, oil-soaked sands, and rock scrapings, concluded that exposed samples had undergone extensive weathering, evidenced by a loss of saturated and aromatic compounds and a substantial increase in oxygenated compounds, termed ‘oxyhydrocarbons’

(OxHC) (Aeppli *et al.*, 2012). A similar study carried out on sand patties collected at an even later time point concluded that the abundance of OxHC can increase with time, further suggesting that weathering continues in samples deposited and exposed on beaches (White *et al.*, 2016). Data from these studies demonstrated that the chemical composition of the entrained oil can change over time as a result of photooxidation and biodegradation processes (Aeppli *et al.*, 2012, Hall *et al.*, 2013, Elango *et al.*, 2014, Gros *et al.*, 2014, Radović *et al.*, 2014).

Long-term, these nearshore buried oil sources are of particular concern due to their mobility and capacity to redistribute in the environment (OSAT-III, 2013, Dalyander *et al.*, 2014) and for the potential to continually contaminate public beaches. One uncertainty with regard to these residues is whether the remaining petroleum constituents are utilized by microbial communities once they are deposited on beaches. Microbial biodegradation of petroleum has been extensively studied and shown to be vital to remediation of contaminated systems, particularly in marine environments (Leahy & Colwell, 1990, Prince, 1993, Atlas, 1995, Harayama *et al.*, 1999, Head *et al.*, 2006, McGenity *et al.*, 2012). The response of the microbial communities to DWH contamination was widely studied in the years following the spill. Several reports showed that indigenous microbial populations in the deep-sea water column, sediment, and coastal beaches and marshes rapidly responded to the presence of hydrocarbons and mediated oil transformation processes (for review, see Joye *et al.*, 2014, Kimes *et al.*, 2014, King, 2015). However, very few studies have

focused specifically on the microbial communities associated with oil:sand aggregates. Thus far, research on sand patties has indicated that microbial communities can vary between aggregates, and taxa with known hydrocarbon-degrading ability have been detected. As a result of the Texas City “Y” spill in Galveston Bay, the community composition of tar balls was reported to vary when compared to the peripheral beach sand and included hydrocarbon-degraders such as *Alcanivorax* and *Pseudoalteromonas* (Bacosa *et al.*, 2016). Urbano *et al* (2013) used DGGE analysis to characterize microbial communities of DWH sand patties and detected hydrocarbon-degrading taxa (e.g., *Mycobacterium, Stenotrophomonas*), as well as differences in community compositions between supratidal and intertidal samples. Phospholipid fatty acid analyses, along with radiocarbon measurements of oil extracted from DWH-sourced sand patties, has demonstrated that the microbial communities associated with aggregates are distinct from those of non-oiled sand and also that these microorganisms can assimilate oil-derived components (Bostic, 2016). Fungal species have been isolated from DWH sand patties and were found to be capable of hydrocarbon degradation, indicating that higher eukaryotic organisms may also play a role in transformation of hydrocarbons in these aggregates (Simister *et al.*, 2015). We conducted a preliminary survey of two sand patties collected from the coast of Alabama in January 2014 and subjected them to metagenomic sequencing. Results from taxonomic classification based on partial 16S rRNA genes demonstrated that populations varied between aggregates collected at different locations (i.e., Fort Morgan

versus Gulf Shores) (Figure S1, Table S1). *Pseudospirillium* and *Pseudoalteromonas* were abundant in both sand patties, and several observed taxa (e.g., *Pseudoalteromonas*, *Colwellia*) were consistent with other studies that investigated the response of microbial communities to the DWH spill (Figure S1) (Kostka *et al.*, 2011, Bælum *et al.*, 2012, Redmond & Valentine, 2012, Dubinsky *et al.*, 2013, Gutierrez *et al.*, 2013, Yang *et al.*, 2016). Analyses also revealed the presence of genes associated with both aerobic and anaerobic hydrocarbon degradation pathways (Figure S2).

The aim of study herein was to expand upon our preliminary work and to characterize multiple sand patties from different GoM beaches using a meta-omics approach (i.e., 16S rRNA community analysis, metagenomics, and metabolomics) to assess the composition, functional potential, and activity among aggregates deposited at different locations. It was hypothesized that the community profiles and metabolic potential for hydrocarbon degradation within oil:sand aggregates would differ between geographical locations (i.e., where they are deposited), and that microbial communities would mediate hydrocarbon transformation processes *in situ*. Knowledge about the community structure and the metabolic function of aggregate populations will allow for a better understanding of the ultimate fate of residual oil and the role microorganisms have in further mediation of ecosystem recovery.

MATERIALS & METHODS

Sampling Sites and Sample Collection. Oil:sand aggregates, peripheral beach sand, and seawater samples were collected from Fort Morgan (FM) and Gulf Shores (GS), Alabama (Figure S3) in September 2014. Two separate locations in Gulf Shores were sampled, denoted as Gulf Shores Site 1 (GS-1) and Gulf Shores Site 2 (GS-2). Sand patty samples were identified on the beach, GPS coordinates recorded (Table S2), and patties aseptically transferred to individual methanol-washed glass collection jars (Fisher Scientific, Pittsburgh, PA, USA). Surface seawater at each site was collected in acid-washed, autoclaved 2L-polypropylene wide mouth bottles (VWR®, Radnor, PA, USA) via submersion. Biomass was subsequently obtained via syringe-filtering collected seawater through 0.45 µm Supor membranes (Pall Life Sciences, Ann Arbor, MI, USA) (60 mL per filter), and individual filters were aseptically transferred into MO BIO Powersoil® Bead Tubes (MO BIO Laboratories, Carlsbad, CA, USA). Beach sand was also collected in acid-washed, autoclaved 2L-polypropylene wide mouth bottles (VWR®, Radnor, PA, USA) using an ethanol-sterilized hand shovel. Three 2-L bottles of beach sand were collected from Fort Morgan and Gulf Shores Site 2, and one bottle was collected from Gulf Shores Site 1. All samples were placed on dry ice for transport back to the laboratory and stored at -80°C until analysis.

Water Analysis. Redox potential, temperature, and pH of surface water were measured at each location using an OAKTON pH 11 series meter (OAKTON Instruments, Vernon Hills, IL, USA). Seawater was collected in 15

mL centrifuge tubes (VWR®, Radnor, PA, USA), immediately placed on dry ice for transport back to the laboratory, and kept at -80°C until analysis. Anion exchange chromatography was used to measure seawater nitrate, nitrite, and sulfate concentrations using a Dionex ICS-1100 (Dionex, Sunnyvale, CA, USA) operated with an IonPac AS23 column, a 4.5 mM Na_2CO_3 and 0.8 mM $NaHCO_3$ eluent, and a flow rate of 1 mL min^{-1}. Four replicates per site were filtered through 0.2 µm PTFE-membrane syringe filters (VWR®, Radnor, PA, USA) to remove particulates and diluted fifty-fold in deionized water prior to ion chromatography.

Aggregate and Beach Sand Subsampling. A total of 1, 13, and 20 sand patties were collected at Gulf Shores Site 1, Gulf Shores Site 2, and Fort Morgan, respectively. Aggregates were weighed to ensure that each sample chosen for further investigation contained enough material for subsequent analyses (Table S3). The three largest aggregates were chosen from Fort Morgan. Only one sample was found and collected from Gulf Shores Site 1, and therefore, was the only sample to analyze. Five sand patties were chosen from Gulf Shores Site 2 due to the overall smaller size of these samples to ensure that at least triplicate samples were successful in all downstream analyses. Sand patties were homogenized and subsampled for the various assays to allow for correlation among analyses. For this, individual sand patties were homogenized in their glass collection jars using a sterile spatula and subsampled for oil extraction and characterization, DNA extraction and

sequencing, and for metabolite profiling. Peripheral beach sand samples were subsampled to serve as controls.

Oil Extraction and Characterization. Oil present in aggregates was extracted and analyzed to confirm that sand patties originated from MC252 oil and to determine types of oil constituents present, along with the extent of weathering. Homogenized aggregate subsamples and beach sand controls (~1 g) were extracted with dichloromethane:methanol (90:10, v/v) and brought to concentrations of 10-50 mg mL^{-1}. GCxGC-FID analysis was conducted as previously described (Aeppli *et al.*, 2012, Aeppli *et al.*, 2014). Samples were injected in 1 µl-volumes in a GCxGC-FID system (Leco, St. Joseph, MI) fitted with a Restek Rtx-1 column (60 m, 0.25 mm ID, 0.25 µm thickness; first dimension) and a SGE BPX-50 column (1.5 m, 0.10 mm ID, 0.10 µm thickness; second dimension). A carrier gas of H_2 was used at a flow rate of 1 ml min^{-1}. Ovens were programmed at 40° for 10 min, 40-340° at 1.25°C min^{-1} and at 45°C for 10 min, 45-355°C at 1.29°C min^{-1}, respectively. Compounds used to calculate biomarker ratios were identified based on elution order and standards. Quantification of saturate, aromatic, and oxygenated fractions was performed via thin layer-chromatography-FID (TLC-FID) as previously described (Aeppli *et al.*, 2012, Aeppli *et al.*, 2014). Extracts were spotted on a silica-gel-sintered glass rod and sequentially developed in hexane (26 min), toluene (12 min), and dichloromethane:methanol (97:3) (5 min). Rods were dried between each development for 1 min at 500 mbar at 70°C, and subsequently scanned using

an Iatroscan MK-5 TLC-FID system (Iatron, Tokyo, Japan) using a 30 sec scan time and flow rate of 2 L min^{-1} air and 160 mL min^{-1} H_2.

DNA Extraction. Triplicate technical replicates were generated for each homogenized sand patty as well as for each jar of beach sand (Figure S3). Approximately 1 g of homogenized sand patty or beach sand sample was transferred to MO BIO PowerSoil® Bead Tubes (MO BIO Laboratories, Carlsbad, CA, USA). For seawater samples, the MO BIO tubes containing filtered seawater biomass (see "*Sample Collection*") were thawed prior to extraction. Genomic DNA was extracted according to the manufacturer's instructions. DNA was quantified using a Qubit® 2.0 Fluorometer and the Qubit® dsDNA BR Assay Kit (ThermoFisher, Waltham, MA, USA).

16S rRNA Gene Sequencing. The taxonomic composition of microbial communities was investigated via 16S rRNA gene sequencing. Amplification was performed with two series of PCR using a 5' M13 tag on a universal 519F primer (5'-GTA AAA CGA CGG CCA GCA CMG CCC C-3') and a universal Bac-785R reverse primer (5'-TAC NVG GGT ATC TAA TCC-3') as previously described (Wawrik *et al.*, 2012, Klindworth *et al.*, 2013). First, amplification was carried out using 'untagged' primers with reaction volumes of 50 µl, each containing 25 µl of PCR Master Mix (2X) (Invitrogen, Waltham, MA, USA), 1 µl of forward and reverse primers, and 2 µl of template. Thermocycler conditions were as follows: 95°C for 2 min, 30 cycles of 95°C for 30 s, 55°C for 1 min, and 72°C for 1.5 min, with a final extension step at 72°C for 10 min. Resulting PCR products were purified with a QIAGEN QIAquick PCR Purification Kit (QIAGEN,

Valencia, CA, USA) according to the manufacturer's instructions. A second amplification step was carried out to incorporate Illumina barcode sequences to the PCR product. Reactions were carried out in 30-µl total volumes, and each contained 15 µl of PCR Master Mix (2X) (Invitrogen, Waltham, MA, USA), 0.15 µl of 'untagged' 785R primer (100 µM stock concentration), 1 µl of 'tagged' forward primer (10 µM stock), and 2 µl of cleaned PCR product. Thermocycler parameters remained as described above for six cycles. Both 'untagged' and 'tagged' PCR products were analyzed via gel electrophoresis to confirm efficient amplification and barcoding. Barcoded PCR products were combined in equal amounts (5 µl per sample), cleaned as described above, and sequenced via Illumina MiSeq (300v2) at the Oklahoma Medical Research Foundation (Oklahoma City, OK, USA).

16S rRNA Gene Sequence Analysis. Resulting 16S rRNA gene sequences were analyzed via QIIME (Version 1.9.0) (Caporaso *et al.*, 2010a) using MGMIC, an in-house, web-based automated application for next-generation sequencing read analysis. Read quality was assessed via FastQC (Version 0.11.2) (Andrews, 2010), reads trimmed to a quality score of 30, and adapter sequences trimmed via Cutadapt (Martin, 2011). Reads were then paired, and only overlapping reads were retained. Remaining sequences were grouped into operational taxonomic units (OTUs) at a 97% identity level and aligned to the SILVA reference database (Pruesse *et al.*, 2007) with PyNAST (Caporaso *et al.*, 2010b). Taxonomy was subsequently assigned to sequences and taxa plots generated. Frequency data were arcsine-square-root

transformed prior to statistical analyses using a student's t-test. Core taxa, defined here as any group accounting for 1% or more of a library, were further analyzed via PC-ORD (Version 6, MjM Software) to investigate similarities and/or differences among samples. Non-metric multidimensional scaling (NMDS) was employed to visualize grouping patterns of phylogenetic communities. NMDS ordination was plotted with two axes and a Bray-Curtis distance measure. Ordination analyses were conducted 1000 times with actual data and 1000 with randomized versions of the data to ensure that the lowest stress value (i.e., the best fit of the data) was achieved. A multi-response permutation procedure (MRPP) analysis using a Bray-Curtis distance measure was performed to test for differences among samples within a group (i.e., within a sampling location) (McCune *et al.*, 2002). Community richness, evenness, and diversity were also measured.

Metagenomic Sequencing. Genomic DNA obtained from aggregates, beach sand, and seawater was used to investigate the metabolic potential of the microbial communities through metagenomic sequencing. Libraries were prepared using a Nextera XT DNA Library Preparation Kit (Illumina, San Diego, CA, USA). Technical replicate DNA extractions (described above) were pooled to generate metagenomic samples (Figure S3). Combined samples were diluted as needed to produce approximately 0.2 ng/µl concentrations for a total of 1 ng input DNA as suggested by the Nextera protocol. Library preparations were carried out according to the manufacturer's instructions with the exception of one sample, FM8. Due to the extremely low DNA template concentration for

this sample (approximately 0.05 ng/µl), nine separate Nextera 'tagmentations' were carried out and subsequently combined prior to the PCR clean-up step. Individual libraries were validated for size distribution with an Agilent Bioanalyzer using a High Sensitivity DNA kit (Agilent Technologies, Santa Clara, California, USA) following the manufacturer's instructions. Library normalization of amplified samples was modified from the Nextera protocol due to low concentrations among several samples after PCR clean-up. Manual normalization was conducted via pooling 2.4 nM (molarity calculated based on DNA quantity and measured library size distributions) of each sample. Libraries were then sequenced via Illumina HiSeq 3000 at the Oklahoma Medical Research Foundation (Oklahoma City, OK, USA).

Metagenomic Sequence Analysis. Resulting metagenomic sequences were also analyzed using the in-house MGMIC pipeline to detect functional genes associated with hydrocarbon degradation. Raw forward and reverse paired-end metagenomic reads (250 bp) were uploaded to MGMIC, and read quality was first evaluated by FastQC (Version 0.11.2) (Andrews, 2010). Illumina and Nextera adapters were detected and removed using custom scripts in conjunction with Trim Galore! (Krueger, 2015) and Cutadapt (Martin, 2011). Reads with a quality score below 30 and any sequencing artifacts were removed using homerTools (Heinz *et al.*, 2010). Sequences were screened for a minimum length of 100 nucleotides via Trimmomatic (Bolger *et al.*, 2014), and biopieces (Hansen, 2010) was used to remove unpaired reads and to convert

resulting high-quality sequences into fasta format. FastQC analyses were repeated to assess these quality-control steps.

The resulting unassembled reads were analyzed for presence/absence and abundance of functional genes of interest via USEARCH (Version 8.1) (Edgar, 2010). For sequences to be classified as a hit, reads required 60% identity over at least 35 amino acids. These parameters were chosen based on preliminary analyses varying both the percent identity (50%, 55%, 60%, 65%, 70%, and 75%) and the minimum amino acid length (25, 30, 35, and 40 amino acids) to determine which parameters resulted in confident classifications. Functional gene databases associated with aerobic and anaerobic hydrocarbon degradation pathways were manually generated and curated (Callaghan & Wawrik, 2016). These included: Ass/Mas, alkylsuccinate synthase/(1-methylalkyl)succinate synthase; Abc, anaerobic benzene carboxylase; Ahy, alkane C2 methylene hydroxylase; Apc, acetophenone carboxylase; Bss, benzylsuccinate synthase; Cmd, *p*-cymene dehydrogenase; Ebd, ethylbenzene dehydrogenase; Hbs, hydroxybenzylsuccinate synthase; Ibs, 4-isopropylbenzylsuccinate synthase; Nms, napthyl-2-methylsuccinate synthase; Ped, phenylethanol dehydrogenase; Ppc, phenylphosphate carboxylase; and Pps, phenylphosphate synthase. AromaDeg, a publically available database containing dioxygenases involved in aromatic hydrocarbon transformation processes (Duarte *et al.*, 2014) was also used. In addition, the different classes of oxygenases contained within the AromaDeg database were investigated individually. These included: benzoate, biphenyl, phthalate,

salicylate, protocatechuate, homoprotocatechuate, gentisate, and extradiol dioxygenases (EXDO) of monocyclic, bicyclic, and miscellaneous substrates (Duarte *et al.*, 2014).

Sequences were also interrogated for marker genes associated with electron-accepting and nutrient cycling processes via USEARCH analysis (Version 8.1) (Edgar, 2010) of reads against the KOBAS database (Xie *et al.*, 2011). The top resulting hits from these analyses were retained and catalogued via KEGG orthology (KO) number. Commonly used molecular markers were analyzed here to assess the involvement of aggregate-associated microorganisms in various nitrogen cycling pathways (i.e., nitrogen fixation, nitrification, dissimilatory nitrate reduction to ammonia (DNRA), denitrification, and anaerobic ammonium oxidation (anammox)), oxidation and reduction of sulfur species, carbon fixation via the Wood-Ljungdahl and photosynthetic pathways, and methanogenesis (Table S4). It should be noted that marker genes involved in anammox have KO numbers not included in the KOBAS database used. Therefore, analyses of these genes were conducted by manually generating databases for marker genes based on amino acid sequences associated with the KEGG entry, and reads were analyzed via MGMIC as described above.

The number of sequence hits to each of the gene databases was normalized to the beta subunit of RNA polymerase (RpoB) hits to account for variations in library size among samples. Normalizations were conducted using either bacterial, archaeal, or prokaryotic (bacterial + archaeal) RpoB hits based

on which domain(s) the marker genes have been detected in, and ratios are reported in the text.

High Performance Liquid Chromatography/High Resolution Mass Spectrometry (HPLC/HRMS). Mass spectrometry was utilized for metabolomic profiling with the aim to identify compounds indicative of aerobic and/or anaerobic hydrocarbon transformation. Sand patty and beach sand samples (~1 g per sample) were acidified with 4N HCl (2 mL) and sonicated for 30 minutes. MS-grade ethyl acetate was subsequently added (2 mL) to each sample, the mixture vortexed, and the organic phase carefully removed. Ethyl acetate extraction was repeated once and volumes combined. Samples were dried under N_2 prior to reconstitution in HPLC-grade isopropanol (1 mL). Each sample was filtered through a 0.2 µm filter and concentrated to 100 µL volumes by evaporation. Initially, HPLC-HRMS analyses were conducted in triplicate for each sample on an Agilent 1290 binary UPLC interfaced to an Agilent 6538 UHD Accurate Mass QTOF mass spectrometer. The UPLC separation used injection volumes of 5 µl, with a Waters Acquity HSS C18 SB analytical column (2.1 x 100 mm, 1.8 µm) and VanGuard Acquity HSS C18 SB guard column (2.1 x 5 mm, 1.8 µm), and a flow rate of 400 µL min^{-1}. Each series of three injections were separated by at least one isopropanol (MS-grade) injection blank. In the mass spectrometer, compounds were ionized using electrospray in negative ion mode. Mass spectrometer parameters were as follows: ion-source gas temperature of 325°C, capillary voltage of 3500V, fragmentor voltage of 160V, nebulizer pressure of 20 psi, sheath gas flow of

10L min^{-1}, an *m/z* range of 50-1100, data acquisition rate of 4 GHz, and one spectrum recorded per second. HPLC-HRMS raw data were analyzed using Mass Hunter and Mass Profiler Professional software to putatively identify metabolites. Based on putative identifications, several sand patty samples were subsequently reanalyzed, along with available standards. These analyses were performed in duplicate using 10-µl injections, a Waters Acquity BEH C18 analytical column (2.1 x 100 mm, 1.7 µm) and VanGuard Acquity BEH C18 guard column (2.1 x 5 mm, 1.8 µm), and using the parameters described above. Standards included 2-benzylsuccinic acid, C_{10} and C_{16} alkylsuccinic acids, *p*-, *m*-, and *o*-toluic acid, benzoic acid, 3-hydroxybenzoic acid, 4-hydroxybenzoic acid, (R)-2-phenylpropionic acid, and (S)-2-phenylpropionic acid.

RESULTS

Water Analysis. Surface water measurements at each of the three sites included temperature, pH, redox potential, and anion concentrations. Temperature, pH, and redox measurements at each of the three collection sites ranged from 24.6°C to 26.6°C, 7.76 to 7.91, and -69.9 to -74.1mV, respectively (Table S5). Sulfate concentrations were also similar among sites and ranged from 23.47 ± 1.47 to 24.78 ± 3.01 mM (Table S5). Nitrate and nitrite were undetectable (data not shown).

Characterization of Extracted Oil. Biomarker ratios were used to fingerprint the oil extracted from aggregates. Ratios revealed that each of the nine aggregates was derived from DWH oil (Table S6). Further analysis via GCxGC-FID confirmed that each of the aggregates was highly weathered, demonstrated by the substantial loss of oil constituents originally present in MC252 crude oil (Figures S4A-K). A large proportion of oil constituents, including short chain *n*-alkanes, BTEX, and low-molecular-weight PAHs (e.g., naphthalene, phenanthrene) were no longer detectable (data not shown). TLC-FID measurements revealed a decrease in both the saturate (F_{Sat}) and aromatic (F_{Aro}) fractions with an increase in oxygenated fractions (F_{OxHC1} and F_{OxHC2}) compared to MC252 crude oil (Figure 1). Relative abundances of the saturate and aromatic fractions were high (48% and 34%, respectively) in MC252 crude oil, and the $F_{OxHC1+2}$ fraction made up only 18% of the total mass of the oil. In contrast, relative abundances of $F_{OxHC1+2}$ ranged from 56-76% in the aggregates, whereas saturated and aromatic fractions ranged from 8-34% (Figure 1).

Microbial Community Analysis via 16S rRNA Sequencing. Partial 16S rRNA genes were sequenced from a total of 57 sand patty, beach sand, and seawater samples, and library sizes ranged from 11,355 to 42,621 reads per sample (Table S7), with a median of 25,609 reads. Proteobacteria comprised the largest phylum among aggregates, ranging from approximately 29-88% of total reads (Table S8A). Within Proteobacteria, sequences classified largely as Gammaproteobacteria, Alphaproteobacteria, or Betaproteobacteria

with the majority assigned to Gammaproteobacteria (ranged from ~10-74% of total reads) (Table S9). Alpha- and Betaproteobacteria ranged from approximately 1-29% and approximately 0.02-7% of the total population, respectively (Table S9A). Deltaproteobacteria populations were abundant in only two of the aggregates: FM8 (11.43% ± 0.85%) and GS1 (16.61% ± 0.22%) (Table S9A).

Commonly detected groups within Gammaproteobacteria included *Marinobacter*, Acidithiobacillales KCM-B-112, *Halomonas*, *Alcanivorax*, *Idiomarina*, *Pseudoxanthomonas*, *Pseudospirillum*, *Lysobacter, Pseudomonas*, as well as Gammaproteobacteria-Other (Figures 2A-C). However, the presence of these specific taxa varied among sand patties. Alteromonadales was significantly higher in FM8 (8.00% ± 1.46%) and FM16 (14.97% ± 1.67%) than in all other samples ($p \leq 1.18E-03$). Within Altermonadales, FM8 consisted of mostly *Marinobacter* (6.84% ± 1.12%), whereas FM16 consisted of *Marinobacter* (4.95% ± 0.37%), *Idiomarina* (4.13% ± 1.34%), and Alteromonadales-Other (5.23% ± 2.39%). The majority of Gammaproteobacteria in FM20 classified as *Pseudoxanthomonas* (18.51% ± 4.54%) and Acidithiobacillales KCM-B-112 (39.43% ± 0.71%). Gammaproteobacteria observed in GS1 mostly classified as *Pseudospirillum* (5.82% ± 1.16%) or were unclassified Gammaproteobacteria. The five sand patty samples investigated from Gulf Shores Site 2 (GS2, GS3, GS7, GS9, GS12) had notable similarities, i.e., the enrichment of Acidithiobacillales KCM-B-112, as was also seen with FM20 (Figures S2A & S2C). Relative abundances

of KCM-B-112 were significantly enriched in FM20, GS2, GS3, GS7, GS9, and GS12 compared to all other aggregates ($p \leq 5.43E-03$), and each of these samples were significantly different to each other due to the large variations of KCM-B-112 relative abundances, which ranged from 18.94% ± 0.30% in GS3 to 50.15% ± 0.58% in GS9 ($p \leq 0.04$). Other notable Gammaproteobacteria present in Gulf Shores Site 2 aggregates consisted of *Lysobacter* (GS7, 8.11% ± 0.08%), *Pseudoxanthomonas* (GS9, 15.68% ± 0.50%), and *Pseudomonas* (GS9, 3.57% ± 0.16%) (Figure 2C).

Alphaproteobacteria taxa also varied among individual samples and largely included *Hyphomonas*, *Thalassopira*, *Parvibaculum*, *Geminicoccus*, *Rhizobium*, *Brevundimonas*, *Sphingomonas*, *Methylobacterium*, *Parvularcula*, *Phenylobacterium*, Rickettsiales TK34, and unclassified Rhodobacteraceae-Other (Figures 2A-C). Rhodobacteriaceae-Other and *Hyphomonas* comprised a large portion of Alphaproteobacteria in FM8, averaging 11.52% ± 0.54% and 4.45% ± 2.01%, respectively. *Parvibaculum* (4.27% ± 0.30%) and *Thalassopira* (2.26% ± 0.41%) were the most abundant alphaproteobacterial genera detected in FM16. Other notable taxa among samples included *Geminicoccus* (GS3, 5.16% ± 0.35%), *Phenylobacterium* (GS7, 6.51% ± 0.15%), *Methylobacterium* (GS9, 4.03% ± 0.25%), and *Parvibaculum* (GS12, 6.65% ± 0.10%). In contrast to other sand patty samples, GS1 had a low abundance of Alphaproteobacteria, with an average of 1.96% ± 0.50% of total sequences attributed to this group.

Betaproteobacteria were not ubiquitous among all aggregates. Observed groups included *Achromobacter* (GS9, 1.87% ± 0.06%), *Variovorax* (GS7,

1.12% ± 0.08%), and *Massilia* (GS3, 1.98% ± 0.12%; GS7, 2.00% ± 0.10%; GS9, 1.19% ± 0.12%). Additionally, unclassified Oxalobacteraceae were detected in FM8 (5.31% ± 0.90%) and FM16 (1.33% ± 0.09%) (Figures 2A-C).

As mentioned above, only two sand patty samples were found to have notable levels of Deltaproteobacteria. GS1 had a significantly higher relative abundance of Deltaproteobacteria compared to all other aggregates, with an average of 16.61% ± 0.22% of total sequences ($p \leq 1.44E-03$). GS1 deltaproteobacterial reads largely classified as Desulfarculaceae (3.02% ± 0.17%), Desulfobacteraceae-Other (3.39% ± 0.64%), *Desulfosarcina* (1.78% ± 0.16%), Desulfobacteraceae-SEEP-SRB1 (1.42% ± 0.28%), Desulfobacteraceae-Sva0081-Sediment Group (1.03% ± 0.15%), Desulfobacteraceae (1.78% ± 0.04%), and *Desulfovibrio* (1.55% ± 0.26%) (Figure 2B). FM8 also had a significantly higher abundance of Deltaproteobacteria compared to the other sand patties, with the exception of GS1, with an average of 11.43% ± 0.85% ($p \leq 1.70E-05$). These sequences mostly classified as *Desulfovibrio* (4.03% ± 0.62%) and *Desulfofustis* (3.57% ± 0.62%) (Figure 2A, Table S10A). Deltaproteobacteria taxa in all of the other aggregates had low overall relative abundances (<1% of all reads) (Table S9).

Although sequences classified as Proteobacteria were the most abundant reads among sand patties, non-proteobacterial taxa were also detected at high relative abundances. Dominant taxa varied among sample and included *Halogranum* (FM16, 10.22% ± 2.66%), Anaerolineaceae (GS1, 4.78% ± 0.36%), Leptospiraceae (GS1, 18.44% ± 2.60%), *Mycobacterium* [(FM20,

7.18% ± 3.28%), (GS2, 6.22% ± 0.32%), (GS3, 5.17% ± 0.23%), (GS7, 5.56% ± 0.36%), (GS12, 5.39% ± 0.19%)], Thermomicrobia-JG30-KF-FM45 (GS12, 11.00% ± 0.45%), and Microbacteriaceae-Other (GS3, 12.08% ± 0.25%) (Figures 2A-C).

Beach sand and seawater samples had distinct populations compared to those observed in aggregates, and similar communities were observed among sand and seawater samples collected at the different locations (Figures 2D and 2E). Major phyla detected in beach sand included Planctomycetes, Proteobacteria, Bacteroidetes, Thaumarchaeota, and cyanobacteria (Figure 2D, Table S8B). Similarly, seawater samples consisted largely of Planctomycetes, Proteobacteria, Bacteroidetes, cyanobacteria, and Euryarcheota (Figure 2E, Table S8C). Several groups were observed in both sand and seawater samples (e.g., Planctomycetaceae, *Rhodopirellula*, *Blastopirellula*, Thermoplasmatales-Marine Group II), and these communities clustered closely in NMDS ordination (Figure 3). As with sand patty samples, the majority of Proteobacterial reads in beach sand and seawater classified as Gammaproteobacteria or Alphaproteobacteria, and to a lesser extent, Deltaproteobacteria. Gammaproteobacteria made up the largest proportion of Proteobacteria, ranging from approximately 6-18% and 7-15% of all beach sand and seawater reads, respectively (Tables S9B and S9C). Dominant gammaproteobacterial taxa in beach sand and seawater were different from those observed in aggregates, and consisted mainly of the uncharacterized BD7-8 marine group and JTB255 marine benthic group in sand, whereas OM60 Nor5 clade and

SAR86 were the dominant gammaproteobacterial lineages in seawater (Figures 2D and 2E).

Collectively, the community analysis of sand patty, beach sand, and seawater samples yielded 1,342 OTUs at the genus level, of which, 135 OTUs were categorized as the 'core' community, defined as any taxa consisting of ≥1% of the population in any library. Core OTUs encompassed approximately 77-96% of total reads (data not shown). A total of ten and seven core OTUs were shared among aggregates and beach sand or aggregates and seawater, respectively (data not shown). NMDS ordination demonstrated that GS1 harbored a distinct core community and that populations in each of the Fort Morgan aggregates were distinct from each other (Figure 3). FM20 was similar in overall community structure with all of the sand patties analyzed from Gulf Shores Site 2 (Figures 2A & 2C). MRPP tests were conducted on samples within a location (i.e., between aggregate, beach sand, and seawater collected on the same beach), and groups were defined as sample type (i.e., sand patties, sand, or seawater). MRPP analyses generate a test statistic (T) that describes how strongly the tested groups are separated (McCune *et al.*, 2002). Results indicated that the groups at each sampling location, that is aggregates, sand, and seawater, are distinct, as indicated by the negative T values (Table S11).

Metagenomic Analysis. Metagenomic sequences were analyzed for presence and for abundance of functional genes to compare the metabolic potentials of microbial communities among samples. RpoB-normalized ratios

were calculated to account for differences among library size and are reported hereafter.

Nitrogen Cycling

Commonly used molecular markers were analyzed to investigate the potential of the aggregate-associated microorganisms in various nitrogen cycling pathways (i.e., nitrogen fixation, nitrification, dissimilatory nitrate reduction to ammonia (DNRA), denitrification, and anaerobic ammonia oxidation (anammox)). Overall, analyses of genes associated with nitrogen cycling show that nitrogen fixation and DNRA are processes that can be carried out by the populations among the sand patties, whereas the potential for denitrification was more variable among aggregates (Figure S5).

Nitrate reductases (NarGHI, NapAB) catalyze the reduction of nitrate to nitrite in DNRA and in denitrification (Zehr & Kudela, 2011). In DNRA, nitrite reductases (NirBD, NrfAH) further reduce nitrite to ammonia (Zehr & Kudela, 2011). Nitrate reductases (NarGHI and NapAB) and nitrite reductases (NirBD and NrfAH) were observed in all sample types (Figures S5A-G). NarGHI ratios were significantly higher in aggregates collected from Gulf Shores Site 2 than in beach sand ($p \leq 0.02$) or seawater ($p \leq 2.06E-03$). Significantly higher ratios were also observed for Fort Morgan sand patties relative to seawater ($p \leq 0.05$), whereas no significant differences were seen between Fort Morgan sand patties and beach sand ($p \leq 0.10$). NapAB sequences were generally more prevalent among beach sand, with significantly higher ratios than in aggregates or seawater at Gulf Shores Site 2 ($p \leq 4.81E-03$). As nitrate reductase enzymes

are involved in several nitrogen cycling processes, nitrite reductases were used as markers to determine the potential of microbial communities for participating in DNRA. NirBD and NrfAH ratios followed a similar trend as those observed with nitrate reductases (Figures S5F-I). NirBD ratios were significantly higher in sand patties from Fort Morgan and Gulf Shores Site 2 than in sand ($p \leq 0.01$) or seawater ($p \leq 0.02$) from these locations. NrfAH sequences were significantly higher in beach sand samples than in aggregates across both Fort Morgan and Gulf Shores Site 2 ($p \leq 0.046$), with the exception of NrfH at Fort Morgan which was only marginally higher than aggregates ($p = 0.056$).

The genetic potential for denitrification, based on the presence of NirK, NirS, NorBC, and NosZ (Zehr & Kudela, 2011), was observed among aggregates, although not consistently, as low ratios were measured in samples from Gulf Shores Site 2 (Figures S5J-N). Beach sand samples had significantly higher ratios than sand patties or seawater for NirK, NirS, and NosZ ($p \leq 0.046$) (Figures S5J, S5K, S5N). In contrast, nitric oxide reductases (NorBC) were observed at higher ratios in sand patties than other genes involved in denitrification, particularly at Fort Morgan (Figures S6L & S6M).

The potential for nitrogen fixation, the conversion of dinitrogen gas to ammonia, was assessed by surveying for nitrogenase proteins (NifDKH) (Zehr & Kudela, 2011). These genes had significantly higher ratios in sand patty samples at both Fort Morgan and Gulf Shores Site 2 ($p \leq 0.048$) than compared to beach sand and seawater samples, with the exception of NifH in Fort Morgan sand patties. These abundances were only marginally significant ($p = 0.055$)

compared to sand and seawater (Figures S5O-Q). No sequences in any of the samples had hits to the AnfG gene, which encodes for the delta subunit of nitrogenase (data not shown).

Nitrification, the oxidation of ammonia to nitrate, is catalyzed by ammonia monooxygenase (AmoCAB), hydroxylamine dehydrogenase (Hao), and nitrate reductase/nitrite oxidoreductase (NxrAB) enzymes (Kowalchuk & Stephen, 2001, Zehr & Kudela, 2011). AmoCAB and Hao sequences were significantly higher in beach sand at both Fort Morgan and Gulf Shores Site 2 ($p \leq 0.03$) than in sand patty or seawater samples (Figures S5R-S5U). NxrAB (NarGH) was present in all samples (Figures S5A-B). However, as nitrate reductases are involved in multiple nitrogen cycling processes, differences among samples cannot be directly linked with nitrification based on NxrAB.

The potential for anaerobic oxidation of ammonia to nitrogen (anammox) was also investigated via analysis of the marker genes hydrazine synthase (Hzs) and hydrazine dehydrogenase (Hdh) (van Niftrik & Jetten, 2012). Few, if any, sequences classified as either Hzs or Hdh among sand patty, beach sand, or seawater samples (data not shown). Only one read among all sand patties samples had sequence similarity to known anammox genes (i.e., hydrazine synthase in GS1) (data not shown). Beach sand and seawater samples had slightly more reads that classified as either hydrazine synthase or hydrazine dehydrogenase, but detection was sporadic and resulted in extremely low ratios (data not shown).

Sulfur Cycling

Genes encoding proteins involved in dissimilatory sulfate reduction, adenylylsulfate reductase (AprAB) and dissimilatory sulfite reductase (DsrAB), had the highest ratios in GS1 (Figures S6A-D). These genes were also detected at relatively high abundances in FM8, consistent with the presence of Deltaproteobacteria among both GS1 and FM8, and were observed in beach sand and seawater as well, although at overall lower ratios (Figures S6A-D). Normalized ratios were significantly lower in Gulf Shores Site 2 sand patty samples compared to beach sand and seawater samples ($p \leq 2.71E-04$). Ratios from individual aggregates collected from Fort Morgan varied (Figures S6A-D), and therefore, were not significantly different than beach sand or seawater samples collected from this location ($p \geq 0.31$).

Several sulfur oxidation genes were also investigated. Aggregate populations appeared to possess the metabolic potential for oxidation of sulfur species to varying extents and through multiple pathways. The various subunits of the SOX complex, the most well-characterized sulfur oxidation enzyme complex (Friedrich *et al.*, 2001, Ghosh & Dam, 2009), were detected at the highest ratios in FM8 (Figures S6E-K). Genes encoding the SOX proteins also appeared to be widespread among beach sand and seawater samples, but gene ratios were consistently lower in Gulf Shores Site 2 sand patties than in corresponding beach sand or seawater (Figures S6E-K). Oxidation of sulfur species through less-characterized pathways can involve thiosulfate dehydrogenase (DoxD), sulfide:quinone oxidoreductase (Sqr), sulfide

dehydrogenase/flavocytochrome c (FccAB), and sulfur oxygenase/reductase (Sor) enzymes (Ghosh & Dam, 2009). Of these, Sqr sequences were observed most commonly (Figure S6P) and were significantly higher among aggregates from both Fort Morgan and Gulf Shores Site 2 than in beach sand or seawater samples ($p \leq 0.03$).

Methanogenesis

On trend with the detection of genes for sulfate reduction, methyl-coenzyme M reductase (McrABG) and heterodisulfide reductase (HdrABC), genes typically involved in the final steps of methanogenesis, ratios were elevated in GS1. These genes were also observed at high ratios in FM8 and/or FM16 (Figures S7A-F). Few, if any, beach sand and seawater samples had sequences classified as McrABG, whereas HdrABC hits were observed within these samples (Figures S7A-F).

Carbon Fixation

Gene inventories were surveyed for carbon-monoxide dehydrogenase genes (CooSF) in order to determine if populations possessed the potential for carbon fixation through the Wood-Ljungdahl pathway. Surveys suggested that there was potential for carbon fixation associated with GS1 and FM8 sand patties (Figures S8A-B). Additionally, ratios of the large subunit of ribulose-biphosphate carboxylase (RbcL), the key enzyme involved in carbon fixation in photosynthetic organisms, were significantly higher in seawater samples than in beach sand or sand patties from each location ($p \leq 4.69E-03$) (Figure S8C).

Aerobic Hydrocarbon Degradation

Functional gene profiles revealed differences in the metabolic potential for hydrocarbon degradation among samples (Figures 4B-D). With respect to the inventory of genes associated with aerobic hydrocarbon degradation pathways, FM16 demonstrated a strong aerobic degradation signature, with high ratios of monooxygenases involved in alkane hydroxylation (AlkB, CYP153) (Nie *et al.*, 2014) (Figures 4B and S12), and dioxygenases involved in a number of aromatic ring activation and cleavage reactions, including those involved in aerobic transformation of benzene, toluene, benzoate, naphthalene, biphenyl, among several other compounds (AromaDeg) (Duarte *et al.*, 2014) (Figures 4B and S12). FM8 also displayed the potential for aerobic degradation, although to a lesser extent than FM16 (Figures 4B and S12). No significant differences in AlkB or CYP153 ratios were observed between Fort Morgan aggregates compared to beach sand or seawater due to the variation between the different sand patties collected at this location ($p \geq 0.17$). Sand patty profiles generally had higher ratios of CYP153 than sand or seawater samples, whereas ratios indicated a more widespread distribution of dioxygenases (Figures 4B and S12). Both sand patties and beach sand samples collected at Fort Morgan had significantly higher dioxygenase ratios than seawater ($p \leq 4.56E-03$), whereas the variation observed among Gulf Shores Site 2 sand patties resulted in a significant difference measured only between beach sand and seawater dioxygenase ratios ($p = 0.047$).

The results of the AromaDeg analyses demonstrated a ubiquitous presence of dioxygenases among the different sample types (Figures 4B, S12,

S13). Sand patties had the highest variation, particularly within samples collected from Gulf Shores Site 2. Specifically, GS12 contained the overall highest ratio, and GS9 had the lowest (Figure S13). In an attempt to interrogate differences in the types of dioxygenases present within samples, individual classes of proteins contained within the AromaDeg database were analyzed separately. Benzoate and biphenyl oxygenase sequences were detected most frequently among sand patties (Figures S13B-C), and aggregates also had the highest ratios of hits to the three individual databases of extradiol oxygenases (EXDO) (Figures S13F-H). No significant differences in benzoate oxygenases, biphenyl oxygenases, or EXDO ratios were observed among Gulf Shores Site 2 aggregates compared to sand and seawater at the same location ($p \geq 0.06$). In contrast, significantly higher ratios of benzoate oxygenases ($p \leq 0.03$), biphenyl oxygenases ($p \leq 6.94E-03$), EXDO monocyclic oxygenases ($p \leq 5.43E-03$), and EXDO miscellaneous oxygenases ($p \leq 0.01$) were observed between Fort Morgan aggregates and sand/seawater samples. Fort Morgan sand patties also had a significantly higher ratio of hits to the salicylate oxygenase database than beach sand and seawater samples ($p \leq 0.02$).

Anaerobic Hydrocarbon Degradation

Several genes associated with the anaerobic activation of hydrocarbons were identified in GS1, consistent with this sample having high ratios of AprAB and DsrAB. Most notably, genes involved in the addition of hydrocarbons to fumarate (i.e., 'fumarate addition'), including the catalytic subunits of alkylsuccinate synthase/(1-methylalkyl)succinate synthase (AssA/MasD),

benzylsuccinate synthase (BssA), napthyl-2-methylsuccinate synthase (NmsA), hydroxybenzylsuccinate synthase (HbsA), and 4-isopropylbenzylsuccinate synthase (IbsA) (Strijkstra *et al.*, 2014, Wilkes *et al.*, 2016, Heider *et al.*, 2016a) were considerably higher in GS1 than in all other sand patty, sand, or seawater samples (Figure S9). The ratios of alkylsuccinate synthase/(1-methylalkyl)succinate synthase, which catalyzes the addition of *n*-alkanes to fumarate (Wilkes *et al.*, 2016), was much higher than those associated with the activation of aromatic compounds (Figure S9). FM8 was also observed to have consistently higher ratios of these genes than the other samples analyzed (Figure S9).

The potential for other mechanisms of anaerobic hydrocarbon transformation was also investigated. Specifically, gene inventories were surveyed for genes involved in anaerobic hydroxylation processes, such as ethylbenzene dehydrogenase (Ebd), *p*-cymene dehydrogenase (Cmd), and a putative alkane C2-methylene hydroxylase enzyme (Ahy) (Heider *et al.*, 2016b). Ratios of the catalytic subunit of ethylbenzene dehydrogenase, EbdA, were highest in GS1 (Figure S10), whereas the ratios of genes involved in the downstream reactions of ethylbenzene degradation (i.e., phenylethanol dehydrogenase (Ped) and acetophenone carboxylase (Apc), (Heider *et al.*, 2016b)), varied among all samples, with no clear trend observed among aggregates compared to beach sand or seawater (Figure S10). The first step in anaerobic hydroxylation of *p*-cymene is catalyzed by *p*-cymene dehydrogenase (Cmd) (Strijkstra *et al.*, 2014), and ratios of CmdA and CmdB were variable

among individual samples (Figure S11B). Activation of *n*-alkanes via anaerobic hydroxylation is proposed to be catalyzed by a putative alkane C2-methylene hydroxylase, AhyABCD (Heider & Schühle, 2013, Heider *et al.*, 2016b). The maximum ratios of each of the subunits of this enzyme were observed in GS1 (Figure S11A). Together, EbdB, CmdB, and AhyB ratios were higher than expected compared to those calculated for the other subunits of these proteins (Figures S10B, S11A, and S11B). Further analysis of EbdB, CmdB, and AhyB sequences indicated that many of these hits are similar to nitrate reductases (data not shown).

Hydrocarbons can also be activated under anaerobic conditions via carboxylation processes (Rabus *et al.*, 2016). Anaerobic benzene carboxylase (AbcA) ratios were significantly higher in sand patties than in seawater collected at respective locations ($p = 0.03$ for Fort Morgan; $p = 3.25E-03$ at Gulf Shores Site 2), but no significant differences were observed between aggregates and beach sand ($p \geq 0.08$) (Figure S11C). The potential for the anaerobic activation of phenol was assessed by surveys of phenylphosphate synthase (PpsAB) and phenylphosphate carboxylase (PpcABCD). Phenol is activated to a phenylphosphate intermediate via PpsAB and then carboxylated by PpcABCD (Boll & Fuchs, 2005). The abundance of these genes varied among individual samples, although GS1 had consistently high ratios with these enzymes (Figure S11D).

Metabolite Profiling

Metabolomic surveys were conducted to determine whether hydrocarbon transformation processes occur within aggregates deposited on coastal beaches. Extracted ion chromatograms (EICs) were obtained from the raw HPLC/HRMS data of oil:sand aggregates. EICs for the molecule ions ($M\text{-}H^-$) of potential metabolites generally contained a number of peaks, some of which overlapped in HPLC retention time (data not shown), rendering unequivocal identifications of these compounds extremely difficult. However, targeted searches for metabolites associated with hydrocarbon transformation processes produced a number of potential candidates from the aggregates. These included benzoic acid, phenylpentanoic acid, phenanthrene carboxylic acid, along with C_{10} to C_{22} alkylsuccinic acids, among several others (data not shown). These compounds were putatively identified through the *m/z* (mass-to-charge) ratios of the ($M\text{-}H^-$) ions. For the majority of compounds detected, several isomers were identified at different retention times. None of these compounds were detected in any of the beach sand samples analyzed (data not shown). In order to provide stronger evidence for the presence of these metabolites, multiple aggregate samples (i.e., FM8, FM20, GS7) were subsequently reanalyzed in conjunction with several available standards. Overall, metabolites confirmed based on mass and retention times of standards included *p*-toluic acid, *m*-toluic acid, *o*-toluic acid, 3-hydroxybenzoic acid, 2-phenylpropionic acid, benzylsuccinic acid, as well as alkylsuccinic acids (data not shown).

DISCUSSION

The DWH spill was a catastrophic event. Of the vast amounts of crude oil released during the spill, much of it was removed through active clean-up efforts (e.g., burning, skimming, chemical dispersant application) or was removed through natural weathering processes (e.g., evaporation, dissolution, biodegradation) (Ramseur, 2010). However, an unknown amount of hydrocarbons was buried in the deep seabed (Valentine *et al.*, 2014) and at various unknown locations along the coast (Hayworth *et al.*, 2011). Residual oil contamination in nearshore coastal environments allows for re-oiling of the shoreline in the form of oil:sand aggregates (i.e., sand patties, tar balls, oil-soaked sands, surface residue balls) (Hayworth *et al.*, 2011, OSAT-III, 2013). As these aggregates are responsible for continued contamination of environmentally and economically important ecosystems, it is important to understand the chemical and biological nature of these residues. The aim of this study was to characterize the microbial communities associated with DWH-sourced sand patties and to determine the biodegradation potential of the entrained oil once aggregates are deposited on GoM beaches.

Sand patties analyzed here contained oil derived from the DWH spill as confirmed through biomarker ratios (Table S6). A concurrent increase in the oxygenated fractions and decrease in the saturate and aromatic fractions was observed in oil extracted from patties (Figure 1). This signifies a high degree of weathering (Aeppli *et al.*, 2012) and is in agreement with previous studies that concluded ‘oxyhydrocarbons’ (OxHC) can make up a substantial portion of the

extractable compounds from aggregates (Aeppli *et al.*, 2012, White *et al.*, 2016). When OxHC fractions were normalized to C_{30}-hopane, an increase was observed in relation to this recalcitrant marker (data not shown), indicating that these oxygenated compounds are newly formed and likely represent oil degradation products (Aeppli *et al.*, 2014). Data collected here is also in agreement with a previous report indicating that weathered oil profiles were somewhat uniform between samples (White *et al.*, 2016), as all nine aggregates exhibited severe weathering profiles and were depleted in many of the oil constituents originally present in MC252 oil (Figures S4A-K). Multiple reports have confirmed that DWH-sourced oil constituents undergo molecular changes (e.g., incorporation of oxygen molecules) as a result of weathering (Aeppli *et al.*, 2012, Hall *et al.*, 2013, Gros *et al.*, 2014, Radović *et al.*, 2014, Ruddy *et al.*, 2014, White *et al.*, 2016), leading to formation of compounds such as carboxylic acids, alcohols, and ketones (Aeppli *et al.*, 2012, Ruddy *et al.*, 2014), and that aggregates exhibit signatures of biodegradation (Aeppli *et al.*, 2012, Elango *et al.*, 2014, Gros *et al.*, 2014, Bostic, 2016). Biodegradation potential of both residual hydrocarbons and oxygenated degradation products likely exists within aggregates. However, there are currently no published reports of conclusive *in situ* biodegradation activity.

To date, relatively little is known with regard to the structure and metabolic potential of the microbial communities associated with DWH sand patties. Based on our preliminary metagenomic survey (Figures S1 and S2, Table S1), we hypothesized that the microbial communities associated with

sand patties and their metabolic potentials would differ between individual aggregates. In the study herein, populations were found to be highly variable among geographical locations (i.e., where they were deposited) and also among aggregates collected from the same location (i.e., at Fort Morgan). The genetic potential for hydrocarbon degradation through aerobic and/or anaerobic processes also varied among samples and was consistent with observations from 16S rRNA profiles. Beach sand and seawater, sources of microbes associated with aggregates, had distinct communities compared to all of the aggregates interrogated here. NMDS analysis (Figure 3) indicated that differences between individual aggregate populations were as large as the differences in populations of aggregates to sand/seawater communities and were much larger than those between sand and seawater samples. It can be hypothesized that community succession associated with sand patties potentially undergoes distinctly different trajectories, which is likely as a result of the specific conditions (e.g., nutrient availability, moisture content, types of substrates available, residence time) that each aggregate is subjected to during transport and deposition.

A number of striking differences were observed among aggregates with regard to the 16S rRNA community profiles as well as with the functional gene profiles associated with nutrient cycling and terminal electron-accepting processes. Overall, the individual aggregates demonstrated either an anaerobic, facultative anaerobic, or aerobic signature. Collectively, results of both the 16S rRNA gene profiling (e.g., high relative abundance of sulfate-

reducing taxa) (Figure 2B) and metagenomic analyses (e.g., high ratios of AprAB, DsrAB) (Figures 6A-D) indicated that GS1, the one sand patty collected at Gulf Shores Site 1, differed substantially from all other samples and that anaerobic processes were likely dominant in this aggregate. Although no quantitative data were collected for moisture or nutrient content (e.g., nitrate, ammonia, and sulfate concentrations), GS1 was collected in the intertidal zone and would have been subjected to tidal activity. If this aggregate had recently washed ashore and was saturated with seawater, the high relative abundance of anaerobic taxa and anaerobic functional genes could potentially be explained by the presence of anoxic microniches.

Both aerobic and anaerobic signatures were observed in FM8. Community profiles for FM8 included a high relative abundance of anaerobes, particularly sulfate-reducing taxa (e.g., *Desulfovibrio*, *Desulfofustis*) (Figure 2A), as well as a number of aerobic and facultative anaerobic taxa (e.g., *Marinobacter*, *Alcanivorax*, *Hyphomonas*, *Pseudomonas*, *Bacillus*) (Figure 2A). Correspondingly, functional gene profiles suggested that both aerobic and anaerobic processes were important in FM8. Genes involved in DNRA and denitrification (NapAB, NrfAH, NirK, NirS, NorBC, NosZ) were present in FM8, as were those involved in dissimilatory sulfate reduction (AprAB, DsrAB) and carbon fixation via the Wood-Ljungdahl pathway (CooFS) indicating the importance of anaerobic processes within this sample. Additionally, genes associated with oxidation processes were also observed, most notably with the SOX system genes (Figures S6E-K). Together, data indicate that FM8 shared

similarity with GS1 with regard to the importance of anaerobic processes but was substantially different in that aerobic systems were also likely relevant in this sample.

In contrast to GS1 and FM8, the remainder of the aggregates investigated had predominantly aerobic 16S rRNA and functional gene signatures. The community profile of FM16 revealed that aerobic hydrocarbon degraders made up a relatively large proportion of the overall community (e.g., *Alcanivorax*, *Marinobacter*, *Thalassospira*, *Parvibaculum*) (Figure 2A). Many of the taxa present in FM16 have previously been identified as either capable of utilizing hydrocarbon substrates or have been observed/enriched in hydrocarbon-contaminated systems (Coulon *et al.*, 2007, Kodama *et al.*, 2008, Zhao *et al.*, 2008, Vila *et al.*, 2010, Wang *et al.*, 2010, Li *et al.*, 2012, Rosario-Passapera *et al.*, 2012, Yergeau *et al.*, 2012, Gutierrez *et al.*, 2013, Liu & Liu, 2013, Sherry *et al.*, 2013, Fathepure, 2014, Joye *et al.*, 2014, Kappell *et al.*, 2014, Liang *et al.*, 2015, Shao *et al.*, 2015, Liang *et al.*, 2016, Mishamandani *et al.*, 2016, Ruiz *et al.*, 2016), and several taxa have also been reported in studies focused on contamination from the DWH spill (Gutierrez *et al.*, 2013, Liu & Liu, 2013, Looper *et al.*, 2013, Joye *et al.*, 2014, Kappell *et al.*, 2014, Atlas *et al.*, 2015). With regard to the metabolic potential of the microbial community, nitrogen fixation appeared to be a central nitrogen cycling process in FM16, but that the community also did appear able to participate in denitrification. Genes involved in oxidation of sulfur species were observed, whereas genes involved in reductive processes (e.g., AprAB, DsrAB, CooFS) were not abundant, with

the exception of heterodisulfide reductase (Figures S7A-C). The high ratios observed for heterodisulfide reductase in FM16, as well as GS1 and FM8, are likely due to hits to heterodisulfide reductase homologs present in non-methanogen taxa, as methanogens were not abundant in any of the aggregates. Homologs of heterodisulfide reductase genes have been found in a number of non-methanogenic taxa, particularly within sulfate-reducing bacteria (Pereira *et al.,* 2011, Callaghan *et al.*, 2012, Ramos *et al.*, 2015), and these genes have been proposed to be involved in energy conversion processes (Thauer *et al.*, 2008), which may explain the unexpectedly high detection of these sequences in samples without methanogens.

Interestingly, FM20, as well as the five samples collected from Gulf Shores Site 2 (GS2, GS3, GS7, GS9, GS12) had similar overall community compositions. One notable trend among these aggregates was the presence of *Mycobacterium*. *Mycobacterium* species are metabolically diverse organisms, capable of utilizing a variety of hydrocarbons including *n*-alkanes (Watkinson & Morgan, 1991, Churchill *et al.*, 1999, Bogan *et al.*, 2003), aromatics (Burback & Perry, 1993, Solano-Serena *et al.*, 2000), and PAHs (Kim *et al.*, 2010). *Mycobacterium* has also been observed in microbial communities that responded to the DWH spill (Looper *et al.*, 2013, Atlas *et al.*, 2015), and in DWH-sourced oil:sand aggregates (Urbano *et al.*, 2013). The frequent detection among aggregates in this study may suggest that *Mycobacterium* plays a role in hydrocarbon transformation in sand patties as was suggested by Urbano *et al* (2013), potentially due to the ability of this taxa to withstand desiccating

conditions. Several other taxa observed within these patties were organisms with known or suspected hydrocarbon-degrading capabilities that have been previously reported in GoM microbial communities associated with DWH contamination, including *Pseudoxanthomonas*, *Pseudomonas*, *Sphingomonas*, *Nocardioides*, and *Streptomyces* (Dubinsky *et al.*, 2013, Looper *et al.*, 2013, Mortazavi *et al.*, 2013, Urbano *et al.*, 2013) (Figures 2A & 2C; Table S10A-C). These aggregates also had an enrichment of the uncharacterized taxa Acidithiobacillales KCM-B-112 (Figures 2A and 2C). The order Acidithiobacillales has only a few characterized members and are described as sulfur-utilizing autotrophs (Garrity *et al.*, 2015). The SILVA database (Pruesse *et al.*, 2007, Quast *et al.*, 2013) contains approximately 900 16S rRNA gene sequences associated with KCM-B-112. These 16S rRNA gene sequences were submitted and classified as various uncultured prokaryotes and were obtained from a variety of environments including, but not limited to, petroleum-contaminated soil and sand, heavy metal-contaminated soil, asphalt seeps, oil-containing bioreactors, and oil sands tailings ponds (SILVA, 2007). Many of the SILVA listings classified sequences as related to known sulfur-oxidizers. However, some of the gene sequences were obtained from clones related to *Methylococcus capsulatus*, a methanotroph capable of nitrogen-fixation (Kasai *et al.*, 2005). Interestingly, the type strain of Acidithiobacillales, *Acidithiobacillus ferrooxidans*, can fix nitrogen (Mackintosh, 1978), and *nif* genes have been found in the genome of *A. ferrooxidans* (Valdés *et al.*, 2008). NifDHK genes were abundant among aggregates in this study (Figures S5O-Q). Given that

16S rRNA gene phylogeny and function are not necessarily correlated, it is unclear what role Acidithiobacillales KCM-B-112 could be playing in these sand patties. It can be postulated that a potential functional niche of KCM-B-112 is to provide an ammonia source to the microbial population through nitrogen fixation. However, further bioinformatic analyses would be needed to determine which taxa the observed *nif* gene sequences were attributed to, which is beyond the scope of this study. Genes involved in sulfur oxidation were also present among these aggregates, but were generally less abundant overall compared to beach sand or seawater (Figures S6E-P). Genes of reductive processes (e.g., AprAB, DsrAB, CooFS) were low among FM20 and the Gulf Shores Site 2 aggregates (Figures S6A-D, S7D-F, and S8A-C), further suggesting that anaerobic processes were not dominant among populations associated with these samples.

In comparison, the community compositions and functional genes detected in beach sand and seawater, initial sources of aggregate inocula, were distinct compared to all sand patties. Both beach sand and seawater contained taxa commonly found in marine systems (e.g., Gammaproteobacteria, Deltaproteobacteria, Plantomycetes, Bacteroidetes, Actinobacteria, Firmicutes) (Mills *et al.*, 2008, Biers *et al.*, 2009, Zinger *et al.*, 2011, Gobet *et al.*, 2012, King *et al.*, 2012, Newton *et al.*, 2013), and communities were similar between samples collected at each of the three locations (Figures 2D and 2E). Several taxa were shared between sand and seawater samples (e.g., Planctomycetaceae, *Rhodopirellula*, *Blastopirellula*), and samples clustered

together in NMDS ordination (Figure 3), indicating that these samples were more similar to each other than to any of the aggregates. Functional gene profiles of beach sand and seawater communities were also different from those associated with sand patties. Beach sand and seawater are both known to harbor diverse microbial populations with broad metabolic capabilities (Biers *et al.*, 2009, Zinger *et al.*, 2011, Gobet *et al.*, 2012, Williams & Cavicchioli, 2014). Functional gene profiles observed among sand and seawater samples in this study are representative of marine systems, as the genetic potential for various carbon, nitrogen, and sulfur cycling processes was observed (Figure 4A).

One of the main goals of this study was to investigate whether the microbial communities within aggregates had the functional potential to attenuate residual hydrocarbons. Interrogation of the genetic capacity for hydrocarbon transformation within aggregate-associated populations revealed that there was also considerable dissimilarity in the biodegradation potential of each sand patty. In GS1, metagenomic analyses indicated that the associated microbial community was capable of participating in a range of anaerobic hydrocarbon pathways, particularly those of 'fumarate addition' (Figures 4C, 4D, and S9A-E). Proteins of the 'fumarate addition' pathways catalyze the addition of *n*-alkanes (AssA/MasD), toluene and xylene (BssA), *p*-cymene (IbsA), *p*-cresol (HbsA), and 2-methylnapthalene (Nms/Mns) to fumarate to form succinic acid metabolites (Rabus *et al.*, 2016). Overall, AssA/MasD was more prevalent than sequences typically associated with activation of aromatic compounds

(Figure S9), implying that organisms capable of degrading *n*-alkanes may be more prevalent in this sample. Genes associated with other anaerobic processes, including anaerobic ethylbenzene hydroxylation (EbdA), anaerobic phenol carboxylation (PpsAB, PpcABC), and anaerobic benzene carboxylation (AbcA) were also present in GS1 (Figures 4D, S10, and S11), further corroborating the likely importance of anaerobic transformation pathways within this sample. Interestingly, a large number of sequences in GS1 classified as EbdB (Figure S10B). Ethylbenzene dehydrogenase is a DMSO reductase-type II molybdenum type protein (Johnson *et al.*, 2001), as are *p*-cymene dehydrogenase (Cmd) and dissimilatory nitrate reductases (Heider *et al.*, 2016b). The alpha- and beta-subunits of ethylbenzene dehydrogenase are similar to nitrate reductases (Heider *et al.*, 2016b), and a closer inspection of the sequences classified as EbdB via BLAST largely returned nitrate reductases (data not shown), explaining the apparent widespread distribution of putative EbdB sequences among all samples types. A putative alkane C2 methylene hydroxylase (AhyABCD) (Figure S11A), a protein that was first detected in the alkane/alkene-utilizing sulfate-reducer, *Desulfococcus oleovorans* Hxd3 (Callaghan *et al*., 2008), was also prevalent in GS1. It has been proposed that this enzyme may be involved in the anaerobic hydroxylation of alkanes (Heider & Schühle, 2013, Heider *et al.*, 2016b), although the requisite metabolites have not yet been detected. The putative alkane C2 methylene hydroxylase has sequence similarity to ethylbenzene dehydrogenase (Heider & Schühle, 2013, Heider *et al.*, 2016b), and therefore,

the frequent detection among samples, as suggested by observed ratios of AhyB, should also be interpreted with caution.

Similarly as was seen with the 16S rRNA and nutrient cycling profiles, genes involved in both aerobic and anaerobic hydrocarbon degradation pathways were detected in FM8. With regard to anaerobic degradation processes, genes involved in alkane and mono-aromatic hydrocarbon addition to fumarate (e.g., AssA/MasD, BssA) were prevalent (Figure S9), and genes involved in other anaerobic pathways (e.g., Ahy, Abc, Pps) were also detected (Figure S11) but were detected less frequently than those of 'fumrate addition', particularly for AssA/MasD (Figure S9B). These data suggest that *n*-alkane activation via 'fumarate addition' may be an important process within FM8, as was observed with GS1, and also that the community can participate in transformation of a range of hydrocarbons. Additionally, the microbial community associated with FM8 is capable of hydroxylating alkanes (i.e., via AlkB and CYP153), as well as carrying out transformation of range of aromatic compounds as demonstrated by the various dioxygenases detected with the AromaDeg database (Figure S13).

The remainder of the sand patties investigated displayed predominantly aerobic signatures. For FM16, data indicate the potential for aerobic hydrocarbon transformation as demonstrated by the occurrence of mono- and dioxygenases (Figures 4B, S12, and S13) and of known aerobic hydrocarbon-degraders (e.g., *Marinobacter*, *Alcanivorax*) (Nie *et al.*, 2014) (Figure 2A). Aerobic processes also seemed more prevalent in the aggregates analyzed at

Gulf Shores Site 2. Interestingly, although overall community composition between these Gulf Shores Site 2 aggregates was similar (Figure 3), differences were observed with regard to the functional gene profiles related to hydrocarbon transformation. For example, GS12 had the highest observed ratio of AromaDeg sequences, whereas GS9 had the lowest (Figures S12 and S13). These varying patterns suggest that aggregates can become enriched in genes for specific metabolic pathways but can also become depleted compared to the background (i.e., sand/seawater) metabolic potential.

The microbial community in beach sand and seawater had the genetic capacity for hydrocarbon degradation, and in general, genes of aerobic pathways were detected more frequently (Figures S9-S13). These data are not surprising given that the GoM is regularly exposed to hydrocarbons through natural seeps and anthropogenic inputs (NRC, 2003), and the indigenous microbial populations are diverse and capable of utilizing petroleum constituents (for review, see Joye *et al.*, 2014, Kimes *et al.*, 2014, King *et al.*, 2015). Sand and seawater samples exhibited a more consistent detection of the various genes analyzed than sand patty samples, which seems to indicate that aggregate-associated populations can become enriched in genes associated with hydrocarbon transformation compared to the background beach sand and seawater (e.g., GS1: AssA, FM16: CYP153), but can also become depleted relative to the background (e.g., GS9: AromaDeg).

One of the goals of this study was to investigate whether genetic potential for hydrocarbon transformation could be correlated with evidence of *in*

situ activity. To our knowledge, this is the first report of identification of putative hydrocarbon transformation metabolites within DWH-sourced aggregates through mass spectrometry analysis. The presence of hydrocarbon-degrading taxa and genes involved in the transformation of oil constituents suggested that the sand patty-associated microbial communities were able to degrade hydrocarbons. Targeted metabolite profiling was conducted in an attempt to identify requisite metabolites of known pathways via QTOF mass spectrometry. Identification of metabolites was challenging due to the limited sand patty material available for analyses, the extremely low concentrations of putative metabolites, and the complexity of the metabolite signatures. The presence of several compounds was confirmed based on mass and retention times of available standards. These included benzylsuccinic acid, alkylsuccinic acids, toluic acid, hydroxybenzoic acid, and phenylpropionic acid. A number of other compounds were identified as putative metabolites associated with hydrocarbon degradation processes (e.g., phenanthrene carboxylic acid, benzoylacetate, acenapthylmethylsuccinic acid) based on known retention times of these compounds. However, conclusive identification of these putatively identified metabolites was not possible. None of the confirmed or putative metabolites were detected in beach sand control samples.

Given that the requisite parent compounds (e.g., BTEX, short-chain *n*-alkanes, naphthalene, phenanthrene) were no longer detectable based on GCxGC analyses, metabolite detection in these aggregates should be interpreted with caution. It may be possible that these putative compounds were

derived from biological transformation of trace concentrations of parent hydrocarbons that were below the detection limits of the GCxGC method, or that they represent products from biotransformation processes that occurred at an earlier time. With respect to the latter, these putative compounds may not have been further transformed to end products due to limitations in nutrients or changes in redox conditions. Alternatively, the putative detections may have been accidental. Compounds that are produced directly via biological transformations can be detected using HPLC/HRMS (Picó & Barceló, 2015). However, the weathering of the residual oil in aggregates can also occur as a result of abiotic reactions. The resulting mixture of 'oxyhydrocarbons' can be challenging to characterize beyond identification of chemical functionalities (e.g., alcohols, ketones) (Aeppli *et al.*, 2012, Ray *et al.*, 2014, Ruddy *et al.*, 2014), and the complexity of traces in this study further corroborates this.

CONCLUSIONS

DWH-sourced sand patties represent contaminating oil that persists in the environment that has continued to wash ashore years after the spill. Chemical analyses of these aggregates have consistently shown that they are highly weathered, likely through both photooxidation and biodegradation processes (Aeppli *et al.*, 2012, Hall *et al.*, 2013, Aeppli *et al.*, 2014, Gros *et al.*, 2014, White *et al.*, 2016), but little is known with regard to the microbial ecology of these residues. Several conclusions can be drawn from the results of this study. Distinct microbial populations are associated with individual aggregates, and many community members have known or suspected hydrocarbon-

degrading capabilities. These putative hydrocarbon-degraders vary in abundance between sand patties, as does the genetic potential for aerobic and/or anaerobic hydrocarbon transformation. Overall, the data suggest that oil:sand aggregates are distinct entities that differ from background beach sand and seawater and also likely from other sand patties. These differences are presumably the result of the environmental conditions that each aggregate is subjected to over time, including aggregate residence time in seawater versus on land, moisture and nutrient content due to seawater inundation and/or precipitation, as well as available residual hydrocarbons. Results provide evidence that microbial communities associated with aggregates are capable of hydrocarbon transformation, and that they may play a vital role in the long-term attenuation of residual oil from the DWH spill.

FIGURES

Figure 1. Relative abundance of saturate (F_{Sat}), aromatic (F_{Aro}), and oxygenated (F_{OxHC1} and F_{OxHC2}) fractions measured via TLC-FID for MC252 crude oil and oil:sand aggregates collected from Fort Morgan (FM), Gulf Shores (GS) Site 1 and Site 2 locations.

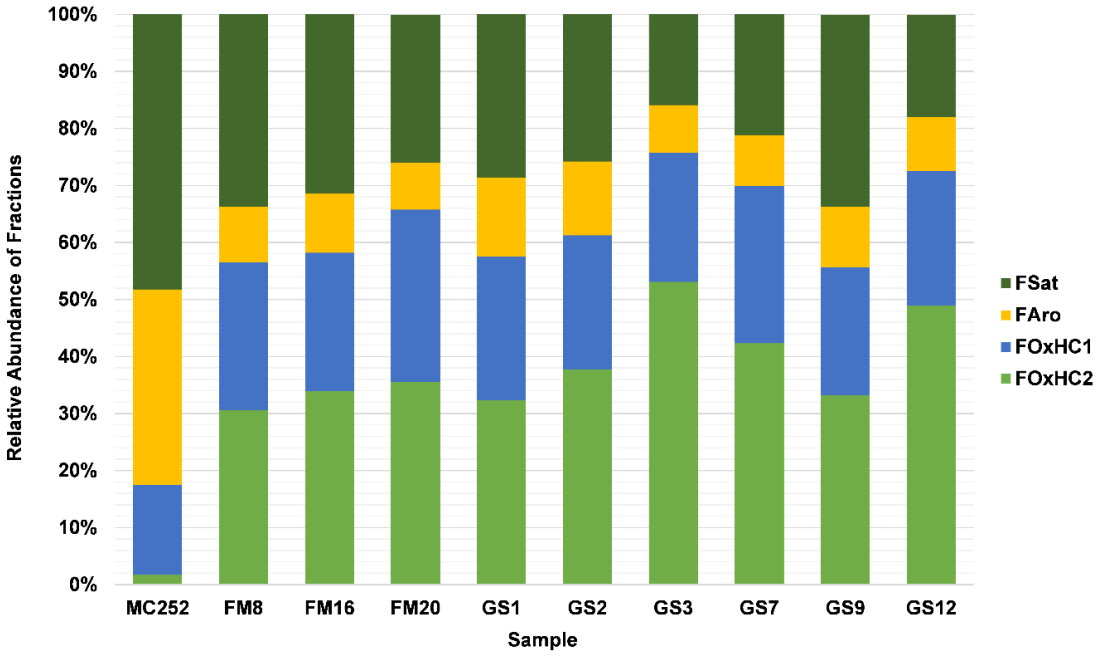

Figure 2. Microbial community composition as determined by Illumina sequencing of partial 16S rRNA gene sequences from **(A)** Fort Morgan aggregates, **(B)** the Gulf Shores Site 1 aggregate, **(C)** Gulf Shores Site 2 aggregates, **(D)** beach sand, and **(E)** seawater samples. Each sample was subjected to triplicate DNA extractions, and each replicate is indicated by the triplicate bar graphs for each sample. Reads were analyzed using QIIME (Version 1.9.0) (Caporaso *et al*, 2010a) and classified to the genus level when possible. Minor phylogenetic groups, which could not be visually resolved in the bar graphs, are not included in the legend. Sand and seawater samples from Gulf Shores locations are denoted as from Site 1 (GS-1) or Site 2 (GS-2). Note: beach sand samples sequenced from Gulf Shores Site 1 are technical replicates.

A.


FM8
Unassigned; Other
Spirochaeta
Pseudomonas
Alcanivorax
Marinobacter
Acidithiobacillales; KCM-B-112
Gammaproteobacteria; Other
Cystobacter
Desulfovibrio
Desulfofustis
Oxalobacteraceae; Other
Pelagibius
Rhodobacteraceae; Other
Oceanicaulis
Hyphomonas
Planctomycetaceae
Bacillus
Chloroplast
Demequnia
FM16
Unassigned; Other
Halomonas
Alcanivorax
Idiomarina
Marinobacter
Altermonadaceae; Other
Acidithiobacillales; KCM-B-112
Gammaproteobacteria; Other
Thalassospira
Rhodobacteraceae; Other
Parvibaculum
Phyllobacteriaceae; Other
Parvularcula
Hyphomonas
Planctomycetaceae
Planctomyces
Halobacillus
Anaerolineaceae
Salegentibacter
Muricauda
Gramella
Halolamina
Halogranum
FM20
Unassigned; Other
Pseudoxanthomonas
Salinicola
Cobetia
Acidithiobacillales; KCM-B-112
Gammaproteobacteria; Other
Oxalobacteraceae; Other
Sphingomonas
Erythrobacteraceae
Rickettsiales; TK34
Rhodospirillaceae; Other
Geminicoccus
Rhizobium
Alphaproteobacterium; E6aD10
Brevundimonas
Chloroplast
Nocardioides
Mycobacterium

B.

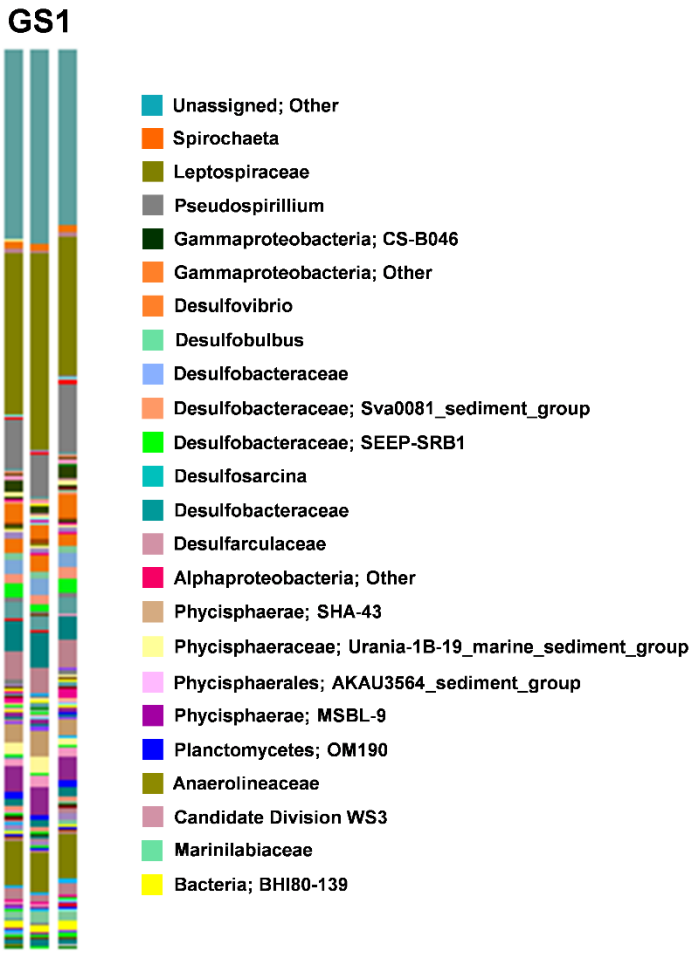
GS1
Unassigned; Other
Spirochaeta
Leptospiraceae
Pseudospirillium
Gammaproteobacteria; CS-B046
Gammaproteobacteria; Other
Desulfovibrio
Desulfobulbus
Desulfobacteraceae
Desulfobacteraceae; Sva0081_sediment_group
Desulfobacteraceae; SEEP-SRB1
Desulfosarcina
Desulfobacteraceae
Desulfarculaceae
Alphaproteobacteria; Other
Phycisphaerae; SHA-43
Phycisphaeraceae; Urania-1B-19_marine_sediment_group
Phycisphaerales; AKAU3564_sediment_group
Phycisphaerae; MSBL-9
Planctomycetes; OM190
Anaerolineaceae
Candidate Division WS3
Marinilabiaceae
Bacteria; BHI80-139

C.

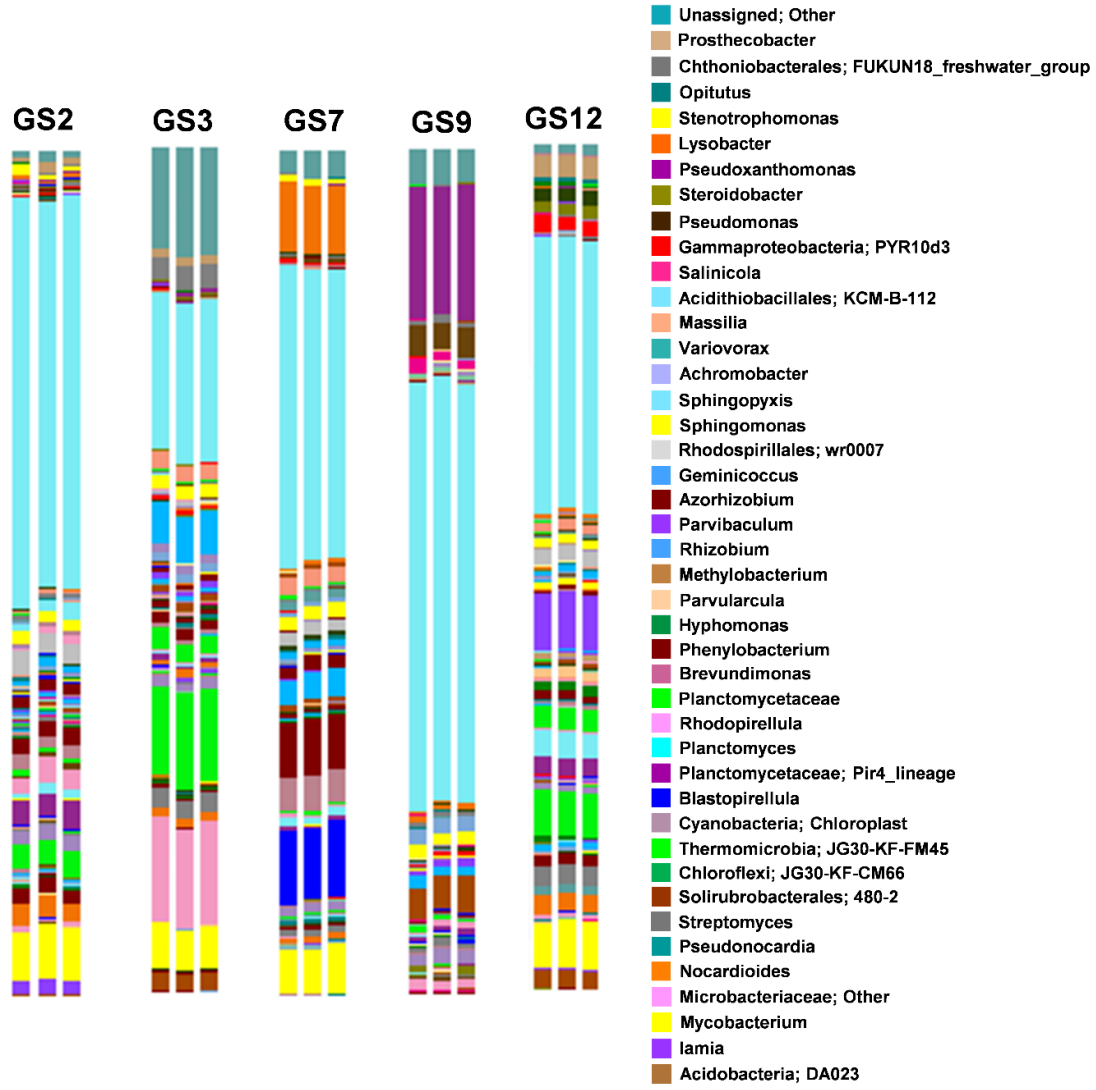
GS2
GS3
GS7
GS9
GS12
Unassigned; Other
Prosthecobacter
Chthoniobacterales; FUKUN18_freshwater_group
Opitutus
Stenotrophomonas
Lysobacter
Pseudoxanthomonas
Steroidobacter
Pseudomonas
Gammaproteobacteria; PYR10d3
Salinicola
Acidithiobacillales; KCM-B-112
Massilia
Variovorax
Achromobacter
Sphingopyxis
Sphingomonas
Rhodospirillales; wr0007
Geminicoccus
Azorhizobium
Parvibaculum
Rhizobium
Methylobacterium
Parvularcula
Hyphomonas
Phenylobacterium
Brevundimonas
Planctomycetaceae
Rhodopirellula
Planctomyces
Planctomycetaceae; Pir4_lineage
Blastopirellula
Cyanobacteria; Chloroplast
Thermomicrobia; JG30-KF-FM45
Chloroflexi; JG30-KF-CM66
Solirubrobacterales; 480-2
Streptomyces
Pseudonocardia
Nocardioides
Microbacteriaceae; Other
Mycobacterium
Iamia
Acidobacteria; DA023

D.

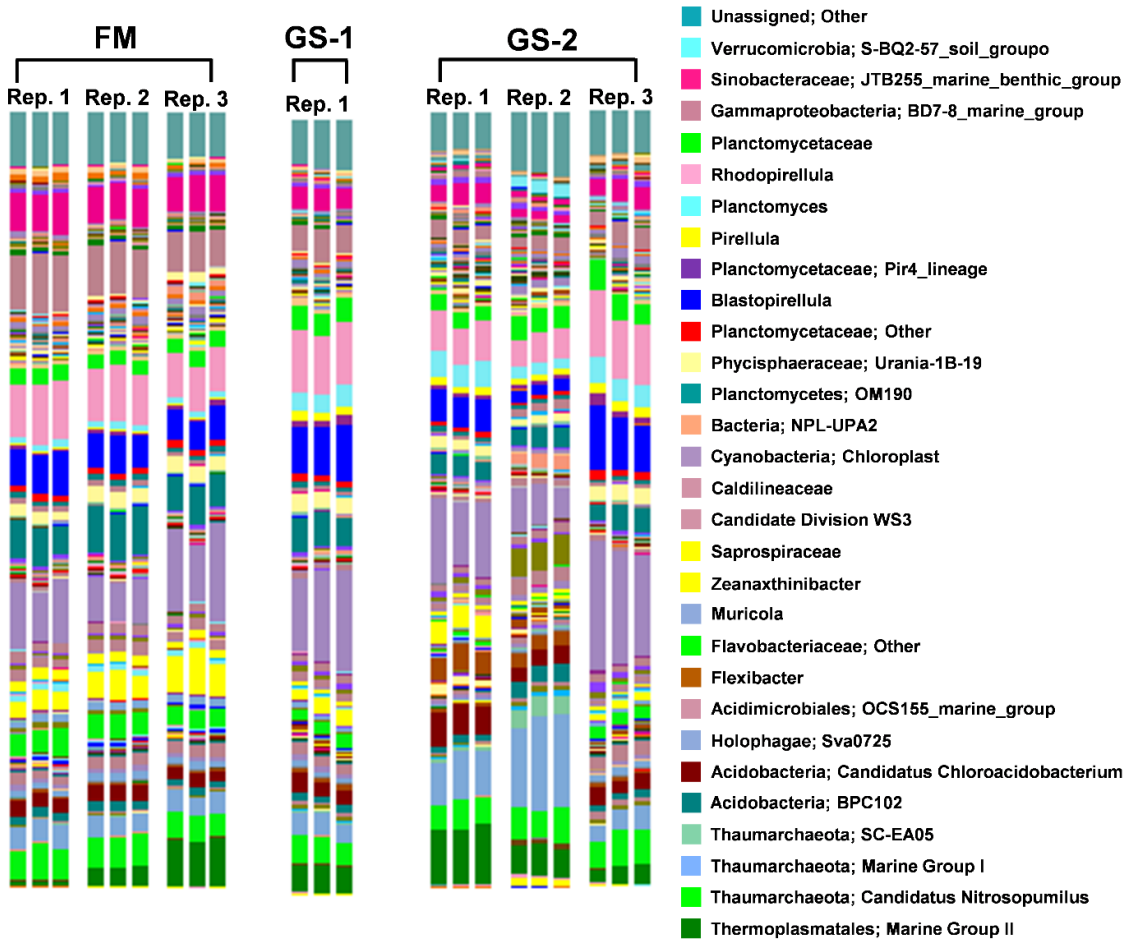
FM
GS-1
GS-2
Rep. 1
Rep. 2
Rep. 3
Rep. 1
Rep. 1
Rep. 2
Rep. 3
Unassigned; Other
Verrucomicrobia; S-BQ2-57_soil_groupo
Sinobacteraceae; JTB255_marine_benthic_group
Gammaproteobacteria; BD7-8_marine_group
Planctomycetaceae
Rhodopirellula
Planctomyces
Pirellula
Planctomycetaceae; Pir4_lineage
Blastopirellula
Planctomycetaceae; Other
Phycisphaeraceae; Urania-1B-19
Planctomycetes; OM190
Bacteria; NPL-UPA2
Cyanobacteria; Chloroplast
Caldilineaceae
Candidate Division WS3
Saprospiraceae
Zeanaxthinibacter
Muricola
Flavobacteriaceae; Other
Flexibacter
Acidimicrobiales; OCS155_marine_group
Holophagae; Sva0725
Acidobacteria; Candidatus Chloroacidobacterium
Acidobacteria; BPC102
Thaumarchaeota; SC-EA05
Thaumarchaeota; Marine Group I
Thaumarchaeota; Candidatus Nitrosopumilus
Thermoplasmatales; Marine Group II

E.

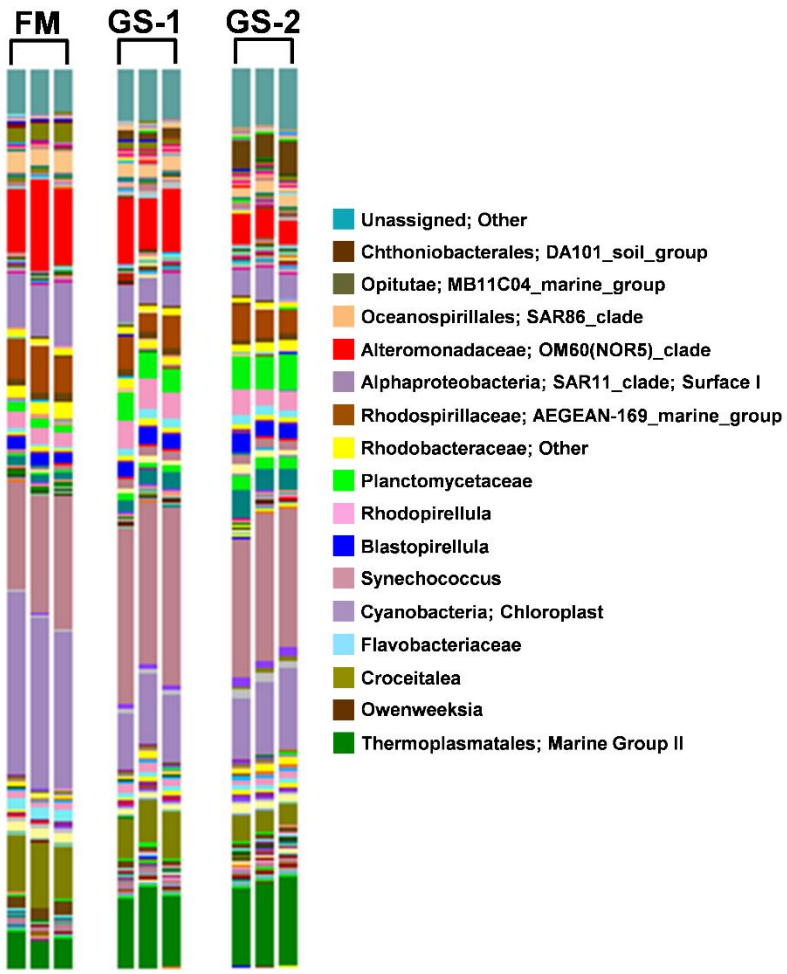
FM
GS-1
GS-2
Unassigned; Other
Chthoniobacterales; DA101_soil_group
Opitutae; MB11C04_marine_group
Oceanospirillales; SAR86_clade
Alteromonadaceae; OM60(NOR5)_clade
Alphaproteobacteria; SAR11_clade; Surface I
Rhodospirillaceae; AEGEAN-169_marine_group
Rhodobacteraceae; Other
Planctomycetaceae
Rhodopirellula
Blastopirellula
Synechococcus
Cyanobacteria; Chloroplast
Flavobacteriaceae
Croceitalea
Owenweeksia
Thermoplasmatales; Marine Group II

Figure 3. Non-metric multidimensional scaling (NMDS) ordination of core microbial communities. Core taxa were defined as any group accounting for 1% or more of sequences in any sample. NMDS plot was generated using a Bray-Curtis distance measure in PC-ORD (Version 6, MjM Software). Sand and seawater (SW) samples are labeled according to site: Fort Morgan (FM), Gulf Shores Site 1 (GS-1) or Gulf Shores Site 2 (GS-2).

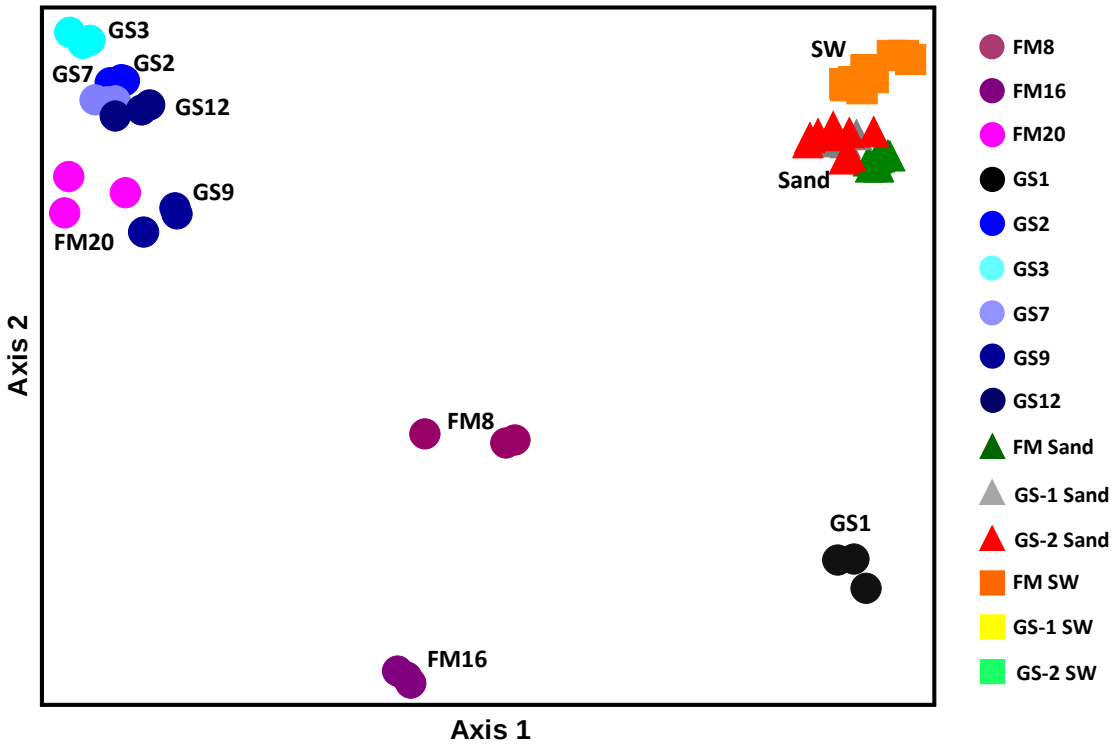

Figure 4. Heatmap of normalized ratios calculated for gene sequences involved in **(A)** biogeochemical cycling, **(B)** aerobic hydrocarbon transformation pathways as well as genes involved in **(C)** anaerobic pathways of samples collected from Fort Morgan (FM), Gulf Shores Site 1 (GS.1), and Gulf Shores Site 2 (GS.2) with AssA ratios plotted and **(D)** without AssA ratios plotted. Heatmaps were generated using Heatmap Builder® (Version 1.1) with dataset-normalized sorting so that the highest ratio in each set of functional genes corresponds to the darkest grid color. Abbreviations: Nar, nitrate reductase; Nir, nitrite reductase; Nap, nitrate reductase; Nrf, nitrate reductase; Nor, nitric oxide reductase; Nos, nitrous oxide reductase; Nif, nitrogenase; Amo, ammonia monooxygenase; Hao, hydroxylamine dehydrogenase; Apr, adenylylsulfate reductase; Dsr, dissimilatory sulfite reductase; Sox, sulfur-oxidizing protein; Sqr, sulfide:quinone oxidoreductase; Dox, thiosulfate dehydrogenase; Fcc, sulfide dehydrogenase; Sor, sulfur oxygenase; Coo, carbon monoxide dehydrogenase; Rbc, ribulose-bisphosphate carboxylase; Alk, alkane monooxygenase; CYP153, cytochrome P450 alkane hydroxylase; Ass, alkylsuccinate synthase; Mas, (methyl)alkylsuccinate synthase; Bss, benzylsuccinate synthase; Ibs, (4-isopropylbenzyl)succinate synthase; Nms, 2-napthylmethylsuccinate synthase; Hbs, hydroxybenzylsuccinate synthase; Ahy, alkane C2 methylene hydroxylase; Ebd, ethylbenzene dehydrogenase; Ped, phenylethanol dehydrogenase; Apc, acetophenone carboxylase; Cmd, *p*-cymene dehydrogenase; Abc, anaerobic benzene dehydrogenase; Pps, phenylphosphate synthase; Ppc, phenylphosphate carboxylase.

A.

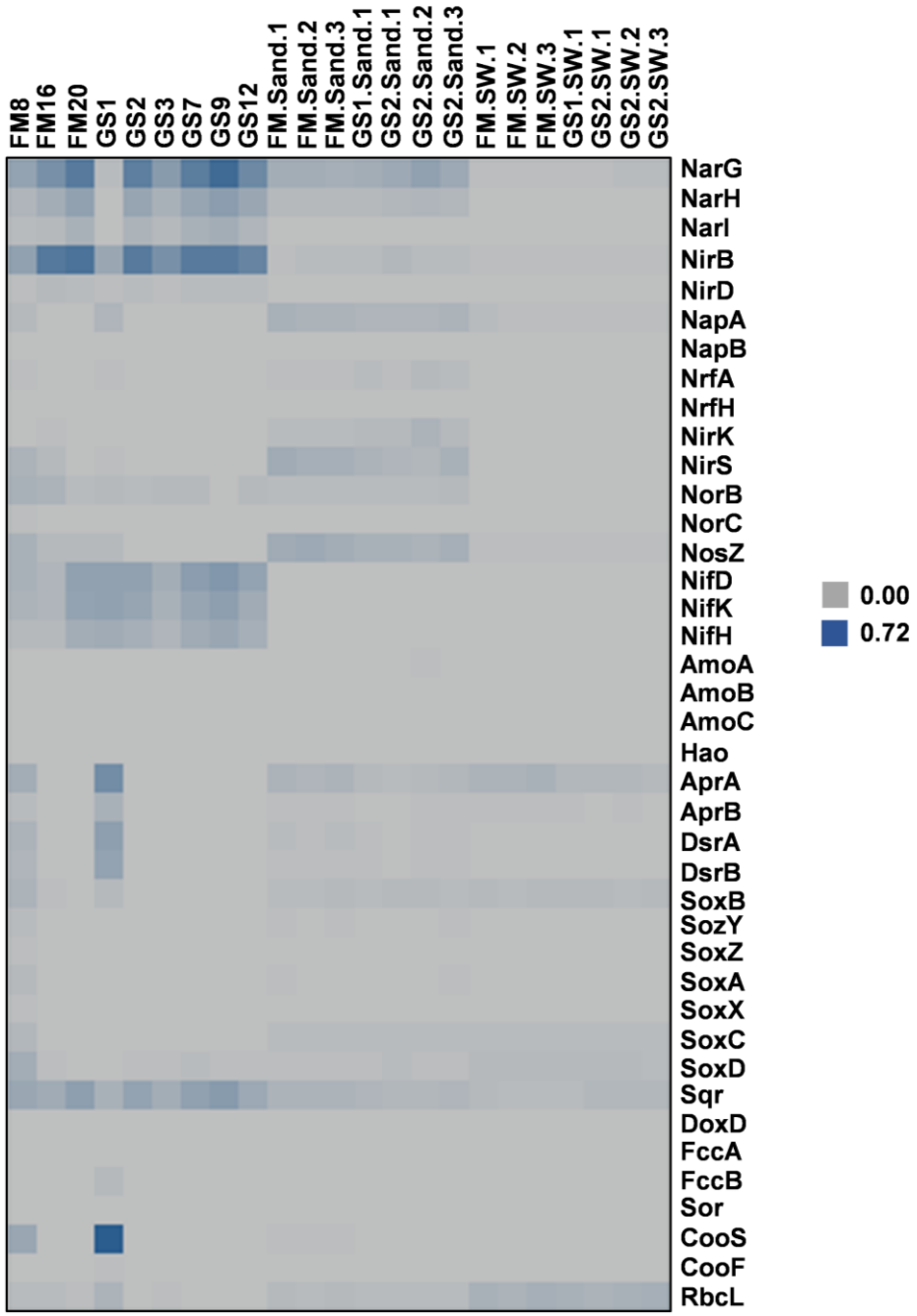
FM8
FM16
FM20
GS1
GS2
GS3
GS7
GS9
GS12
FM.Sand.1
FM.Sand.2
FM.Sand.3
GS1.Sand.1
GS2.Sand.1
GS2.Sand.2
GS2.Sand.3
FM.SW.1
FM.SW.2
FM.SW.3
GS1.SW.1
GS2.SW.1
GS2.SW.2
GS2.SW.3
NarG
NarH
NarI
NirB
NirD
NapA
NapB
NrfA
NrfH
NirK
NirS
NorB
NorC
NosZ
NifD
NifK
NifH
AmoA
AmoB
AmoC
Hao
AprA
AprB
DsrA
DsrB
SoxB
SozY
SoxZ
SoxA
SoxX
SoxC
SoxD
Sqr
DoxD
FccA
FccB
Sor
CooS
CooF
RbcL
0.00
0.72

B.

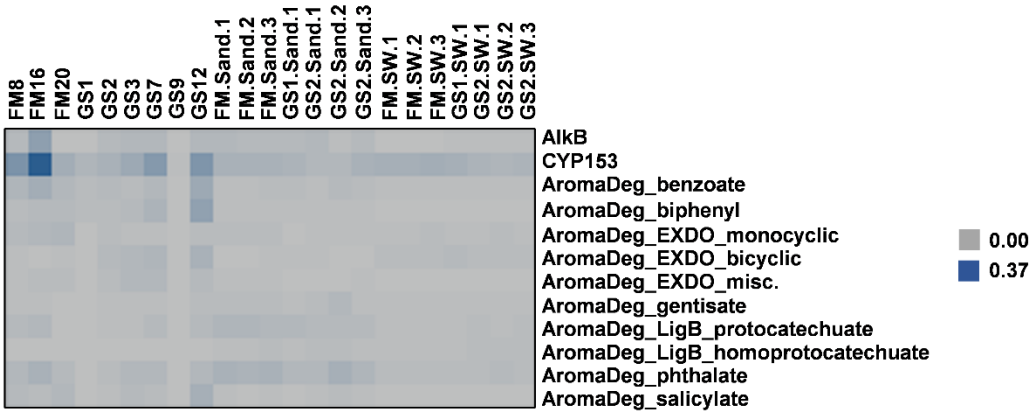
FM8
FM16
FM20
GS1
GS2
GS3
GS7
GS9
GS12
FM.Sand.1
FM.Sand.2
FM.Sand.3
GS1.Sand.1
GS2.Sand.1
GS2.Sand.2
GS2.Sand.3
FM.SW.1
FM.SW.2
FM.SW.3
GS1.SW.1
GS2.SW.1
GS2.SW.2
GS2.SW.3
AlkB
CYP153
AromaDeg_benzoate
AromaDeg_biphenyl
AromaDeg_EXDO_monocyclic
AromaDeg_EXDO_bicyclic
AromaDeg_EXDO_misc.
AromaDeg_gentisate
AromaDeg_LigB_protocatechuate
AromaDeg_LigB_homoprotocatechuate
AromaDeg_phthalate
AromaDeg_salicylate
0.00
0.37

C.

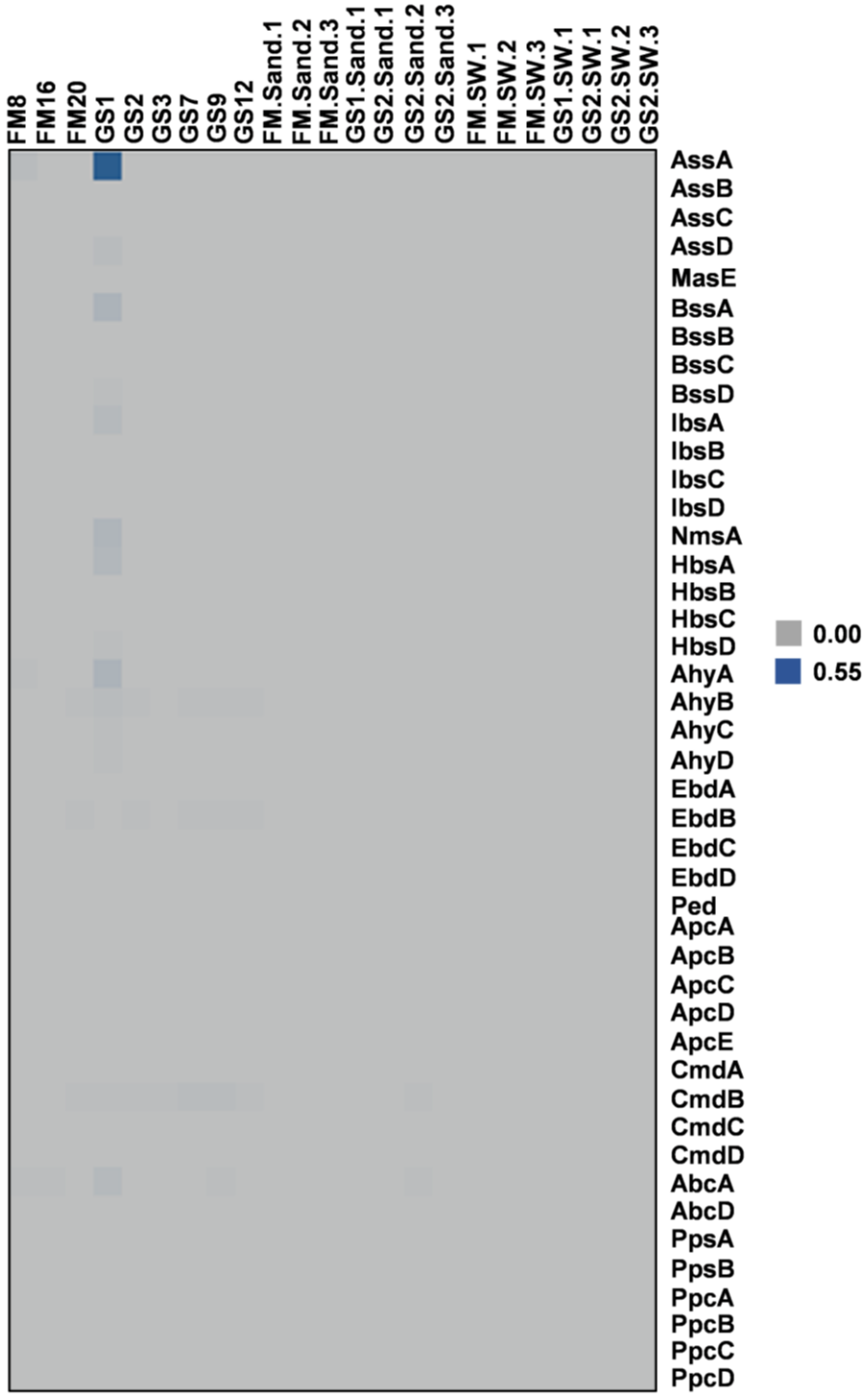
FM8
FM16
FM20
GS1
GS2
GS3
GS7
GS9
GS12
FM.Sand.1
FM.Sand.2
FM.Sand.3
GS1.Sand.1
GS2.Sand.1
GS2.Sand.2
GS2.Sand.3
FM.SW.1
FM.SW.2
FM.SW.3
GS1.SW.1
GS2.SW.1
GS2.SW.2
GS2.SW.3
AssA
AssB
AssC
AssD
MasE
BssA
BssB
BssC
BssD
IbsA
IbsB
IbsC
IbsD
NmsA
HbsA
HbsB
HbsC
HbsD
AhyA
AhyB
AhyC
AhyD
EbdA
EbdB
EbdC
EbdD
Ped
ApcA
ApcB
ApcC
ApcD
ApcE
CmdA
CmdB
CmdC
CmdD
AbcA
AbcD
PpsA
PpsB
PpcA
PpcB
PpcC
PpcD
0.00
0.55

D.

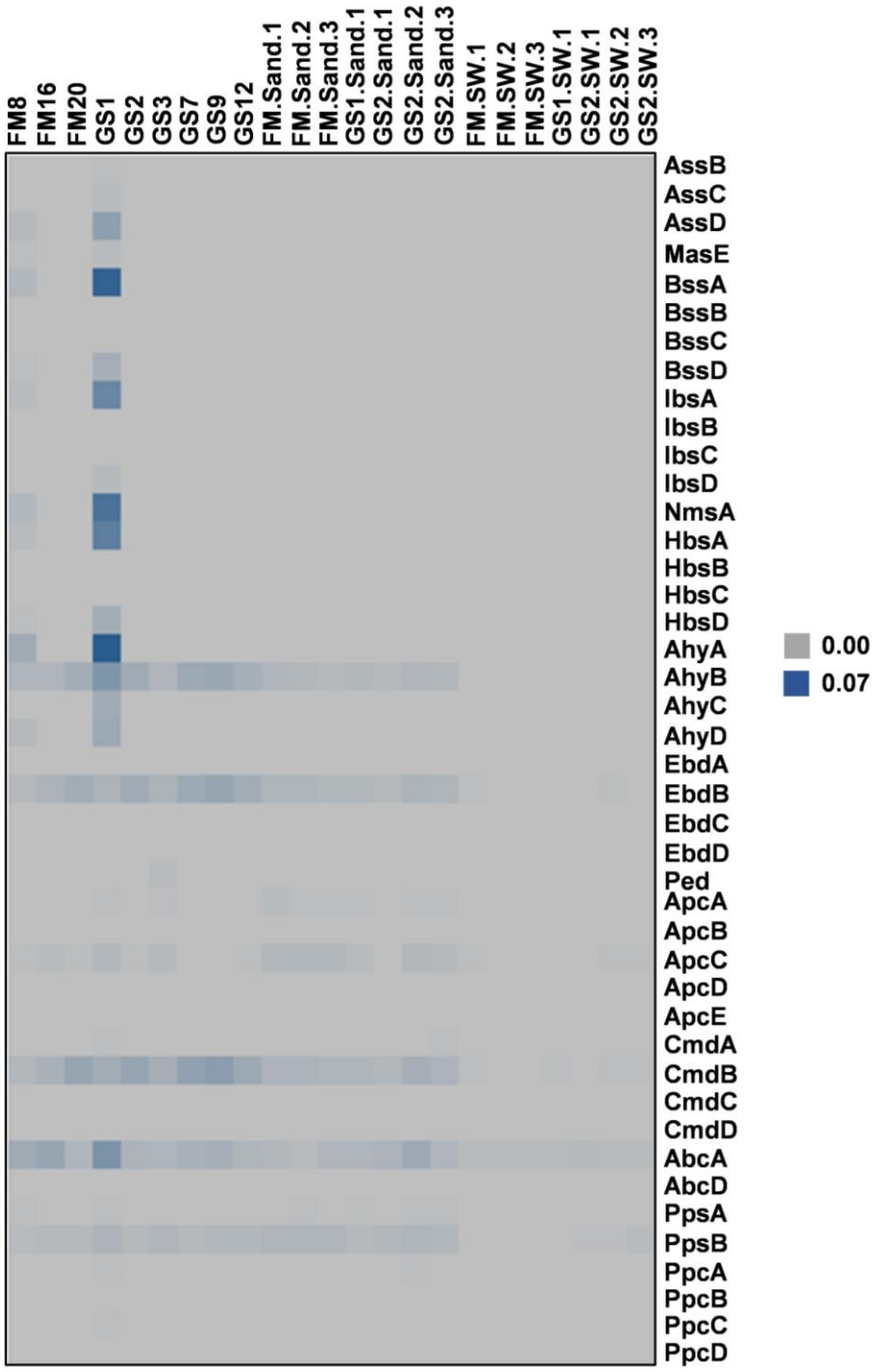
FM8
FM16
FM20
GS1
GS2
GS3
GS7
GS9
GS12
FM.Sand.1
FM.Sand.2
FM.Sand.3
GS1.Sand.1
GS2.Sand.1
GS2.Sand.2
GS2.Sand.3
FM.SW.1
FM.SW.2
FM.SW.3
GS1.SW.1
GS2.SW.1
GS2.SW.2
GS2.SW.3
AssB
AssC
AssD
MasE
BssA
BssB
BssC
BssD
IbsA
IbsB
IbsC
IbsD
NmsA
HbsA
HbsB
HbsC
HbsD
AhyA
AhyB
AhyC
AhyD
EbdA
EbdB
EbdC
EbdD
Ped
ApcA
ApcB
ApcC
ApcD
ApcE
CmdA
CmdB
CmdC
CmdD
AbcA
AbcD
PpsA
PpsB
PpcA
PpcB
PpcC
PpcD
0.00
0.07

REFERENCES

Aeppli C, Nelson RK, Radović JR, Carmichael CA, Valentine DL & Reddy CM. (2014) Recalcitrance and degradation of petroleum biomarkers upon abiotic and biotic natural weathering of Deepwater Horizon oil. *Environ Sci Technol* **48**:6726-6734.

Aeppli C, Carmichael CA, Nelson RK, Lemkau KL, Graham WM, Redmond MC, Valentine DL & Reddy CM. (2012) Oil weathering after the Deepwater Horizon disaster led to the formation of oxygenated residues. *Environ Sci Technol* **46**:8799-8807.

Andrews S. (2010) FastQC: a quality control tool for high throughput sequence data. Available online at: http://www.bioinformatics.babraham.ac.uk/projects/fastqc.

Atlas RM. (1995) Petroleum biodegradation and oil spill bioremediation. *Marine Poll Bull* **31**:178-182.

Atlas RM, Stoeckel DM, Faith SA, Minard-Smith A, Thorn JR & Benotti MJ. (2015) Oil biodegradation and oil-degrading microbial populations in marsh sediments impacted by oil from the Deepwater Horizon well blowout. *Environ Sci Technol* **49**:8356-8366.

Bacosa HP, Thyng KM, Plunkett S, Erdner DL & Liu Z. (2016) The tarballs on Texas beaches following the 2014 Texas City "Y" spill: modeling, chemical, and microbiological studies. *Marine Poll Bull* **109**:236-244.

Bælum J, Borglin S, Chakraborty R*, et al.* (2012) Deep-sea bacteria enriched by oil and dispersant from the Deepwater Horizon spill. *Environ Microbiol* **14**:2405-2416.

Biers EJ, Sun S & Howard EC. (2009) Prokaryotic genomes and diversity in surface ocean waters: interrogating the global ocean sampling metagenome. *Appl Environ Microbiol* **75**:2221-2229.

Bogan BW, Lahner LM, Sullivan WR & Paterek JR. (2003) Degradation of straight-chain aliphatic and high-molecular-weight polycyclic aromatic hydrocarbons by a strain of Mycobacterium austroafricanum. *J Appl Microbiol* **94**:230-239.

Bolger AM, Lohse M & Usadel B. (2014) Trimmomatic: a flexible trimmer for Illumina sequence data. *Bioinformatics* **30**:2114-2120.

Boll M & Fuchs G. (2005) Unusual reactions involved in anaerobic metabolism of phenolic compounds. *Biol Chem* **386**:989-997.

Bostic, JT (2016). Biodegradation of highly weathered DWH oil. Thesis, University of South Carolina, Columbia, South Carolina, USA.

Burback BL & Perry JJ. (1993) Biodegradation and biotransformation of groundwater pollutant mixtures by Mycobacterium vaccae. *Appl Environ Microbiol* **59**:1025-1029.

Callaghan AV, R.N. Austin, J.T. Groves, J.J. Kukor, R. Rabus, F. Widdel, *et al.* (2008) The complete genome sequence of *Desulfococcus oleovorans* Hxd3, a sulfate-reducing, alkane-degrading bacterium. Boston, MA

Callaghan AV, Morris BEL, Pereira IAC, McInerney MJ, Austin RN, Groves JT, Kukor JJ, Suflita JM, Young LY, Zylstra GJ & Wawrik B. (2012) The genome sequence of *Desulfatibacillum alkenivorans* AK-01: a blueprint for anaerobic alkane oxidation. *Environ Microbiol* **14**:101-113.

Callaghan AV & Wawrik B. (2016) *AnHyDeg: a curated database of anaerobic hydrocarbon degradation genes*. Available online at: https://github.com/AnaerobesRock/AnHyDeg.

Caporaso JG, Kuczynski J, Stombaugh J*, et al.* (2010a) QIIME allows analysis of high-throughput community sequencing data. *Nat Meth* **7**:335-336.

Caporaso JG, Bittinger K, Bushman FD, DeSantis TZ, Andersen GL & Knight R. (2010b) PyNAST: a flexible tool for aligning sequences to a template alignment. *Bioinformatics* **26**:266-267.

Churchill SA, Harper JP & Churchill PF. (1999) Isolation and characterization of a Mycobacterium species capable of degrading three- and four-ring aromatic and aliphatic hydrocarbons. *Appl Environ Microbiol* **65**:549-552.

Clement TP, Hayworth JS & Mulabagal V. (2011) Is submerged Deepwater Horizon oil degrading offshore? Comparison of the chemical signatures of tar mat samples deposited by Tropical Storm Lee in September 2011 with oil mousse samples collected in June 2010. http://eng.auburn.edu/files/acad_depts/civil/oil-spill-research.pdf.

Clement TP, Hayworth JS, Mulabugal V, John GF & Yin F. (2012) Impact of Hurricane Issac on mobilizing Deepwater Horizon oil spill residues along Alabama's coastline - a physicochemical characterization study. http://www.eng.auburn.edu/files/acad_depts/civil/oil-research-isaac.pdf.

Coulon F, McKew BA, Osborn AM, McGenity TJ & Timmis KN. (2007) Effects of temperature and biostimulation on oil-degrading microbial communities in temperate estuarine waters. *Environ Microbiol* **9**:177-186.

Dalyander PS, Long JW, Plant NG & Thompson DM. (2014) Assessing mobility and redistribution patterns of sand and oil agglomerates in the surf zone. *Marine Poll Bulletin* **80**:200-209.

Duarte M, Jauregui R, Vilchez-Vargas R, Junca H & Pieper DH. (2014) AromaDeg, a novel database for phylogenomics of aerobic bacterial degradation of aromatics. *Database*. bau: 118.

Dubinsky EA, Conrad ME, Chakraborty R*, et al.* (2013) Succession of hydrocarbon-degrading bacteria in the aftermath of the Deepwater Horizon oil spill in the Gulf of Mexico. *Environ Sci Technol* **47**:10860-10867.

Edgar RC. (2010) Search and clustering orders of magnitude faster than BLAST. *Bioinformatics* **26**:2460-2461.

Elango V, Urbano M, Lemelle KR & Pardue JH. (2014) Biodegradation of MC252 oil in oil:sand aggregates in a coastal headland beach environment. *Front Microbiol* **5**:161.

Fathepure BZ. (2014) Recent studies in microbial degradation of petroleum hydrocarbons in hypersaline environments. *Front Microbiol* **5**:173.

Friedrich CG, Rother D, Bardischewsky F, Quentmeier A & Fischer J. (2001) Oxidation of reduced inorganic sulfur compounds by bacteria: emergence of a common mechanism? *Appl Environ Microbiol* **67**:2873-2882.

Garrity GM, Bell JA & Lilburn T. (2015) Acidithiobacillales ord. nov. In: Whitman WB, *et al.* (eds.) *Bergey's Manual of Systematics of Archaea and Bacteria*. John Wiley & Sons, Inc.

Ghosh W & Dam B. (2009) Biochemistry and molecular biology of lithotrophic sulfur oxidation by taxonomically and ecologically diverse bacteria and archaea. *FEMS Microbiol Rev* **33**:999-1043.

Gobet A, Boer SI, Huse SM, van Beusekom JEE, Quince C, Sogin ML, Boetius A & Ramette A. (2012) Diversity and dynamics of rare and of resident bacterial populations in coastal sands. *ISME J* **6**:542-553.

Gros J, Reddy CM, Aeppli C, Nelson RK, Carmichael CA & Arey JS. (2014) Resolving biodegradation patterns of persistent saturated hydrocarbons in weathered oil samples from the Deepwater Horizon disaster. *Environ Sci Technol* **48**:1628-1637.

Gutierrez T, Singleton DR, Berry D, Yang T, Aitken MD & Teske A. (2013) Hydrocarbon-degrading bacteria enriched by the Deepwater Horizon oil spill identified by cultivation and DNA-SIP. *ISME J* **7**:2091-2104.

Hall GJ, Frysinger GS, Aeppli C, Carmichael CA, Gros J, Lemkau KL, Nelson RK & Reddy CM. (2013) Oxygenated weathering products of Deepwater Horizon oil come from surprising precursors. *Marine Poll Bull* **75**:140-149.

Hansen MA. (2010) Biopieces. Available online at: http://maasha.github.io/biopieces/.

Harayama S, Kishira H, Kasai Y & Shutsubo K. (1999) Petroleum biodegradation in marine environments. *J Mol Microbiol Biotechnol* **1**:63-70.

Hayworth J, Clement T & Valentine J. (2011) Deepwater Horizon oil spill impacts on Alabama beaches. *Hydrol Earth Syst Sci* **15**:3639-3649.

Head IM, Jones DM & Roling WFM. (2006) Marine microorganisms make a meal of oil. *Nat Rev Micro* **4**:173-182.

Heider J & Schühle K. (2013) Anaerobic biodegradation of hydrocarbons including methane. In: Rosenberg E, DeLong EF, Lory S, Stackebrandt E, & Thompson F (eds.). *The Prokaryotes: Prokaryotic Physiology and Biochemistry,*(Rosenberg E, DeLong EF, Lory S, Stackebrandt E & Thompson F, eds.), p.605-634. Springer-Verlag, Berlin, Heidelberg.

Heider J, Szaleniec M, Martins BM, Seyhan D, Buckel W & Golding BT. (2016a) Structure and function of benzylsuccinate synthase and related fumarate-adding glycyl radical enzymes. *J Mol Microbiol Biotechnol* **26**:9-44.

Heider J, Szaleniec M, Sünwoldt K & Boll M. (2016b) Ethylbenzene dehydrogenase and related molybdenum enzymes involved in oxygen-independent alkyl chain hydroxylation. *J Mol Microbiol Biotechnol* **26**:45-62.

Heinz S, Benner C, Spann N, Bertolino E, Lin YC, Laslo P, Cheng JX, Murre C, Singh H & Glass CK. (2010) Simple combinations of lineage-determining transcription factors prime cis-regulatory elements required for macrophage and B cell identities. *Mol Cell* **38**:576-589.

Horel A, Bernard RJ & Mortazavi B. (2014) Impact of crude oil exposure on nitrogen cycling in a previously impacted Juncus roemerianus salt marsh in the northern Gulf of Mexico. *Environ Sci Pollut Res* **21**:6982-6993.

Johnson HA, Pelletier DA & Spormann AM. (2001) Isolation and characterization of anaerobic ethylbenzene dehydrogenase, a novel Mo-Fe-S enzyme. *J Bacteriol* **183**:4536-4542.

Jørgensen BB. (1982) Mineralization of organic matter in the sea bed - the role of sulphate reduction. *Nature* **296**:643-645.

Joye SB, Teske AP & Kostka JE. (2014) Microbial dynamics following the Macondo oil well blowout across Gulf of Mexico environments. *BioScience* **64**:766-777.

Kappell AD, Wei Y, Newton RJ, Van Nostrand JD, Zhou J, McLellan SL & Hristova KR. (2014) The polycyclic aromatic hydrocarbon degradation potential of Gulf of Mexico native coastal microbial communities after the Deepwater Horizon oil spill. *Front Microbiol* **5**:205.

Kasai Y, Takahata Y, Hoaki T & Watanabe K. (2005) Physiological and molecular characterization of a microbial community established in unsaturated, petroleum-contaminated soil. *Environ Microbiol* **7**:806-818.

Kim SJ, Kweon O & Cerniglia CE. (2010) Degradation of polycyclic aromatic hydrocarbons by Mycobacterium strains. In: Timmis KN, McGenity TJ, van der Meer JR, & de Lorenzo V (eds.). *Handbook of Hydrocarbon and Lipid Microbiology*. p.1865-1879. Springer-Verlag, Berlin, Heidelberg.

Kimes NE, Callaghan AV, Suflita JM & Morris PJ. (2014) Microbial transformation of the Deepwater Horizon oil spill—past, present, and future perspectives. *Front Microbiol* **5**:603.

King GM, Smith CB, Tolar B & Hollibaugh JT. (2012) Analysis of composition and structure of coastal to mesopelagic bacterioplankton communities in the northern Gulf of Mexico. *Front Microbiol* **3**:438.

King GM, Kostka JE, Hazen TC, & Sobecky PA. (2015) Microbial responses to the Deepwater Horizon oil spill: from coastal wetlands to the deep sea. *Annu Rev Mar Sci* **7**:377-401.

Klindworth A, Pruesse E, Schweer T, Peplies J, Quast C, Horn M & Glöckner FO. (2013) Evaluation of general 16S ribosomal RNA gene PCR primers for classical and next-generation sequencing-based diversity studies. *Nucleic Acids Res* **41**.

Kodama Y, Stiknowati LI, Ueki A, Ueki K & Watanabe K. (2008) Thalassospira tepidiphila sp. nov., a polycyclic aromatic hydrocarbon-degrading bacterium isolated from seawater. *Int J Syst Evol Microbiol* **58**:711-715.

Kostka JE, Prakash O, Overholt WA, Green SJ, Freyer G, Canion A, Delgardio J, Norton N, Hazen TC & Huettel M. (2011) Hydrocarbon-degrading bacteria

and the bacterial community response in Gulf of Mexico beach sands impacted by the Deepwater Horizon oil spill. *Appl Environ Microbiol* **77**:7962-7974.

Kowalchuk GA & Stephen JR. (2001) Ammonia-oxidizing bacteria: a model for molecular microbial ecology. *Annu Rev Microbiol* **55**:485-529.

Krueger F. (2015) Trim Galore. Available online at: https://www.bioinformatics.babraham.ac.uk/projects/trim_galore/.

Leahy JG & Colwell RR. (1990) Microbial degradation of hydrocarbons in the environment. *Microbiol Rev* **54**:305-315.

Li H, Zhang Q, Wang XL, Ma XY, Lin KF, Liu YD, Gu JD, Lu SG, Shi L, Lu Q, & Shen TT. (2012) Biodegradation of benzene homologues in contaminated sediment of the East China Sea. *Bioresour Technol* **124**:129-136.

Liang B, Wang LY, Mbadinga SM, Liu JF, Yang S-Z, Gu JD & Mu BZ. (2015) Anaerolineaceae and Methanosaeta turned to be the dominant microorganisms in alkanes-dependent methanogenic culture after long-term of incubation. *AMB Express* **5**:37.

Liang B, Wang LY, Zhou Z, Mbadinga SM, Zhou L, Liu JF, Yang SZ, Gu JD & Mu BZ. (2016) High frequency of Thermodesulfovibrio spp. and Anaerolineaceae in association with Methanoculleus spp. in a long-term incubation of n-alkanes-degrading methanogenic enrichment culture. *Front Microbiol* **7**:1431.

Liu Z & Liu J. (2013) Evaluating bacterial community structures in oil collected from the sea surface and sediment in the northern Gulf of Mexico after the Deepwater Horizon oil spill. *MicrobiologyOpen* **2**:492-504.

Looper JK, Cotto A, Kim B-Y, Lee MK, Liles MR, Chadhain SMN & Son A. (2013) Microbial community analysis of Deepwater Horizon oil-spill impacted sites along the Gulf coast using functional and phylogenetic markers. *Env Sci Process Impact* **15**:2068-2079.

Mackintosh ME. (1978) Nitrogen fixation by Thiobacillus ferrooxidans. *Microbiology* **105**:215-218.

Martin M. (2011) Cutadapt removes adapter sequences from high-throughput sequencing reads. EMBnet.journal. **17**:10-12.

McCune B, Grace JB & Urban DL. (2002) *Analysis of ecological communities*. Oregon, USA: MjM Software.

McGenity TJ, Folwell BD, McKew BA & Sanni GO. (2012) Marine crude-oil biodegradation: a central role for interspecies interactions. *Aquat Biosyst* **8**:10.

McNutt MK, Camilli R, Guthrie GD, Hsieh PA, Labson VF, Lehr WJ, Maclay D, Ratzel AC & Sogge MK. (2011) *Assessment of flow rate estimates for the Deepwater Horizon/Macondo well oil spill*. US Department of the Interior.

McNutt MK, Camilli R, Crone TJ, Guthrie GD, Hsieh PA, Ryerson TB, Savas O & Shaffer F. (2012) Review of flow rate estimates of the Deepwater Horizon oil spill. *Proc Natl Acad Sci* **109**:20260-20267.

Michel J, Owens EH, Zengel S, Graham A, Nixon Z, Allard T, Holton W, Reimer PD, Lamarche A, White M, Rutherford N, Childs C, Mauseth G, Challenger G, & Taylor E. (2013) Extent and degree of shoreline oiling: Deepwater Horizon oil spill, Gulf of Mexico, USA. *PLOS ONE* **8**:e65087.

Mills HJ, Hunter E, Humphrys M, Kerkhof L, McGuinness L, Huettel M & Kostka JE. (2008) Characterization of nitrifying, denitrifying, and overall bacterial communities in permeable marine sediments of the northeastern Gulf of Mexico. *Appl Environ Microbiol* **74**:4440-4453.

Mishamandani S, Gutierrez T, Berry D & Aitken MD. (2016) Response of the bacterial community associated with a cosmopolitan marine diatom to crude oil shows a preference for the biodegradation of aromatic hydrocarbons. *Environ Microbiol* **18**:1817-1833.

Mortazavi B, Horel A, Beazley MJ & Sobecky PA. (2013) Intrinsic rates of petroleum hydrocarbon biodegradation in Gulf of Mexico intertidal sandy sediments and its enhancement by organic substrates. *J Hazard Mater* **244–245**:537-544.

Mulabagal V, Yin F, John GF, Hayworth JS & Clement TP. (2013) Chemical fingerprinting of petroleum biomarkers in Deepwater Horizon oil spill samples collected from Alabama shoreline. *Mar Poll Bull* **70**:147-154.

Newton RJ, Huse SM, Morrison HG, Peake CS, Sogin ML & McLellan SL. (2013) Shifts in the microbial community composition of Gulf Coast beaches following beach oiling. *PLOS ONE* **8**:e74265.

Nie Y, Chi CQ, Fang H, Liang JL, Lu SL, Lai GL, Tang YQ & Wu XL. (2014) Diverse alkane hydroxylase genes in microorganisms and environments. *Sci Rep* **4**:4968.

Nixon Z, Zengel S, Baker M, Steinhoff M, Fricano G, Rouhani S & Michel J. (2016) Shoreline oiling from the Deepwater Horizon oil spill. *Mar Poll Bul* **107**:170-178.

National Research Council, NRC. (2003) *Oil in the sea III: inputs, fates, and effects*. National Academies Press. Washington, D.C.

Operational Science Advisory Team, OSAT-II. (2011) Summary report for fate and effects of remnant oil remaining in the beach environment. https://www.restorethegulf.gov/sites/default/files/u316/OSAT-2%20Report%20no%20ltr.pdf.

Operational Science Advisory Team, OSAT-III. (2013) Investigation of recurring residual oil in discrete shoreline areas in the eastern area of responsibility. https://www.restorethegulf.gov/sites/default/files/u372/OSAT%20III%20Eastern%20States.pdf.

Pereira IAC, Ramos AR, Grein F, Marques MC, da Silva SM, & Venceslau SS. (2011). A comparative genoic analysis of energy metabolism in sulfate reducing bacteria and archaea. *Front Microbiol*. **2**:69.

Picó Y & Barceló D. (2015) Transformation products of emerging contaminants in the environment and high-resolution mass spectrometry: a new horizon. *Anal Bioanal Chem* **407**:6257-6273.

Prince RC. (1993) Petroleum spill bioremediation in marine environments. *Crit Rev Microbiol* **19**:217-240.

Pruesse E, Quast C, Knittel K, Fuchs BM, Ludwig W, Peplies J & Glöckner FO. (2007) SILVA: a comprehensive online resource for quality checked and aligned ribosomal RNA sequence data compatible with ARB. *Nucleic Acids Res* **35**:7188-7196.

Quast C, Pruesse E, Yilmaz P, Gerken J, Schweer T, Yarza P, Peplies J & Glöckner FO (2013) The SILVA ribosomal RNA gene database project: improved data processing and web-based tools. *Nucleic Acids Res* **41**:D590-D596.

Rabus R, Boll M, Heider J*, et al.* (2016) Anaerobic microbial degradation of hydrocarbons: from enzymatic reactions to the environment. *J Mol Microbiol Biotechnol* **26**:5-28.

Radović JR, Aeppli C, Nelson RK, Jimenez N, Reddy CM, Bayona JM & Albaigés J. (2014) Assessment of photochemical processes in marine oil spill fingerprinting. *Marine Poll Bull* **79**:268-277.

Ramos AR, Grein F, Oliveira GP, Venceslau SS, Keller KL, Wall JD & Pereira IAC. (2015) The FlxABCD-HdrABC proteins correspond to a novel NADH dehydrogenase/heterodisulfide reductase widespread in anaerobic bacteria and

involved in ethanol metabolism in Desulfovibrio vulgaris Hildenborough. *Environ Microbiol* **17**:2288-2305.

Ramseur JL. (2010) Deepwater Horizon oil spill: the fate of the oil. Congressional Research Service, Washington, D.C. Congressional Research Service Report 7-5700. fas.org/spg/crs.misc.R41531.pdf.

Ray PZ, Chen H, Podgorski DC, McKenna AM & Tarr MA. (2014) Sunlight creates oxygenated species in water-soluble fractions of Deepwater horizon oil. *J Hazard Mater* **280**:636-643.

Redmond MC & Valentine DL. (2012) Natural gas and temperature structured a microbial community response to the Deepwater Horizon oil spill. *Proc Natl Acad Sci USA* **109**:20292-20297.

Rosario-Passapera R, Keddis R, Wong R, Lutz RA, Starovoytov V & Vetriani C. (2012) Parvibaculum hydrocarboniclasticum sp. nov., a mesophilic, alkane-oxidizing alphaproteobacterium isolated from a deep-sea hydrothermal vent on the East Pacific Rise. *Int J Syst Evol Microbiol* **62**:2921-2926.

Ruddy BM, Huettel M, Kostka JE, Lobodin VV, Bythell BJ, McKenna AM, Aeppli C, Reddy CM, Nelson RK, Marshall AG, & Rodgers RP. (2014) Targeted petroleomics: analytical investigation of Macondo well oil oxidation products from Pensacola Beach. *Energy & Fuels* **28**:4043-4050.

Ruiz ON, Brown LM, Striebich RC, Smart CE, Bowen LL, Lee JS, Little BJ, Mueller SS & Gunasekera TS. (2016) Effect of conventional and alternative fuels on a marine bacterial community and the significance to bioremediation. *Energy & Fuels* **30**:434-444.

Shao Z, Yuan J, Lai Q & Zheng T. (2015) The diversity of PAH-degrading bacteria in a deep-sea water column above the Southwest Indian Ridge. *Front Microbiol* **6**:853.

Sherry A, Gray ND, Ditchfield AK, Aitken CM, Jones DM, Röling WFM, Hallmann C, Larter SR, Bowler BFJ & Head IM. (2013) Anaerobic biodegradation of crude oil under sulphate-reducing conditions leads to only modest enrichment of recognized sulphate-reducing taxa. *Int Biodeterior Biodegradation* **81**:105-113.

SILVA. (2007) SILVA: High quality ribosomal RNA databases. Available online at: https://www.arb-silva.de/.

Simister RL, Poutasse CM, Thurston AM, Reeve JL, Baker MC & White HK. (2015) Degradation of oil by fungi isolated from Gulf of Mexico beaches. *Marine Poll Bull* **100**:327-333.

Solano-Serena F, Marchal R, Casarégola S, Vasnier C, Lebeault JM & Vandecasteele JP. (2000) A Mycobacterium strain with extended capacities for degradation of gasoline hydrocarbons. *Appl Environ Microbiol* **66**:2392-2399.

Strijkstra A, Trautwein K, Jarling R, Wöhlbrand L, Dörries M, Reinhardt R, Drozdowska M, Golding BT, Wilkes H & Rabus R. (2014) Anaerobic activation of p-cymene in denitrifying Betaproteobacteria: methyl group hydroxylation versus addition to fumarate. *Appl Environ Microbiol* **80**:7592-7603.

Tarr M, Zito P, Overton EB, Olson GM, Adhikari PL & Reddy CM. (2016) Weathering of oil spilled in the marine environment. *Oceanography*. **29**:126-135.

Thauer RK, Kaster AK, Seedorf H, Buckel W, & Hedderich R. (2008). Methanogenic archaea: ecologically relevant differences in energy conservation. *Nature Rev Microbiol*. **6**:579-591.

Urbano M, Elango V & Pardue JH. (2013) Biogeochemical characterization of MC252 oil:sand aggregates on a coastal headland beach. *Marine Poll Bull* **77**:183-191.

Valdés J, Pedroso I, Quatrini R, Dodson RJ, Tettelin H, Blake R, Eisen JA & Holmes DS. (2008) Acidithiobacillus ferrooxidans metabolism: from genome sequence to industrial applications. *BMC Genomics* **9**:597-597.

Valentine DL, Fisher GB, Bagby SC, Nelson RK, Reddy CM, Sylva SP & Woo MA. (2014) Fallout plume of submerged oil from Deepwater Horizon. *Proc Natl Acad Sci* **111**:15906-15911.

van Niftrik L & Jetten MSM. (2012) Anaerobic ammonium-oxidizing bacteria: unique microorganisms with exceptional properties. *Microbiol Mol Biol Rev* **76**:585-596.

Vila J, Nieto JM, Mertens J, Springael D & Grifoll M. (2010) Microbial community structure of a heavy fuel oil-degrading marine consortium: linking microbial dynamics with polycyclic aromatic hydrocarbon utilization. *FEMS Microbiol Ecol* **73**:349-362.

Wang L, Wang W, Lai Q & Shao Z. (2010) Gene diversity of CYP153A and AlkB alkane hydroxylases in oil-degrading bacteria isolated from the Atlantic Ocean. *Environ Microbiol* **12**:1230-1242.

Warnock AM, Hagen SC & Passeri DL. (2015) Marine tar residues: a review. *Water Air Soil Pollut* **226**:68.

Watkinson RJ & Morgan P. (1991) Physiology of aliphatic hydrocarbon-degrading microorganisms. In: Ratledge, C (ed.). P*hysiology of Biodegradative Microorganisms.* p.79-92. Springer Netherlands, Dordrecht.

Wawrik B, Mendivelso M, Parisi VA*,* Suflita JM, Davidova IA, Marks CR, Van Nostrand JD, Liang Y, Zhou J, Huizinga BJ, Strapoć D, & Callaghan AV. (2012) Field and laboratory studies on the bioconversion of coal to methane in the San Juan Basin. *FEMS Microbiol Ecol* **81**:26-42.

White HK, Wang CH, Williams PL, Findley DM, Thurston AM, Simister RL, Aeppli C, Nelson RK & Reddy CM. (2016) Long-term weathering and continued oxidation of oil residues from the Deepwater Horizon spill. *Marine Poll Bull* **113**:380-386.

Wilkes H, Buckel W, Golding BT & Rabus R. (2016) Metabolism of hydrocarbons in alkane-utilizing anaerobic bacteria. *J Mol Microbiol Biotechnol* **26**:138-151.

Williams TJ & Cavicchioli R. (2014) Marine metaproteomics: deciphering the microbial metabolic food web. *Trends Microbiol* **22**:248-260.

Xie C, Mao X, Huang J, Ding Y, Wu J, Dong S, Kong L, Gao G, Li CY & Wei L. (2011) KOBAS 2.0: a web server for annotation and identification of enriched pathways and diseases. *Nucleic Acids Res* **39**:W316-W322.

Yang T, Nigro LM, Gutierrez T, D'Ambrosio L, Joye SB, Highsmith R & Teske A. (2016) Pulsed blooms and persistent oil-degrading bacterial populations in the water column during and after the Deepwater Horizon blowout. *Deep Sea Res Part II Top Stud Oceanogr* **129**:282-291.

Yergeau E, Sanschagrin S, Beaumier D & Greer CW. (2012) Metagenomic analysis of the bioremediation of diesel-contaminated Canadian High Arctic soils. *PLOS ONE* **7**:e30058.

Zehr JP & Kudela RM. (2011) Nitrogen cycle of the open ocean: from genes to ecosystems. *Annu Rev Mar Sci* **3**:197-225.

Zhao B, Wang H, Mao X & Li R. (2008) Biodegradation of phenanthrene by a halophilic bacterial consortium under aerobic conditions. *Curr Microbiol* **58**:205-210.

Zinger L, Amaral-Zettler LA, Fuhrman JA, Horner-Devine MC, Huse SM, Welch DBM, Martiny JBH, Sogin M, Boetius A & Ramette A. (2011) Global patterns of bacterial beta-diversity in seafloor and seawater ecosystems. *PLOS ONE* **6**:e24570.

Appendix I: Chapter 1 Supplemental Materials

Table S1. Longitudinal and latitudinal coordinates of stations sampled in Chesapeake Bay.

Station Designation	Latitude	Longitude	Salinity PSU	Water Temp. ˚C
908	39° 08.00N	76° 19.84W	9.9	28
858	38° 58.01N	76° 23.04W	11.9	29
818	38° 17.79N	76° 17.28W	15.3	29
707	37° 07.02N	76° 06.94W	27.3	24

Table S2. Alkylsuccinate synthase (*assA*) and benzylsuccinate synthase (*bssA*) primer sequences used for the interrogation of Chesapeake Bay sediments (adapted from Callaghan *et al.*, 2010).

Primer Set	Alkylsuccinate Synthase (*assA*) and Benzylsuccinate Synthase (*bssA*) Primer Sequences[a]		Predicted Amplicon Size (bp)	Target
1[b]	*ass/bss*F: *ass/bss*R:	5'-TTTGAGTGCATCCGCCAYGGICT-3' 5'-TCGTCRTTGCCCCATTTIGGIGC-3'	*assA*: 661 *bssA*: 682	*assA* *bssA*
2	1213F: 1987R:	5'-GACATGACCGAYGCCATYCT-3' 5'-TCRTCGTCRTTGCCCCAYTT-3'	793	*bssA*
3	1294F: 1936R:	5'-TTSGARTGCATCCGNCACGGN-3' 5'-TCRTCATTNCCCCAYTTNGG-3'	661	*assA*
4	1294F: 2457R:	5'-TTSGARTGCATCCGNCACGGN-3' 5'-TTGTCCTGNGTYTTGCGG-3'	1180	*assA*
5	1294F: 1936R:	5'-TTYGAGTGYATNCGCCASGGC-3' 5'-TCRTCATTNCCCCAYTTNGG-3'	661	*assA*
6	1294F: 2457R:	5'-TTYGAGTGYATNCGCCASGGC-3' 5'-TTGTCCTGNGTYTTGCGG-3'	1180	*assA*
7	1432F: 1936R:	5'-CCNACCACNAAGCAYGG-3' 5'-TCRTCATTNCCCCAYTTNGG-3'	523	*assA*
8	1432F: 2457R	5'-CCNACCACNAAGCAYGG-3' 5'-TTGTCCTGNGTYTTGCGG-3'	1042	*assA*
9[b]	1432F: *ass/bss*R:	5'-CCNACCACNAAGCAYGG-3' 5'-TCGTCRTTGCCCCATTTIGGIGC-3'	523	*assA*

[a]Positions within the *assA* gene are relative *to assA1* (2,505 bp) in *Desulfatibacillum alkenivorans* strain AK-01 (Accession number DQ826035); Positions within the *bssA* gene are relative to *bssA* (2,586 bp) in *Thauera aromatica* K172 (Accession number AJ001848). [b]The *ass/bss* F positions relative to *assA1* and *bssA* are 1294 and 1321, respectively; the *ass/bss* R positions in *assA1* and *bssA* are 1933 and 1981, respectively.

Table S3. Microcosms established with sediment core material under **(A)** sulfate-reducing conditions and **(B)** methanogenic conditions. All treatments were established in triplicate. Initial sulfate concentrations were approximately 25 mM; hexadecane was amended as an overlay. Sterile controls were autoclaved at 121°C for three consecutive days. Positive controls were amended with *Desulfatibacillum alkenivorans* strain AK-01 (10% v/v). An X indicates inclusion into the microcosm.

(A) Sulfate-Reducing Microcosms

Treatment	Sulfate	Sediment	Autoclaved	$C_{16}H_{34}$	*D. alkenivorans* AK-01
Active enrichments	X	X		X	
Positive controls	X	X		X	X
Background controls	X	X			
Abiotic media controls	X			X	
Sterile controls	X	X	X	X	

(B) Methanogenic Microcosms

Treatment	Sulfate	Sediment	Autoclaved	$C_{16}H_{34}$	*D. alkenivorans* AK-01
Active enrichments		X		X	
Positive controls		X		X	X
Background controls		X			
Abiotic media controls				X	
Sterile controls		X	X	X	

Table S4. Phylogenetic analysis of bacterial 16S rRNA genes detected in Chesapeake Bay sediments at the family level of taxonomic classification. All data are shown as percentages of detected sequences for each respective sequence library. Note: Horizon 6 at Station 908 is designated as 908D.

	908 A %	908 B %	908 C %	908D A %	908D B %	908D C %	858 A %	858 B %	858 C %	818 A %	818 B %	818 C %	707 A %	707 B %	707 C %
Acidobacteria;Acidobacteria_Gp1;Gp1	0.40	0.28	0.23	0.34	0.20	0.16	0.05	0.18	0.07	0.13	0.03	0.18	0.19	0.30	0.23
Acidobacteria;Acidobacteria_Gp21;Gp21	0.77	0.74	0.94	0.54	0.40	0.28	0.64	0.47	0.41	0.00	0.11	0.13	0.12	0.09	0.15
Acidobacteria;Acidobacteria_Gp22;Gp22	0.44	0.84	0.58	0.51	0.14	0.06	0.09	0.10	0.12	0.00	0.03	0.03	0.02	0.05	0.03
Acidobacteria;Acidobacteria_Gp23;Gp23	0.80	0.59	0.74	0.58	0.51	0.28	0.80	0.76	0.67	0.00	0.05	0.13	0.24	0.12	0.30
Acidobacteria;Acidobacteria_Gp3;Gp3	0.09	0.06	0.25	0.58	0.40	0.32	0.14	0.08	0.31	0.28	0.16	0.28	0.32	0.21	0.30
Acidobacteria;Acidobacteria_Gp4;Gp4	0.00	0.06	0.05	0.00	0.00	0.00	0.00	0.00	0.00	0.00	0.00	0.00	0.00	0.00	0.00
Acidobacteria;Acidobacteria_Gp5;Gp5	0.00	0.00	0.05	0.00	0.00	0.00	0.00	0.03	0.02	0.00	0.00	0.00	0.00	0.00	0.00
Acidobacteria;Acidobacteria_Gp6;Gp6	0.69	0.43	0.33	0.27	0.17	0.00	0.05	0.00	0.10	0.00	0.00	0.05	0.00	0.00	0.00
Acidobacteria;Acidobacteria_Gp9;Gp9	0.02	0.06	0.08	0.00	0.06	0.03	0.00	0.00	0.00	0.00	0.00	0.08	0.19	0.19	0.23
Acidobacteria;Holophagae;Holophagales;Holophagaceae	0.04	0.03	0.05	0.03	0.03	0.03	0.00	0.05	0.02	0.00	0.00	0.03	0.00	0.00	0.00
Actinobacteria;Actinobacteria;Acidimicrobidae;Acidimicrobiales	0.33	0.16	0.30	0.47	0.34	0.19	0.18	0.24	0.12	0.03	0.00	0.00	0.02	0.09	0.13
Actinobacteria;Actinobacteria;Acidimicrobidae;Acidimicrobidae_incertae_sedis	0.33	0.22	0.18	0.20	0.23	0.06	0.02	0.10	0.12	0.00	0.08	0.03	0.07	0.12	0.03
Actinobacteria;Actinobacteria;Acidimicrobidae;unclassified_Acidimicrobidae	0.29	0.43	0.38	0.30	0.28	0.09	0.39	0.21	0.31	0.00	0.05	0.03	0.00	0.00	0.05
Actinobacteria;Actinobacteria;Actinobacteridae;Actinomycetales	0.71	0.96	0.64	2.24	1.42	2.47	0.66	0.84	0.81	1.94	1.70	1.95	1.36	2.04	1.93

Actinobacteria;Actinobacteria;Rubrobacteridae;Rubrobacterales	0.00	0.00	0.00	0.03	0.00	0.06	0.00	0.00	0.00	0.08	0.03	0.00	0.05	0.09	0.10
Actinobacteria;Actinobacteria;Rubrobacteridae; Solirubrobacterales	0.09	0.03	0.05	0.03	0.09	0.00	0.05	0.03	0.05	0.10	0.16	0.05	0.00	0.00	0.05
Actinobacteria;Actinobacteria;unclassified_Actinobacteria	0.15	0.03	0.08	0.07	0.14	0.13	0.37	0.31	0.45	0.08	0.03	0.28	0.46	0.42	0.98
Aquificae;Aquificae;Aquificales;Desulfurobacteriaceae	0.00	0.00	0.00	0.00	0.00	0.00	0.02	0.00	0.00	0.00	0.08	0.08	0.00	0.00	0.00
Bacteroidetes;Bacteroidetes_incertae_sedis;Prolixibacter	0.00	0.00	0.00	0.00	0.00	0.00	0.05	0.05	0.10	0.00	0.00	0.00	0.00	0.00	0.00
Bacteroidetes;Bacteroidia;Bacteroidales;Porphyromonadaceae	0.11	0.06	0.10	0.00	0.00	0.00	0.11	0.13	0.00	0.03	0.00	0.00	0.02	0.00	0.03
Bacteroidetes;Flavobacteria;Flavobacteriales;Cryomorphaceae	0.07	0.16	0.05	0.64	0.43	0.57	0.57	0.66	0.36	0.05	0.03	0.03	0.02	0.02	0.05
Bacteroidetes;Flavobacteria;Flavobacteriales;Flavobacteriaceae	1.99	3.29	2.36	0.03	0.00	0.00	1.28	1.81	2.03	0.00	0.03	0.15	0.02	0.00	0.00
Bacteroidetes;Flavobacteria;Flavobacteriales; unclassified_Flavobacteriales	0.00	0.00	0.00	0.00	0.00	0.00	0.00	0.03	0.00	0.00	0.00	0.10	0.00	0.00	0.00
Bacteroidetes;Sphingobacteria;Sphingobacteriales; Cytophagaceae	0.22	0.09	0.23	0.00	0.00	0.00	0.00	0.00	0.00	0.10	0.00	0.00	0.00	0.00	0.00
Bacteroidetes;Sphingobacteria;Sphingobacteriales; Flammeovirgaceae	0.49	0.25	0.46	0.03	0.00	0.06	0.05	0.03	0.05	0.08	0.00	0.00	0.02	0.14	0.03
Bacteroidetes;Sphingobacteria;Sphingobacteriales; Saprospiraceae	0.13	0.00	0.03	0.00	0.00	0.00	0.00	0.00	0.00	0.00	0.00	0.00	0.00	0.00	0.00
Bacteroidetes;Sphingobacteria;Sphingobacteriales; unclassified_Sphingobacteriales	0.07	0.00	0.08	0.07	0.00	0.16	0.09	0.08	0.05	0.00	0.00	0.00	0.00	0.00	0.00
Bacteroidetes;unclassified_Bacteroidetes;Other	1.57	1.99	1.47	0.58	0.60	0.19	0.85	0.58	0.72	0.36	0.13	0.46	0.49	0.49	0.88
Chloroflexi;Anaerolineae;Anaerolineales;Anaerolineaceae	1.28	1.24	1.52	1.12	1.53	1.90	0.94	0.71	1.22	0.43	0.76	0.97	1.80	1.67	2.13
Chloroflexi;Caldilineae;Caldilineales;Caldilineaceae	0.33	0.22	0.20	0.20	0.31	0.32	0.16	0.16	0.10	0.08	0.16	0.23	0.36	0.44	0.40
Chloroflexi;Chloroflexi;Chloroflexales;Chloroflexaceae	0.11	0.03	0.20	1.08	1.19	0.98	0.80	0.16	0.45	0.00	0.00	0.00	0.00	0.00	0.05
Chloroflexi;Dehalococcoidetes;Dehalococcoides	0.20	0.16	0.30	0.85	1.39	0.85	0.85	0.73	0.69	3.86	4.10	3.79	0.90	0.91	1.05
Chloroflexi;Dehalococcoidetes;Dehalogenimonas	6.55	6.89	7.44	26.68	23.51	24.29	13.57	10.62	12.22	32.52	34.96	30.10	20.54	21.88	21.93
Chloroflexi;Thermomicrobia;Sphaerobacteridae; Sphaerobacterales	0.00	0.00	0.00	0.03	0.03	0.03	0.00	0.00	0.02	0.03	0.11	0.03	0.00	0.00	0.00

Chloroflexi;unclassified_Chloroflexi;Other	0.73	0.93	0.71	1.35	1.70	1.58	1.07	1.57	0.86	0.10	0.40	0.59	1.19	1.07	1.28
Cyanobacteria;Cyanobacteria;Chloroplast;Bacillariophyta	0.11	0.09	0.15	0.03	0.00	0.06	0.41	0.79	0.62	0.13	0.13	0.10	0.00	0.00	0.00
Cyanobacteria;Cyanobacteria;Chloroplast;unclassified_Chloroplast	0.00	0.00	0.00	0.07	0.00	0.00	0.02	0.00	0.07	0.03	0.03	0.00	0.00	0.00	0.00
Cyanobacteria;Cyanobacteria;Family_II;GpIIa	0.00	0.00	0.00	0.00	0.03	0.00	0.09	0.05	0.14	0.00	0.11	0.00	0.00	0.00	0.00
Cyanobacteria;Cyanobacteria;Family_XI;GpXI	0.02	0.03	0.03	0.07	0.00	0.06	0.00	0.03	0.02	0.00	0.00	0.00	0.05	0.05	0.03
Cyanobacteria;Cyanobacteria;Family_XIII;GpXIII	0.00	0.00	0.00	0.00	0.00	0.00	0.05	0.05	0.02	0.00	0.00	0.00	0.00	0.00	0.00
Cyanobacteria;Cyanobacteria;unclassified_Cyanobacteria	0.11	0.00	0.23	0.27	0.06	0.22	0.11	0.03	0.10	0.20	0.11	0.15	0.05	0.02	0.05
Deferribacteres;Deferribacteres;Deferribacterales;Deferribacteraceae	0.38	0.34	0.46	0.61	0.37	0.22	0.23	0.29	0.17	0.10	0.19	0.18	0.46	0.16	0.25
Deferribacteres;Deferribacteres;Deferribacterales; Deferribacterales_incertae_sedis	2.43	2.58	2.39	0.47	0.28	0.25	1.94	1.29	1.36	0.28	0.38	0.51	0.95	0.81	1.75
Deinococcus-Thermus;Deinococci;Deinococcales;Deinococcaceae	0.00	0.00	0.05	0.00	0.00	0.00	0.00	0.00	0.00	0.00	0.00	0.00	0.36	0.05	0.10
Firmicutes;Bacilli;Bacillales;Bacillaceae	0.13	0.16	0.15	0.14	0.06	0.25	0.14	0.31	0.43	0.38	0.40	0.26	0.17	0.35	0.38
Firmicutes;Bacilli;Bacillales;Paenibacillaceae	0.07	0.03	0.05	0.30	0.43	0.28	0.25	0.45	0.38	0.08	0.13	0.13	0.17	0.12	0.13
Firmicutes;Bacilli;Bacillales;Staphylococcaceae	0.04	0.03	0.00	0.03	0.03	0.00	0.00	0.03	0.05	0.00	0.22	0.00	0.00	0.00	0.00
Firmicutes;Bacilli;Bacillales;Thermoactinomycetaceae	0.02	0.00	0.05	0.00	0.00	0.00	0.00	0.00	0.02	0.00	0.00	0.00	0.07	0.19	0.05
Firmicutes;Bacilli;Bacillales;unclassified_Bacillales	0.04	0.03	0.05	0.00	0.09	0.03	0.02	0.00	0.02	0.00	0.00	0.00	0.02	0.00	0.00
Firmicutes;Bacilli;Lactobacillales;Enterococcaceae	0.11	0.03	0.08	0.00	0.00	0.06	0.09	0.18	0.26	0.00	0.03	0.05	0.22	0.14	0.15
Firmicutes;Bacilli;Lactobacillales;Lactobacillaceae	0.00	0.00	0.00	0.00	0.00	1.36	0.00	0.00	0.00	0.00	0.00	0.10	0.00	0.00	0.00
Firmicutes;Bacilli;Lactobacillales;Streptococcaceae	0.00	0.00	0.03	0.03	0.11	7.69	0.00	0.00	0.00	0.05	0.00	0.05	0.00	0.00	0.03
Firmicutes;Clostridia;Clostridiales;Clostridiaceae	0.33	0.34	0.23	0.37	0.40	0.09	0.80	0.55	0.41	0.36	0.51	0.20	0.15	0.28	0.25
Firmicutes;Clostridia;Clostridiales;Eubacteriaceae	0.00	0.03	0.00	0.07	0.20	0.03	0.21	0.00	0.17	0.00	0.00	0.00	0.00	0.00	0.00

Firmicutes;Clostridia;Clostridiales;Eubacteriaceae	0.00	0.03	0.00	0.07	0.20	0.03	0.21	0.00	0.17	0.00	0.00	0.00	0.00	0.00	0.00
Firmicutes;Clostridia;Clostridiales;Incertae_Sedis_XI	0.31	0.09	0.28	0.68	0.40	0.54	0.16	0.24	0.07	0.00	0.30	0.03	0.34	0.02	0.08
Firmicutes;Clostridia;Clostridiales;Incertae_Sedis_XIV	0.89	0.59	0.84	0.07	0.09	0.09	0.89	0.60	0.60	0.10	0.13	0.36	0.75	0.60	0.95
Firmicutes;Clostridia;Clostridiales;Peptococcaceae	0.07	0.16	0.10	0.00	0.03	0.00	0.16	0.03	0.10	0.05	0.00	0.15	0.02	0.07	0.25
Firmicutes;Clostridia;Clostridiales;Peptostreptococcaceae	0.13	0.03	0.15	0.20	0.14	0.06	0.14	0.05	0.07	0.00	0.00	0.00	0.02	0.21	0.03
Firmicutes;Clostridia;Clostridiales;Veillonellaceae	0.02	0.09	0.03	0.03	0.03	0.03	0.02	0.03	0.02	0.03	0.05	0.00	0.00	0.00	0.00
Firmicutes;Clostridia;Clostridiales;unclassified_Clostridiales	2.66	2.20	3.30	1.39	1.56	1.42	1.51	2.18	1.98	0.79	1.03	1.13	1.43	1.84	1.48
Firmicutes;Clostridia;Natranaerobiales;Natranaerobiaceae	0.02	0.03	0.08	0.00	0.06	0.00	0.11	0.05	0.02	0.03	0.03	0.08	0.00	0.00	0.00
Firmicutes;Clostridia;Thermoanaerobacterales; Thermoanaerobacteraceae	0.09	0.00	0.03	0.07	0.03	0.09	0.18	0.16	0.02	0.05	0.03	0.03	0.10	0.23	0.28
Firmicutes;Clostridia;unclassified_Clostridia	2.21	2.08	2.74	4.74	5.67	4.81	3.91	3.75	3.66	2.12	2.21	3.28	2.99	3.39	4.08
Firmicutes;Erysipelotrichi;Erysipelotrichales;Erysipelotrichaceae	0.11	0.12	0.10	0.07	0.06	0.03	0.07	0.03	0.12	0.00	0.13	0.08	0.19	0.00	0.13
Firmicutes;unclassified_Firmicutes;Other	0.89	1.24	1.45	1.35	1.50	1.14	6.03	4.62	5.04	0.03	0.00	0.03	0.00	0.02	0.00
Gemmatimonadetes;Gemmatimonadetes;Gemmatimonadales; Gemmatimonadaceae	1.08	0.68	1.02	0.68	0.82	0.60	0.23	0.18	0.22	0.05	0.22	0.10	0.58	0.56	0.48
Lentisphaerae;Lentisphaeria;Victivallales;Victivallaceae	0.00	0.00	0.00	0.00	0.20	0.09	0.05	0.08	0.17	0.20	0.11	0.05	0.07	0.07	0.03
Nitrospira;Nitrospira;Nitrospirales;Nitrospiraceae	3.03	3.69	3.05	0.20	0.43	0.13	0.89	0.84	0.79	0.10	0.00	0.20	0.12	0.09	0.48
OD1;OD1_genera_incertae_sedis;Other	0.00	0.25	0.00	0.00	0.00	0.00	0.00	0.00	0.02	0.00	0.00	0.00	0.00	0.00	0.00
OP10;OP10_genera_incertae_sedis;Other	0.20	0.12	0.36	0.81	0.60	0.25	0.41	0.55	0.50	0.36	0.43	0.72	0.56	0.39	0.75
Proteobacteria;Alphaproteobacteria;Caulobacterales;Caulobacteraceae	0.13	0.12	0.05	0.07	0.03	0.06	0.00	0.00	0.02	0.00	0.00	0.00	0.15	0.09	0.00

Proteobacteria;Alphaproteobacteria;Kordiimonadales;Kordiimonadaceae	0.02	0.00	0.00	0.03	0.03	0.06	0.00	0.00	0.00	0.00	0.00	0.00	0.00	0.00	0.00
Proteobacteria;Alphaproteobacteria;Rhizobiales;Hyphomicrobiaceae	0.15	0.28	0.20	0.14	0.09	0.19	0.00	0.05	0.02	0.10	0.00	0.00	0.00	0.00	0.00
Proteobacteria;Alphaproteobacteria;Rhizobiales;Methylobacteriaceae	0.00	0.00	0.00	0.03	0.06	0.00	0.02	0.03	0.00	0.23	0.27	0.10	0.05	0.02	0.03
Proteobacteria;Alphaproteobacteria;Rhizobiales;Methylocystaceae	0.29	0.25	0.05	0.07	0.14	0.00	0.07	0.08	0.02	0.36	0.16	0.20	0.15	0.09	0.15
Proteobacteria;Alphaproteobacteria;Rhizobiales;Rhodobiaceae	0.33	0.25	0.15	0.14	0.06	0.19	0.25	0.24	0.14	0.05	0.03	0.05	0.02	0.00	0.05
Proteobacteria;Alphaproteobacteria;Rhodobacterales;Rhodobacteraceae	0.09	0.06	0.08	0.03	0.03	0.00	0.09	0.21	0.12	0.03	0.08	0.00	0.00	0.02	0.00
Proteobacteria;Alphaproteobacteria;Rhodospirillales;Acetobacteraceae	0.11	0.09	0.13	0.17	0.11	0.09	0.14	0.00	0.02	0.05	0.19	0.13	0.12	0.19	0.25
Proteobacteria;Alphaproteobacteria;Rhodospirillales;Rhodospirillaceae	0.51	0.22	0.56	0.30	0.48	0.25	0.30	0.37	0.17	0.38	0.22	0.15	0.39	0.51	0.83
Proteobacteria;Alphaproteobacteria;Rickettsiales;SAR11	0.00	0.00	0.00	0.00	0.00	0.00	0.00	0.00	0.00	0.05	0.16	0.00	0.00	0.00	0.00
Proteobacteria;Alphaproteobacteria;Sneathiellales;Sneathiellaceae	0.00	0.00	0.00	0.00	0.00	0.00	0.00	0.00	0.00	0.00	0.00	0.00	0.02	0.05	0.03
Proteobacteria;Alphaproteobacteria;Sphingomonadales;Sphingomonadaceae	0.02	0.03	0.00	0.00	0.03	0.06	0.00	0.00	0.00	0.00	0.00	0.00	0.00	0.00	0.00
Proteobacteria;Alphaproteobacteria;unclassified_Alphaproteobacteria	0.00	0.00	0.00	0.00	0.06	0.03	0.32	0.29	0.31	0.08	0.13	0.10	0.07	0.00	0.10
Proteobacteria;Betaproteobacteria;Burkholderiales;Burkholderiaceae	0.51	0.31	0.30	0.58	0.62	0.76	0.16	0.29	0.19	0.33	0.22	0.18	0.05	0.12	0.10
Proteobacteria;Betaproteobacteria;Burkholderiales; Burkholderiales_incertae_sedis	0.71	0.56	0.64	0.47	0.31	0.54	0.05	0.10	0.07	0.00	0.00	0.00	0.00	0.00	0.05
Proteobacteria;Betaproteobacteria;Burkholderiales;Comamonadaceae	0.02	0.03	0.00	0.07	0.00	0.03	0.00	0.00	0.07	0.00	0.03	0.00	0.22	0.07	0.03
Proteobacteria;Betaproteobacteria;Burkholderiales;Oxalobacteraceae	0.00	0.00	0.00	0.00	0.00	0.00	0.00	0.00	0.00	0.43	0.00	0.00	0.00	0.00	0.00
Proteobacteria;Betaproteobacteria;Burkholderiales; unclassified_Burkholderiales	1.04	1.27	1.24	0.24	0.03	0.06	0.09	0.26	0.29	0.00	0.00	0.00	0.00	0.00	0.00
Proteobacteria;Betaproteobacteria;Rhodocyclales;Rhodocyclaceae	0.60	0.47	0.46	0.03	0.11	0.03	0.11	0.29	0.19	0.00	0.00	0.00	0.00	0.00	0.00

Proteobacteria;Betaproteobacteria;unclassified_Betaproteobacteria	1.20	0.96	1.65	0.14	0.26	0.06	0.05	0.05	0.02	0.00	0.00	0.00	0.00	0.00	0.00
Proteobacteria;Deltaproteobacteria;Desulfobacterales; Desulfobacteraceae	14.41	16.67	14.86	10.26	9.98	9.84	10.92	14.29	14.37	7.11	6.24	8.71	17.78	13.80	12.95
Proteobacteria;Deltaproteobacteria;Desulfobacterales; Desulfobulbaceae	5.75	4.75	4.32	0.30	0.40	0.22	0.82	0.58	0.60	0.10	0.08	0.74	0.00	0.05	0.05
Proteobacteria;Deltaproteobacteria;Desulfobacterales; unclassified_Desulfobacterales	0.07	0.06	0.10	0.00	0.00	0.00	0.02	0.03	0.10	0.00	0.00	0.00	0.00	0.00	0.00
Proteobacteria;Deltaproteobacteria;Desulfovibrionales; Desulfonatronaceae	0.07	0.00	0.05	0.00	0.03	0.00	0.00	0.00	0.00	0.00	0.00	0.00	0.00	0.00	0.00
Proteobacteria;Deltaproteobacteria;Desulfovibrionales; Desulfovibrionaceae	0.02	0.16	0.03	0.24	0.45	0.60	0.07	0.05	0.36	0.08	0.03	0.05	0.07	0.12	0.03
Proteobacteria;Deltaproteobacteria;Desulfurellales;Desulfurellaceae	0.02	0.00	0.05	0.81	0.40	1.08	0.02	0.03	0.02	0.51	0.32	0.26	0.12	0.07	0.10
Proteobacteria;Deltaproteobacteria;Desulfuromonadales; Desulfuromonadaceae	0.51	0.59	0.56	0.00	0.00	0.06	0.14	0.29	0.22	0.08	0.11	0.23	0.15	0.19	0.15
Proteobacteria;Deltaproteobacteria;Myxococcales;Cystobacterineae	0.04	0.00	0.13	0.14	0.06	0.03	0.14	0.10	0.24	0.13	0.22	0.23	0.39	0.30	0.50
Proteobacteria;Deltaproteobacteria;Myxococcales;Nannocystineae	0.02	0.06	0.05	0.30	0.09	0.00	0.02	0.08	0.00	0.03	0.24	0.00	0.00	0.09	0.15
Proteobacteria;Deltaproteobacteria;Myxococcales;Sorangiineae	0.91	1.12	1.09	0.07	0.14	0.06	0.48	0.52	0.43	0.00	0.03	0.05	0.12	0.33	0.38
Proteobacteria;Deltaproteobacteria;Myxococcales; unclassified_Myxococcales	0.27	0.65	0.43	0.03	0.00	0.00	0.02	0.03	0.10	0.15	0.00	0.10	0.00	0.00	0.00
Proteobacteria;Deltaproteobacteria;Syntrophobacterales; Syntrophaceae	1.88	2.17	2.16	1.42	1.70	2.28	12.59	12.01	11.59	0.10	0.16	0.08	0.44	0.21	0.28
Proteobacteria;Deltaproteobacteria;Syntrophobacterales; Syntrophobacteraceae	2.61	3.63	2.03	0.14	0.09	0.13	0.69	0.45	0.36	0.00	0.00	0.03	0.56	0.58	0.45
Proteobacteria;Deltaproteobacteria;Syntrophobacterales; unclassified_Syntrophobacterales	0.29	0.19	0.15	0.07	0.00	0.13	0.14	0.13	0.05	1.61	1.40	1.66	1.38	1.35	1.95
Proteobacteria;Deltaproteobacteria;Syntrophorhabdaceae; Syntrophorhabdus	0.07	0.03	0.00	0.03	0.00	0.03	0.02	0.03	0.05	0.00	0.00	0.00	0.00	0.00	0.00
Proteobacteria;Deltaproteobacteria;unclassified_Deltaproteobacteria	5.95	7.05	6.02	5.38	7.69	5.66	3.77	4.51	4.16	10.76	11.20	9.68	10.03	10.31	7.85
Proteobacteria;Epsilonproteobacteria;Campylobacterales; Helicobacteraceae	0.00	0.00	0.03	0.00	0.00	0.00	0.00	0.10	0.02	0.00	0.00	0.00	0.00	0.00	0.00

Proteobacteria;Epsilonproteobacteria;Nautiliales;Nautiliaceae	0.09	0.19	0.18	0.71	0.77	0.66	0.05	0.08	0.07	0.03	0.03	0.00	0.05	0.07	0.13
Proteobacteria;Gammaproteobacteria;Alteromonadales; Alteromonadaceae	0.00	0.12	0.05	0.00	0.00	0.00	0.00	0.03	0.02	0.03	0.00	0.03	0.00	0.00	0.00
Proteobacteria;Gammaproteobacteria;Chromatiales;Chromatiaceae	1.55	0.90	1.02	0.03	0.00	0.00	0.32	0.03	0.07	0.00	0.00	0.18	0.00	0.02	0.03
Proteobacteria;Gammaproteobacteria;Chromatiales; Ectothiorhodospiraceae	0.00	0.03	0.00	0.00	0.00	0.00	0.09	0.00	0.05	0.00	0.00	0.08	0.10	0.49	0.08
Proteobacteria;Gammaproteobacteria;Chromatiales; unclassified_Chromatiales	2.57	1.96	2.41	0.30	0.03	0.03	0.37	0.52	0.60	0.03	0.00	0.15	0.02	0.14	0.03
Proteobacteria;Gammaproteobacteria; Gammaproteobacteria_incertae_sedis;Sedimenticola	0.49	0.31	0.25	0.07	0.11	0.13	0.09	0.24	0.24	0.15	0.03	0.46	0.00	0.00	0.10
Proteobacteria;Gammaproteobacteria; Gammaproteobacteria_incertae_sedis;Thiohalophilus	0.22	0.19	0.66	0.03	0.03	0.00	0.82	0.39	0.72	0.05	0.00	0.08	0.00	0.02	0.05
Proteobacteria;Gammaproteobacteria;Legionellales;Legionellaceae	0.00	0.00	0.00	0.00	0.00	0.00	0.05	0.00	0.00	0.15	0.08	0.13	0.00	0.02	0.08
Proteobacteria;Gammaproteobacteria;Methylococcales; Methylococcaceae	0.02	0.03	0.00	0.00	0.03	0.00	0.05	0.00	0.00	0.00	0.03	0.00	0.15	0.05	0.03
Proteobacteria;Gammaproteobacteria;Oceanospirillales; Halomonadaceae	0.07	0.06	0.10	0.00	0.06	0.00	0.18	0.03	0.10	0.00	0.00	0.00	0.00	0.00	0.00
Proteobacteria;Gammaproteobacteria;Xanthomonadales; Sinobacteraceae	0.55	0.50	0.56	0.03	0.03	0.00	0.43	0.21	0.62	0.00	0.00	0.00	0.00	0.00	0.00
Proteobacteria;Gammaproteobacteria;Xanthomonadales; Xanthomonadaceae	0.18	0.43	0.15	0.03	0.06	0.03	0.27	0.13	0.48	0.00	0.00	0.00	0.07	0.00	0.08
Proteobacteria;Gammaproteobacteria; unclassified_Gammaproteobacteria	6.71	6.11	6.07	1.19	1.99	0.79	3.72	3.91	3.66	0.95	0.86	1.97	0.63	0.49	2.10
Proteobacteria;unclassified_Proteobacteria;Other	0.00	0.00	0.00	0.00	0.00	0.00	0.02	0.24	0.05	0.00	0.00	0.00	0.00	0.00	0.00
Spirochaetes;Spirochaetes;Spirochaetales;Brachyspiraceae	0.02	0.00	0.00	0.03	0.03	0.00	0.02	0.05	0.02	0.03	0.00	0.00	0.00	0.00	0.10
Spirochaetes;Spirochaetes;Spirochaetales;Spirochaetaceae	2.59	2.27	2.34	4.54	5.84	4.74	4.91	6.48	4.42	1.51	1.03	1.13	0.39	0.46	0.78
Spirochaetes;Spirochaetes;Spirochaetales; Spirochaetales_incertae_sedis	0.00	0.00	0.00	0.07	0.00	0.00	0.02	0.00	0.00	0.00	0.03	0.00	0.05	0.05	0.00
Thermotogae;Thermotogae;Thermotogales;Thermotogaceae	0.09	0.00	0.00	0.00	0.00	0.00	0.00	0.00	0.02	0.00	0.00	0.03	0.00	0.00	0.00

Verrucomicrobia;Spartobacteria; Spartobacteria_genera_incertae_sedis	0.00	0.00	0.00	0.00	0.03	0.00	0.43	0.24	0.24	0.00	0.00	0.00	0.02	0.07	0.08
Verrucomicrobia;Verrucomicrobiae;Verrucomicrobiales; Verrucomicrobiaceae	0.11	0.03	0.03	0.00	0.00	0.00	0.05	0.08	0.05	0.00	0.00	0.00	0.05	0.07	0.00
WS3;WS3_genera_incertae_sedis;Other	1.46	0.53	1.27	0.98	1.28	0.73	0.64	0.42	0.84	1.05	0.76	0.82	0.49	0.26	0.35
Unclassified	6.22	5.52	6.17	6.03	5.64	4.68	6.24	5.98	5.86	12.30	10.72	9.50	8.64	8.55	8.20
None;Other;Other;Other;Other	3.92	3.48	3.63	12.60	11.91	10.63	6.78	7.34	7.43	15.19	14.82	14.98	18.77	20.70	16.98

Table S5. Phylogenetic analysis of archaeal 16S rRNA genes detected in Chesapeake Bay sediments at the family level of taxonomic classification. All data are shown as percentages of detected sequences for each respective sequence library. Note: Horizon 6 at Station 908 is designated as 908D.

	908 A %	908 B %	908 C %	908D A %	908D B %	908D C %	858 A %	858 B %	858 C %	818 A %	818 B %	818 C %	707 A %	707 B %	707 C %
Crenarchaeota;Thermoprotei;Sulfolobales;Sulfolobaceae	0.00	0.00	0.00	0.00	0.00	0.00	0.00	0.00	0.05	0.00	0.00	0.00	0.00	0.00	0.00
Crenarchaeota;Thermoprotei;Thermoproteales;Thermofilaceae	0.27	0.33	0.40	0.63	0.95	0.61	0.11	0.00	0.21	0.70	0.58	0.83	0.58	0.90	0.50
Crenarchaeota;Thermoprotei;Thermoproteales;Thermoproteaceae	0.00	0.00	0.00	0.00	0.00	0.00	0.00	0.00	0.00	0.00	0.00	0.00	0.00	0.06	0.00
Crenarchaeota;Thermoprotei;Thermoproteales;unclassified_Thermoproteales	0.14	0.05	0.06	0.04	0.30	0.22	0.11	0.00	0.00	0.13	0.48	0.37	0.41	0.18	0.67
Crenarchaeota;Thermoprotei;unclassified_Thermoprotei	8.24	6.07	7.42	12.02	13.97	11.60	5.88	4.02	4.04	79.77	69.51	60.94	32.13	35.90	25.38
Euryarchaeota;Halobacteria;Halobacteriales;Halobacteriaceae	0.00	0.00	0.00	0.00	0.00	0.00	0.00	0.00	0.00	0.00	0.00	0.00	0.00	0.00	0.04
Euryarchaeota;Methanobacteria;Methanobacteriales;Methanobacteriaceae	0.00	0.00	0.00	0.00	0.00	0.00	0.06	0.00	0.05	0.00	0.00	0.00	0.06	0.00	0.00
Euryarchaeota;Methanococci;Methanococcales;Methanococcaceae	0.00	0.00	0.00	0.00	0.00	0.00	0.00	0.00	0.00	0.06	0.00	0.00	0.00	0.00	0.00
Euryarchaeota;Methanomicrobia;Methanomicrobiales;Incertae_sedis_1	0.00	0.00	0.06	0.00	0.00	0.00	0.00	0.00	0.00	0.00	0.00	0.28	0.00	0.00	0.00
Euryarchaeota;Methanomicrobia;Methanomicrobiales;Methanocorpusculaceae	0.00	0.00	0.00	0.00	0.00	0.00	0.00	0.00	0.00	0.13	0.00	0.00	0.00	0.00	0.00
Euryarchaeota;Methanomicrobia;Methanomicrobiales;Methanomicrobiaceae	5.49	3.52	6.21	8.93	9.47	13.34	18.08	14.51	14.19	0.25	0.29	0.64	0.99	0.54	0.42
Euryarchaeota;Methanomicrobia;Methanosarcinales;Methanosaetaceae	12.64	10.85	10.70	9.35	12.43	11.51	7.51	12.35	9.09	0.06	0.19	0.18	0.06	0.06	0.00
Euryarchaeota;Methanomicrobia;Methanosarcinales;Methanosarcinaceae	18.96	14.64	20.47	13.54	13.80	12.68	21.47	20.75	23.29	0.45	0.39	0.37	1.39	1.62	1.09
Euryarchaeota;Methanomicrobia;Methanosarcinales;unclassified_Methanosarcinales	0.69	0.49	1.09	0.38	0.30	0.96	0.51	0.58	1.33	0.25	1.36	0.74	1.05	0.24	0.50
Euryarchaeota;Thermococci;Thermococcales;Thermococcaceae	0.00	0.00	0.00	0.00	0.00	0.00	0.00	0.00	0.00	0.00	0.00	0.00	0.06	0.06	0.13
Euryarchaeota;Thermoplasmata;Thermoplasmatales;Ferroplasmataceae	0.14	0.11	0.00	0.04	0.00	0.00	0.11	0.12	0.05	0.13	0.00	0.09	0.17	0.42	0.21

Euryarchaeota;Thermoplasmata;Thermoplasmatales; Picrophilaceae	19.92	26.36	18.98	11.89	11.25	10.17	9.44	11.54	11.16	0.45	0.87	0.28	0.29	0.06	0.46
Euryarchaeota;Thermoplasmata;Thermoplasmatales; unclassified_Thermoplasmatales	1.51	0.92	1.09	1.48	0.95	0.39	2.60	2.21	2.71	1.53	3.10	3.86	5.11	4.93	4.69
Euryarchaeota;unclassified_Euryarchaeota;Other	23.63	28.85	22.60	36.10	30.31	33.10	26.10	27.74	25.84	8.21	11.42	17.65	35.85	31.99	45.39
Korarchaeota;Korarchaeota_genera_incertae_sedis;Other	0.00	0.05	0.06	0.04	0.06	0.26	0.06	0.00	0.00	0.06	0.19	0.18	0.06	0.42	0.17
Unclassified	8.38	7.75	10.87	5.54	6.22	5.17	7.97	6.18	7.97	7.82	11.62	13.60	21.79	22.61	20.35

Table S6. Results from PerMANOVA and MRPP analyses of sequenced core bacterial and archaeal communities. PerMANOVA (permutation-based multivariate analysis of variance) was performed using the Bray-Curtis distance measure and 5000 permutations. An F statistic in a PerMANOVA analysis indicates the likelihood of no difference among groups, with a higher value suggesting a larger difference among samples. MRPP (multi-response permutation procedure) analysis was also conducted using Bray-Curtis as a distance measure. Test statistic (T) describes how strongly the groups are separated, with a more negative value indicating a greater level of separation. The chance-corrected within-group agreement of the MRPP analysis, represented by A, indicates homogeneity within-groups compared to what is randomly expected. All analyses were performed in PC-ORD (Version 6, MjM Software).

BACTERIA	
PerMANOVA	**MRPP**
F = 35.56	T = -7.04
p = 2.0E-04	Observed δ = 0.55E-01
	Expected δ = 0.17
	p = 1.80E-06
	A = 0.68
ARCHAEA	
PerMANOVA	**MRPP**
F = 67.24	T = -6.00
p = 2.0E-04	Observed δ = 0.53E-01
	Expected δ = 0.23
	p = 2.24E-05
	A = 0.77

Table S7. Diversity indices and descriptive information of core taxa in bacterial and archaeal communities**.** A total of 21 core bacterial classes were found among all samples, whereas a total of 6 core classes of archaea were found among all samples. All statistics were calculated in PC-ORD (Version 6, MjM Software). Notation: S - number of taxa in each sample; E - evenness; H - Shannon Diversity index; and D' - Simpson's Diversity for an infinite population. D' is the complement of Simpson's original index, and indicates the likelihood that two individuals from a population would be different if chosen randomly.

		Bacteria		
Sample*	**S**	**E**	**H**	**D'**
908A	21	0.94	2.86	0.93
908B	21	0.93	2.83	0.93
908C	21	0.94	2.86	0.93
908H6A	21	0.92	2.81	0.93
908H6B	21	0.93	2.83	0.93
908H6C	21	0.92	2.80	0.93
858A	21	0.93	2.83	0.93
858B	21	0.93	2.82	0.93
858C	21	0.93	2.83	0.93
818A	20	0.84	2.53	0.89
818B	18	0.86	2.48	0.89
818C	20	0.87	2.59	0.90
707A	19	0.87	2.58	0.90
707B	20	0.86	2.58	0.90
707C	20	0.89	2.67	0.91
		Archaea		
Sample	**S**	**E**	**H**	**D'**
908A	6	0.93	1.66	0.80
908B	6	0.93	1.66	0.79
908C	6	0.94	1.68	0.80
908H6A	6	0.92	1.64	0.79
908H6B	6	0.93	1.66	0.79
908H6C	6	0.92	1.64	0.79
858A	6	0.92	1.65	0.78
858B	6	0.90	1.60	0.77
858C	6	0.92	1.64	0.78
818A	6	0.77	1.37	0.65
818B	6	0.84	1.50	0.71
818C	6	0.87	1.55	0.74
707A	6	0.94	1.69	0.80
707B	6	0.94	1.68	0.80
707C	6	0.92	1.64	0.78

*Letters refer to sample replicates

Table S8. Copy numbers of *dsrA* and bacterial 16S rRNA gene sequences per gram of wet sediment. Values represent averages and standard deviations of triplicate replicates.

Station	Avg. # of *dsrA* gene copies g^{-1} wet sediment	Avg. # of bacterial 16S rRNA gene copies g^{-1} wet sediment	Relative % of *dsrA* gene sequences
Station 908			
Horizon 1 (surface)	$2.98 \times 10^6 \pm 1.11 \times 10^6$	$5.63 \times 10^7 \pm 1.47 \times 10^7$	5.28
Horizon 2	$1.33 \times 10^6 \pm 2.14 \times 10^5$	$3.25 \times 10^7 \pm 4.29 \times 10^6$	4.09
Horizon 3	$5.84 \times 10^5 \pm 1.04 \times 10^5$	$3.43 \times 10^7 \pm 9.19 \times 10^6$	1.71
Horizon 4	$4.69 \times 10^5 \pm 8.46 \times 10^4$	$2.54 \times 10^7 \pm 4.26 \times 10^6$	1.84
Horizon 5	$4.10 \times 10^5 \pm 1.97 \times 10^5$	$2.27 \times 10^7 \pm 7.40 \times 10^6$	1.81
Horizon 6	$1.01 \times 10^5 \pm 4.51 \times 10^4$	$1.05 \times 10^7 \pm 3.76 \times 10^5$	0.96
Station 858			
Horizon 1 (surface)	$6.02 \times 10^5 \pm 9.63 \times 10^4$	$3.68 \times 10^7 \pm 4.33 \times 10^6$	1.64
Horizon 2	$5.27 \times 10^5 \pm 3.39 \times 10^5$	$3.02 \times 10^7 \pm 1.35 \times 10^7$	1.86
Horizon 3	$5.31 \times 10^5 \pm 1.11 \times 10^5$	$3.37 \times 10^7 \pm 6.84 \times 10^6$	1.58
Horizon 4	$5.46 \times 10^5 \pm 2.56 \times 10^5$	$3.23 \times 10^7 \pm 1.01 \times 10^7$	1.69
Horizon 5	$4.11 \times 10^5 \pm 6.72 \times 10^4$	$2.36 \times 10^7 \pm 1.19 \times 10^6$	1.75
Horizon 6	$3.23 \times 10^5 \pm 8.62 \times 10^4$	$2.10 \times 10^7 \pm 2.59 \times 10^6$	1.53
Horizon 7	$3.36 \times 10^5 \pm 5.02 \times 10^4$	$2.25 \times 10^7 \pm 5.89 \times 10^6$	1.49
Station 818			
Horizon 1 (surface)	$3.42 \times 10^5 \pm 2.55 \times 10^5$	$9.59 \times 10^6 \pm 4.00 \times 10^6$	3.47
Horizon 2	$1.47 \times 10^5 \pm 2.56 \times 10^4$	$7.39 \times 10^6 \pm 5.05 \times 10^5$	1.99
Horizon 3	$1.17 \times 10^5 \pm 9.46 \times 10^4$	$6.07 \times 10^6 \pm 2.77 \times 10^6$	1.92
Horizon 4	$3.78 \times 10^4 \pm 1.96 \times 10^4$	$6.19 \times 10^6 \pm 7.30 \times 10^5$	0.61
Horizon 5	$9.93 \times 10^3 \pm 7.57 \times 10^3$	$4.30 \times 10^6 \pm 1.03 \times 10^6$	0.23
Station 707			
Horizon 1 (surface)	$6.58 \times 10^5 \pm 2.01 \times 10^5$	$2.53 \times 10^7 \pm 3.47 \times 10^6$	2.60
Horizon 2	$1.63 \times 10^6 \pm 2.03 \times 10^6$	$2.94 \times 10^7 \pm 1.25 \times 10^7$	5.55
Horizon 3	$7.46 \times 10^5 \pm 4.92 \times 10^5$	$2.40 \times 10^7 \pm 1.59 \times 10^7$	3.11
Horizon 4	$2.35 \times 10^5 \pm 1.58 \times 10^5$	$1.08 \times 10^7 \pm 1.64 \times 10^6$	2.18

Table S9. Copy numbers of *mcrA* and archaeal 16S gene sequences per gram of wet sediment. Values represent averages and standard deviations of triplicate replicates.

Station	Avg. # of *mcrA* gene copies g^{-1} wet sediment	Avg. # of archaeal 16S rRNA gene copies g^{-1} wet sediment	Relative % of *mcrA* gene sequences
Station 908			
Horizon 1 (surface)	$3.42 \times 10^6 \pm 1.98 \times 10^6$	$1.41 \times 10^8 \pm 4.49 \times 10^7$	2.43
Horizon 2	$3.03 \times 10^6 \pm 3.83 \times 10^5$	$6.29 \times 10^7 \pm 1.43 \times 10^7$	4.82
Horizon 3	$1.76 \times 10^6 \pm 6.68 \times 10^5$	$6.04 \times 10^7 \pm 1.47 \times 10^7$	2.92
Horizon 4	$2.68 \times 10^6 \pm 8.04 \times 10^5$	$4.18 \times 10^7 \pm 1.10 \times 10^7$	6.41
Horizon 5	$2.32 \times 10^6 \pm 1.60 \times 10^6$	$4.65 \times 10^7 \pm 2.43 \times 10^7$	4.98
Horizon 6	$2.76 \times 10^5 \pm 1.07 \times 10^5$	$1.04 \times 10^7 \pm 1.60 \times 10^6$	2.65
Station 858			
Horizon 1 (surface)	$5.85 \times 10^6 \pm 3.94 \times 10^6$	$1.04 \times 10^8 \pm 9.88 \times 10^6$	5.65
Horizon 2	$3.70 \times 10^6 \pm 2.35 \times 10^6$	$7.18 \times 10^7 \pm 4.96 \times 10^7$	5.15
Horizon 3	$2.69 \times 10^6 \pm 3.96 \times 10^5$	$1.05 \times 10^8 \pm 4.98 \times 10^6$	2.56
Horizon 4	$3.94 \times 10^6 \pm 1.15 \times 10^6$	$1.11 \times 10^8 \pm 4.99 \times 10^7$	3.56
Horizon 5	$4.51 \times 10^6 \pm 1.84 \times 10^5$	$6.19 \times 10^7 \pm 5.05 \times 10^6$	7.30
Horizon 6	$3.03 \times 10^6 \pm 6.97 \times 10^5$	$3.94 \times 10^7 \pm 1.15 \times 10^7$	7.69
Horizon 7	$3.31 \times 10^6 \pm 6.34 \times 10^5$	$4.74 \times 10^7 \pm 2.30 \times 10^7$	6.98
Station 818			
Horizon 1 (surface)	$1.10 \times 10^5 \pm 7.31 \times 10^4$	$1.37 \times 10^7 \pm 9.83 \times 10^6$	0.80
Horizon 2	$8.60 \times 10^4 \pm 9.78 \times 10^3$	$6.81 \times 10^6 \pm 7.36 \times 10^5$	1.26
Horizon 3	$6.92 \times 10^4 \pm 1.57 \times 10^4$	$4.91 \times 10^6 \pm 2.63 \times 10^6$	1.41
Horizon 4	$9.43 \times 10^4 \pm 2.96 \times 10^4$	$6.07 \times 10^6 \pm 1.55 \times 10^6$	1.55
Horizon 5	$5.10 \times 10^4 \pm 8.03 \times 10^3$	$3.71 \times 10^6 \pm 1.09 \times 10^6$	1.37
Station 707			
Horizon 1 (surface)	$5.09 \times 10^5 \pm 2.59 \times 10^5$	$7.43 \times 10^7 \pm 2.29 \times 10^7$	0.69
Horizon 2	$4.29 \times 10^5 \pm 3.34 \times 10^5$	$1.20 \times 10^8 \pm 1.15 \times 10^8$	0.36
Horizon 3	$4.15 \times 10^5 \pm 2.13 \times 10^5$	$6.11 \times 10^7 \pm 4.30 \times 10^7$	0.68
Horizon 4	$1.07 \times 10^5 \pm 1.81 \times 10^4$	$1.81 \times 10^7 \pm 8.94 \times 10^6$	0.59

Table S10. Detection of *assA* and *bssA* in Bay sediments. The number of detected OTUs is designated for each station. Note: N.D. designates that the gene of interest was not detected based on the primers used in this study.

Station	***assA***	***bssA***
908 (surface horizon)	4 OTUs	1 OTU
908 (horizon 6)	1 OTU	N.D.
858	4 OTUs	1 OTU
818	4 OTUs	ND
707	5 OTUs	ND

Table S11. Sulfate concentrations (mM) in microcosms after 672 days of incubation. Microcosm treatments were established in triplicate, and sulfate was monitored via ion chromatography. *D. alkenivorans* strain AK-01 positive controls were amended with additional sulfate when sulfate was depleted to approximately 2-3 mM. The incubation time required for this sulfate depletion in positive controls varied among the stations and among the replicates at each station. The range of time points designating when replicates at each station were amended with sulfate are indicated below. The treatments are as follows: (1) Active enrichments amended with sediment and hexadecane; (2) Positive controls amended with sediment, hexadecane and *Desulfatibacillum alkenivorans* strain AK-01; (3) Background controls containing medium and sediment; (4) Abiotic media controls containing medium and hexadecane; and (5) Sterile controls amended with sediment and hexadecane and autoclaved at 121°C for three consecutive days. Values represent the averages and standard deviations of triplicate replicates. Note: values shown in red are statistically significant from time-zero measurements.

Station	Active Enrichments		Positive Controls			Background Controls		Abiotic Controls		Sterile Controls	
	T-0	T-96 weeks	T-0	Sulfate Amendment	T-96 weeks**	T-0	T-96 weeks	T-0	T-96 weeks	T-0	T-96 weeks
908 Surface	23.72 ± 1.20	20.02 ± 1.46	25.95 ± 2.48	T-32 – T-52 weeks	16.87 ± 4.16	25.32 ± 1.84	22.55 ± 0.22	25.72 ± 0.84	25.17 ± 0.04	24.56 ± 1.21	23.98 ± 0.15
908 Horizon 6	24.80 ± 0.98	21.67 ± 0.39	23.72 ± 0.26	T-20 – T-44 weeks	3.47 ± 5.62	24.86 ± 0.64	22.78 ± 0.39	25.22 ± 1.37	24.64 ± 0.71	24.63 ± 0.65	23.69 ± 0.30
858 Surface	25.46 ± 1.06	20.82 ± 0.81	22.52 ± 1.82	After T-40 weeks	11.93 ± 0.25	24.29 ± 1.49	21.85 ± 0.25	26.33 ± 1.31	24.10 ± 0.39	23.04 ± 1.37	22.92 ± 0.16
818 Surface	24.58*	19.15*	24.46 ± 1.00	T-24 – T-32 weeks	10.21 ± 1.98	24.30 ± 0.48	19.29 ± 0.79	25.79 ± 0.91	22.56 ± 1.21	24.98 ± 0.21	22.42 ± 0.25
707 Surface	25.29 ± 0.46	13.76 ± 6.54	23.81 ± 0.58	T-24 – T-36 weeks	12.17 ± 5.30	24.97 ± 0.21	20.10 ± 0.60	25.88 ± 1.07	22.09 ± 2.04	24.91 ± 0.21	22.86 ± 0.39

*No standard deviation calculated. Only two replicates for this condition.
**Values represent sulfate concentrations after 672 days of incubation (T-96 weeks). These are amounts remaining after initial sulfate depletion, re-amendment at time points indicated (AK-01 positive controls), and subsequent sulfate utilization.

Table S12. Methane production (mM) in microcosms established under sulfate-reducing and methanogenic conditions after 672 days of incubation. Treatments were established in triplicate as follows: (1) Active enrichments amended with sediment and hexadecane; (2) Positive controls amended with sediment, hexadecane and *Desulfatibacillum alkenivorans* strain AK-01, (3) Background controls containing medium and sediment, (4) Abiotic media controls containing medium and hexadecane, and (5) Sterile controls amended with sediment and hexadecane and autoclaved at 121°C for three consecutive days. Values represent averages and standard deviations of triplicate replicates. Note: values shown in red are statistically significant from time-zero measurements.

Treatment	Sulfate-Reducing Conditions	Methanogenic Conditions
Station 908		
(1) Active enrichments	1.37 ± 0.52	3.15 ± 0.64
(2) Positive controls	1.61 ± 0.41	2.49 ± 0.42
(3) Background controls	0.18 ± 0.11	1.93 ± 0.40
(4) Abiotic media controls	0.00	0.00
(5) Sterile controls	0.00	0.00
Station 908, Horizon 6		
(1) Active enrichments	1.00 ± 0.48	2.69 ± 0.27
(2) Positive controls	0.20 ± 0.02	2.18 ± 0.08
(3) Background controls	0.60 ± 0.36	1.02 ± 0.42
(4) Abiotic media controls	0.00	0.00
(5) Sterile controls	0.001 ± 0.002	0.001 ± 0.002
Station 858		
(1) Active enrichments	2.05 ± 0.61	4.15 ± 1.15
(2) Positive controls	2.01 ± 0.27	3.32 ± 0.37
(3) Background controls	0.23 ± 0.08	2.19 ± 0.17
(4) Abiotic media controls	0.00	0.00
(5) Sterile controls	0.004 ± 0.001	0.005 ± 0.001
Station 818		
(1) Active enrichments	0.02*	0.06 ± 0.02
(2) Positive controls	0.07 ± 0.04	0.54 ± 0.39
(3) Background controls	0.01 ± 0.004	0.48 ± 0.40
(4) Abiotic media controls	0.00	0.00
(5) Sterile controls	0.00	0.00
Station 707		
(1) Active enrichments	0.04 ± 0.01	1.20 ± 0.25
(2) Positive controls	0.18 ± 0.07	1.28 ± 0.28
(3) Background controls	0.02 ± 0.02	0.41 ± 0.55
(4) Abiotic media controls	0.00	0.00
(5) Sterile controls	0.00	0.00

*No standard deviation calculated. Only two replicates for this condition.

Figure S1. Map of the Chesapeake Bay including the longitudinal and latitudinal coordinates of stations that were sampled in August 2010.

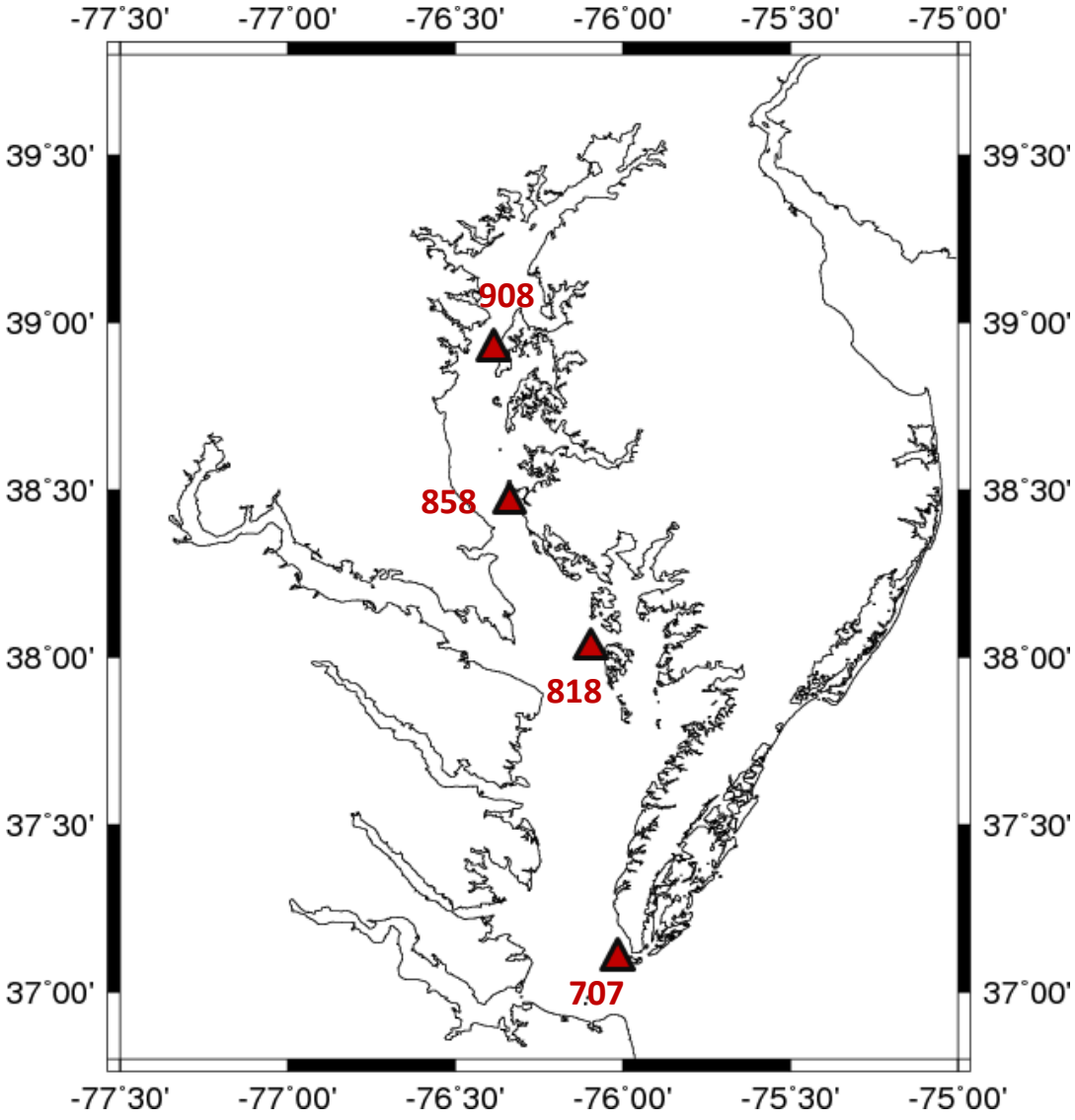

Figure S2. Dissolved oxygen data collected in 2009 along the vertical section of the Chesapeake Bay. Data were obtained from the Chesapeake Bay Program Water Quality Database (http://www.chesapeakebay.net/data/downloads/cbp_water_quality_database_1984_present). Approximate station locations sampled for the study herein are labeled in blue.

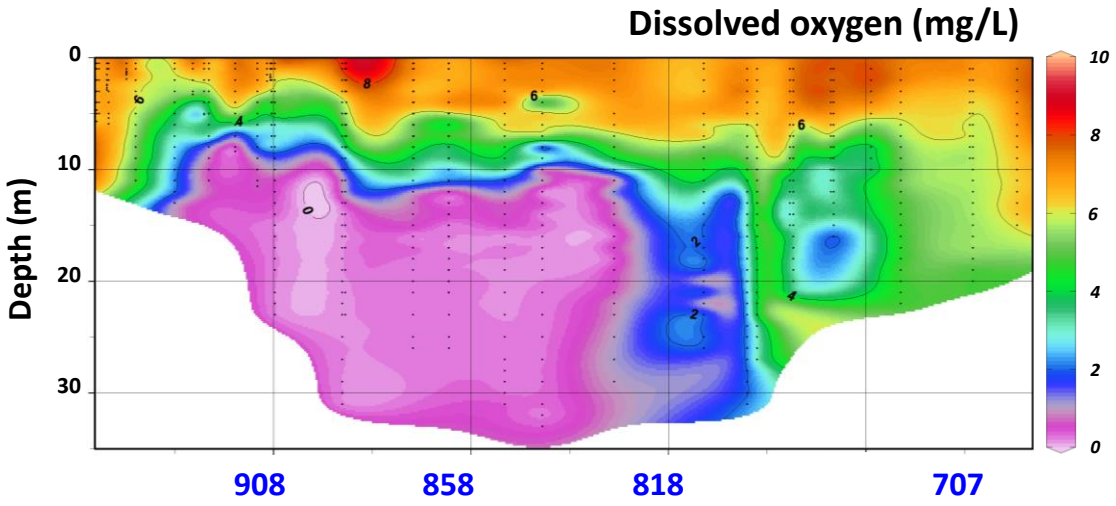

Figure S3. Dissolved oxygen data collected in 2010 along the vertical section of the Chesapeake Bay. Data were obtained from the Chesapeake Bay Program Water Quality Database (http://www.chesapeakebay.net/data/downloads/cbp_water_quality_database_1984_present). Approximate station locations sampled for the study herein are labeled in blue.

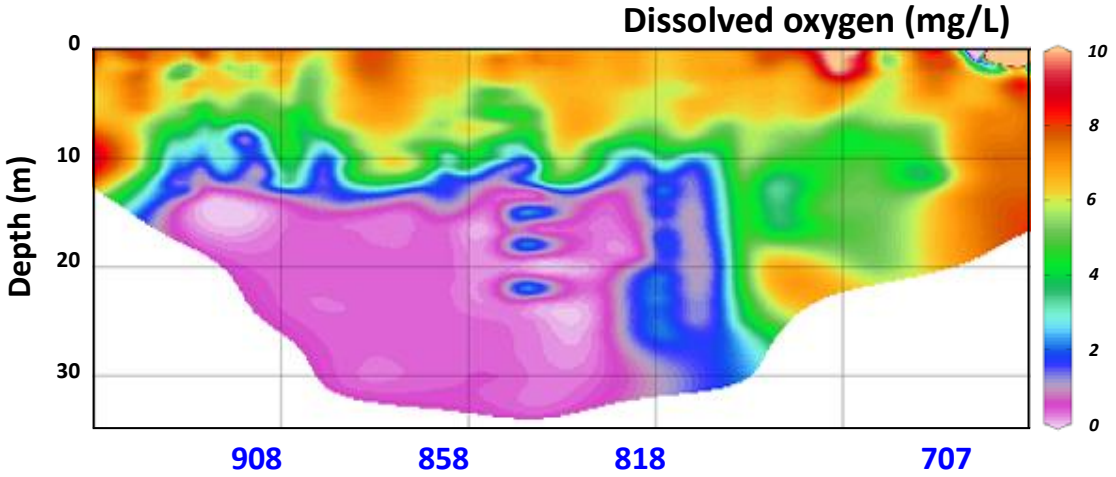

Figure S4. Non-metric multidimensional scaling (NMDS) plot of core **(A)** bacterial and **(B)** archaeal communities. Core bacterial and archaeal taxa are considered taxonomic groups that make up ≥ 1% of the total population in any sequenced library. These core taxa were analyzed using PC-ORD (Version 6, MiM Software) to determine similarities and/or differences in microbial populations among locations in Chesapeake Bay. NMDS plots were constructed using the Bray-Curtis distance measure, rotated with orthogonal principal axes, and analyzed using 1000 permutations. Samples are labeled according to station number and replicate (A, B, or C). Surface and depth horizons at station 908 are differentiated as follows: 908s_A-C (surface horizon) and 908d_A-C (depth horizon).

A.

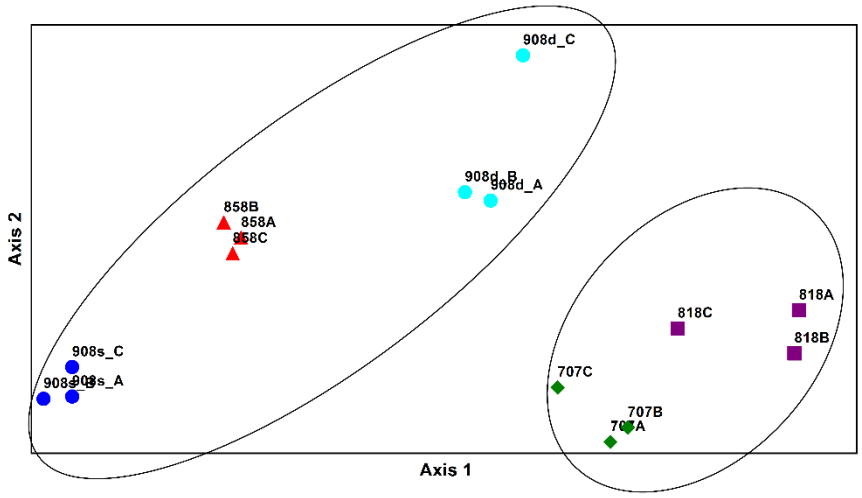

B.

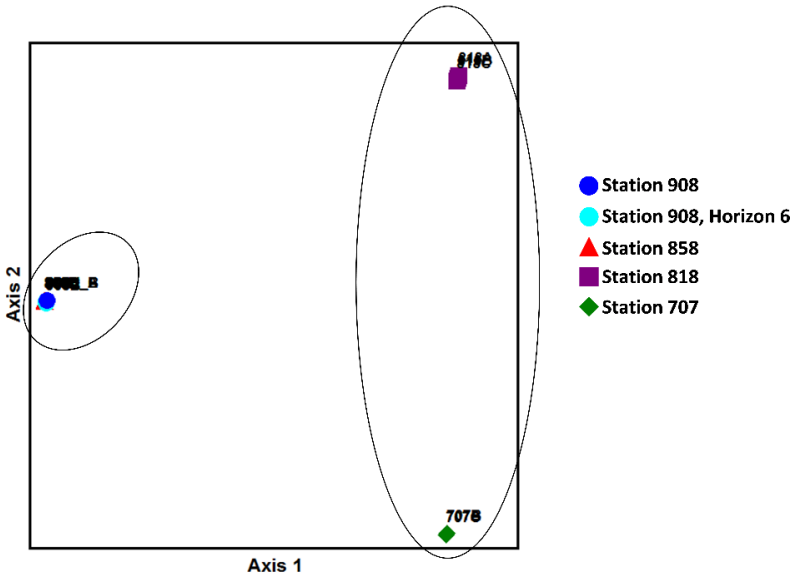

Figure S5. Distribution of **(A)** sulfate-reducing microorganisms and **(B)** methanogens in Chesapeake Bay sediment horizons. Relative percentages of microorganisms were determined via qPCR analysis of *dsrA* and bacterial 16S rRNA gene sequences for sulfate-reducers and *mcrA* and archaeal 16S rRNA gene sequences for methanogens. Calculations assume single copies of *dsrA, mcrA,* and 16S rRNA genes per cell. Analyses were conducted in triplicate, and averages were used to determine percentages shown below. Note: stations have different numbers of horizons due to the ability to core the different types of Bay sediment.

A.

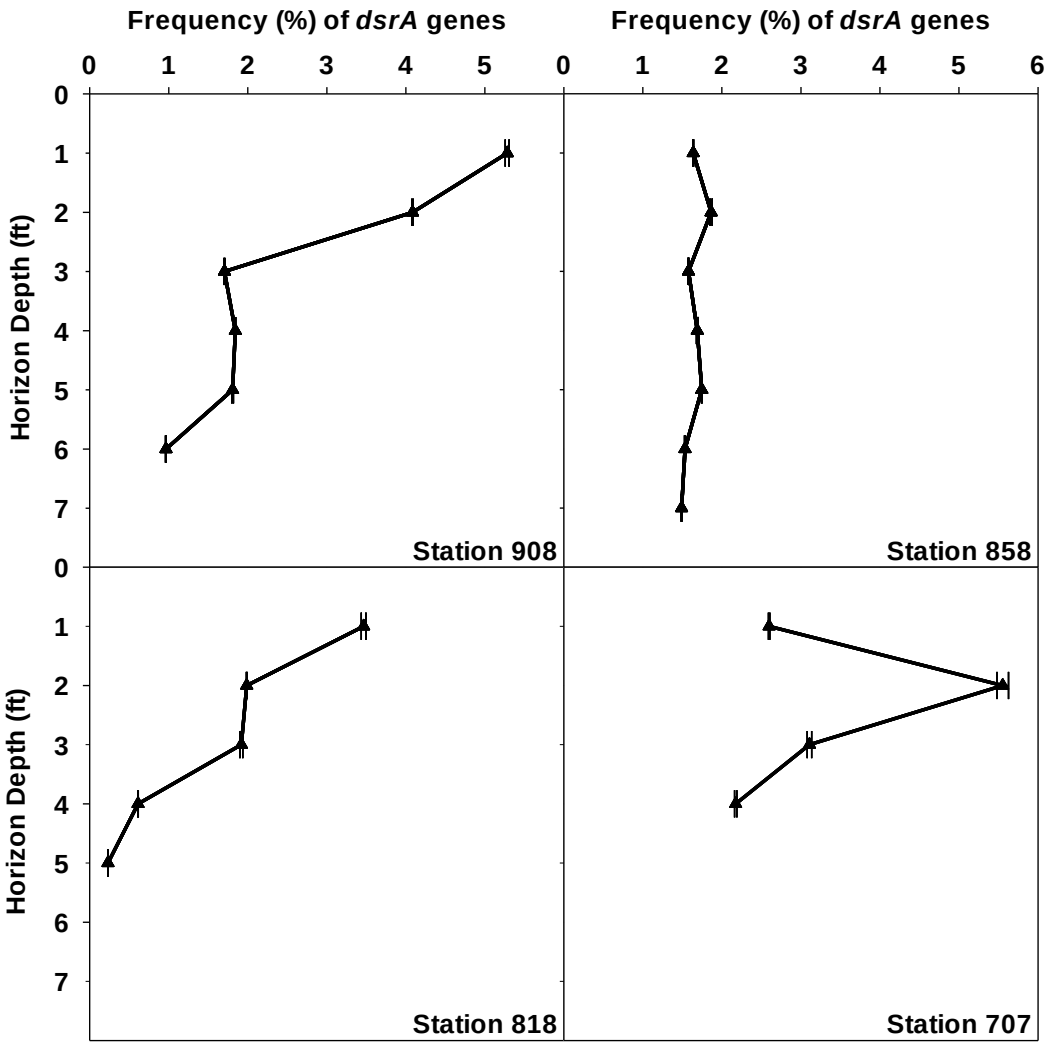

B.

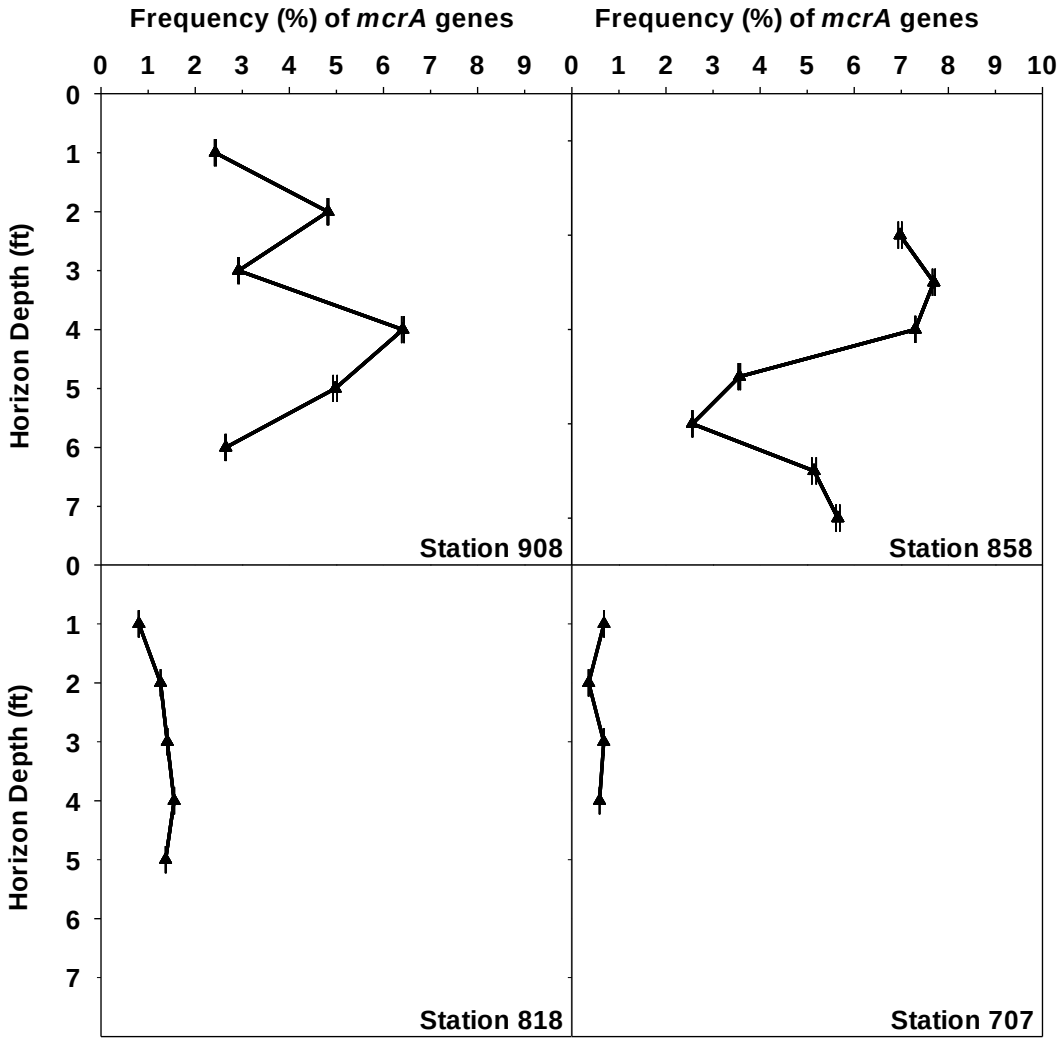
Frequency (%) of *mcrA* genes
Frequency (%) of *mcrA* genes
Horizon Depth (ft)
Horizon Depth (ft)
Station 908
Station 858
Station 818
Station 707

Figure S6. Sulfate loss in microcosms established under sulfate-reducing conditions with Chesapeake Bay sediment. Green bars indicate time-zero measurements, and the yellow bars indicate measurements at an incubation time-point for each station *prior* to sulfate re-amendment of the AK-01 controls. The incubation times required for sulfate depletion to *near* 2-3 mM varied among the stations (as shown below), occurring as follows: station 858 - 40 weeks of incubation; station 908 - 32 weeks; station 908 (horizon 6) - 20 weeks; and 24 weeks for stations 818 and 707. AK-01 positive controls were amended with additional sulfate when initial concentrations were depleted to 2-3 mM (See Table S8). *Enrichment cultures were allowed to incubate for a total of 672 days (not shown).* Treatments were established in triplicate as follows: (1) Active enrichments amended with sediment and hexadecane; (2) Positive controls amended with sediment, hexadecane, and *Desulfatibacillum alkenivorans* strain AK-01, (3) Background controls containing medium and sediment, (4) Abiotic media controls containing medium and hexadecane, and (5) Sterile controls amended with sediment and hexadecane and autoclaved at 121°C for three consecutive days. Data represent averages of triplicate incubations. Note: an asterisk (*) indicates a significant difference between sulfate concentrations at time-zero and the later time point.

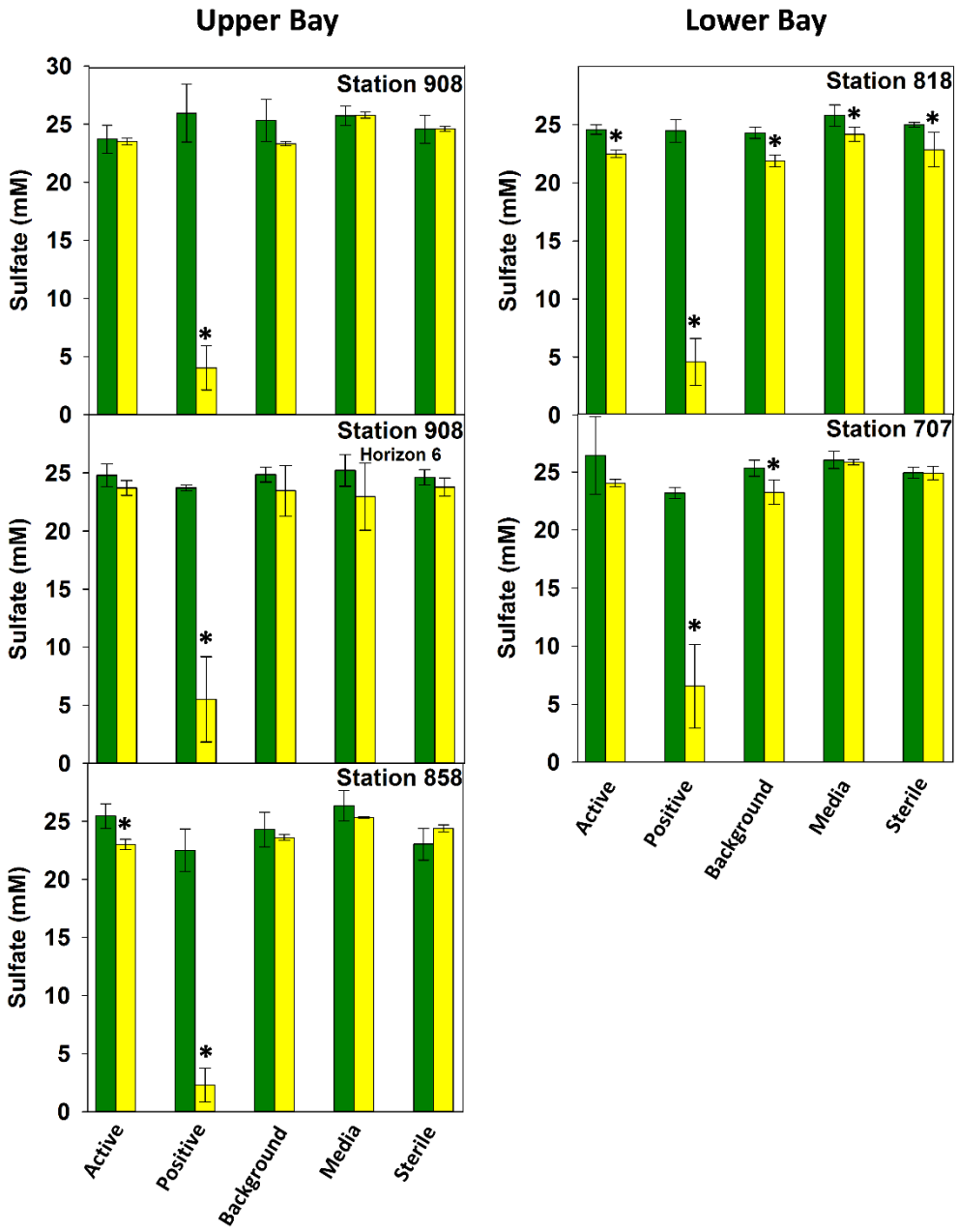
Upper Bay
Lower Bay
Station 908
Station 908
Horizon 6
Station 858
Station 818
Station 707
Sulfate (mM)
0
5
10
15
20
25
30
*
Active
Positive
Background
Media
Sterile

OXFORD UNIVERSITY PRESS LICENSE TERMS AND CONDITIONS

May 04, 2017

This Agreement between Jamie M Johnson Duffner ("You") and Oxford University Press ("Oxford University Press") consists of your license details and the terms and conditions provided by Oxford University Press and Copyright Clearance Center.

License Number	4102200770753
License date	May 04, 2017
Licensed content publisher	Oxford University Press
Licensed content publication	FEMS Microbiology Ecology
Licensed content title	Interrogation of Chesapeake Bay sediment microbial communities for intrinsic alkane-utilizing potential under anaerobic conditions
Licensed content author	Johnson, Jamie M.; Wawrik, Boris
Licensed content date	2015-02-24
Type of Use	Thesis/Dissertation
Institution name	
Title of your work	Microbial Ecology of Coastal Ecosystems: Investigations of the Genetic Potential for Anaerobic Hydrocarbon Transformation and the Response to Hydrocarbon Exposure
Publisher of your work	n/a
Expected publication date	May 2017
Permissions cost	0.00 USD
Value added tax	0.00 USD
Total	0.00 USD
Requestor Location	Jamie M Johnson Duffner 770 Van Vleet Oval NORMAN, OK 73019 United States Attn: Jamie M Johnson Duffner
Publisher Tax ID	GB125506730
Billing Type	Invoice
Billing Address	Jamie M Johnson Duffner 770 Van Vleet Oval NORMAN, OK 73019 United States Attn: Jamie M Johnson Duffner
Total	0.00 USD
Terms and Conditions	

STANDARD TERMS AND CONDITIONS FOR REPRODUCTION OF MATERIAL FROM AN OXFORD UNIVERSITY PRESS JOURNAL

1. Use of the material is restricted to the type of use specified in your order details.
2. This permission covers the use of the material in the English language in the following territory: world. If you have requested additional permission to translate this material, the terms and conditions of this reuse will be set out in clause 12.
3. This permission is limited to the particular use authorized in (1) above and does not allow you to sanction its use elsewhere in any other format other than specified above, nor does it apply to quotations, images, artistic works etc that have been reproduced from other sources which may be part of the material to be used.
4. No alteration, omission or addition is made to the material without our written consent. Permission must be re-cleared with Oxford University Press if/when you decide to reprint.
5. The following credit line appears wherever the material is used: author, title, journal, year, volume, issue number, pagination, by permission of Oxford University Press or the sponsoring society if the journal is a society journal. Where a journal is being published on behalf of a learned society, the details of that society must be included in the credit line.
6. For the reproduction of a full article from an Oxford University Press journal for whatever purpose, the corresponding author of the material concerned should be informed of the proposed use. Contact details for the corresponding authors of all Oxford University Press journal contact can be found alongside either the abstract or full text of the article concerned, accessible from www.oxfordjournals.org Should there be a problem clearing these rights, please contact journals.permissions@oup.com
7. If the credit line or acknowledgement in our publication indicates that any of the figures, images or photos was reproduced, drawn or modified from an earlier source it will be necessary for you to clear this permission with the original publisher as well. If this permission has not been obtained, please note that this material cannot be included in your publication/photocopies.
8. While you may exercise the rights licensed immediately upon issuance of the license at the end of the licensing process for the transaction, provided that you have disclosed complete and accurate details of your proposed use, no license is finally effective unless and until full payment is received from you (either by Oxford University Press or by Copyright Clearance Center (CCC)) as provided in CCC's Billing and Payment terms and conditions. If full payment is not received on a timely basis, then any license preliminarily granted shall be deemed automatically revoked and shall be void as if never granted. Further, in the event that you breach any of these terms and conditions or any of CCC's Billing and Payment terms and conditions, the license is automatically revoked and shall be void as if never granted. Use of materials as described in a revoked license, as well as any use of the materials beyond the scope of an unrevoked license, may constitute copyright infringement and Oxford University Press reserves the right to take any and all action to protect its copyright in the materials.
9. This license is personal to you and may not be sublicensed, assigned or transferred by you to any other person without Oxford University Press's written permission.
10. Oxford University Press reserves all rights not specifically granted in the combination of (i) the license details provided by you and accepted in the course of this licensing transaction, (ii) these terms and conditions and (iii) CCC's Billing and Payment terms and conditions.
11. You hereby indemnify and agree to hold harmless Oxford University Press and CCC, and their respective officers, directors, employs and agents, from and against any and all claims arising out of your use of the licensed material other than as specifically authorized pursuant to this license.
12. Other Terms and Conditions:

v1.4

Questions? customercare@copyright.com or +1-855-239-3415 (toll free in the US) or +1-978-646-2777.

Appendix II: Chapter 2 Supplemental Materials

Table S1. Sediment descriptions and latitude and longitude coordinates from each coastal sampling location in Biloxi, Mississippi.

	Site Description	Latitude	Longitude
Site 1	Medium-grain sandy upper layer and dark gray fine-grain lower layer; some noticeable sulfide odor. Marsh grass vegetation nearby.	N 30°22.470	W 088°47.597
Site 2	Sandy sediment, uniform with depth. No vegetation.	N 30°14.854	W 088°44.162
Site 3	Medium-grain sandy upper layer and dark-gray silt-like grain lower layer; some noticeable sulfide odor. Marsh grass vegetation nearby.	N 30°20.591	W 088°45.067

Table S2. Surface water measurements taken at sampling locations in Biloxi, Mississippi.

	Site 1	Site 2	Site 3
Temperature (°C)	27.6	26.9	27.5
pH	7.8	8.1	6.7
Salinity (ppt)	13	26	10
Redox Potential (mV)	-72.4	90.0	-10.5

Table S3. Ion concentrations measured in coastal water samples. Sulfate and chloride measurements conducted via ion exchange chromatography of four replicates per site. Nitrate, nitrite, and phosphate concentrations were determined via colorimetric assays. Note: **Surface** indicates water samples collected slightly offshore. **Overlying** indicates water overlying sediment collected onshore. N.D. = not detected.

	Site 1		Site 2		Site 3	
	Surface	**Overlying**	**Surface**	**Overlying**	**Surface**	**Overlying**
Sulfate (mM)	9.42 ± 0.04	8.05 ± 0.86	19.47 ± 0.06	16.58 ± 0.05	7.83 ± 0.04	9.26 ± 0.28
Chloride (mM)	264.84 ± 2.25	190.47 ± 58.74	542.78 ± 1.15	467.21 ± 2.61	225.15 ± 0.62	248.81 ± 32.33
Nitrate (mM)	0.01 ± 0.009	N.D.	N.D.	N.D.	N.D.	N.D.
Nitrite (mM)	N.D.	N.D.	N.D.	N.D.	N.D.	N.D.
Phosphate (mM)	0.02 ± 0.005	0.02 ± 0.001	N.D.	0.07 ± 0.002	0.018 ± 0.01	N.D.

Table S4. Average relative abundances of total Deltaproteobacteria detected in field (i.e., T-0) sediment communities based on 16S rRNA gene analyses. Note: values represent averages of 3-4 replicates. Significant p values are indicated in red.

	Site 1	Site 2	Site 3
	Jar A		
Average (%)	7.31 ± 0.17	2.54 ± 0.22	12.24 ± 0.49
T-test	**Site 1 vs. Site 2**	**Site 2 vs. Site 3**	**Site 1 vs. Site 3**
p value	3.40E-06	7.10E-07	1.30E-04
	Jar B		
Average (%)	4.43 ± 0.18	2.40 ± 0.12	7.82 ± 2.55
T-test	**Site 1 vs. Site 2**	**Site 2 vs. Site 3**	**Site 1 vs. Site 3**
p value	2.20E-05	0.03	0.07

Table S5. Multi-response permutational procedure (MRPP) analysis of field (i.e., T-0) sediment samples collected at Sites 1, 2, and 3. MRPP was conducted in PC-ORD (Version 6, MjM Software) using a Bray-Curtis distance measure with groups defined by site (i.e., Site 1, Site 2, Site 3). The test statistic, T, describes how strongly groups are separated from each other, with a more negative value indicative of a greater degree of separation. The chance-corrected within-group agreement, A, indicates within-group homogeneity compared to random chance. A maximum value of A=1 indicates that all samples within a group are identical. The p value indicates within-group replicates are statistically similar to each other than to replicates in other groups.

	T-0 Sediment
T	-8.89
A	0.32
p value	4.95E-06

Table S6. Diversity indices and descriptive information of Deltaproteobacteria communities sequenced from field (i.e., T-0) sediment samples at **(A)** Site 1, **(B)** Site 2, and **(C)** Site 3. A total of 105 deltaproteobacterial OTUs were detected in sediment at the genus level (97% similarity). Data were calculated in PC-ORD (Version 6, MjM Software). Abbreviations: S - number of taxa in each sample, E - evenness, H - Shannon Diversity index, and D' - Simpson's Diversity for an infinite population. D' is the complement of Simpson's original index and indicates the likelihood that two individuals from a population would be different, if chosen randomly.

A.

Sample	S	E	H	D'
Jar A, Rep. 1	50	0.927	3.627	0.966
Jar A, Rep. 2	61	0.917	3.772	0.969
Jar A, Rep. 3	68	0.927	3.913	0.974
Jar B, Rep. 1	61	0.962	3.955	0.978
Jar B, Rep. 2	78	0.947	4.127	0.981
Jar B, Rep. 3	64	0.966	4.017	0.979
Jar B, Rep. 4	82	0.953	4.202	0.982

B.

Sample	S	E	H	D'
Jar A, Rep. 1	51	0.964	3.789	0.974
Jar A, Rep. 2	56	0.953	3.836	0.974
Jar A, Rep. 3	74	0.935	4.026	0.977
Jar A, Rep. 4	60	0.947	3.878	0.974
Jar B, Rep. 1	70	0.938	3.984	0.976
Jar B, Rep. 2	55	0.949	3.801	0.972
Jar B, Rep. 3	50	0.953	3.728	0.971

C.

Sample	S	E	H	D'
Jar A, Rep. 1	38	0.962	3.499	0.966
Jar A, Rep. 2	80	0.922	4.038	0.977
Jar A, Rep. 3	70	0.933	3.963	0.977
Jar B, Rep. 1	82	0.936	4.126	0.980
Jar B, Rep. 2	67	0.929	3.908	0.975
Jar B, Rep. 3	58	0.936	3.801	0.973

Table S7. Relative abundances of the most abundant taxa within the total Deltaproteobacteria population in field (i.e., T-0) sediment samples from Site 1 **(A)** Jar A and **(B)** Jar B. Values were calculated based on the relative abundances of individual taxa and the relative abundance of total Deltaproteobacteria and represent averages from 3-4 replicates per jar.

A.

Deltaproteobacteria Taxa	Average (%)
Desulfarculaceae; g	14.51 ± 0.81
Nitrospinaceae; g	10.67 ± 1.76
Desulfonauticus	5.26 ± 0.66
Sh765B-TzT-29	17.70 ± 2.12
Syntrophaceae; g	6.43 ± 0.47
Bacteriovoracaceae; g	3.97 ± 0.19
Desulfobacteraceae; Other	2.92 ± 1.21
Desulfobacteraceae; SEEP-SRB1	2.14 ± 0.87
Desulfobacteraceae; Sva0081_sediment_group	3.28 ± 0.53
Desulfobulbus	2.46 ± 0.08
Sva0485; f; g	3.25 ± 0.69
Desulfobacca	3.01 ± 0.34
Syntrophobacteraceae; g	4.83 ± 1.09

B.

Deltaproteobacteria Taxa	Average (%)
Desulfarculaceae; g	3.61 ± 0.17
Desulfobacteraceae; Sva0081_sediment_group	9.65 ± 0.75
Desulfobacteraceae; g	2.82 ± 0.84
Desulfobulbus	3.90 ± 0.67
Desulfobulbaceae; MSBL7	1.84 ± 1.15
Desulfonauticus	8.53 ± 1.57
Desulfuromonadaceae; Other	4.09 ± 0.97
Desulfuromonadales; Sva1033; g	2.75 ± 0.50
GR-WP33-30; f; g	2.40 ± 0.78
Nannocystineae; g	2.08 ± 1.02
Sandaracinaceae	5.84 ± 1.08
Sh765B-TzT-29	6.78 ± 1.06

Table S8. Relative abundances of the most abundant taxa within the total Deltaproteobacteria population in field (i.e., T-0) sediment samples from Site 2 **(A)** Jar A and **(B)** Jar B. Values were calculated based on the relative abundances of individual taxa and the relative abundance of total Deltaproteobacteria and represent averages from 3-4 replicates per jar.

A.

Deltaproteobacteria Taxa	Average (%)
Bdellovibrionaceae; OM27_clade	3.43 ± 0.58
Desulfobacteraceae; Sva0081_sediment_group	5.29 ± 1.68
Desulfonauticus	13.83 ± 1.40
Desulfuromonadales; GR-WP33-58; g	3.16 ± 0.24
GR-WP33-30; f; g	3.99 ± 0.62
Myxococcales; 0319-6G20; g	2.50 ± 0.64
Haliangium	3.74 ± 0.52
Sandaracinaceae	11.30 ± 2.06
SAR324_clade, Marine_group_B f; g	2.98 ± 0.58
Sh765B-TzT-29	11.21 ± 0.66

B.

Deltaproteobacteria Taxa	Average (%)
Bdellovibrio	2.65 ± 0.53
Desulfobacteraceae; Sva0081_sediment_group	4.69 ± 0.80
Desulfonauticus	15.17 ± 0.36
Desulfothermus	1.79 ± 0.71
Desulfuromonadales; GR-WP33-58; g	3.46 ± 0.66
GR-WP33-30; f; g	5.53 ± 1.48
Haliangium	5.08 ± 1.62
Sandaracinaceae	9.26 ± 1.77
SAR324_clade, Marine_group_B; f; g	2.56 ± 1.33
Sh765B-TzT-29	14.36 ± 1.22

Table S9. Relative abundances of the most abundant taxa within the total Deltaproteobacteria population in field (i.e., T-0) sediment samples from Site 3 **(A)** Jar A and **(B)** Jar B. Values were calculated based on the relative abundances of individual taxa and the relative abundance of total Deltaproteobacteria and represent averages from 3-4 replicates per jar.

A.

Deltaproteobacteria Taxa	Average (%)
43F-1404R; f; g	3.79 ± 1.31
Desulfarculaceae; g	7.70 ± 1.49
Desulfobacteraceae; Sva0081_sediment_group	9.20 ± 2.65
Desulfobacteraceae; g	3.05 ± 0.20
Desulfonauticus	4.54 ± 0.64
Desulfuromonas	2.65 ± 1.30
Geoalkalibacter	3.98 ± 0.88
GR-WP33-30; f; g	6.08 ± 0.94
Sh765B-TzT-29; f; g	9.59 ± 1.15
Desulfobacca	8.42 ± 2.36
Syntrophobacteraceae; g	5.52 ± 1.90
Desulfobacteraceae;Other	2.79 ± 0.96
Desulfobulbus	2.64 ± 0.65
Nitrospinaceae; g	2.71 ± 0.23
Nannocystineae; g	2.13 ± 0.27

B.

Deltaproteobacteria Taxa	Average (%)
43F-1404R; f; g	2.76 ± 1.35
Desulfarculaceae; g	7.58 ± 0.95
Desulfobacteraceae; Other	2.97 ± 0.21
Desulfobacteraceae; SEEP-SRB1	2.45 ± 1.00
Desulfobacteraceae; Sva0081_sediment_group	6.60 ± 1.81
Desulfobulbus	4.20 ± 1.40
Nitrospinaceae; g	4.57 ± 0.42
Desulfonauticus	5.92 ± 2.17
Geoalkalibacter	2.42 ± 1.49
Geobacter	4.06 ± 2.85
GR-WP33-30; f; g	4.29 ± 1.67
Sh765B-TzT-29; f; g	8.08 ± 1.61
Sva0485; f; g	3.26 ± 1.65
Desulfobacca	8.38 ± 2.44
Syntrophobacteraceae; g	5.81 ± 1.49

Table S10. Change in relative abundances of total Deltaproteobacteria from samples collected in the field (i.e., T-0) compared to SRA samples from **(A)** Jar A and **(B)** Jar B. Values represent averages of 3-4 replicates per site. Significant p values are denoted in red. N.A. indicates repeat SRAs that were not conducted separately.

A.

	T-0, Jar A	Source Oil	0.1% & 10% Source Oil	50% & 100% Source Oil	Pyrene
Site 1	7.31 ± 0.17 %	7.61% ± 0.72%	8.12% ± 0.58%	7.02 % ± 0.14%	6.88% ± 0.41%
t-tests		**T-0 vs Source Oil**	**T-0 vs 0.1% Repeats**	**T-0 vs 50% Repeats**	**T-0 vs Pyrene**
p values		0.59	0.10	0.09	0.21
Site 2	2.54% ± 0.22%	2.13% ± 0.50%	N.A.	2.11% ± 0.38%	1.33% ± 0.22%
t-tests		**T-0 vs Source Oil**	**T-0 vs 0.1% Repeats**	**T-0 vs 50% Repeats**	**T-0 vs Pyrene**
p values		0.24	N.A.	0.15	5.49E-04
Site 3	12.24% ± 0.90%	12.77% ± 0.58%	N.A.	10.05% ± 0.62%	8.49% ± 1.99%
t-tests		**T-0 vs Source Oil**	**T-0 vs 0.1% Repeats**	**T-0 vs 50% Repeats**	**T-0 vs Pyrene**
p values		0.33	N.A.	8.13E-03	0.04

B.

	T-0, Jar B	Anthracene	Mix
Site 1	4.43% ± 0.18%	4.31% ± 0.69%	5.42% ± 0.15%
t-tests		**T-0 vs Anthracene**	**T-0 vs Mix**
p values		0.69	3.01E-04
Site 2	2.40% ± 0.12%	2.68% ± 0.36%	5.81% ± 0.77%
t-tests		**T-0 vs Anthracene**	**T-0 vs Mix**
p values		0.32	1.31E-03
Site 3	7.82% ± 2.55%	11.42% ± 0.90%	12.07% ± 0.69%
t-tests		**T-0 vs Anthracene**	**T-0 vs Mix**
p values		0.08	0.04

Table S11. Average relative abundances of deltaproteobacterial taxa sequenced from field (i.e., T-0) sediment and SRA samples from **(A)** Site 1, **(B)** Site 2, and **(C)** Site 3. Data obtained through analysis of 16S rRNA gene sequences analyzed via QIIME (Version 1.9.0) (Caporaso *et al.*, 2010a). Values represent averages of 3-4 replicates per sample.

A.

	T-0 Jar A (%)	Source Oil (%)	0.1% & 10% Source Oil (%)	50% & 100% Source Oil (%)	Pyrene (%)	T-0 Jar B (%)	Anth. (%)	Mix (%)
Other	0.01	0.01	0.03	0.01	0.01	0.01	0.00	0.01
10bav-F6; f; g	0.00	0.00	0.01	0.00	0.00	0.00	0.00	0.00
43F-1404R; f; g	0.09	0.05	0.10	0.04	0.08	0.02	0.03	0.02
Bdellovibrionales; Bacteriovoracaceae;Other	0.00	0.00	0.00	0.00	0.00	0.01	0.00	0.00
Bdellovibrionales; Bacteriovoracaceae; Bacteriovorax	0.00	0.00	0.00	0.00	0.00	0.01	0.00	0.00
Bdellovibrionales; Bacteriovoracaceae; Deferrisoma	0.00	0.01	0.00	0.00	0.01	0.00	0.01	0.00
Bdellovibrionales; Bacteriovoracaceae; Peredibacter	0.01	0.00	0.00	0.01	0.00	0.01	0.00	0.00
Bdellovibrionales; Bacteriovoracaceae; g	0.29	0.24	0.24	0.24	0.13	0.02	0.00	0.02
Bdellovibrionales; Bdellovibrionaceae; Bdellovibrio	0.02	0.02	0.04	0.01	0.05	0.09	0.04	0.03
Bdellovibrionales; Bdellovibrionaceae; OM27_clade	0.01	0.01	0.01	0.03	0.01	0.08	0.03	0.04
DTB120; f; g	0.01	0.00	0.00	0.00	0.00	0.00	0.00	0.00
Desulfarculales; Desulfarculaceae;Other	0.00	0.00	0.00	0.00	0.00	0.00	0.00	0.00
Desulfarculales; Desulfarculaceae; Desulfarculus	0.01	0.00	0.03	0.01	0.01	0.01	0.00	0.00
Desulfarculales; Desulfarculaceae; g	1.06	1.07	0.95	0.79	0.72	0.16	0.10	0.20
Desulfobacterales;Other;Other	0.00	0.00	0.00	0.00	0.00	0.00	0.00	0.00
Desulfobacterales; Desulfobacteraceae;Other	0.21	0.04	0.08	0.06	0.11	0.09	0.07	0.07
Desulfobacterales; Desulfobacteraceae; Desulfatibacillum	0.00	0.00	0.00	0.00	0.01	0.00	0.00	0.00
Desulfobacterales; Desulfobacteraceae; Desulfatiferula	0.00	0.00	0.00	0.00	0.00	0.00	0.01	0.00
Desulfobacterales; Desulfobacteraceae; Desulfatirhabdium	0.00	0.01	0.00	0.01	0.00	0.00	0.00	0.01
Desulfobacterales; Desulfobacteraceae; Desulfobacter	0.00	0.08	0.01	0.03	0.00	0.03	0.03	0.01
Desulfobacterales; Desulfobacteraceae; Desulfobacterium	0.00	0.00	0.01	0.00	0.01	0.00	0.03	0.04
Desulfobacterales; Desulfobacteraceae; Desulfobacula	0.00	0.02	0.02	0.05	0.05	0.02	0.12	0.13
Desulfobacterales; Desulfobacteraceae; Desulfocella	0.00	0.00	0.00	0.00	0.00	0.00	0.00	0.00
Desulfobacterales; Desulfobacteraceae; Desulfobotulus	0.00	0.00	0.01	0.01	0.00	0.00	0.00	0.00
Desulfobacterales; Desulfobacteraceae; Desulfococcus	0.04	0.02	0.06	0.01	0.02	0.03	0.04	0.03
Desulfobacterales; Desulfobacteraceae; Desulfofaba	0.01	0.03	0.01	0.02	0.01	0.01	0.01	0.01
Desulfobacterales; Desulfobacteraceae; Desulfofrigus	0.00	0.00	0.00	0.01	0.00	0.00	0.02	0.02
Desulfobacterales; Desulfobacteraceae; Desulfosalsimonas	0.00	0.00	0.01	0.01	0.01	0.01	0.02	0.11
Desulfobacterales; Desulfobacteraceae; Desulfosarcina	0.01	0.02	0.06	0.05	0.03	0.10	0.11	0.15
Desulfobacterales; Desulfobacteraceae; Desulfospira	0.00	0.00	0.00	0.03	0.00	0.02	0.04	0.01
Desulfobacterales; Desulfobacteraceae; Desulfotignum	0.01	0.00	0.01	0.01	0.01	0.11	0.02	0.01
Desulfobacterales; Desulfobacteraceae; SEEP-SRB1	0.16	0.64	0.72	0.57	0.46	0.09	0.11	0.23

Desulfobacterales; Desulfobacteraceae; Sva0081_sediment_group	0.24	0.33	0.44	0.30	0.21	0.43	0.46	0.58
Desulfobacterales; Desulfobacteraceae; g	0.06	0.11	0.13	0.12	0.05	0.12	0.12	0.16
Desulfobacterales; Desulfobulbaceae;Other	0.01	0.01	0.11	0.08	0.04	0.04	0.13	0.18
Desulfobacterales; Desulfobulbaceae; Desulfobulbus	0.18	0.18	0.21	0.21	0.11	0.17	0.20	0.25
Desulfobacterales; Desulfobulbaceae; Desulfocapsa	0.00	0.01	0.01	0.03	0.01	0.00	0.05	0.02
Desulfobacterales; Desulfobulbaceae; Desulfopila	0.00	0.02	0.07	0.12	0.04	0.08	0.13	0.20
Desulfobacterales; Desulfobulbaceae; Desulforhopalus	0.00	0.00	0.00	0.01	0.01	0.00	0.02	0.07
Desulfobacterales; Desulfobulbaceae; Desulfotalea	0.00	0.00	0.00	0.00	0.00	0.00	0.00	0.00
Desulfobacterales; Desulfobulbaceae; Desulfurivibrio	0.01	0.01	0.01	0.02	0.01	0.03	0.08	0.02
Desulfobacterales; Desulfobulbaceae; MSBL7	0.01	0.02	0.05	0.05	0.02	0.08	0.05	0.05
Desulfobacterales; Desulfobulbaceae; SEEP-SRB2	0.03	0.08	0.09	0.06	0.03	0.01	0.01	0.02
Desulfobacterales; Desulfobulbaceae; SEEP-SRB4	0.00	0.00	0.00	0.00	0.00	0.01	0.00	0.00
Desulfobacterales; Desulfobulbaceae; g	0.02	0.02	0.09	0.13	0.06	0.09	0.32	0.31
Desulfobacterales; Nitrospinaceae; Candidatus_Entotheonella	0.02	0.02	0.01	0.00	0.00	0.04	0.03	0.03
Desulfobacterales; Nitrospinaceae; Nitrospina	0.00	0.00	0.00	0.00	0.00	0.01	0.00	0.00
Desulfobacterales; Nitrospinaceae; g	0.77	0.82	0.76	0.71	1.26	0.08	0.17	0.21
Desulfovibrionales; Desulfohalobiaceae;Other	0.00	0.00	0.00	0.00	0.00	0.00	0.00	0.00
Desulfovibrionales;Other;Other	0.00	0.00	0.00	0.00	0.00	0.00	0.00	0.00
Desulfovibrionales; Desulfohalobiaceae; Desulfonauticus	0.38	0.00	0.00	0.00	0.00	0.38	0.00	0.00
Desulfovibrionales; Desulfohalobiaceae; Desulfothermus	0.04	0.00	0.00	0.00	0.00	0.03	0.00	0.00
Desulfovibrionales; Desulfohalobiaceae; Desulfovermiculus	0.00	0.00	0.00	0.00	0.00	0.00	0.00	0.00
Desulfovibrionales; Desulfomicrobiaceae; Desulfomicrobium	0.00	0.00	0.00	0.01	0.00	0.00	0.00	0.00
Desulfovibrionales; Desulfovibrionaceae;Other	0.00	0.00	0.00	0.00	0.02	0.00	0.00	0.00
Desulfovibrionales; Desulfovibrionaceae; Desulfovibrio	0.01	0.01	0.01	0.02	0.01	0.01	0.01	0.02
Desulfurellales; Desulfurellaceae; g	0.01	0.01	0.02	0.01	0.01	0.01	0.00	0.02
Desulfuromonadales;Other;Other	0.04	0.09	0.13	0.06	0.04	0.03	0.04	0.02
Desulfuromonadales; 21f08; g	0.00	0.01	0.00	0.00	0.00	0.00	0.00	0.00
Desulfuromonadales; AKYG597; g	0.00	0.00	0.00	0.00	0.00	0.00	0.00	0.00
Desulfuromonadales; BVA18; g	0.00	0.00	0.00	0.00	0.00	0.00	0.00	0.00
Desulfuromonadales; Desulfuromonadaceae;Other	0.01	0.02	0.02	0.01	0.01	0.18	0.01	0.01
Desulfuromonadales; Desulfuromonadaceae; Desulfuromonas	0.14	0.02	0.05	0.05	0.05	0.05	0.04	0.02
Desulfuromonadales; Desulfuromonadaceae; Desulfuromusa	0.00	0.01	0.10	0.11	0.09	0.02	0.25	0.24
Desulfuromonadales; Desulfuromonadaceae; Pelobacter	0.02	0.13	0.15	0.18	0.14	0.04	0.06	0.19
Desulfuromonadales; GR-WP33-58; g	0.02	0.00	0.00	0.01	0.00	0.07	0.03	0.04
Desulfuromonadales; Geobacteraceae;Other	0.00	0.00	0.01	0.01	0.00	0.01	0.03	0.01
Desulfuromonadales; Geobacteraceae; Geoalkalibacter	0.04	0.04	0.03	0.02	0.01	0.01	0.01	0.03
Desulfuromonadales; Geobacteraceae; Geobacter	0.04	0.02	0.03	0.01	0.03	0.02	0.01	0.02
Desulfuromonadales; Geobacteraceae; Geopsychrobacter	0.00	0.00	0.00	0.00	0.00	0.01	0.00	0.00
Desulfuromonadales; Geobacteraceae; Geothermobacter	0.00	0.01	0.03	0.02	0.00	0.03	0.02	0.05
Desulfuromonadales; M113; g	0.00	0.00	0.00	0.00	0.00	0.00	0.00	0.00
Desulfuromonadales; Sva1033; g	0.00	0.02	0.08	0.05	0.02	0.12	0.17	0.18

FW113; f; g	0.01	0.00	0.02	0.02	0.04	0.01	0.00	0.01
GR-WP33-30; f; g	0.09	0.03	0.07	0.06	0.05	0.11	0.06	0.09
Myxococcales;Other;Other	0.01	0.00	0.00	0.01	0.00	0.00	0.00	0.00
Myxococcales; 0319-6G20; g	0.03	0.01	0.01	0.01	0.00	0.04	0.05	0.06
Myxococcales; Cystobacteraceae; Anaeromyxobacter	0.00	0.00	0.00	0.01	0.00	0.00	0.00	0.00
Myxococcales; Cystobacterineae;Other	0.00	0.00	0.00	0.00	0.00	0.00	0.00	0.00
Myxococcales; Cystobacterineae; g	0.04	0.01	0.02	0.04	0.01	0.04	0.05	0.04
Myxococcales; FFCH16767; g	0.00	0.00	0.00	0.00	0.00	0.00	0.00	0.00
Myxococcales; Haliangiaceae; Haliangium	0.08	0.03	0.06	0.06	0.03	0.03	0.05	0.05
Myxococcales; MSB-4B10; g	0.00	0.01	0.02	0.01	0.00	0.00	0.00	0.00
Myxococcales; Nannocystaceae;Other	0.00	0.00	0.00	0.00	0.00	0.00	0.00	0.01
Myxococcales; Nannocystaceae; Enhygromyxa	0.01	0.01	0.01	0.03	0.01	0.00	0.00	0.01
Myxococcales; Nannocystaceae; Nannocystis	0.00	0.01	0.00	0.00	0.00	0.01	0.01	0.01
Myxococcales; Nannocystaceae; g	0.00	0.00	0.00	0.01	0.00	0.01	0.00	0.02
Myxococcales; Nannocystineae; Nannocystaceae	0.00	0.00	0.00	0.00	0.00	0.00	0.00	0.00
Myxococcales; Nannocystineae; g	0.06	0.10	0.03	0.05	0.02	0.09	0.04	0.04
Myxococcales; Phaselicystidaceae; Phaselicystis	0.00	0.00	0.01	0.00	0.00	0.01	0.00	0.01
Myxococcales; Polyangiaceae;Other	0.01	0.00	0.00	0.01	0.00	0.00	0.00	0.00
Myxococcales; Polyangiaceae; Byssovorax	0.01	0.00	0.00	0.01	0.00	0.00	0.00	0.00
Myxococcales; Polyangiaceae; Chondromyces	0.00	0.00	0.00	0.00	0.00	0.00	0.00	0.00
Myxococcales; Polyangiaceae; Sorangium	0.01	0.01	0.02	0.01	0.01	0.00	0.00	0.01
Myxococcales; Sandaracinaceae; Sandaracinus	0.00	0.01	0.01	0.02	0.00	0.01	0.00	0.00
Myxococcales; Sorangiineae;Other	0.00	0.00	0.00	0.00	0.00	0.00	0.00	0.00
Myxococcales; Sorangiineae; Sandaracinaceae	0.07	0.10	0.10	0.13	0.06	0.26	0.19	0.18
Myxococcales; Sorangiineae; g	0.04	0.03	0.02	0.03	0.01	0.02	0.01	0.02
Myxococcales; VHS-B3-70; g	0.04	0.02	0.04	0.04	0.00	0.00	0.00	0.00
Myxococcales; mle1-27; g	0.00	0.00	0.00	0.00	0.00	0.00	0.00	0.00
Order_Incertae_Sedis; Syntrophorhabdaceae; Syntrophorhabdus	0.00	0.00	0.00	0.00	0.01	0.00	0.00	0.00
SAR324_clade(Marine_group_B); f; g	0.11	0.04	0.05	0.00	0.03	0.10	0.01	0.02
Sh765B-TzT-29; f; g	1.29	1.77	1.44	1.19	1.97	0.30	0.33	0.37
Sva0485; f; g	0.24	0.23	0.30	0.17	0.09	0.06	0.02	0.08
Syntrophobacterales; Syntrophaceae;Other	0.01	0.00	0.01	0.00	0.00	0.00	0.00	0.00
Syntrophobacterales; Syntrophaceae; Desulfobacca	0.22	0.18	0.13	0.17	0.18	0.04	0.01	0.07
Syntrophobacterales; Syntrophaceae; Desulfomonile	0.02	0.02	0.04	0.02	0.02	0.01	0.02	0.01
Syntrophobacterales; Syntrophaceae; Smithella	0.00	0.00	0.01	0.00	0.00	0.00	0.00	0.00
Syntrophobacterales; Syntrophaceae; Syntrophus	0.02	0.01	0.01	0.04	0.00	0.00	0.00	0.00
Syntrophobacterales; Syntrophaceae; g	0.47	0.40	0.27	0.23	0.21	0.03	0.03	0.03
Syntrophobacterales; Syntrophobacteraceae;Other	0.00	0.00	0.00	0.01	0.00	0.00	0.00	0.00
Syntrophobacterales; Syntrophobacteraceae; Desulforhabdus	0.00	0.04	0.01	0.03	0.00	0.01	0.01	0.02
Syntrophobacterales; Syntrophobacteraceae; Syntrophobacter	0.01	0.00	0.00	0.00	0.01	0.00	0.01	0.01
Syntrophobacterales; Syntrophobacteraceae; g	0.35	0.29	0.33	0.21	0.11	0.06	0.06	0.10

Desulfobacterales; Desulfobacteraceae; Desulfofrigus	0.00	0.00	0.00	0.00	0.00	0.00	0.00	0.00
Desulfobacterales; Desulfobacteraceae; Desulfonema	0.00	0.00	0.00	0.00	0.00	0.00	0.00	0.00
Desulfovibrionales;Other;Other	0.00	0.00	0.00	0.00	0.00	0.00	0.00	0.00
Desulfovibrionales; Desulfovibrionaceae; Desulfocurvus	0.00	0.00	0.00	0.00	0.00	0.00	0.00	0.00
Desulfuromonadales; 008E09-B-D-P15; g	0.00	0.00	0.00	0.00	0.00	0.00	0.00	0.00
Syntrophobacterales;Other;Other	0.00	0.00	0.00	0.00	0.00	0.00	0.00	0.00
Syntrophobacterales; Syntrophobacteraceae; Desulfacinum	0.00	0.00	0.00	0.00	0.00	0.00	0.00	0.00

B.

	T-0 Jar A (%)	Source Oil (%)	50% & 100% Source Oil (%)	Pyrene (%)	T-0 Jar B (%)	Anth. (%)	Mix (%)
Other	0.01	0.00	0.00	0.01	0.00	0.00	0.00
10bav-F6; f; g	0.00	0.00	0.00	0.00	0.00	0.00	0.00
43F-1404R; f; g	0.02	0.01	0.02	0.01	0.02	0.00	0.01
Bdellovibrionales; Bacteriovoracaceae;Other	0.01	0.01	0.00	0.00	0.01	0.00	0.00
Bdellovibrionales; Bacteriovoracaceae; Bacteriovorax	0.01	0.00	0.00	0.00	0.01	0.00	0.00
Bdellovibrionales; Bacteriovoracaceae; Deferrisoma	0.00	0.00	0.00	0.00	0.00	0.00	0.00
Bdellovibrionales; Bacteriovoracaceae; Peredibacter	0.02	0.01	0.00	0.00	0.02	0.00	0.01
Bdellovibrionales; Bacteriovoracaceae; g	0.03	0.04	0.01	0.01	0.03	0.00	0.01
Bdellovibrionales; Bdellovibrionaceae; Bdellovibrio	0.09	0.05	0.03	0.02	0.06	0.02	0.01
Bdellovibrionales; Bdellovibrionaceae; OM27_clade	0.09	0.07	0.01	0.03	0.06	0.00	0.00
DTB120; f; g	0.00	0.00	0.00	0.00	0.00	0.00	0.00
Desulfarculales; Desulfarculaceae;Other	0.00	0.00	0.00	0.00	0.00	0.00	0.00
Desulfarculales; Desulfarculaceae; Desulfarculus	0.00	0.00	0.00	0.00	0.00	0.00	0.00
Desulfarculales; Desulfarculaceae; g	0.06	0.01	0.06	0.03	0.05	0.03	0.03
Desulfobacterales;Other;Other	0.00	0.00	0.00	0.00	0.00	0.00	0.00
Desulfobacterales; Desulfobacteraceae;Other	0.03	0.03	0.05	0.01	0.02	0.00	0.03
Desulfobacterales; Desulfobacteraceae; Desulfatibacillum	0.00	0.00	0.00	0.00	0.00	0.00	0.00
Desulfobacterales; Desulfobacteraceae; Desulfatiferula	0.00	0.01	0.00	0.00	0.00	0.00	0.00
Desulfobacterales; Desulfobacteraceae; Desulfatirhabdium	0.00	0.00	0.00	0.00	0.00	0.00	0.00
Desulfobacterales; Desulfobacteraceae; Desulfobacter	0.00	0.00	0.00	0.00	0.00	0.01	0.00
Desulfobacterales; Desulfobacteraceae; Desulfobacterium	0.00	0.00	0.01	0.00	0.00	0.08	0.18
Desulfobacterales; Desulfobacteraceae; Desulfobacula	0.00	0.01	0.07	0.01	0.00	0.17	1.08
Desulfobacterales; Desulfobacteraceae; Desulfocella	0.00	0.00	0.00	0.00	0.00	0.00	0.00
Desulfobacterales; Desulfobacteraceae; Desulfobotulus	0.00	0.00	0.00	0.00	0.00	0.00	0.00
Desulfobacterales; Desulfobacteraceae; Desulfococcus	0.00	0.00	0.00	0.00	0.00	0.00	0.00
Desulfobacterales; Desulfobacteraceae; Desulfofaba	0.00	0.01	0.20	0.01	0.00	0.38	1.24
Desulfobacterales; Desulfobacteraceae; Desulfofrigus	0.00	0.00	0.00	0.00	0.00	0.00	0.00
Desulfobacterales; Desulfobacteraceae; Desulfosalsimonas	0.00	0.01	0.00	0.00	0.00	0.01	0.04
Desulfobacterales; Desulfobacteraceae; Desulfosarcina	0.03	0.01	0.03	0.04	0.02	0.05	0.06
Desulfobacterales; Desulfobacteraceae; Desulfospira	0.00	0.01	0.00	0.00	0.00	0.00	0.00
Desulfobacterales; Desulfobacteraceae; Desulfotignum	0.01	0.00	0.00	0.00	0.01	0.02	0.00
Desulfobacterales; Desulfobacteraceae; SEEP-SRB1	0.01	0.01	0.01	0.00	0.01	0.02	0.03
Desulfobacterales; Desulfobacteraceae; Sva0081_sediment_group	0.14	0.11	0.07	0.10	0.11	0.06	0.15
Desulfobacterales; Desulfobacteraceae; g	0.03	0.02	0.09	0.01	0.03	0.04	0.13
Desulfobacterales; Desulfobulbaceae;Other	0.00	0.03	0.02	0.00	0.00	0.03	0.08
Desulfobacterales; Desulfobulbaceae; Desulfobulbus	0.03	0.04	0.03	0.01	0.02	0.02	0.02
Desulfobacterales; Desulfobulbaceae; Desulfocapsa	0.00	0.00	0.00	0.00	0.00	0.01	0.04

Desulfobacterales; Desulfobulbaceae; Desulfopila	0.02	0.05	0.16	0.09	0.01	0.42	1.22
Desulfobacterales; Desulfobulbaceae; Desulforhopalus	0.00	0.00	0.00	0.00	0.00	0.01	0.01
Desulfobacterales; Desulfobulbaceae; Desulfotalea	0.00	0.00	0.00	0.00	0.00	0.00	0.00
Desulfobacterales; Desulfobulbaceae; Desulfurivibrio	0.01	0.00	0.00	0.00	0.01	0.00	0.00
Desulfobacterales; Desulfobulbaceae; MSBL7	0.00	0.00	0.00	0.01	0.00	0.00	0.01
Desulfobacterales; Desulfobulbaceae; SEEP-SRB2	0.00	0.00	0.00	0.00	0.00	0.00	0.00
Desulfobacterales; Desulfobulbaceae; SEEP-SRB4	0.01	0.00	0.00	0.00	0.00	0.00	0.00
Desulfobacterales; Desulfobulbaceae; g	0.05	0.02	0.07	0.03	0.02	0.18	0.16
Desulfobacterales; Nitrospinaceae; Candidatus_Entotheonella	0.03	0.03	0.01	0.00	0.05	0.00	0.01
Desulfobacterales; Nitrospinaceae; Nitrospina	0.01	0.02	0.00	0.01	0.01	0.02	0.00
Desulfobacterales; Nitrospinaceae; g	0.04	0.01	0.02	0.01	0.03	0.02	0.02
Desulfovibrionales; Desulfohalobiaceae;Other	0.00	0.00	0.00	0.00	0.00	0.00	0.00
Desulfovibrionales;Other;Other	0.00	0.00	0.00	0.00	0.00	0.00	0.00
Desulfovibrionales; Desulfohalobiaceae; Desulfonauticus	0.35	0.00	0.01	0.00	0.37	0.02	0.00
Desulfovibrionales; Desulfohalobiaceae; Desulfothermus	0.05	0.00	0.00	0.00	0.04	0.00	0.00
Desulfovibrionales; Desulfohalobiaceae; Desulfovermiculus	0.00	0.00	0.00	0.00	0.00	0.00	0.00
Desulfovibrionales; Desulfomicrobiaceae; Desulfomicrobium	0.00	0.00	0.00	0.00	0.00	0.00	0.00
Desulfovibrionales; Desulfovibrionaceae;Other	0.00	0.00	0.00	0.00	0.00	0.00	0.00
Desulfovibrionales; Desulfovibrionaceae; Desulfovibrio	0.00	0.00	0.00	0.00	0.00	0.00	0.00
Desulfurellales; Desulfurellaceae; g	0.00	0.01	0.02	0.01	0.01	0.01	0.00
Desulfuromonadales;Other;Other	0.01	0.00	0.01	0.00	0.01	0.00	0.00
Desulfuromonadales; 21f08; g	0.00	0.01	0.00	0.00	0.00	0.00	0.00
Desulfuromonadales; AKYG597; g	0.00	0.00	0.00	0.00	0.00	0.00	0.00
Desulfuromonadales; BVA18; g	0.00	0.00	0.00	0.00	0.00	0.00	0.00
Desulfuromonadales; Desulfuromonadaceae;Other	0.01	0.00	0.00	0.00	0.01	0.00	0.00
Desulfuromonadales; Desulfuromonadaceae; Desulfuromonas	0.02	0.01	0.00	0.00	0.01	0.01	0.00
Desulfuromonadales; Desulfuromonadaceae; Desulfuromusa	0.00	0.01	0.02	0.01	0.00	0.06	0.11
Desulfuromonadales; Desulfuromonadaceae; Pelobacter	0.01	0.02	0.01	0.01	0.01	0.01	0.01
Desulfuromonadales; GR-WP33-58; g	0.08	0.10	0.01	0.04	0.08	0.00	0.00
Desulfuromonadales; Geobacteraceae;Other	0.00	0.01	0.02	0.01	0.00	0.01	0.01
Desulfuromonadales; Geobacteraceae; Geoalkalibacter	0.01	0.00	0.00	0.00	0.01	0.00	0.00
Desulfuromonadales; Geobacteraceae; Geobacter	0.01	0.01	0.00	0.00	0.01	0.00	0.00
Desulfuromonadales; Geobacteraceae; Geopsychrobacter	0.00	0.00	0.00	0.00	0.00	0.00	0.00
Desulfuromonadales; Geobacteraceae; Geothermobacter	0.00	0.00	0.02	0.00	0.00	0.00	0.00
Desulfuromonadales; M113; g	0.00	0.01	0.00	0.00	0.00	0.00	0.00
Desulfuromonadales; Sva1033; g	0.00	0.00	0.01	0.00	0.00	0.01	0.00
FW113; f; g	0.00	0.00	0.00	0.01	0.00	0.00	0.00
GR-WP33-30; f; g	0.10	0.14	0.10	0.11	0.13	0.11	0.10
Myxococcales;Other;Other	0.00	0.00	0.00	0.00	0.00	0.00	0.00
Myxococcales; 0319-6G20; g	0.06	0.08	0.06	0.01	0.04	0.01	0.00
Myxococcales; Cystobacteraceae; Anaeromyxobacter	0.00	0.00	0.00	0.00	0.00	0.00	0.00

Myxococcales; Cystobacterineae;Other	0.00	0.00	0.01	0.00	0.00	0.00	0.00
Myxococcales; Cystobacterineae; g	0.04	0.04	0.03	0.03	0.04	0.01	0.03
Myxococcales; FFCH16767; g	0.00	0.00	0.00	0.00	0.00	0.00	0.00
Myxococcales; Haliangiaceae; Haliangium	0.10	0.16	0.10	0.11	0.12	0.09	0.08
Myxococcales; MSB-4B10; g	0.00	0.00	0.00	0.00	0.00	0.00	0.00
Myxococcales; Nannocystaceae;Other	0.00	0.00	0.00	0.00	0.01	0.00	0.00
Myxococcales; Nannocystaceae; Enhygromyxa	0.00	0.00	0.00	0.01	0.01	0.00	0.00
Myxococcales; Nannocystaceae; Nannocystis	0.02	0.01	0.00	0.00	0.02	0.00	0.00
Myxococcales; Nannocystaceae; g	0.02	0.02	0.03	0.02	0.01	0.00	0.00
Myxococcales; Nannocystineae; Nannocystaceae	0.01	0.00	0.00	0.01	0.00	0.00	0.00
Myxococcales; Nannocystineae; g	0.05	0.04	0.03	0.00	0.03	0.02	0.03
Myxococcales; Phaselicystidaceae; Phaselicystis	0.00	0.01	0.00	0.00	0.00	0.00	0.00
Myxococcales; Polyangiaceae;Other	0.00	0.00	0.00	0.00	0.00	0.00	0.00
Myxococcales; Polyangiaceae; Byssovorax	0.00	0.00	0.00	0.00	0.00	0.00	0.00
Myxococcales; Polyangiaceae; Chondromyces	0.00	0.00	0.00	0.00	0.00	0.00	0.00
Myxococcales; Polyangiaceae; Sorangium	0.00	0.00	0.00	0.00	0.00	0.00	0.00
Myxococcales; Sandaracinaceae; Sandaracinus	0.00	0.02	0.01	0.02	0.01	0.01	0.03
Myxococcales; Sorangiineae;Other	0.00	0.01	0.00	0.00	0.00	0.00	0.00
Myxococcales; Sorangiineae; Sandaracinaceae	0.28	0.28	0.16	0.08	0.23	0.18	0.29
Myxococcales; Sorangiineae; g	0.04	0.02	0.00	0.03	0.02	0.00	0.02
Myxococcales; VHS-B3-70; g	0.00	0.00	0.00	0.00	0.00	0.00	0.00
Myxococcales; mle1-27; g	0.00	0.00	0.00	0.00	0.00	0.00	0.00
Order_Incertae_Sedis; Syntrophorhabdaceae; Syntrophorhabdus	0.00	0.00	0.00	0.00	0.00	0.00	0.00
SAR324_clade(Marine_group_B); f; g	0.07	0.00	0.00	0.01	0.06	0.00	0.01
Sh765B-TzT-29; f; g	0.28	0.48	0.46	0.26	0.34	0.47	0.37
Sva0485; f; g	0.02	0.02	0.01	0.01	0.01	0.01	0.00
Syntrophobacterales; Syntrophaceae;Other	0.00	0.00	0.00	0.00	0.00	0.00	0.00
Syntrophobacterales; Syntrophaceae; Desulfobacca	0.03	0.00	0.00	0.02	0.03	0.01	0.04
Syntrophobacterales; Syntrophaceae; Desulfomonile	0.00	0.01	0.00	0.01	0.00	0.01	0.02
Syntrophobacterales; Syntrophaceae; Smithella	0.00	0.00	0.00	0.00	0.00	0.00	0.00
Syntrophobacterales; Syntrophaceae; Syntrophus	0.00	0.00	0.00	0.00	0.00	0.00	0.00
Syntrophobacterales; Syntrophaceae; g	0.01	0.00	0.01	0.01	0.02	0.02	0.03
Syntrophobacterales; Syntrophobacteraceae;Other	0.00	0.00	0.01	0.00	0.00	0.00	0.00
Syntrophobacterales; Syntrophobacteraceae; Desulforhabdus	0.00	0.00	0.00	0.00	0.00	0.00	0.00
Syntrophobacterales; Syntrophobacteraceae; Syntrophobacter	0.00	0.00	0.00	0.00	0.00	0.00	0.00
Syntrophobacterales; Syntrophobacteraceae; g	0.03	0.01	0.01	0.00	0.04	0.00	0.01
Desulfobacterales; Desulfobacteraceae; Desulfofrigus	0.00	0.00	0.00	0.00	0.00	0.00	0.00
Desulfobacterales; Desulfobacteraceae; Desulfonema	0.00	0.00	0.00	0.00	0.00	0.00	0.00
Desulfovibrionales;Other;Other	0.00	0.00	0.00	0.00	0.00	0.00	0.00
Desulfovibrionales; Desulfovibrionaceae; Desulfocurvus	0.00	0.00	0.00	0.00	0.00	0.00	0.00
Desulfuromonadales; 008E09-B-D-P15; g	0.00	0.00	0.00	0.00	0.00	0.00	0.00

Syntrophobacterales;Other;Other	0.00	0.00	0.00	0.00	0.00	0.00	0.00
Syntrophobacterales; Syntrophobacteraceae; Desulfacinum	0.00	0.00	0.00	0.00	0.00	0.00	0.00

C.

	T-0 Jar A (%)	Source Oil (%)	50% & 100% Source Oil (%)	Pyrene (%)	T-0 Jar B (%)	Anth. (%)	Mix (%)
Other	0.01	0.04	0.04	0.03	0.01	0.03	0.03
10bav-F6; f; g	0.02	0.01	0.00	0.01	0.01	0.00	0.01
43F-1404R; f; g	0.47	0.56	0.25	0.20	0.25	0.29	0.55
Bdellovibrionales; Bacteriovoracaceae;Other	0.00	0.00	0.00	0.00	0.01	0.00	0.00
Bdellovibrionales; Bacteriovoracaceae; Bacteriovorax	0.01	0.00	0.00	0.00	0.00	0.00	0.00
Bdellovibrionales; Bacteriovoracaceae; Deferrisoma	0.00	0.01	0.02	0.00	0.00	0.01	0.01
Bdellovibrionales; Bacteriovoracaceae; Peredibacter	0.01	0.00	0.00	0.00	0.01	0.00	0.00
Bdellovibrionales; Bacteriovoracaceae; g	0.05	0.02	0.02	0.01	0.03	0.01	0.02
Bdellovibrionales; Bdellovibrionaceae; Bdellovibrio	0.00	0.02	0.00	0.02	0.02	0.04	0.02
Bdellovibrionales; Bdellovibrionaceae; OM27_clade	0.05	0.01	0.04	0.01	0.04	0.00	0.01
DTB120; f; g	0.00	0.00	0.00	0.00	0.00	0.00	0.00
Desulfarculales; Desulfarculaceae;Other	0.00	0.00	0.00	0.00	0.00	0.00	0.00
Desulfarculales; Desulfarculaceae; Desulfarculus	0.10	0.01	0.03	0.02	0.00	0.01	0.01
Desulfarculales; Desulfarculaceae; g	0.94	0.88	0.73	0.62	0.62	0.98	1.10
Desulfobacterales;Other;Other	0.00	0.00	0.00	0.00	0.00	0.00	0.00
Desulfobacterales; Desulfobacteraceae;Other	0.34	0.10	0.06	0.02	0.23	0.06	0.08
Desulfobacterales; Desulfobacteraceae; Desulfatibacillum	0.00	0.00	0.00	0.00	0.00	0.00	0.00
Desulfobacterales; Desulfobacteraceae; Desulfatiferula	0.00	0.00	0.01	0.00	0.00	0.00	0.00
Desulfobacterales; Desulfobacteraceae; Desulfatirhabdium	0.00	0.00	0.01	0.00	0.00	0.00	0.00
Desulfobacterales; Desulfobacteraceae; Desulfobacter	0.00	0.00	0.00	0.00	0.00	0.01	0.00
Desulfobacterales; Desulfobacteraceae; Desulfobacterium	0.00	0.00	0.01	0.01	0.00	0.01	0.00
Desulfobacterales; Desulfobacteraceae; Desulfobacula	0.00	0.01	0.01	0.01	0.00	0.05	0.03
Desulfobacterales; Desulfobacteraceae; Desulfocella	0.00	0.00	0.00	0.00	0.00	0.00	0.00
Desulfobacterales; Desulfobacteraceae; Desulfobotulus	0.00	0.00	0.00	0.00	0.00	0.00	0.00
Desulfobacterales; Desulfobacteraceae; Desulfococcus	0.00	0.00	0.00	0.01	0.01	0.00	0.01
Desulfobacterales; Desulfobacteraceae; Desulfofaba	0.07	0.10	0.05	0.08	0.04	0.14	0.11
Desulfobacterales; Desulfobacteraceae; Desulfofrigus	0.00	0.01	0.00	0.01	0.00	0.01	0.00
Desulfobacterales; Desulfobacteraceae; Desulfosalsimonas	0.05	0.03	0.02	0.04	0.01	0.05	0.05
Desulfobacterales; Desulfobacteraceae; Desulfosarcina	0.05	0.03	0.04	0.01	0.01	0.04	0.05
Desulfobacterales; Desulfobacteraceae; Desulfospira	0.00	0.01	0.00	0.00	0.00	0.01	0.00
Desulfobacterales; Desulfobacteraceae; Desulfotignum	0.00	0.00	0.01	0.01	0.01	0.00	0.00
Desulfobacterales; Desulfobacteraceae; SEEP-SRB1	0.21	0.54	0.57	0.55	0.17	0.78	0.61
Desulfobacterales; Desulfobacteraceae; Sva0081_sediment_group	1.11	1.65	1.17	1.14	0.47	1.68	1.52
Desulfobacterales; Desulfobacteraceae; g	0.38	0.25	0.25	0.19	0.15	0.26	0.25
Desulfobacterales; Desulfobulbaceae;Other	0.02	0.02	0.06	0.03	0.01	0.04	0.06
Desulfobacterales; Desulfobulbaceae; Desulfobulbus	0.33	0.47	0.51	0.29	0.29	0.53	0.58
Desulfobacterales; Desulfobulbaceae; Desulfocapsa	0.01	0.00	0.03	0.01	0.00	0.03	0.02

Desulfobacterales; Desulfobulbaceae; Desulfopila	0.01	0.03	0.03	0.01	0.01	0.06	0.02
Desulfobacterales; Desulfobulbaceae; Desulforhopalus	0.00	0.00	0.00	0.00	0.00	0.00	0.00
Desulfobacterales; Desulfobulbaceae; Desulfotalea	0.00	0.00	0.00	0.00	0.00	0.00	0.00
Desulfobacterales; Desulfobulbaceae; Desulfurivibrio	0.17	0.03	0.04	0.03	0.08	0.01	0.02
Desulfobacterales; Desulfobulbaceae; MSBL7	0.01	0.04	0.06	0.02	0.00	0.06	0.06
Desulfobacterales; Desulfobulbaceae; SEEP-SRB2	0.00	0.01	0.00	0.02	0.01	0.00	0.00
Desulfobacterales; Desulfobulbaceae; SEEP-SRB4	0.00	0.00	0.00	0.00	0.00	0.00	0.00
Desulfobacterales; Desulfobulbaceae; g	0.01	0.03	0.04	0.03	0.03	0.05	0.07
Desulfobacterales; Nitrospinaceae; Candidatus_Entotheonella	0.09	0.05	0.05	0.03	0.07	0.03	0.06
Desulfobacterales; Nitrospinaceae; Nitrospina	0.00	0.00	0.00	0.00	0.00	0.00	0.00
Desulfobacterales; Nitrospinaceae; g	0.33	0.37	0.51	0.65	0.35	0.75	0.58
Desulfovibrionales; Desulfohalobiaceae;Other	0.00	0.00	0.00	0.00	0.00	0.00	0.00
Desulfovibrionales;Other;Other	0.00	0.00	0.00	0.00	0.00	0.00	0.00
Desulfovibrionales; Desulfohalobiaceae; Desulfonauticus	0.55	0.00	0.00	0.00	0.41	0.00	0.00
Desulfovibrionales; Desulfohalobiaceae; Desulfothermus	0.03	0.00	0.00	0.00	0.06	0.00	0.00
Desulfovibrionales; Desulfohalobiaceae; Desulfovermiculus	0.00	0.00	0.00	0.00	0.00	0.00	0.00
Desulfovibrionales; Desulfomicrobiaceae; Desulfomicrobium	0.00	0.00	0.00	0.00	0.00	0.00	0.00
Desulfovibrionales; Desulfovibrionaceae;Other	0.00	0.00	0.00	0.00	0.00	0.00	0.00
Desulfovibrionales; Desulfovibrionaceae; Desulfovibrio	0.05	0.07	0.10	0.03	0.04	0.05	0.04
Desulfurellales; Desulfurellaceae; g	0.03	0.08	0.03	0.02	0.03	0.02	0.03
Desulfuromonadales;Other;Other	0.07	0.19	0.14	0.09	0.02	0.14	0.11
Desulfuromonadales; 21f08; g	0.00	0.02	0.01	0.01	0.00	0.04	0.02
Desulfuromonadales; AKYG597; g	0.04	0.01	0.00	0.02	0.01	0.01	0.02
Desulfuromonadales; BVA18; g	0.01	0.00	0.00	0.00	0.00	0.00	0.00
Desulfuromonadales; Desulfuromonadaceae;Other	0.05	0.02	0.02	0.00	0.02	0.00	0.01
Desulfuromonadales; Desulfuromonadaceae; Desulfuromonas	0.33	0.21	0.08	0.08	0.07	0.06	0.09
Desulfuromonadales; Desulfuromonadaceae; Desulfuromusa	0.01	0.01	0.02	0.02	0.00	0.01	0.03
Desulfuromonadales; Desulfuromonadaceae; Pelobacter	0.09	0.13	0.08	0.04	0.02	0.09	0.10
Desulfuromonadales; GR-WP33-58; g	0.02	0.01	0.01	0.00	0.05	0.01	0.01
Desulfuromonadales; Geobacteraceae;Other	0.00	0.00	0.00	0.00	0.00	0.00	0.00
Desulfuromonadales; Geobacteraceae; Geoalkalibacter	0.49	0.39	0.22	0.26	0.22	0.22	0.33
Desulfuromonadales; Geobacteraceae; Geobacter	0.14	0.13	0.28	0.08	0.38	0.22	0.18
Desulfuromonadales; Geobacteraceae; Geopsychrobacter	0.01	0.00	0.00	0.00	0.02	0.00	0.00
Desulfuromonadales; Geobacteraceae; Geothermobacter	0.01	0.02	0.02	0.03	0.01	0.01	0.02
Desulfuromonadales; M113; g	0.00	0.00	0.00	0.00	0.00	0.00	0.00
Desulfuromonadales; Sva1033; g	0.01	0.00	0.01	0.01	0.03	0.03	0.04
FW113; f; g	0.03	0.03	0.01	0.01	0.03	0.04	0.03
GR-WP33-30; f; g	0.74	0.90	0.48	0.45	0.38	0.44	0.54
Myxococcales;Other;Other	0.01	0.00	0.01	0.00	0.01	0.00	0.00
Myxococcales; 0319-6G20; g	0.03	0.01	0.03	0.02	0.04	0.02	0.01
Myxococcales; Cystobacteraceae; Anaeromyxobacter	0.01	0.00	0.00	0.00	0.00	0.01	0.00

Myxococcales; Cystobacterineae;Other	0.00	0.00	0.00	0.00	0.00	0.00	0.00
Myxococcales; Cystobacterineae; g	0.09	0.08	0.10	0.04	0.06	0.10	0.06
Myxococcales; FFCH16767; g	0.00	0.00	0.00	0.00	0.00	0.00	0.00
Myxococcales; Haliangiaceae; Haliangium	0.12	0.12	0.11	0.07	0.07	0.08	0.08
Myxococcales; MSB-4B10; g	0.01	0.01	0.03	0.00	0.00	0.01	0.00
Myxococcales; Nannocystaceae;Other	0.00	0.00	0.00	0.00	0.00	0.00	0.01
Myxococcales; Nannocystaceae; Enhygromyxa	0.03	0.01	0.02	0.01	0.01	0.00	0.02
Myxococcales; Nannocystaceae; Nannocystis	0.00	0.01	0.01	0.01	0.01	0.01	0.01
Myxococcales; Nannocystaceae; g	0.00	0.01	0.00	0.00	0.00	0.00	0.00
Myxococcales; Nannocystineae; Nannocystaceae	0.00	0.00	0.00	0.00	0.00	0.00	0.00
Myxococcales; Nannocystineae; g	0.26	0.10	0.08	0.08	0.12	0.09	0.14
Myxococcales; Phaselicystidaceae; Phaselicystis	0.02	0.02	0.01	0.00	0.00	0.01	0.01
Myxococcales; Polyangiaceae;Other	0.00	0.03	0.02	0.01	0.01	0.04	0.02
Myxococcales; Polyangiaceae; Byssovorax	0.02	0.01	0.02	0.03	0.02	0.01	0.01
Myxococcales; Polyangiaceae; Chondromyces	0.00	0.00	0.00	0.00	0.00	0.00	0.00
Myxococcales; Polyangiaceae; Sorangium	0.01	0.04	0.04	0.02	0.03	0.01	0.04
Myxococcales; Sandaracinaceae; Sandaracinus	0.04	0.01	0.01	0.00	0.00	0.00	0.01
Myxococcales; Sorangiineae;Other	0.00	0.00	0.00	0.00	0.00	0.00	0.00
Myxococcales; Sorangiineae; Sandaracinaceae	0.13	0.19	0.15	0.08	0.14	0.10	0.12
Myxococcales; Sorangiineae; g	0.13	0.15	0.08	0.03	0.08	0.06	0.11
Myxococcales; VHS-B3-70; g	0.04	0.03	0.03	0.00	0.04	0.01	0.03
Myxococcales; mle1-27; g	0.00	0.00	0.00	0.00	0.00	0.00	0.00
Order_Incertae_Sedis; Syntrophorhabdaceae; Syntrophorhabdus	0.01	0.02	0.01	0.01	0.02	0.03	0.06
SAR324_clade(Marine_group_B); f; g	0.23	0.00	0.01	0.00	0.12	0.01	0.01
Sh765B-TzT-29; f; g	1.18	1.54	1.19	1.06	0.67	1.10	1.03
Sva0485; f; g	0.28	0.25	0.37	0.25	0.26	0.33	0.42
Syntrophobacterales; Syntrophaceae;Other	0.00	0.00	0.00	0.00	0.00	0.00	0.00
Syntrophobacterales; Syntrophaceae; Desulfobacca	1.03	1.57	0.96	0.77	0.72	1.06	0.99
Syntrophobacterales; Syntrophaceae; Desulfomonile	0.08	0.17	0.06	0.05	0.05	0.19	0.16
Syntrophobacterales; Syntrophaceae; Smithella	0.00	0.00	0.00	0.00	0.00	0.00	0.00
Syntrophobacterales; Syntrophaceae; Syntrophus	0.01	0.00	0.00	0.01	0.00	0.01	0.01
Syntrophobacterales; Syntrophaceae; g	0.16	0.12	0.12	0.13	0.10	0.15	0.21
Syntrophobacterales; Syntrophobacteraceae;Other	0.00	0.00	0.00	0.00	0.00	0.01	0.00
Syntrophobacterales; Syntrophobacteraceae; Desulforhabdus	0.00	0.03	0.00	0.00	0.00	0.02	0.03
Syntrophobacterales; Syntrophobacteraceae; Syntrophobacter	0.06	0.02	0.01	0.03	0.02	0.02	0.07
Syntrophobacterales; Syntrophobacteraceae; g	0.67	0.64	0.46	0.49	0.49	0.52	0.84
Desulfobacterales; Desulfobacteraceae; Desulfofrigus	0.00	0.00	0.00	0.00	0.00	0.00	0.00
Desulfobacterales; Desulfobacteraceae; Desulfonema	0.00	0.00	0.00	0.00	0.00	0.00	0.00
Desulfovibrionales;Other;Other	0.00	0.00	0.00	0.00	0.00	0.00	0.00
Desulfovibrionales; Desulfovibrionaceae; Desulfocurvus	0.00	0.00	0.00	0.00	0.00	0.00	0.00
Desulfuromonadales; 008E09-B-D-P15; g	0.00	0.00	0.00	0.00	0.00	0.00	0.00

Syntrophobacterales;Other;Other	0.00	0.00	0.00	0.00	0.00	0.00	0.00
Syntrophobacterales; Syntrophobacteraceae; Desulfacinum	0.00	0.00	0.00	0.00	0.00	0.00	0.00

Table S12. Sulfate reduction rates measured in Site 1 SRAs using a ^{35}S-radiotracer for **(A)** Macondo crude (source) oil, **(B)** pyrene, **(C)** anthracene, and **(D)** anthracene and phenanthrene mix for irradiated versus non-irradiated (dark) aqueous extracts. Incubations included: baseline, containing sediment and seawater, a positive control containing sediment, seawater, and lactate (2 mM), and a sterile sediment and seawater control. Each compound (irradiated or dark) was tested at varying concentrations and compared to endogenous rates (i.e., baseline). Additional amendments were tested after initial incubations were set-up in some instances. In these cases, endogenous controls were re-established each time a SRA was repeated. Values represent averages of triplicate incubations and are reported as a percent increase or decrease from baseline rates. Note: significant p values are denoted in red.

A.

Source Oil

Sample	Average (µmol S/mL/day)	Std. Dev.	p values compared to baseline	% Baseline
Baseline	0.5934	0.1896	n/a	100.00
Lactate	2.8605	0.1150	1.33E-04	482.06
Sterile	0.0069	0.0032	0.04	1.16
1% Irradiated	0.4954	0.1381	0.59	83.49
1% Dark	1.1342	0.4745	0.21	191.13
2% Irradiated	0.7025	0.4300	0.76	118.38
2% Dark	0.4980	0.2866	0.71	83.92
5% Irradiated	1.8212	0.5337	0.04	306.91
5% Dark	0.6632	0.4003	0.83	111.76
Baseline	0.2462	0.0363	n/a	100.00
0.1% Irradiated	0.1669	0.0172	0.05	67.81
0.1% Dark	0.3202	0.0216	0.07	130.07
10% Irradiated	0.2104	0.0372	0.39	85.46
10% Dark	0.2163	0.0472	0.52	87.89
Baseline	0.1258	0.0303	n/a	100.00
50% Irradiated	0.1567	0.0297	0.36	124.57
50% Dark	0.1127	0.0169	0.62	89.58
100% Irradiated	0.1350	0.0165	0.73	107.29
100% Dark	0.1301	0.0095	0.86	103.39

B.

Pyrene

Sample	Average (µmol S/mL/day)	Std. Dev.	p values compared to baseline	% Baseline
Baseline	0.1674	0.0784	n/a	100.00
Lactate	1.7234	0.4496	0.01	1029.61
Sterile	0.0108	0.0012	0.05	6.45
0.1% Irradiated	0.1658	0.0409	0.98	99.08
0.1% Dark	0.2497	0.0766	0.35	149.19
1% Irradiated	0.2391	0.0580	0.36	142.87
1% Dark	0.1844	0.0555	0.81	110.20
2% Irradiated	0.2432	0.0057	0.24	145.31
2% Dark	0.2037	0.1180	0.73	121.72
5% Irradiated	0.2765	0.0909	0.27	165.18
5% Dark	0.1805	0.0497	0.85	107.81
10% Irradiated	0.1530	0.0063	0.85	91.40
10% Dark	0.1268	0.0826	0.64	75.73
Baseline	0.1878	0.0288	n/a	100.00
50% Irradiated	0.1069	0.0389	0.08	56.89
50% Dark	0.1625	0.0274	0.15	86.53

C.

Anthracene

Sample	Average (µmol S/mL/day)	Std. Dev.	p values compared to baseline	% Baseline
Baseline	0.1053	0.0339	n/a	100.00
Lactate	0.7692	0.3710	0.07	730.54
Sterile	0.0082	0.0005	0.02	7.75
0.1% Irradiated	0.1097	0.0110	0.87	104.16
0.1% Dark	0.1872	0.1212	0.41	177.82
1% Irradiated	0.1106	0.0220	0.86	105.03
1% Dark	0.1091	0.0187	0.90	103.59
2% Irradiated	0.1414	0.0497	0.44	134.26
2% Dark	0.0901	0.0125	0.58	85.60
5% Irradiated	0.0998	0.0328	0.88	94.77
5% Dark	0.0939	0.0145	0.68	89.19
10% Irradiated	0.1595	0.0278	0.16	151.48
10% Dark	0.1901	0.0146	0.03	180.54
50% Irradiated	0.0822	0.0095	0.41	78.11
50% Dark	0.1560	0.0633	0.37	148.14

D.

Anthracene & Phenanthrene Mix

Sample	Average (µmol S/mL/day)	Std. Dev.	p values compared to baseline	% Baseline
Baseline	0.0326	0.0049	n/a	100.00
Lactate	0.7489	0.1897	0.01	4590.12
Sterile	0.0037	0.0004	1.22E-03	22.88
0.1% Irradiated	0.1999	0.0987	0.07	612.46
0.1% Dark	0.1025	0.0438	0.09	314.07
1% Irradiated	0.2008	0.0924	0.06	615.47
1% Dark	0.3024	0.1640	0.08	926.75
2% Irradiated	0.2498	0.0607	0.01	765.52
2% Dark	0.1199	0.0701	0.15	367.35
5% Irradiated	0.2160	0.0614	0.01	661.98
5% Dark	0.1216	0.0871	0.22	372.72
10% Irradiated	0.0739	0.0065	1.99E-03	226.42
10% Dark	0.1217	0.0688	0.14	372.93
50% Irradiated	0.1272	0.0512	0.06	389.80
50% Dark	0.1590	0.0628	0.05	487.38

Table S13. Sulfate reduction rates measured in Site 2 SRAs using a ^{35}S-radiotracer at **(A)** Macondo crude (source) oil, **(B)** pyrene, **(C)** anthracene, and **(D)** anthracene and phenanthrene mix for irradiated versus non-irradiated (dark) aqueous extracts. Incubations included: baseline, containing sediment and seawater, a positive control containing sediment, seawater, and lactate (2 mM), and a sterile sediment and seawater control. Each compound (irradiated or dark) was tested at varying concentrations and compared to endogenous rates (i.e., baseline). Additional amendments were tested after initial incubations were set-up in some instances. In these cases, endogenous controls were re-established each time a SRA was repeated. Values represent averages of triplicate incubations and are reported as a percent increase or decrease from baseline rates. Note: significant p values are denoted in red.

A.

Source Oil

Sample	Average (µmol S/mL/day)	Std. Dev.	p values compared to baseline	% Baseline
Baseline	0.0430	0.0166	n/a	100.00
Lactate	0.2178	0.0410	0.01	506.04
Sterile	0.0079	0.0007	0.04	18.34
0.1% Irradiated	0.0359	0.0063	0.60	83.39
0.1% Dark	0.0613	0.0302	0.50	142.29
1% Irradiated	0.0405	0.0069	0.85	94.01
1% Dark	0.1484	0.0665	0.10	344.64
2% Irradiated	0.0447	0.0104	0.91	103.78
2% Dark	0.0944	0.0245	0.07	219.26
5% Irradiated	0.1483	0.0677	0.10	344.39
5% Dark	0.0900	0.0234	0.08	209.06
10% Irradiated	0.0366	0.0128	0.69	85.01
10% Dark	0.1102	0.0756	0.29	256.04
Baseline	0.1540	0.0238	n/a	100.00
50% Irradiated	0.1181	0.0144	0.14	76.68
50% Dark	0.1241	0.0181	0.23	80.61
100 % Irradiated	0.1292	0.0368	0.47	83.90
100% Dark	0.1033	0.0049	0.04	67.11

B.

Pyrene

Sample	Average (µmol S/mL/day)	Std. Dev.	p values compared to baseline	% Baseline
Baseline	0.1354	0.0087	n/a	100.00
Lactate	0.6115	0.3197	0.10	451.73
Sterile	0.0105	0.0018	3.70E-05	7.77
0.1% Irradiated	0.1456	0.0273	0.64	107.57
0.1% Dark	0.1977	0.0371	0.08	146.04
1% Irradiated	0.1688	0.0137	0.04	124.66
1% Dark	0.1796	0.0248	0.08	132.70
2% Irradiated	0.1062	0.0331	0.29	78.42
2% Dark	0.1684	0.0293	0.20	124.40
5% Irradiated	0.1294	0.0121	0.60	95.57
5% Dark	0.1014	0.0117	0.03	74.93
10% Irradiated	0.1119	0.0628	0.63	82.64
10% Dark	0.0967	0.0273	0.12	71.41
Baseline	0.1489	0.0204	n/a	100.00
50% Irradiated	0.0811	0.0055	0.01	54.44
50% Dark	0.1069	0.0178	0.08	71.77

C.

Anthracene

Sample	Average (µmol S/mL/day)	Std. Dev.	p values compared to baseline	% Baseline
Baseline	0.1606	0.0166	n/a	100.00
Lactate	0.4464	0.3123	0.27	278.03
Sterile	0.0068	0.0001	1.98E-04	4.25
0.1% Irradiated	0.1647	0.0312	0.88	102.54
0.1% Dark	0.1353	0.0544	0.56	84.26
1% Irradiated	0.1202	0.0399	0.26	74.89
1% Dark	0.1290	0.0165	0.13	80.31
2% Irradiated	0.1511	0.0377	0.76	94.10
2% Dark	0.1173	0.0206	0.08	73.06
5% Irradiated	0.1340	0.0394	0.43	83.47
5% Dark	0.1157	0.0163	0.05	72.02
10% Irradiated	0.1710	0.0307	0.69	106.52
10% Dark	0.1338	0.0413	0.44	83.31
50% Irradiated	0.0873	0.0193	0.02	54.34
50% Dark	0.1122	0.0343	0.15	69.89

D.

Anthracene & Phenanthrene Mix

Sample	Average (µmol S/mL/day)	Std. Dev.	p values compared to baseline	% Baseline
Baseline	0.0526	0.0051	n/a	100.00
Lactate	0.4190	0.3122	0.17	795.88
Sterile	0.0091	0.0006	2.87E-04	17.38
0.1% Irradiated	0.0597	0.0039	0.19	113.48
0.1% Dark	0.0714	0.0170	0.21	135.66
1% Irradiated	0.0634	0.0110	0.28	120.52
1% Dark	0.0736	0.0123	0.09	139.78
2% Irradiated	0.0595	0.0036	0.20	113.11
2% Dark	0.0570	0.0120	0.66	108.24
5% Irradiated	0.0530	0.0022	0.93	100.67
5% Dark	0.0643	0.0059	0.10	122.10
10% Irradiated	0.0606	0.0103	0.39	115.06
10% Dark	0.0584	0.0122	0.57	110.94
50% Irradiated	0.0485	0.0096	0.62	92.06
50% Dark	0.0512	0.0077	0.83	97.23

Table S14. Sulfate reduction rates measured in Site 3 SRAs using a ^{35}S-radiotracer at **(A)** Macondo crude (source) oil, **(B)** pyrene, **(C)** anthracene, and **(D)** anthracene and phenanthrene mix for irradiated versus non-irradiated (dark) aqueous extracts. Incubations included: baseline, containing sediment and seawater, a positive control containing sediment, seawater, and lactate (2 mM), and a sterile sediment and seawater control. Each compound (irradiated or dark) was tested at varying concentrations and compared to endogenous rates (i.e., baseline). Additional amendments were tested after initial incubations were set-up in some instances. In these cases, endogenous controls were re-established each time a SRA was repeated. Values represent averages of triplicate incubations and are reported as a percent increase or decrease from baseline rates. Note: significant p values are denoted in red.

A.

Source Oil

Sample	Average (µmol S/mL/day)	Std. Dev.	p values compared to baseline	% Baseline
Baseline	0.1492	0.0293	n/a	100.00
Lactate	1.4650	0.1823	5.46E-04	981.93
Sterile	0.0050	0.0006	2.23E-03	3.35
0.1% Irradiated	0.1932	0.0484	0.33	129.51
0.1% Dark	0.1298	0.0270	0.53	86.98
1% Irradiated	0.1502	0.0309	0.97	100.68
1% Dark	0.1086	0.0166	0.08	72.78
2% Irradiated	0.1192	0.0112	0.25	79.87
2% Dark	0.1970	0.0786	0.47	132.07
5% Irradiated	0.1462	0.0171	0.91	97.98
5% Dark	0.1677	0.0166	0.48	122.39
10% Irradiated	0.1865	0.0359	0.32	124.99
10% Dark	0.0773	0.0087	0.08	51.78
Baseline	0.0807	0.0192	n/a	100.00
10% Dark	0.0663	0.0182	0.48	82.17
Baseline	0.0596	0.0183	n/a	100.00
50% Irradiated	0.0667	0.0075	0.64	111.90
50% Dark	0.0544	0.0055	0.72	91.26
100% Irradiated	0.1096	0.0038	0.02	183.79
100% Dark	0.0913	0.0218	0.19	153.03

B.

Pyrene

Sample	Average (µmol S/mL/day)	Std. Dev.	p values compared to baseline	% Baseline
Baseline	0.0713	0.0095	n/a	100.00
Lactate	1.4506	0.2344	1.14E-03	2034.22
Sterile	0.0054	0.0001	6.12E-04	7.55
0.1% Irradiated	0.1248	0.0104	5.80E-03	174.94
0.1% Dark	0.1796	0.0118	5.43E-04	251.82
1% Irradiated	0.1203	0.0361	0.14	168.64
1% Dark	0.1011	0.0234	0.17	141.74
2% Irradiated	0.1303	0.0229	0.03	182.78
2% Dark	0.1213	0.0294	0.08	170.12
5% Irradiated	0.1323	0.0483	0.15	185.58
5% Dark	0.1103	0.0320	0.17	154.68
10% Irradiated	0.1260	0.0385	0.12	176.65
10% Dark	0.1741	0.0214	3.42E-03	244.18
In situ	0.1569	0.0416	n/a	100.00
50% Irradiated	0.1051	0.0132	0.17	66.98
50% Dark	0.1025	0.0176	0.08	65.31

C.

Anthracene

Sample	Average (µmol S/mL/day)	Std. Dev.	p values compared to baseline	% Baseline
Baseline	0.3432	0.0491	n/a	100.00
Lactate	4.1325	0.9102	4.18E-03	1204.03
Sterile	0.0082	0.0011	6.53E-04	2.40
0.1% Irradiated	0.2043	0.0632	0.07	59.53
0.1% Dark	0.3130	0.0766	0.66	91.19
1% Irradiated	0.2650	0.0673	0.26	77.22
1% Dark	0.2703	0.0677	0.28	78.74
2% Irradiated	0.3180	0.0695	0.70	92.66
2% Dark	0.2401	0.0043	0.04	69.94
5% Irradiated	0.4123	0.1292	0.52	120.12
5% Dark	0.3395	0.0796	0.96	98.90
10% Irradiated	0.3754	0.1149	0.73	109.36
10% Dark	0.3592	0.0663	0.80	104.66
50% Irradiated	0.2921	0.0977	0.54	85.09
50% Dark	0.3300	0.0266	0.75	96.15

D.

Anthracene & Phenanthrene Mix

Sample	Average (µmol S/mL/day)	Std. Dev.	p values compared to baseline	% Baseline
Baseline	0.2853	0.0311	n/a	100.00
Lactate	3.9740	0.2377	2.64E-05	1393.14
Sterile	0.0094	0.0007	2.36E-04	3.29
0.1% Irradiated	0.3154	0.0653	0.59	110.57
0.1% Dark	0.3011	0.0095	0.53	105.55
1% Irradiated	0.3686	0.0319	0.06	129.22
1% Dark	0.3437	0.0282	0.12	120.48
2% Irradiated	0.3380	0.0495	0.27	118.48
2% Dark	0.3512	0.0333	0.11	123.12
5% Irradiated	0.4783	0.0415	0.01	167.68
5% Dark	0.3530	0.0412	0.14	123.76
10% Irradiated	0.3777	0.0609	0.13	132.42
10% Dark	0.4813	0.0206	1.75E-03	168.73
50% Irradiated	0.3360	0.0818	0.46	117.81
50% Dark	0.4046	0.0129	0.01	141.84

Figure S1. Non-metric multidimensional scaling (NMDS) ordination of Deltaproteobacteria populations at the time of field sampling (i.e., T-0) compared with Deltaproteobacteria populations at set up of SRAs. NMDS plot was constructed in PC-ORD (Version 6, MjM Software) using a Bray-Curtis distance measure, orthogonal principal axes rotation, and 1000 permutations. SRA repeats included incubations established after initial set-up (i.e., 0.1% and 10% source oil for Site 1; 50% and 100% source oil for all sites).

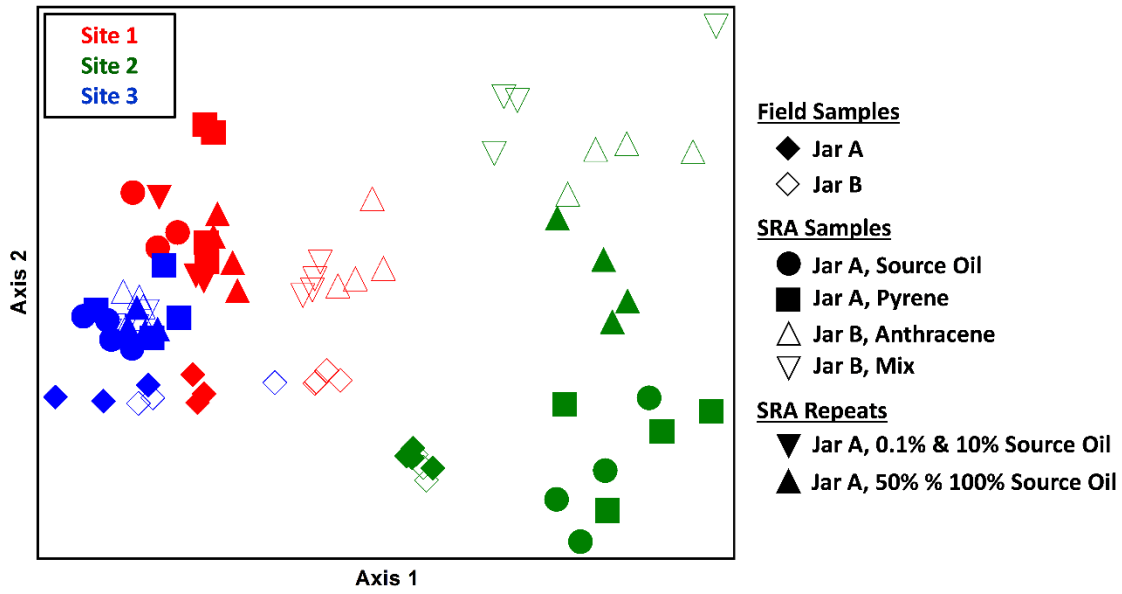

Figure S2. Changes in the relative abundances of Deltaproteobacteria taxa sequenced from Site 1 **(A)** Jar A sediment and **(B)** Jar B sediment collected in the field (i.e., T-0) and at the time of SRA set-up. Community profiles based on taxa detected via 16S rRNA gene sequencing and QIIME analysis (Version 1.9.0) (Caporaso *et al*, 2010a). Minor phylogenetic groups, which could not visually resolved in the bar graphs, are not included in the legend.

A.

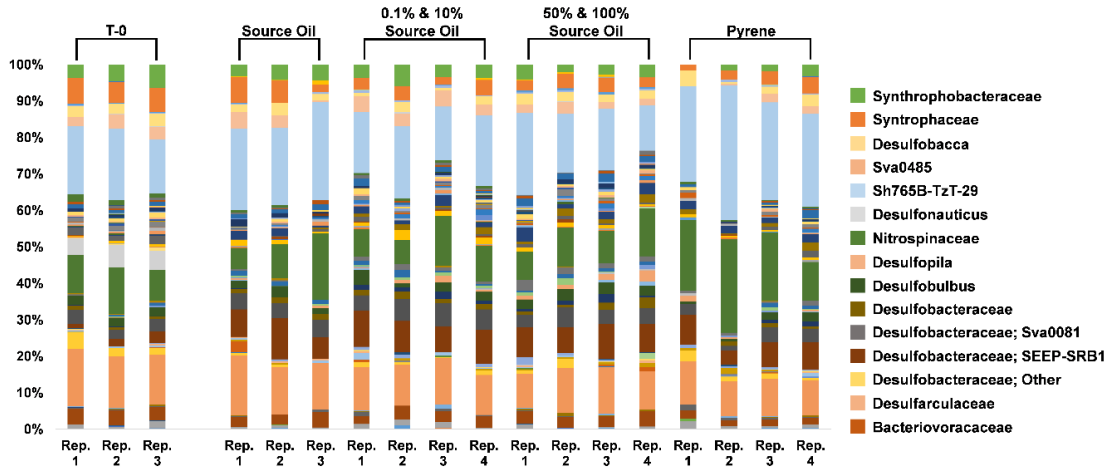

B.

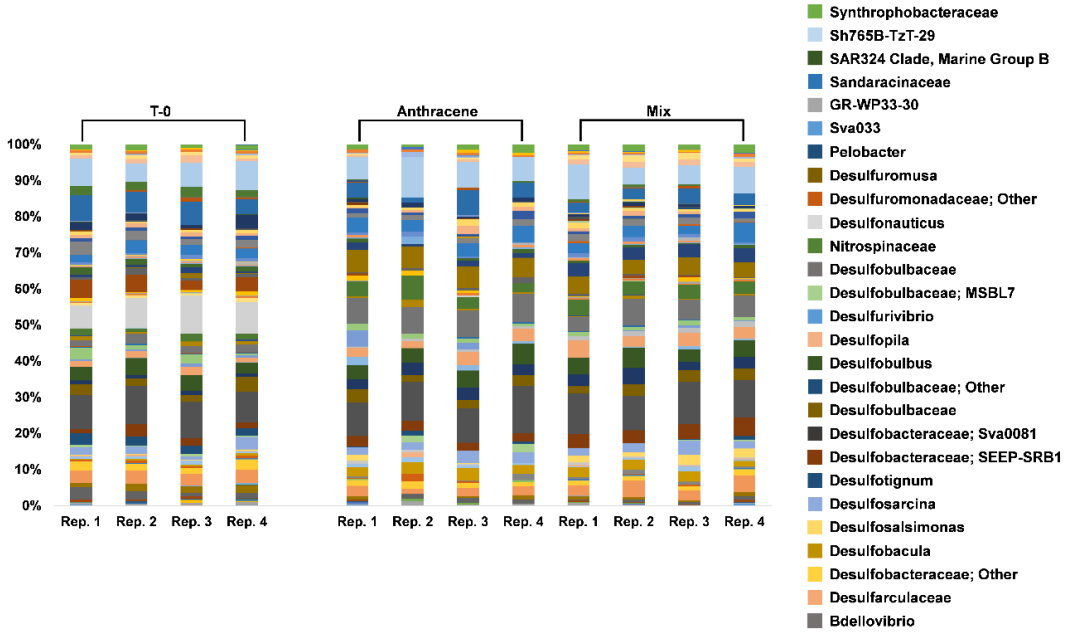

Figure S3. Changes in the relative abundances of Deltaproteobacteria taxa sequenced from Site 2 **(A)** Jar A sediment and **(B)** Jar B sediment collected in the field (i.e., T-0) and at the time of SRA set-up. Community profiles based on taxa detected via 16S rRNA gene sequencing and QIIME analysis (Version 1.9.0) (Caporaso *et al*, 2010a). Minor phylogenetic groups, which could not be visually resolved in the bar graphs, are not included in the legend.

A.

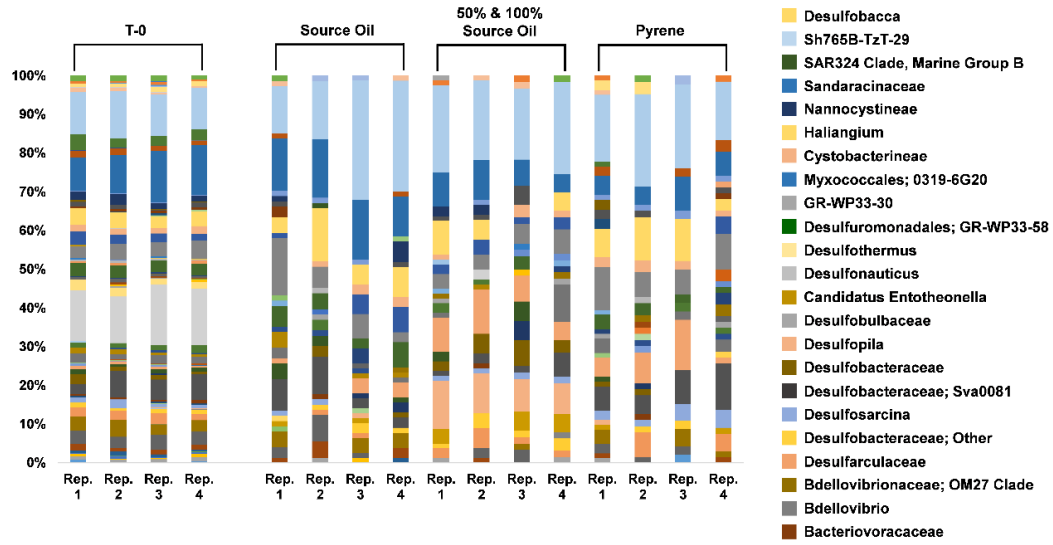

B.

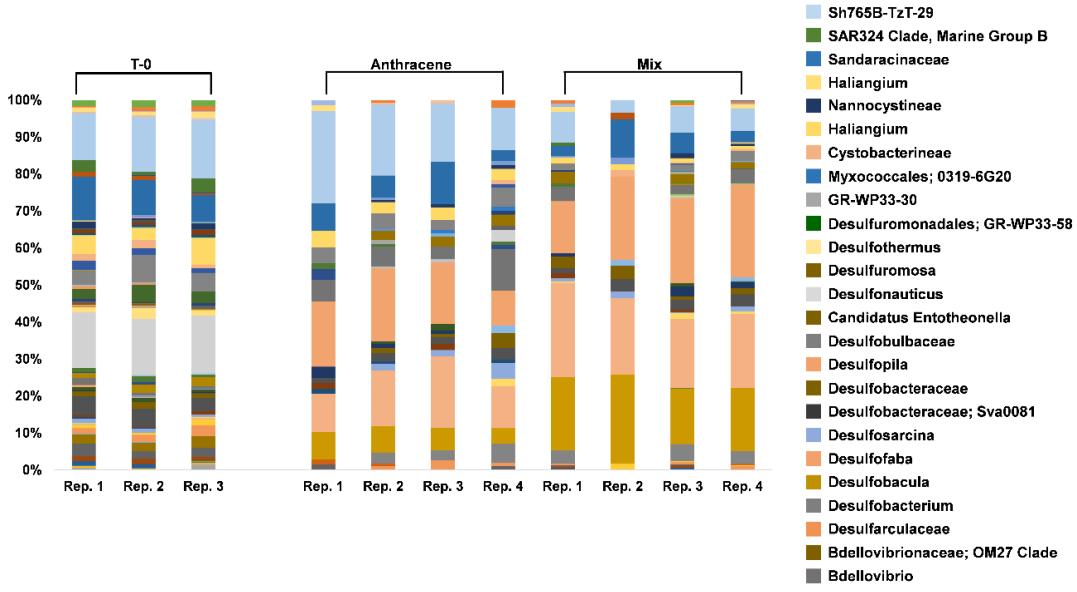

Figure S4. Changes in the relative abundances of Deltaproteobacteria taxa sequenced from Site 3 **(A)** Jar A sediment and **(B)** Jar B sediment collected in the field (i.e., T-0) and at the time of SRA set-up. Community profiles based on taxa detected via 16S rRNA gene sequencing and QIIME analysis (Version 1.9.0) (Caporaso *et al*, 2010a). Minor phylogentic groups, which could not be visually resolved in the bar graphs, are not included in the legend.

A.

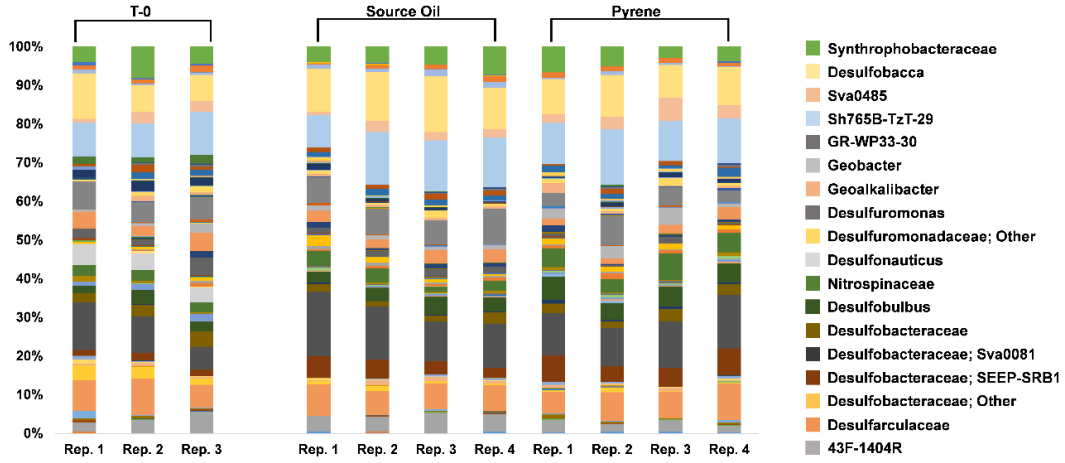

B.

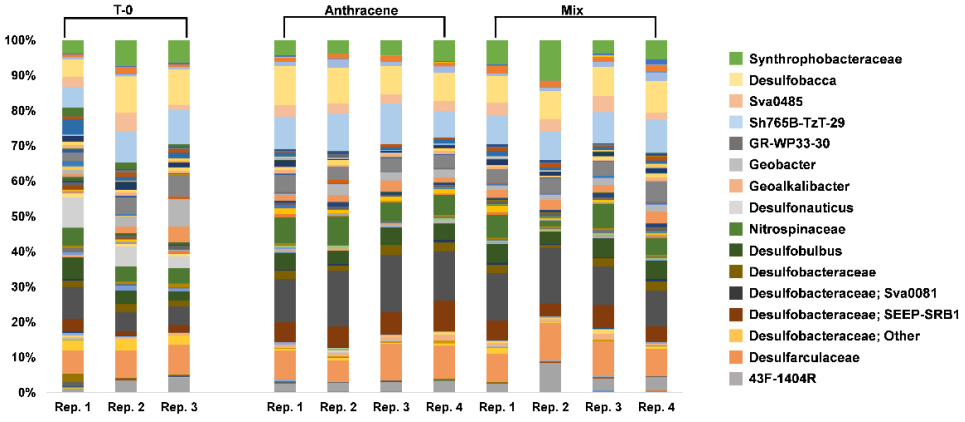

Appendix III: Chapter 3 Supplemental Materials

Table S1. Relative abundances of core taxa in microbial communities, classified at the genus level at 97% similarity, identified via 16S rRNA gene sequences in aggregates collected from Fort Morgan (FM) and Gulf Shores (GS). One aggregate was collected from each location and subsampled to generate technical replicates. Core taxa were defined as any group comprising 1% or more in any library. Technical replicates are denoted as A, B, C.

	FM A (%)	FM B (%)	FM C (%)	GS A (%)	GS B (%)	GS C (%)
Bacteria;Bacteroidetes;Bacteroidia;Bacteroidales;Marinilabiaceae; uncultured	1.87	3.35	1.69	1.08	0.81	0.00
Bacteria;Chloroflexi;Anaerolineae;Anaerolineales;Anaerolineaceae; uncultured	1.00	2.71	2.25	1.51	0.49	0.00
Bacteria;Fusobacteria;Fusobacteriia;BS1-0-74;uncultured bacterium;Other	1.12	1.12	0.70	0.54	0.05	0.00
Bacteria;Proteobacteria;Alphaproteobacteria;4-Org1-14; uncultured alpha proteobacterium;Other	6.59	1.91	2.11	0.12	0.05	0.00
Bacteria;Proteobacteria;Alphaproteobacteria;Rhodobacterales; Rhodobacteraceae;Roseovarius	0.12	1.28	0.42	0.00	0.16	0.22
Bacteria;Proteobacteria;Alphaproteobacteria;Rhodobacterales; Rhodobacteraceae;uncultured	1.99	1.59	1.27	1.20	1.24	1.74
Bacteria;Proteobacteria;Candidatus Thiobios; uncultured gamma proteobacterium;Other;Other	2.11	2.07	2.53	0.18	0.16	0.00
Bacteria;Proteobacteria;Deltaproteobacteria;Desulfarculales; Desulfarculaceae;uncultured	4.48	7.02	6.05	3.43	3.95	4.13
Bacteria;Proteobacteria;Deltaproteobacteria;Desulfobacterales; Desulfobacteraceae;Desulfococcus	0.00	0.16	0.14	0.00	0.43	1.09
Bacteria;Proteobacteria;Deltaproteobacteria;Desulfobacterales; Desulfobacteraceae;Desulfosarcina	6.09	7.02	5.20	0.90	0.92	2.83
Bacteria;Proteobacteria;Deltaproteobacteria;Desulfobacterales; Desulfobacteraceae;SEEP-SRB1	1.24	0.32	0.84	0.42	0.59	1.52
Bacteria;Proteobacteria;Deltaproteobacteria;Desulfobacterales; Desulfobacteraceae;Sva0081 sediment group	0.87	1.44	2.81	1.87	1.46	1.30
Bacteria;Proteobacteria;Deltaproteobacteria;Desulfobacterales; Desulfobacteraceae;uncultured	1.99	2.07	2.67	1.02	1.03	1.09
Bacteria;Proteobacteria;Epsilonproteobacteria;Campylobacterales; Helicobacteraceae;Sulfurimonas	0.00	0.80	0.84	1.08	1.30	1.09
Bacteria;Proteobacteria;Gammaproteobacteria;Acidithiobacillales; Acidithiobacillaceae;Acidithiobacillus	3.23	1.44	1.97	0.36	0.11	0.00

Bacteria;Proteobacteria;Gammaproteobacteria;Alteromonadales;Alteromonadaceae;C1-B045	1.99	0.80	0.70	0.18	0.16	0.00
Bacteria;Proteobacteria;Gammaproteobacteria;Alteromonadales;Alteromonadaceae;OM60(NOR5) clade	0.87	1.12	2.39	0.12	0.00	0.00
Bacteria;Proteobacteria;Gammaproteobacteria;Alteromonadales;Colwelliaceae;Colwellia	0.37	0.00	0.70	1.08	1.57	2.17
Bacteria;Proteobacteria;Gammaproteobacteria;Alteromonadales;Pseudoalteromonadaceae;Pseudoalteromonas	7.96	8.93	3.66	54.49	52.05	38.26
Bacteria;Proteobacteria;Gammaproteobacteria;Alteromonadales;Pseudoalteromonadaceae;uncultured	0.00	0.00	0.00	2.71	1.84	1.74
Bacteria;Proteobacteria;Gammaproteobacteria;Chromatiales;Chromatiaceae;Nitrosococcus	1.24	0.64	0.70	0.12	0.00	0.00
Bacteria;Proteobacteria;Gammaproteobacteria;Chromatiales;Granulosicoccaceae;Granulosicoccus	1.00	1.12	0.56	0.06	0.00	0.00
Bacteria;Proteobacteria;Gammaproteobacteria;Oceanospirillales;Alcanivoracaceae;Alcanivorax	0.50	0.80	0.28	1.51	1.03	0.00
Bacteria;Proteobacteria;Gammaproteobacteria;Oceanospirillales;Alcanivoracaceae;Kangiella	0.75	1.75	0.84	0.18	0.22	0.22
Bacteria;Proteobacteria;Gammaproteobacteria;Oceanospirillales;Oceanospirillaceae;Pseudospirillum	12.06	12.76	17.30	0.96	2.27	2.83
Bacteria;Proteobacteria;Gammaproteobacteria;Order Incertae Sedis;Family Incertae Sedis;Marinicella	1.24	0.48	0.42	0.06	0.05	0.00
Bacteria;Proteobacteria;Gammaproteobacteria;Order Incertae Sedis;Family Incertae Sedis;Sedimenticola	1.12	0.80	0.84	0.00	0.05	0.00
Bacteria;Proteobacteria;Gammaproteobacteria;PYR10d3;uncultured gamma proteobacterium;Other	1.24	0.16	0.56	0.18	0.11	0.00
Bacteria;Proteobacteria;Gammaproteobacteria;Pseudomonadales;Moraxellaceae;Psychrobacter	0.50	1.28	0.84	0.00	0.00	0.00
Bacteria;Proteobacteria;Gammaproteobacteria;Thiotrichales;Piscirickettsiaceae;uncultured	6.72	6.70	8.72	0.54	0.00	0.00
Bacteria;Proteobacteria;Gammaproteobacteria;Vibrionales;Vibrionaceae;Aliivibrio	0.00	0.00	0.00	0.78	0.97	1.52
Bacteria;Proteobacteria;Gammaproteobacteria;Vibrionales;Vibrionaceae;Vibrio	0.50	0.00	0.14	9.39	12.32	19.57
Bacteria;Proteobacteria;Gammaproteobacteria;Xanthomonadales;Sinobacteraceae;JTB255 marine benthic group	0.25	0.96	1.13	0.06	0.05	0.22
Bacteria;Proteobacteria;Gammaproteobacteria;aaa34a10;uncultured bacterium;Other	0.00	0.00	0.00	0.42	0.97	1.74
Bacteria;Proteobacteria;Gammaproteobacteria;uncultured Codakia orbicularis gill symbiont;Other;Other	1.00	0.32	0.42	0.00	0.00	0.00
Total	72.01	72.89	71.73	86.57	86.43	83.26

Table S2. Latitude and longitude coordinates of individual aggregates collected from Fort Morgan (FM) and Gulf Shores (GS) beaches that were subsequently characterized via chemical, molecular, and metabolomic analyses.

Sample	Latitude	Longitude
FM8	30°13'29.9"N	88°00'31.4"W
FM16	30°13'28.5"N	88°00'41.8"W
FM20	30°13'30.6"N	88°00'26.9"W
GS1	30°14'24.6"N	87°44'14.5"W
GS2	30°15'04.5"N	87°39'12.1"W
GS3	30°15'04.6"N	87°39'12.1"W
GS7	30°15'04.3"N	87°39'13.6"W
GS9	30°15'04.4"N	87°39'12.4"W
GS12	30°15'04.6"N	87°39'08.2"W

Table S3. Approximate weights of all aggregates collected from Fort Morgan (FM), Gulf Shores (GS) Site 1 and Site 2. The three largest aggregates from Fort Morgan (FM8, FM16, FM20) and the five largest aggregates from Gulf Shores Site 2 (GS2, GS3, GS7, GS9, GS12), along with the single sample collected from Gulf Shores Site 1 (GS1) were used for subsequent analyses. Note: five samples were chosen from Gulf Shores Site 2 due to the overall smaller size of aggregates at this location to ensure that triplicate samples were available for statistical comparisons.

Fort Morgan		Gulf Shores Site 1		Gulf Shores Site 2	
Aggregate	**Weight (g)**	**Aggregate**	**Weight (g)**	**Aggregate**	**Weight (g)**
1	2.06	1	8.78	2	10.08
2	3.95			3	2.01
3	5.59			4	1.30
4	1.60			5	1.59
5	3.51			6	1.66
6	1.29			7	3.18
7	2.77			8	1.22
8	12.83			9	2.03
9	1.52			10	0.96
10	3.57			11	1.67
11	2.46			12	3.97
12	3.75			13	1.82
13	3.77			14	1.24
14	1.98				
15	4.24				
16	14.00				
17	3.00				
18	3.33				
19	5.31				
20	5.65				

Table S4. KEGG orthology (KO) numbers of functional genes investigated in metagenomic sequences from sand patties, beach sand, and seawater.

Gene	Gene Name	KEGG Orthology Number
RpoB (Bacteria)	DNA-directed RNA polymerase subunit beta	K03043
RpoB (Archaea)	DNA-directed RNA polymerase subunit beta	K13798
NarG	nitrate reductase alpha subunit	K00370
NarH	nitrate reductase beta subunit	K00371
NarI	nitrate reductase gamma subunit	K00374
NapA	periplasmic nitrate reductase	K02567
NapB	cytochrome c-type protein NapB	K02568
NirB	nitrite reductase (NADH) large subunit	K00362
NirD	nitrite reductase (NADH) small subunit	K00363
NrfA	nitrite reductase (cytochrome c-552)	K03385
NrfH	cytochrome c nitrite reductase small subunit	K15876
NirK	nitrite reductase (NO-forming)	K00368
NirS	nitrite reductase (NO-forming) / hydroxylamine reductase	K15864
NorB	nitric oxide reductase subunit B	K04561
NorC	nitric oxide reductase subunit C	K02305
NosZ	nitrous-oxide reductase	K00376
NifD	nitrogenase molybdenum-iron protein alpha chain	K02586
NifK	nitrogenase molybdenum-iron protein beta chain	K02591
NifH	nitrogenase iron protein NifH	K02588
AnfG	nitrogenase delta subunit	K00531
AmoA	methane/ammonia monooxygenase subunit A	K10944
AmoB	methane/ammonia monooxygenase subunit B	K10945
AmoC	methane/ammonia monooxygenase subunit C	K10946

Hao	hydroxylamine dehydrogenase	K10535
Hzs	hydrazine synthase subunit	K20932
Hzs	hydrazine synthase subunit	K20933
Hzs	hydrazine synthase subunit	K20934
Hdh	hydrazine dehydrogenase	K20935
AprA	adenylylsulfate reductase subunit A	K00394
AprB	adenylylsulfate reductase subunit B	K00395
DsrA	dissimilatory sulfite reductase subunit A	K11180
DsrB	dissimilatory sulfite reductase subunit B	K11181
SoxA	sulfur oxidizing protein SoxA	K17222
SoxB	sulfur oxidizing protein SoxB	K17224
SoxC	sulfane dehydrogenase subunit SoxC	K17225
SoxD	cytochrome C	K08738
SoxX	sulfur oxidizing protein SoxX	K17223
SoxY	sulfur oxidizing protein SoxY	K17226
SoxZ	sulfur oxidizing protein SoxZ	K17227
DoxA	thiosulfate dehydrogenase [quinone] small subunit	K16936
DoxD	thiosulfate dehydrogenase [quinone] large subunit	K16937
FccA	cytochrome subunit of sulfide dehydrogenase	K17230
FccB	sulfide dehydrogenase [flavocytochome c] flavoprotein chain	K17229
Sor	sulfur oxygenase/reductase	K16952
Sqr	sulfide:quinone oxidoreductase	K17218
HdrA	heterodisulfide reductase subunit A	K03388
HdrB	heterodisulfide reductase subunit B	K03389
HdrC	heterodisulfide reductase subunit C	K03390
McrA	methyl-coenzyme M reductase subunit alpha	K00399
McrB	methyl-coenzyme M reductase subunit beta	K00401

McrG	methyl-coenzyme M reductase subunit gamma	K00402
CooF	carbon-monoxide dehydrogenase iron sulfur subunit	K00196
CooS	carbon-monoxide dehydrogenase catalytic subunit	K00198
RbcL	ribulose-bisphosphate carboxylase large chain	K01601

Table S5. Water temperature, pH, redox potential, and sulfate concentrations measured from surface water collected at Fort Morgan, Gulf Shores Site 1, and Gulf Shores Site 2.

Site	Water Temperature (°C)	pH	Redox Potential (mV)	Sulfate (mM)
Fort Morgan	26.6	7.91	-71.3	24.78 ± 3.01
Gulf Shores Site 1	24.6	7.76	-74.1	23.47 ± 1.47
Gulf Shores Site 2	25.7	7.79	-69.9	24.01 ± 2.42

Table S6. Average diagnostic biomarker ratios calculated via GCxGC-FID for MC252 crude oil, oil:sand aggregates from this study, and various field samples collected from similar locations (Aeppli *et al.*, 2014). Ratios are denoted as: Ts/Tm: 18α(H)-22,29,30-trinorneohopane/17α(H)-22,29,30-trinorhopane; Ts/H: 18α(H)-22,29,30-trinorneohopane/17α(H),21β(H)-hopane; M/H: 17β(H),21α(H)-hopane/17α(H),21β(H)-hopane; M/NM: 17β(H),21α(H)-hopane/17β(H),21α(H)-30-norhopane; HH(R)/HH(S): 17α(H),21β(H)-22S/R-homohopane; 2HH(S)/H: 17α(H),21β(H)-22S-bishomohopane/17α(H),21β(H)-hopane.

Biomarker Ratio	MC252 crude oil from Aeppli *et al*, 2014	Oil:Sand Aggregates (n = 9)	Samples from Aeppli *et al*, 2014 (n = 46)
Ts/Tm	1.40 ± 0.10	1.36 ± 0.07	1.40 ± 0.10
Ts/H	0.24 ± 0.02	0.24 ± 0.02	0.27 ± 0.02
M/H	0.08 ± 0.01	0.09 ± 0.005	0.09 ± 0.01
M/NM	1.40 ± 0.20	1.45 ± 0.16	1.40 ± 0.10
HH(R)/HH(S)	0.72 ± 0.02	0.72 ± 0.03	0.72 ± 0.03
2HH(S)/H	0.34 ± 0.01	0.33 ± 0.01	0.30 ± 0.03

Table S7. Library sizes of 16S rRNA genes from aggregates, beach sand, and seawater samples. Each aggregate and sand replicate collected were subsampled into three technical replicates, denoted as A, B, C. Seawater was filtered to collect biomass, and three filters at each location were extracted and used for sequencing.

Fort Morgan		Gulf Shores Site 1		Gulf Shores Site 2	
		Aggregates			
FM8A	31809	**GS1A**	37902	**GS2A**	15650
FM8B	26457	**GS1B**	28303	**GS2B**	17005
FM8C	30112	**GS1C**	33769	**GS2C**	20268
FM16A	24907			**GS3A**	20418
FM16B	30191			**GS3B**	21458
FM16C	23894			**GS3C**	18206
FM20A	12879			**GS7A**	14571
FM20B	11355			**GS7B**	29654
FM20C	26209			**GS7C**	16579
				GS9A	22431
				GS9B	18363
				GS9C	19624
				GS12A	20123
				GS12B	21071
				GS12C	23976
		Sand			
Rep. 1A	24987	**Rep. 1A**	29167	**Rep. 1A**	28106
Rep. 1B	32448	**Rep. 1B**	25491	**Rep. 1B**	31199
Rep. 1C	17393	**Rep. 1C**	23473	**Rep. 1C**	30643
Rep. 2A	28806			**Rep. 2A**	20280
Rep. 2B	25609			**Rep. 2B**	29890
Rep. 2C	36868			**Rep. 2C**	22085
Rep. 3A	39996			**Rep. 3A**	28583
Rep. 3B	24260			**Rep. 3B**	24786
Rep. 3C	34410			**Rep. 3C**	11733
		Seawater			
Rep. 1	23646	**Rep. 1**	37004	**Rep. 1**	30465
Rep. 2	31548	**Rep. 2**	42621	**Rep. 2**	29427
Rep. 3	34149	**Rep. 3**	33405	**Rep. 3**	35278

Table S8. Average relative abundances of phyla sequenced from **(A)** aggregates, **(B)** beach sand, and **(C)** seawater (SW) collected from Fort Morgan (FM), Gulf Shores Site 1 (GS-1) and Gulf Shores Site 2 (GS-2). Values represent averages of triplicate libraries generated from technical replicates of each sample.

A.

Phylum	FM8 (%)	FM16 (%)	FM20 (%)	GS1 (%)	GS2 (%)	GS3 (%)	GS7 (%)	GS9 (%)	GS12 (%)
Euryarchaeota	0.14	13.08	0.07	0.16	0.02	0.07	0.05	0.03	0.04
Thaumarchaeota	0.13	0.06	0.07	0.15	0.04	0.04	0.03	0.05	0.06
Acidobacteria	0.49	0.07	0.04	1.41	0.20	2.18	0.06	0.12	2.21
Actinobacteria	5.42	0.15	9.05	0.13	12.84	21.59	8.20	2.13	13.63
Bacteroidetes	2.42	9.63	1.42	2.25	1.20	0.71	1.10	0.39	1.27
Candidate Division BRC1	0.05	0.20	0.00	0.14	0.01	0.00	0.01	0.02	0.01
Candidate Division WS3	0.04	0.01	0.01	1.10	0.01	0.00	0.01	0.01	0.01
Chloroflexi	1.02	2.01	0.52	5.90	3.30	11.12	0.33	0.72	5.95
Cyanobacteria	6.08	0.70	2.00	1.02	2.01	1.53	1.17	2.44	0.92
Firmicutes	4.98	3.90	0.64	0.04	0.18	0.07	0.08	0.43	0.20
NPL-UPA2	0.00	0.00	0.00	0.48	0.00	0.01	0.00	0.00	0.00
Planctomycetes	3.55	4.32	0.98	11.79	8.00	4.52	11.11	2.36	8.59
Proteobacteria	65.10	63.16	82.11	32.33	69.70	41.33	74.56	86.96	61.59
Spirochaetes	1.09	0.44	0.06	18.85	0.13	0.03	0.02	0.02	0.06
Verrucomicrobia	0.51	0.16	0.07	0.13	0.89	3.81	0.10	0.08	3.44
Unassigned	7.85	2.01	2.80	20.72	1.00	12.58	3.01	4.06	1.13

B.

Phylum	FM Rep. 1 (%)	FM Rep. 2 (%)	FM Rep. 3 (%)	GS-1 Rep. 1 (%)	GS-2 Rep. 1 (%)	GS-2 Rep. 2 (%)	GS-2 Rep. 3 (%)
Euryarchaeota	0.81	2.64	6.24	3.86	7.81	5.39	2.51
Thaumarchaeota	7.47	6.78	6.05	6.51	9.90	18.75	6.85
Acidobacteria	5.16	6.02	4.73	6.31	6.86	8.93	6.53
Actinobacteria	1.59	2.04	2.19	2.54	2.37	1.52	3.05
Bacteroidetes	12.30	12.29	12.43	6.66	9.34	2.83	5.54
Candidate Division BRC1	0.06	0.07	0.06	0.10	0.31	0.86	0.17
Candidate Division WS3	1.30	1.56	1.32	1.04	0.72	1.89	0.80
Chloroflexi	2.15	2.26	2.18	2.58	2.28	5.86	2.95
Cyanobacteria	8.20	6.00	10.58	12.42	10.61	6.28	15.61
Firmicutes	0.03	0.02	0.07	0.18	0.19	0.30	0.21
NPL-UPA2	0.37	0.38	0.26	0.30	0.35	1.60	0.15
Planctomycetes	25.80	26.89	23.24	32.20	23.04	18.21	31.84
Proteobacteria	23.25	22.16	21.66	15.72	16.86	13.44	14.39
Spirochaetes	0.07	0.05	0.05	0.04	0.03	0.05	0.04
Verrucomicrobia	2.26	1.91	1.36	1.58	2.50	3.54	2.25
Unassigned	6.92	6.61	5.79	6.08	4.80	7.86	5.60

C.

Phylum	FM SW (%)	GS-1 SW (%)	GS-2 SW (%)
Euryarchaeota	3.57	8.35	9.47
Thaumarchaeota	0.50	0.54	0.78
Acidobacteria	0.44	0.74	0.90
Actinobacteria	0.80	0.90	1.38
Bacteroidetes	14.38	11.78	9.95
Candidate Division BRC1	0.04	0.06	0.12
Candidate Division WS3	0.16	0.15	0.18
Chloroflexi	0.49	0.47	0.71
Cyanobacteria	32.93	27.89	26.89
Firmicutes	0.06	0.14	0.14
NPL-UPA2	0.26	0.29	0.26
Planctomycetes	6.90	14.09	16.23
Proteobacteria	30.19	24.46	19.83
Spirochaetes	0.04	0.03	0.04
Verrucomicrobia	3.09	3.20	5.35
Unassigned	4.90	5.63	6.48

Table S9. Average relative abundances of sequences classified within Proteobacteria in **(A)** aggregates, **(B)** beach sand, and **(C)** seawater samples collected from Fort Morgan (FM), Gulf Shores Site 1 (GS-1), and Gulf Shores Site 2 (GS-2). Values are averages of technical replicates. Values represent averages of triplicate libraries generated from technical replicates of each sample.

A.

Sample	Alpha (%)	Beta (%)	Delta (%)	Gamma (%)
FM8	27.04	6.34	11.43	20.21
FM16	14.59	0.06	0.30	48.00
FM20	15.04	2.13	0.26	64.60
GS1	1.96	0.02	16.61	12.56
GS2	17.76	1.31	0.21	50.40
GS3	18.27	2.54	0.17	20.33
GS7	23.61	4.96	0.24	45.71
GS9	9.87	2.45	0.93	73.56
GS12	20.05	2.06	0.39	38.99

B.

Sample	Alpha (%)	Beta (%)	Delta (%)	Gamma (%)
FM Rep. 1	2.20	0.21	2.67	17.43
FM Rep. 2	1.99	0.21	2.68	16.74
FM Rep. 3	2.10	0.21	2.59	16.27
GS-1 Rep. 1	2.11	0.40	2.22	10.60
GS-2 Rep. 1	3.31	0.94	2.38	9.88
GS-2 Rep. 2	3.40	1.06	2.24	6.24
GS-2 Rep. 3	2.05	0.37	2.63	8.93

C.

Sample	Alpha (%)	Beta (%)	Delta (%)	Gamma (%)
FM SW	15.09	0.15	1.07	13.66
GS-1 SW	10.48	0.22	1.40	12.14
GS-2 SW	9.69	0.31	1.75	7.67

Table S10. Diversity indices and descriptive information of core taxa in technical replicates sampled from aggregates, beach sand, and seawater (SW) collected from **(A)** Fort Morgan (FM), **(B)** Gulf Shores Site 1 (GS-1), and **(C)** Gulf Shores Site 2 (GS-2). All values were calculated in PC-ORD (Version 6, MjM Software). Technical replicates are denoted as A, B, C. Notation: S – number of taxa in each sample; E – evenness; H – Shannon Diversity index; and D' – Simpson's Diversity for an infinite population. D' is the complement of Simpson's original index and indicates the likelihood that two individuals from a population would be different if chosen randomly.

A.

Sample	S	E	H	D’
FM8A	112	0.889	4.196	0.9776
FM8B	110	0.896	4.211	0.9792
FM8C	116	0.892	4.24	0.9791
FM16A	104	0.849	3.945	0.972
FM16B	108	0.837	3.92	0.97
FM16C	103	0.847	3.925	0.9707
FM20A	90	0.835	3.758	0.9551
FM20B	89	0.84	3.771	0.9562
FM20C	100	0.833	3.837	0.9584
FM Sand Rep. 1A	97	0.882	4.037	0.9761
FM Sand Rep. 1B	103	0.871	4.037	0.9758
FM Sand Rep. 1C	97	0.881	4.031	0.9757
FM Sand Rep. 2A	104	0.872	4.048	0.9766
FM Sand Rep. 2B	104	0.871	4.047	0.9765
FM Sand Rep. 2C	97	0.878	4.018	0.9762
FM Sand Rep. 3A	110	0.863	4.057	0.9762
FM Sand Rep. 3B	103	0.871	4.039	0.9764
FM Sand Rep. 3C	110	0.864	4.062	0.9761
FM SW Rep. A	97	0.852	3.898	0.9689
FM SW Rep. B	89	0.853	3.831	0.9672
FM SW Rep. C	94	0.848	3.851	0.9676

B.

Sample	S	E	H	D’
GS1A	104	0.849	3.943	0.9689
GS1B	97	0.843	3.856	0.9656
GS1C	99	0.861	3.954	0.9706
GS-1 Sand Rep. A	116	0.879	4.18	0.9788
GS-1 Sand Rep. B	110	0.879	4.13	0.9776
GS-1 Sand Rep. C	101	0.884	4.079	0.9766
GS-1 SW Rep. A	107	0.863	4.031	0.9732
GS-1 SW Rep. B	115	0.864	4.101	0.9749
GS-1 SW Rep. C	106	0.863	4.026	0.973

C.

Sample	S	E	H	D’
GS2A	94	0.87	3.951	0.9637
GS2B	94	0.863	3.922	0.9643
GS2C	101	0.856	3.951	0.9639
GS3A	89	0.844	3.788	0.9654
GS3B	94	0.837	3.803	0.9648
GS3C	88	0.837	3.746	0.9636
GS7A	92	0.849	3.841	0.9635
GS7B	104	0.837	3.888	0.9646
GS7C	99	0.846	3.886	0.9647
GS9A	102	0.808	3.736	0.9479
GS9B	100	0.813	3.745	0.9485
GS9C	98	0.802	3.677	0.946
GS12A	98	0.855	3.922	0.9682
GS12B	100	0.862	3.968	0.9696
GS12C	102	0.853	3.947	0.9689
GS-2 Sand Rep. 1A	107	0.891	4.164	0.9784
GS-2 Sand Rep. 1B	114	0.891	4.218	0.9796
GS-2 Sand Rep. 1C	115	0.887	4.21	0.9792
GS-2 Sand Rep. 2A	103	0.897	4.159	0.9792
GS-2 Sand Rep. 2B	114	0.877	4.153	0.9784
GS-2 Sand Rep. 2C	97	0.892	4.083	0.9775
GS-2 Sand Rep. 3A	107	0.872	4.074	0.9756
GS-2 Sand Rep. 3B	108	0.877	4.108	0.9767

GS-2 Sand Rep. 3C	94	0.892	4.051	0.9763
GS-2 SW Rep. A	113	0.874	4.133	0.9768
GS-2 SW Rep. B	113	0.877	4.147	0.9768
GS-2 SW Rep. C	113	0.877	4.146	0.9766

Table S11. Results from multi-response permutation procedure (MRPP) of core microbial communities from Fort Morgan (FM), Gulf Shores Site 1 (GS-1), and Gulf Shores Site 2 (GS-2) locations. Analyses were conducted using a Bray-Curtis distance measure. The test statistic (T) designates how strongly the groups are separated, with a more negative value indicative of a greater degree of separation. The chance-corrected within-group agreement, represented by A, indicates homogeneity within groups compared to random expectation, where a maximum of A = 1 describes identical samples within a group. Groups were defined within sampling locations (i.e., Fort Morgan, Gulf Shores Site 1, and Gulf Shores Site 2). All analyses were performed in PC-ORD (Version 6, MjM Software).

	FM	**GS-1**	**GS-2**
T	-11.02	-4.94	-13.07
Observed δ	0.25	0.07	0.29
Expected δ	0.50	0.41	0.52
p values	3.00E-08	3.62E-04	0.00E-08
A	0.50	0.84	0.44

Figure S1. Phylogenetic composition of microbial communities based on 16S rRNA gene sequences from one oil:sand aggregates collected from **(A)** Fort Morgan (FM) and one oil:sand aggregate from **(B)** Gulf Shores (GS) in January 2014. Technical replicates were generated from each aggregate and are denoted A, B, C. Sequences were analyzed via QIIME (Version 1.7.0) (Caporaso *et al.*, 2010a), and grouped into OTUs at 97% similarity. Note: groups are shown to the highest taxonomic resolution possible. Not all phylogenetic groups are included in legends.

A.

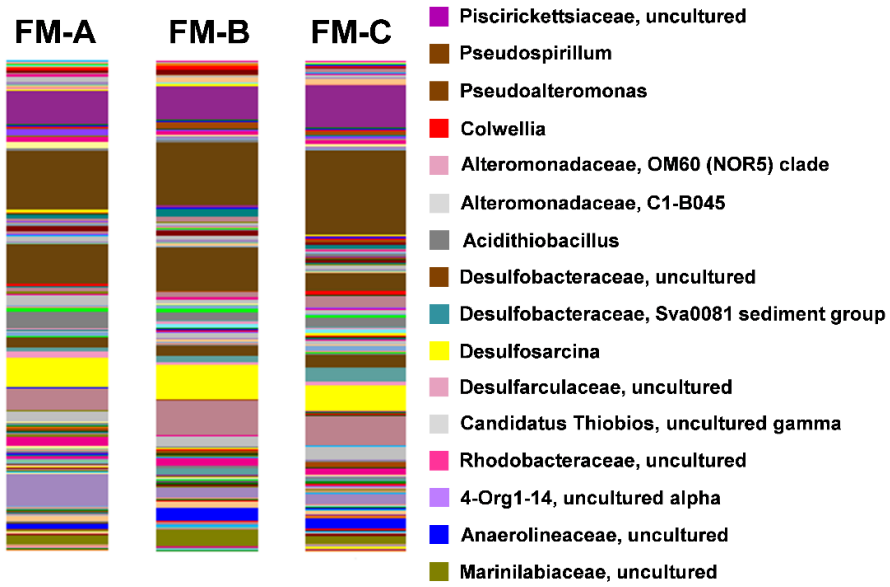

B.

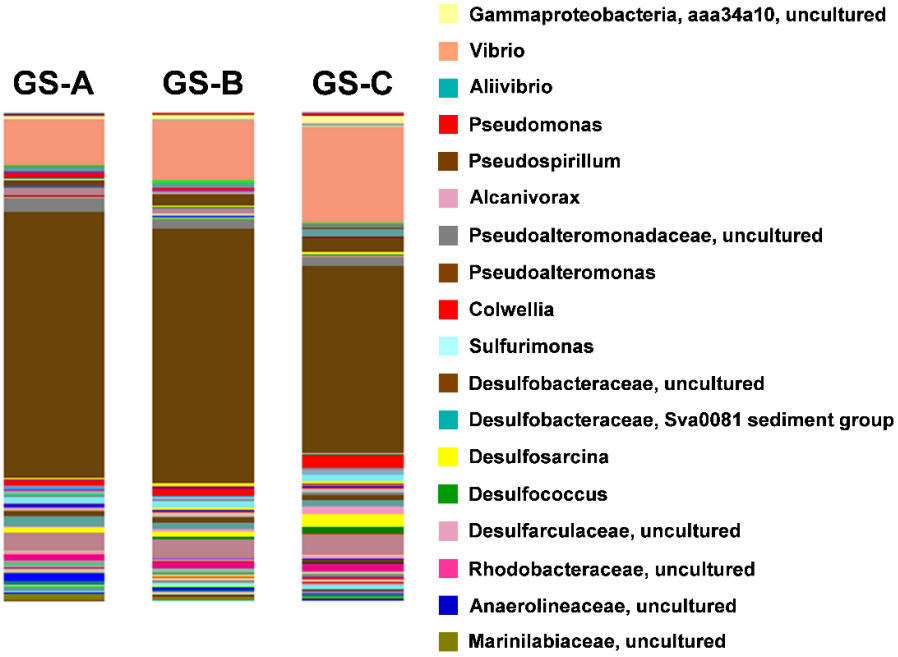

Figure S2. Heatmap of RpoB-normalized ratios calculated for genes involved in aerobic and anaerobic hydrocarbon transformation processes from preliminary sand patties collected in January 2014. Technical replicates were generated from each sand patty collected (i.e., one from Fort Morgan (FM) and one from Gulf Shores (GS) and are denoted as A, B, C. The heatmap was generated using Heatmap Builder® (Version 1.1) with dataset-normalized sorting so that the highest ratio corresponds to the darkest grid color. Abbreviations: Alk, alkane monooxygenase; CYP153, cytochrome P450 alkane hydroxylase; Ass, alkylsuccinate synthase; Bss, benzylsuccinate synthase; Hbs, hydroxybenzylsuccinate synthase; Ibs, (4-isopropylbenzyl)succinate synthase; Nms, 2-napthylmethylsuccinate synthase; Ahy, alkane C2 methylene hydroxylase; Ebd, ethylbenzene dehydrogenase; Abc, anaerobic benzene dehydrogenase.

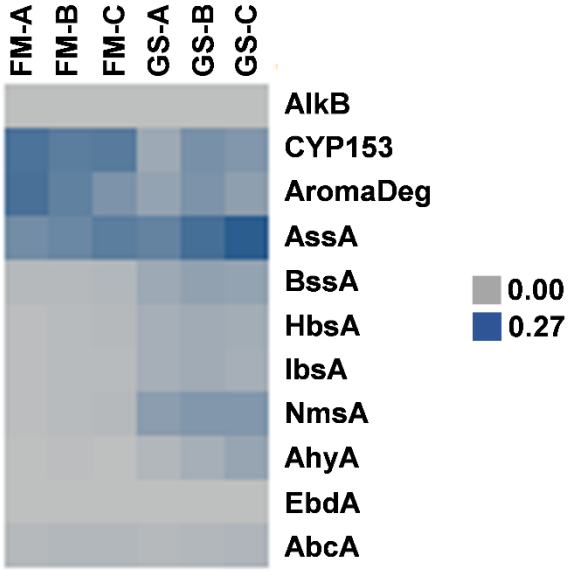

Figure S3. Schematic representation of sampling method. Oil:sand aggregates were homogenized and subsampled for oil characterization and biomarker analysis, 16S rRNA and metagenomic sequencing, and metabolomics. For 16S rRNA gene libraries, triplicate technical replicates were generated by performing DNA extractions on three subsamples for aggregates and beach sand. DNA from technical replicates was subsequently pooled to generate one metagenomic sample per aggregate or beach sand sample. DNA was extracted from triplicate seawater filters and was used to generate both 16S rRNA and metagenomic libraries.

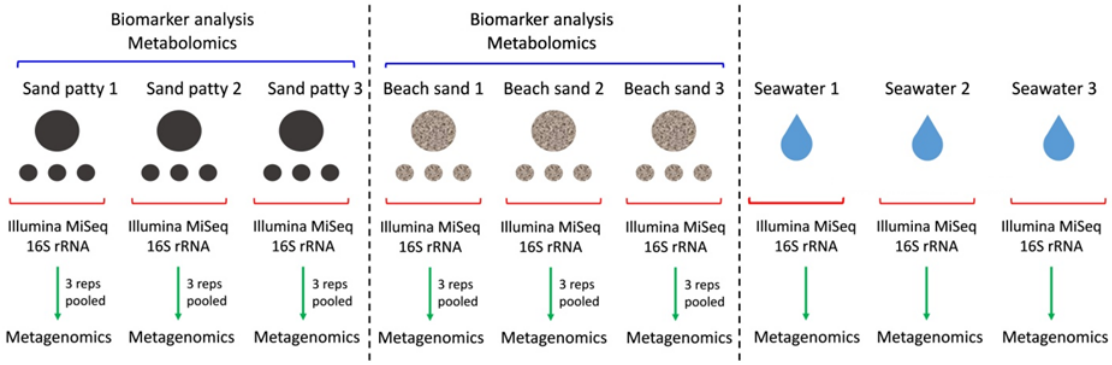

Figure S4. GCxGC-FID chromatographs of oil extracted from **(A)**, **(B)** MC252 crude oil, **(C)** FM8, **(D)** FM16, **(E)** FM20, **(F)** GS1, **(G)** GS2, **(H)** GS3, **(I)** GS7, **(J)** GS9, and **(K)** GS12 aggregates, along with a **(L)** representative sand sample. Note: **(B)** represents MC252 crude oil normalized to C_{30}-hopane.

A.

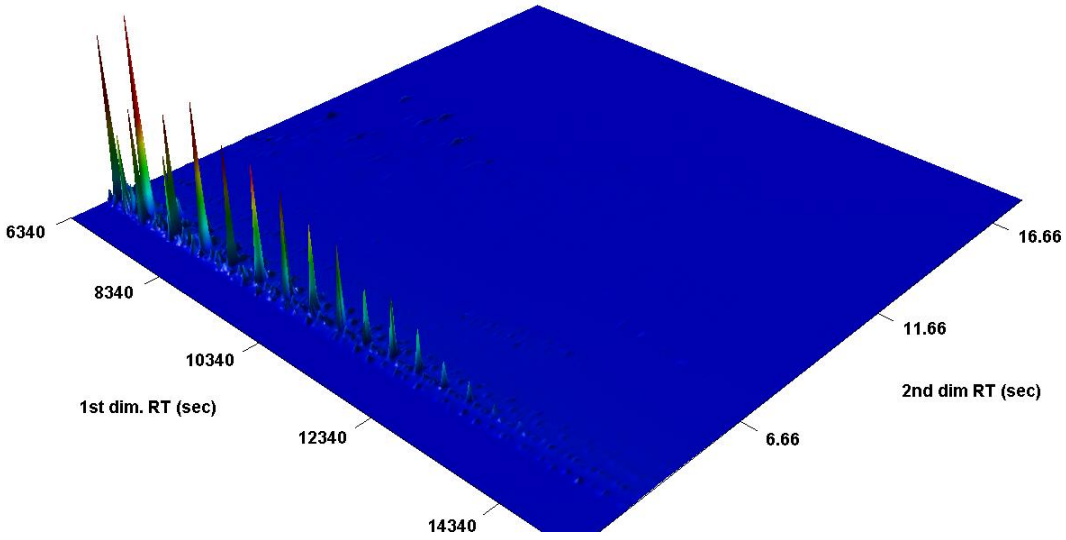

B.

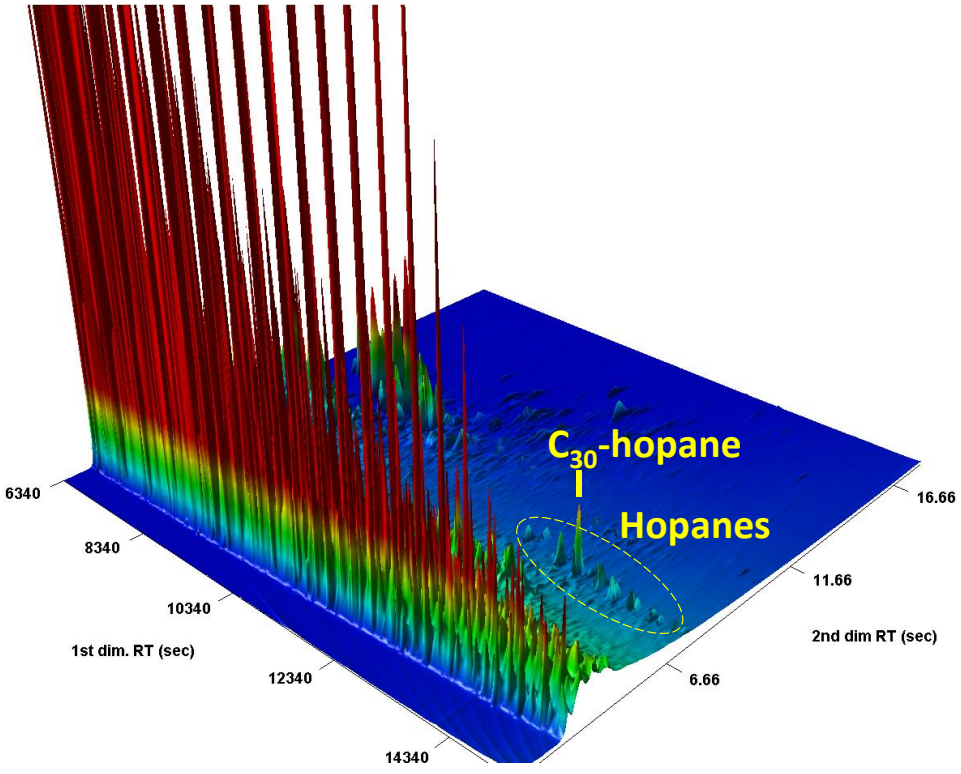

C.

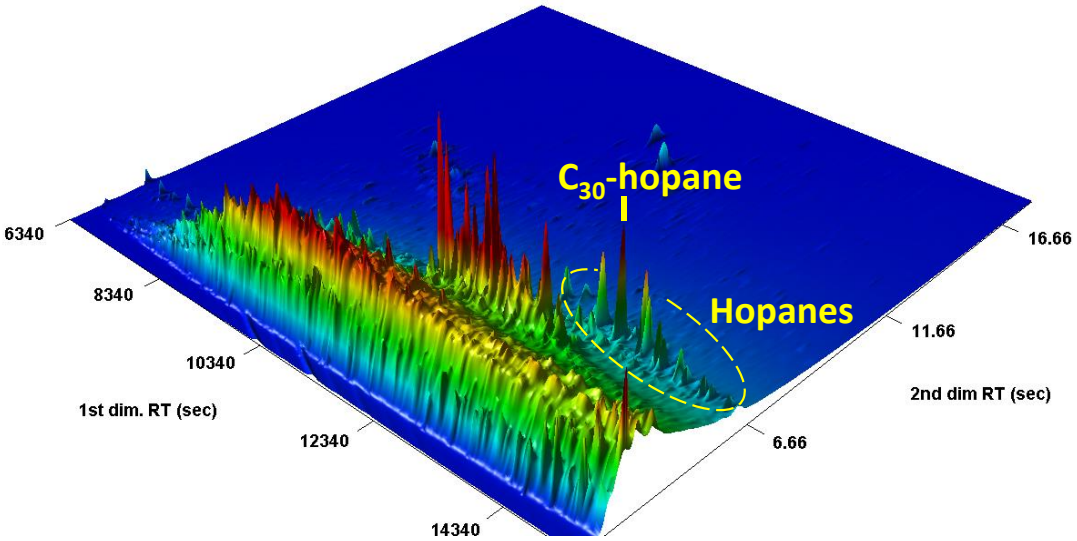
C30-hopane
Hopanes
6340
8340
10340
12340
14340
1st dim. RT (sec)
6.66
11.66
16.66
2nd dim RT (sec)

D.

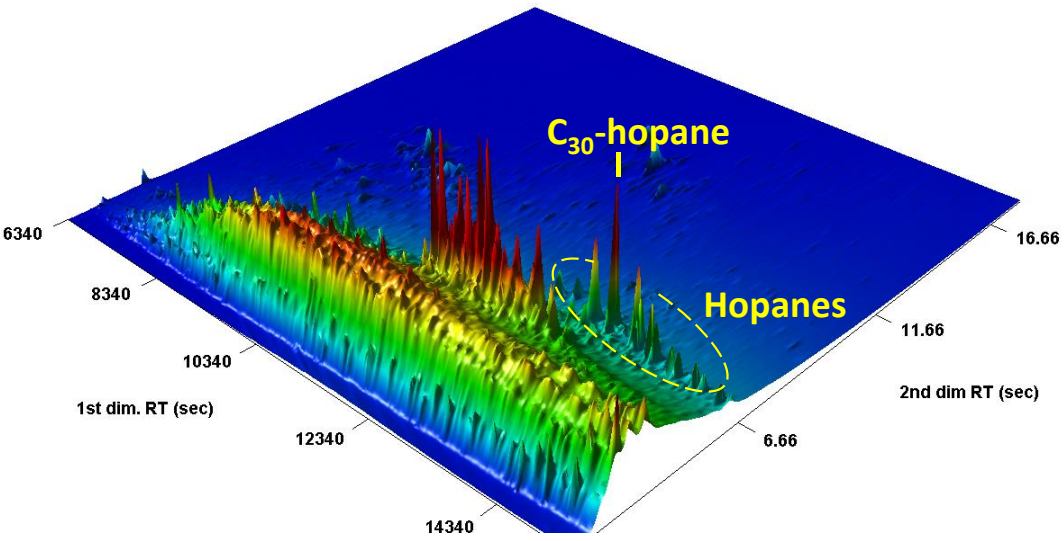
C30-hopane
Hopanes
6340
8340
10340
12340
14340
1st dim. RT (sec)
6.66
11.66
16.66
2nd dim RT (sec)

E.

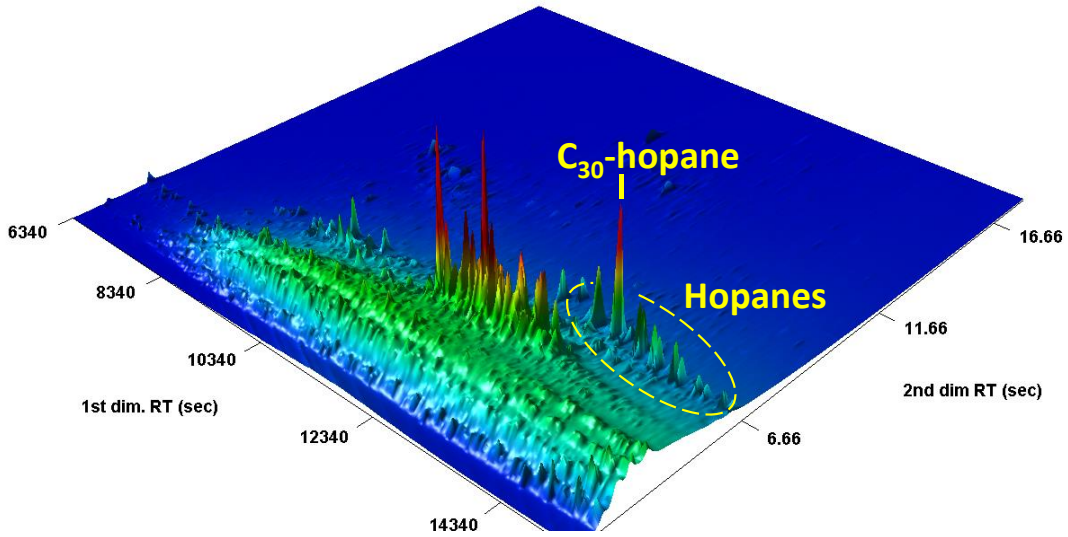
C30-hopane
Hopanes
6340
8340
10340
12340
14340
1st dim. RT (sec)
16.66
11.66
6.66
2nd dim RT (sec)

F.

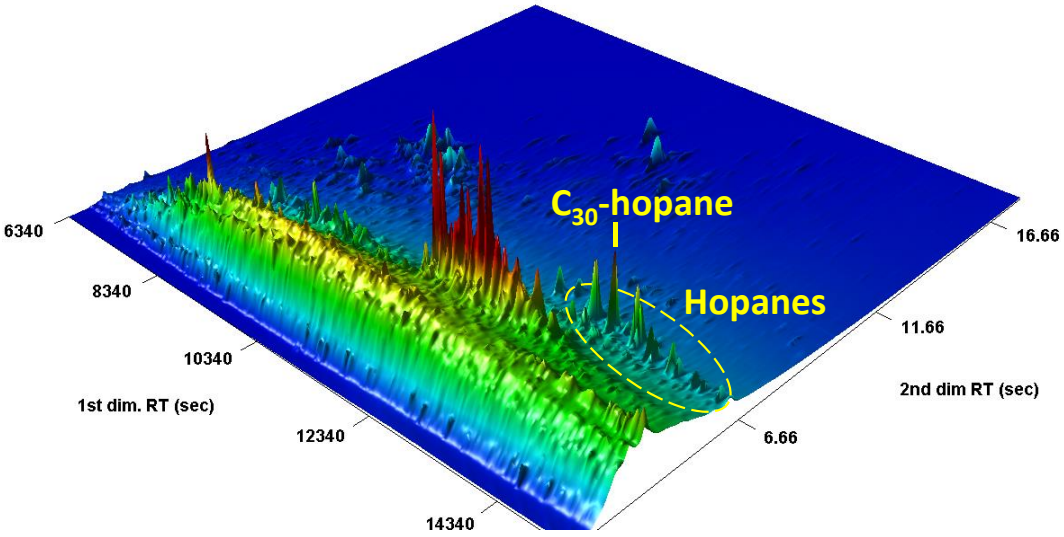
C30-hopane
Hopanes
6340
8340
10340
12340
14340
1st dim. RT (sec)
16.66
11.66
6.66
2nd dim RT (sec)

G.

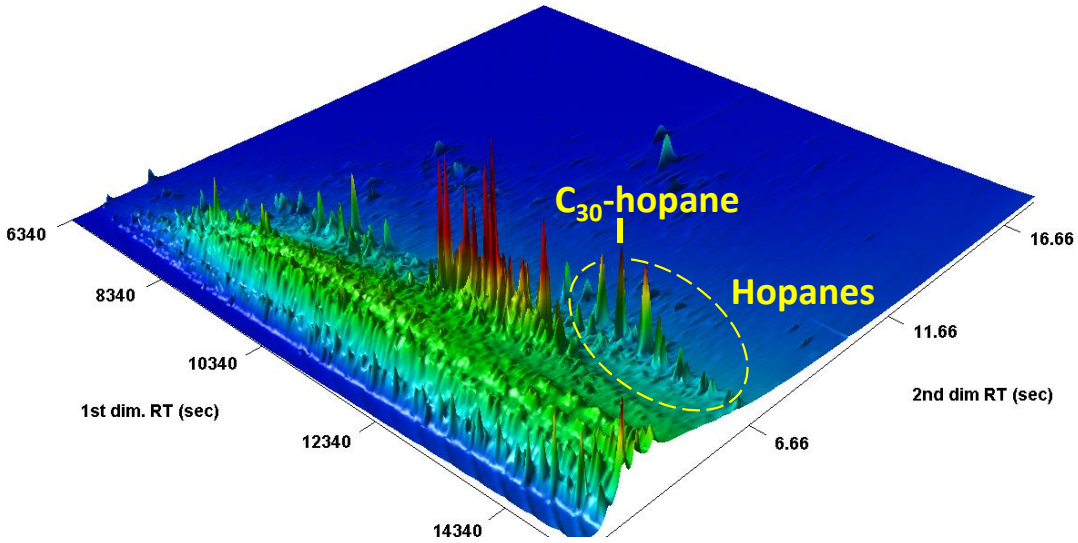
C30-hopane
Hopanes
6340
8340
10340
12340
14340
1st dim. RT (sec)
6.66
11.66
16.66
2nd dim RT (sec)

H.

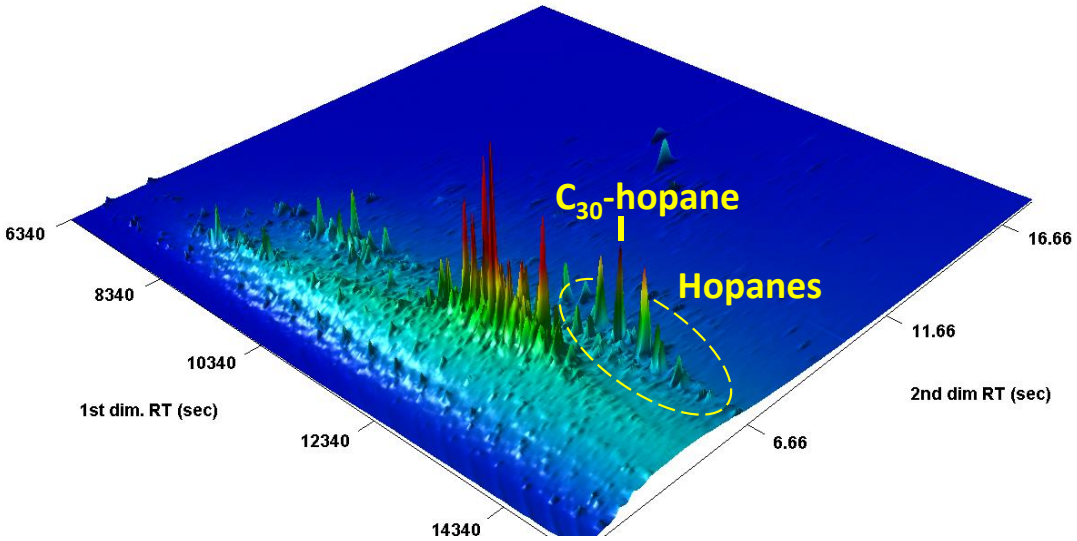
C30-hopane
Hopanes
6340
8340
10340
12340
14340
1st dim. RT (sec)
6.66
11.66
16.66
2nd dim RT (sec)

I.

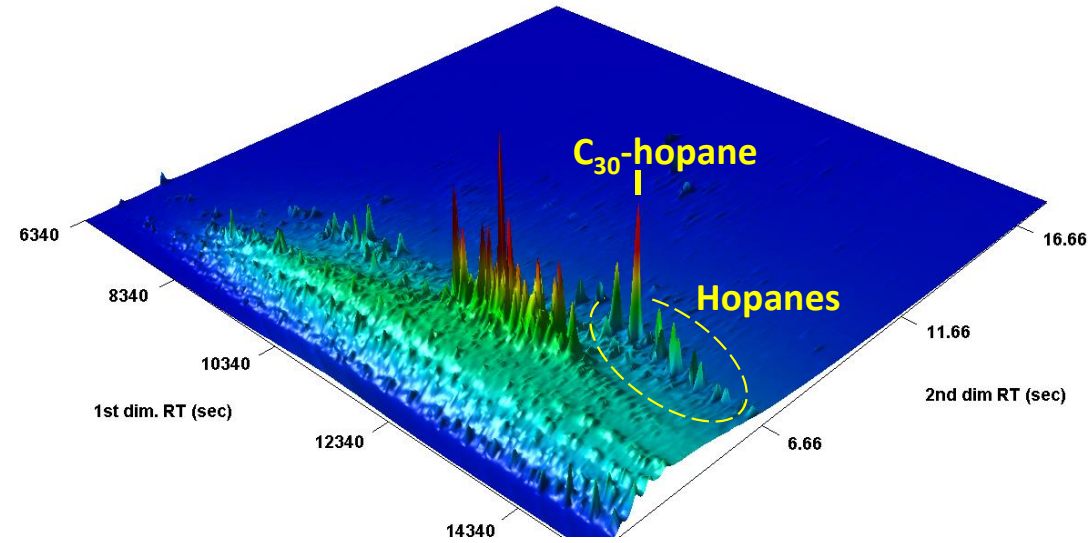
C30-hopane
Hopanes
6340
8340
10340
12340
14340
1st dim. RT (sec)
6.66
11.66
16.66
2nd dim RT (sec)

J.

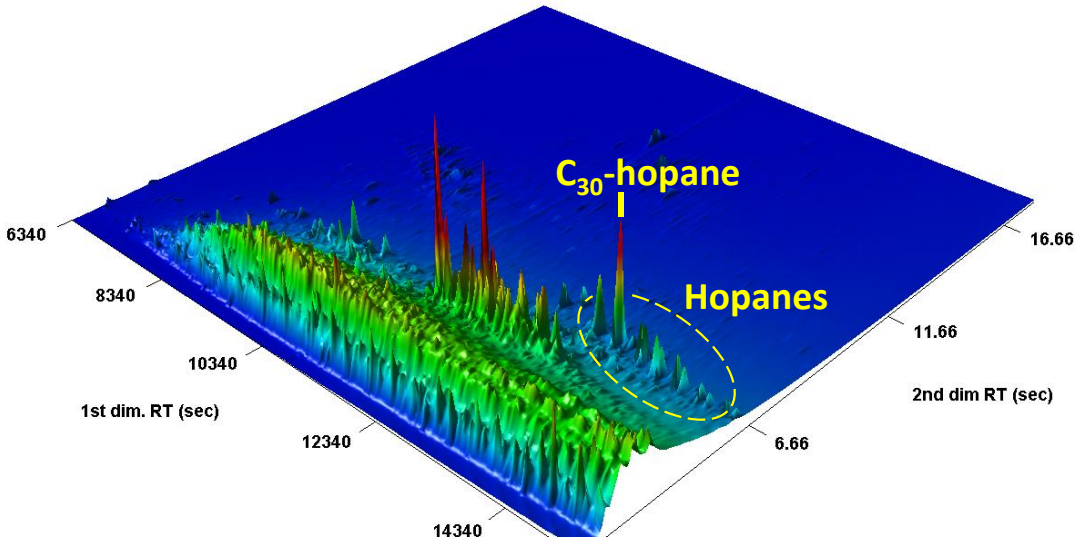
C30-hopane
Hopanes
6340
8340
10340
12340
14340
1st dim. RT (sec)
6.66
11.66
16.66
2nd dim RT (sec)

K.

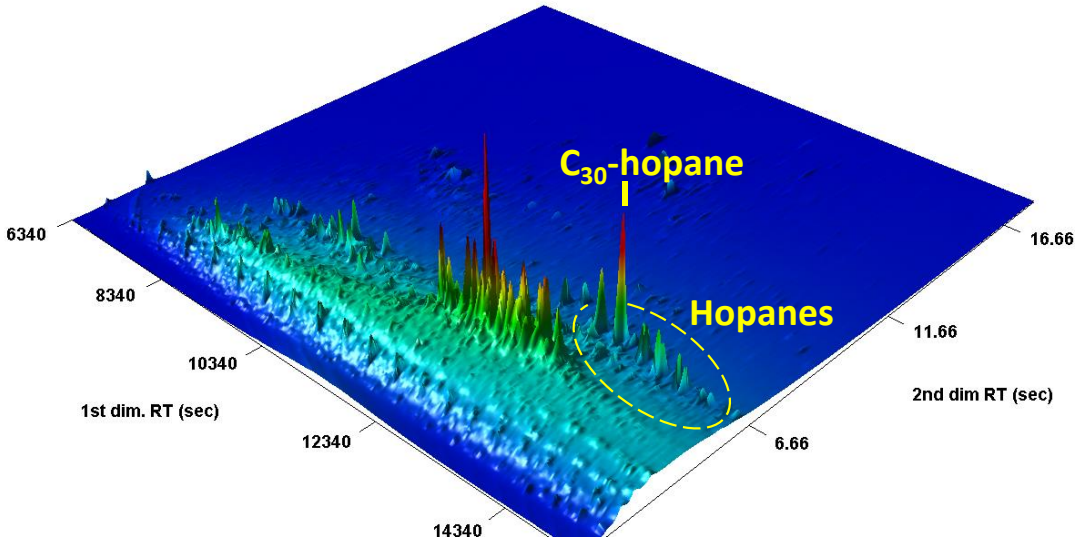
C30-hopane
Hopanes
6340
8340
10340
12340
14340
1st dim. RT (sec)
6.66
11.66
16.66
2nd dim RT (sec)

L.

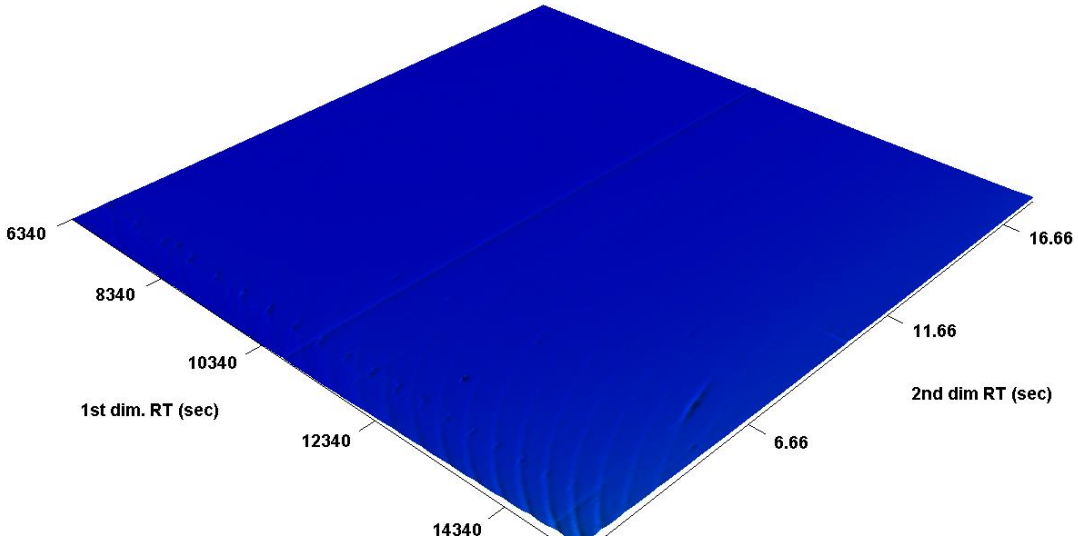
6340
8340
10340
12340
14340
1st dim. RT (sec)
6.66
11.66
16.66
2nd dim RT (sec)

Figure S5. Normalized ratios of functional gene markers associated with nitrogen cycling processes. **(A)** Nitrate reductase alpha subunit, NarG, **(B)** nitrate reductase beta subunit, NarH, **(C)** nitrate reductase gamma subunit, NarI, **(D)** periplasmic nitrate reductase, NapA, **(E)** cytochrome c-type protein, NapB, **(F)** nitrite reductase large subunit, NirB, **(G)** nitrite reductase small subunit, NirD, **(H)** nitrite reductase, NrfA, **(I)** nitrite reductase small subunit, NrfH, **(J)** nitrite reductase (NO-forming), NirK, **(K)** nitrite reductase (NO-forming), NirS, **(L)** nitric oxide reductase subunit B, NorB, **(M)** nitric oxide reductase subunit C, NorC, **(N)** nitrous-oxide reductase, NosZ, **(O)** nitrogenase alpha chain, NifD, **(P)** nitrogenase iron protein, NifH, **(Q)** nitrogenase beta chain, NifK, **(R)** ammonia monooxygenase subunit A, AmoA, **(S)** ammonia monooxygenase subunit B, AmoB, **(T)** ammonia monooxygenase subunit C, AmoC, and **(U)** hydroxylamine dehydrogenase, Hao. Sequence hits normalized to prokaryotic RpoB hits.

A.

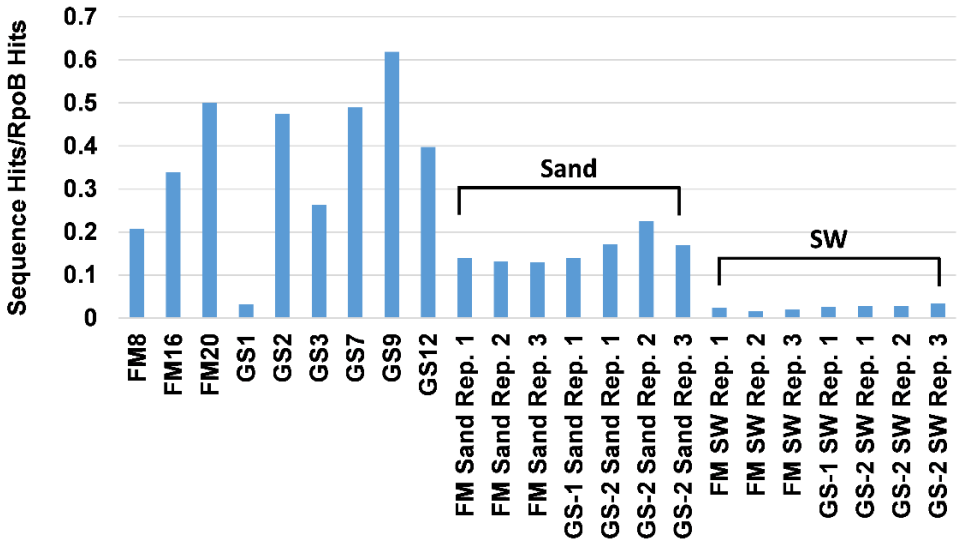

B.

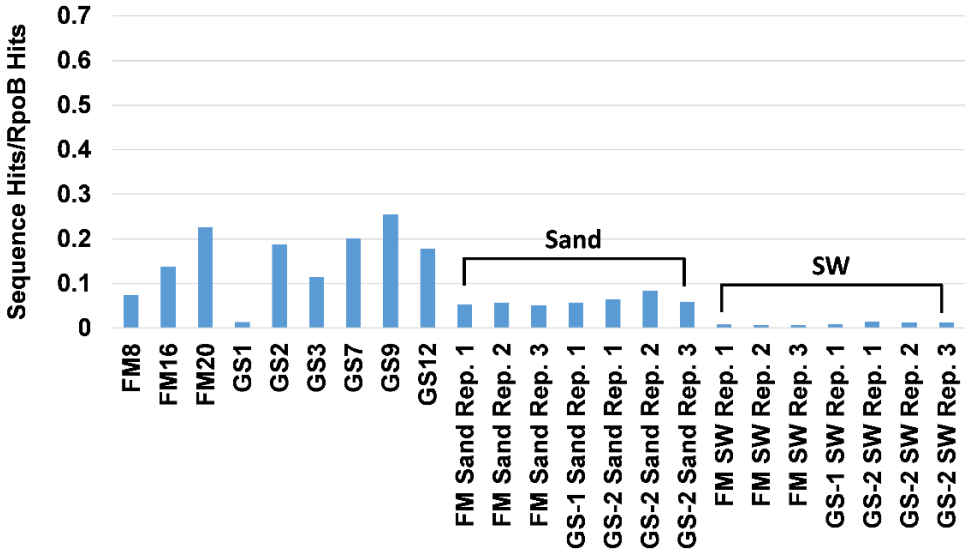
Sequence Hits/RpoB Hits
0.7
0.6
0.5
0.4
0.3
0.2
0.1
0
Sand
SW
FM8
FM16
FM20
GS1
GS2
GS3
GS7
GS9
GS12
FM Sand Rep. 1
FM Sand Rep. 2
FM Sand Rep. 3
GS-1 Sand Rep. 1
GS-2 Sand Rep. 1
GS-2 Sand Rep. 2
GS-2 Sand Rep. 3
FM SW Rep. 1
FM SW Rep. 2
FM SW Rep. 3
GS-1 SW Rep. 1
GS-2 SW Rep. 1
GS-2 SW Rep. 2
GS-2 SW Rep. 3

C.

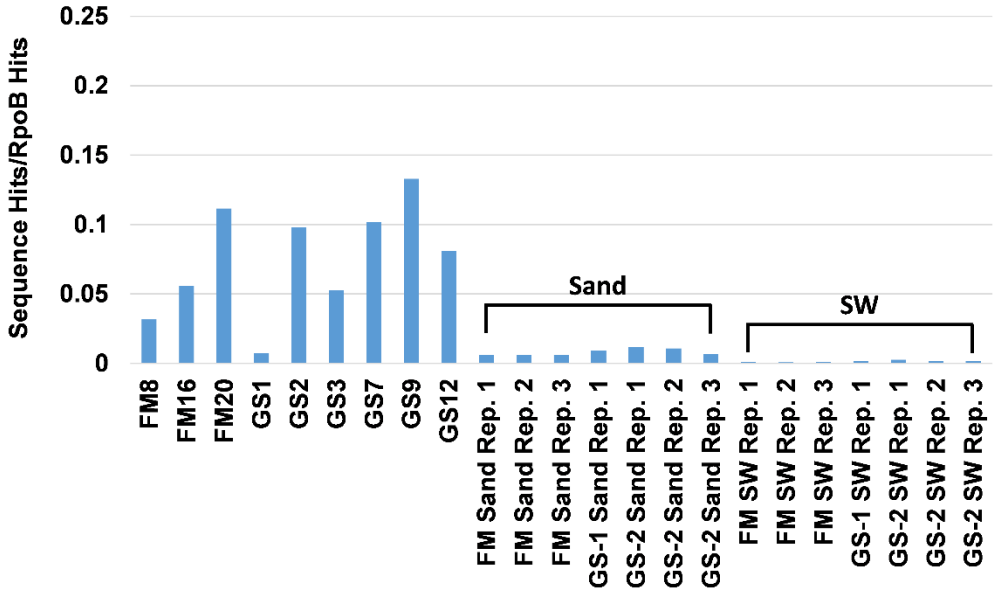
Sequence Hits/RpoB Hits
0.25
0.2
0.15
0.1
0.05
0
Sand
SW
FM8
FM16
FM20
GS1
GS2
GS3
GS7
GS9
GS12
FM Sand Rep. 1
FM Sand Rep. 2
FM Sand Rep. 3
GS-1 Sand Rep. 1
GS-2 Sand Rep. 1
GS-2 Sand Rep. 2
GS-2 Sand Rep. 3
FM SW Rep. 1
FM SW Rep. 2
FM SW Rep. 3
GS-1 SW Rep. 1
GS-2 SW Rep. 1
GS-2 SW Rep. 2
GS-2 SW Rep. 3

D.

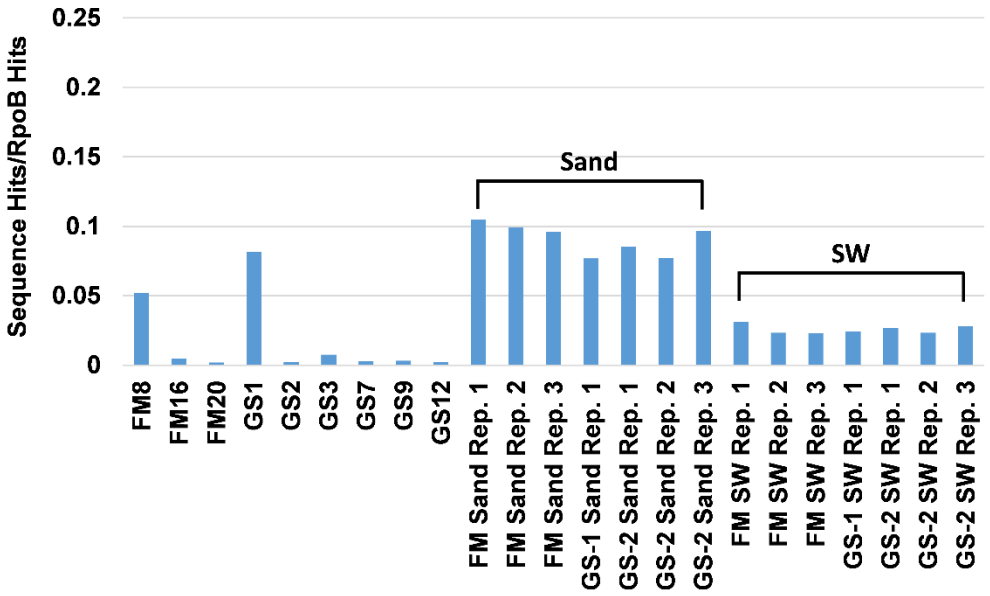
Sequence Hits/RpoB Hits
0.25
0.2
0.15
0.1
0.05
0
Sand
SW
FM8
FM16
FM20
GS1
GS2
GS3
GS7
GS9
GS12
FM Sand Rep. 1
FM Sand Rep. 2
FM Sand Rep. 3
GS-1 Sand Rep. 1
GS-2 Sand Rep. 1
GS-2 Sand Rep. 2
GS-2 Sand Rep. 3
FM SW Rep. 1
FM SW Rep. 2
FM SW Rep. 3
GS-1 SW Rep. 1
GS-2 SW Rep. 1
GS-2 SW Rep. 2
GS-2 SW Rep. 3

E.

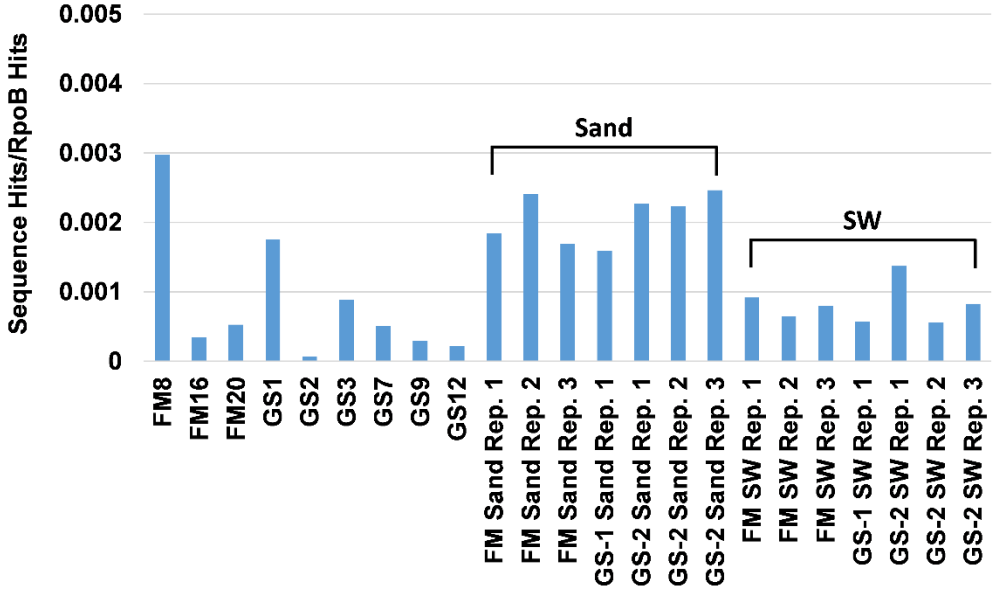
Sequence Hits/RpoB Hits
0.005
0.004
0.003
0.002
0.001
0
Sand
SW
FM8
FM16
FM20
GS1
GS2
GS3
GS7
GS9
GS12
FM Sand Rep. 1
FM Sand Rep. 2
FM Sand Rep. 3
GS-1 Sand Rep. 1
GS-2 Sand Rep. 1
GS-2 Sand Rep. 2
GS-2 Sand Rep. 3
FM SW Rep. 1
FM SW Rep. 2
FM SW Rep. 3
GS-1 SW Rep. 1
GS-2 SW Rep. 1
GS-2 SW Rep. 2
GS-2 SW Rep. 3

F.

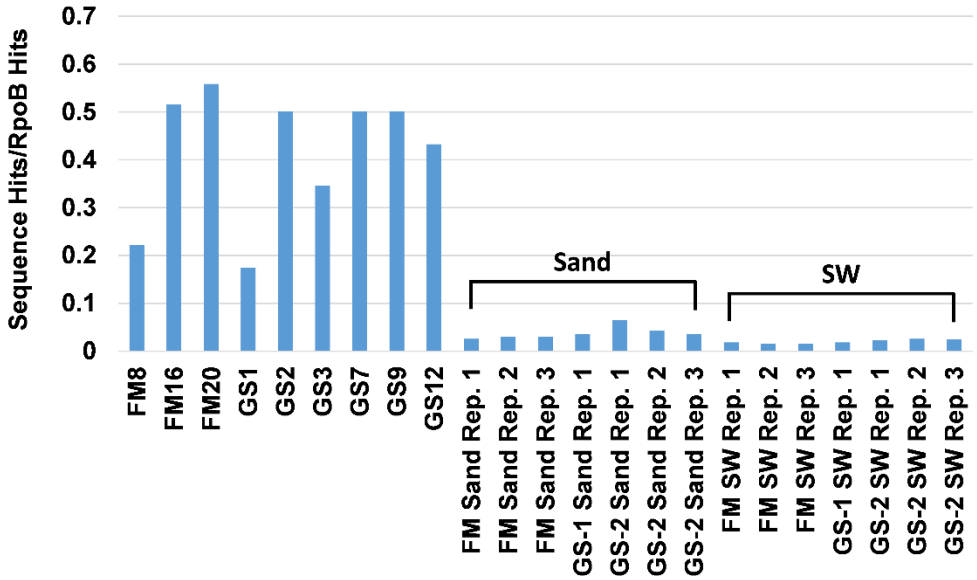
Sequence Hits/RpoB Hits
0.7
0.6
0.5
0.4
0.3
0.2
0.1
0
Sand
SW
FM8
FM16
FM20
GS1
GS2
GS3
GS7
GS9
GS12
FM Sand Rep. 1
FM Sand Rep. 2
FM Sand Rep. 3
GS-1 Sand Rep. 1
GS-2 Sand Rep. 1
GS-2 Sand Rep. 2
GS-2 Sand Rep. 3
FM SW Rep. 1
FM SW Rep. 2
FM SW Rep. 3
GS-1 SW Rep. 1
GS-2 SW Rep. 1
GS-2 SW Rep. 2
GS-2 SW Rep. 3

G.

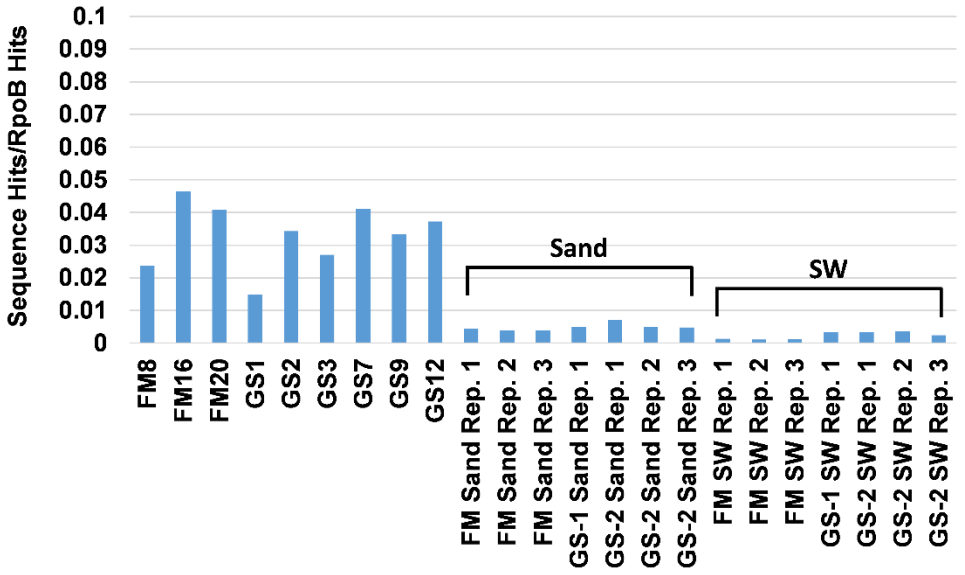
Sequence Hits/RpoB Hits
0.1
0.09
0.08
0.07
0.06
0.05
0.04
0.03
0.02
0.01
0
Sand
SW
FM8
FM16
FM20
GS1
GS2
GS3
GS7
GS9
GS12
FM Sand Rep. 1
FM Sand Rep. 2
FM Sand Rep. 3
GS-1 Sand Rep. 1
GS-2 Sand Rep. 1
GS-2 Sand Rep. 2
GS-2 Sand Rep. 3
FM SW Rep. 1
FM SW Rep. 2
FM SW Rep. 3
GS-1 SW Rep. 1
GS-2 SW Rep. 1
GS-2 SW Rep. 2
GS-2 SW Rep. 3

H.

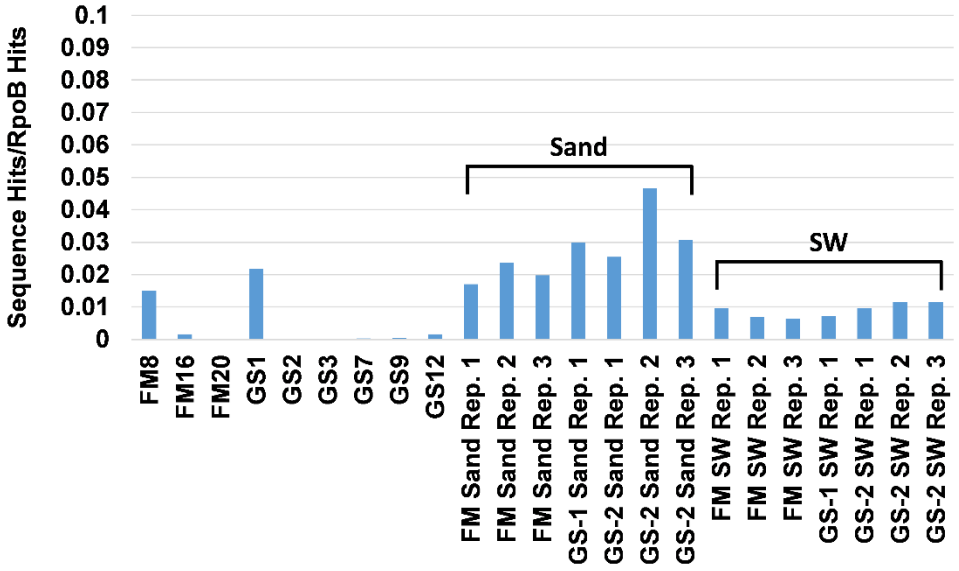
Sequence Hits/RpoB Hits
0.1
0.09
0.08
0.07
0.06
0.05
0.04
0.03
0.02
0.01
0
Sand
SW
FM8
FM16
FM20
GS1
GS2
GS3
GS7
GS9
GS12
FM Sand Rep. 1
FM Sand Rep. 2
FM Sand Rep. 3
GS-1 Sand Rep. 1
GS-2 Sand Rep. 1
GS-2 Sand Rep. 2
GS-2 Sand Rep. 3
FM SW Rep. 1
FM SW Rep. 2
FM SW Rep. 3
GS-1 SW Rep. 1
GS-2 SW Rep. 1
GS-2 SW Rep. 2
GS-2 SW Rep. 3

I.

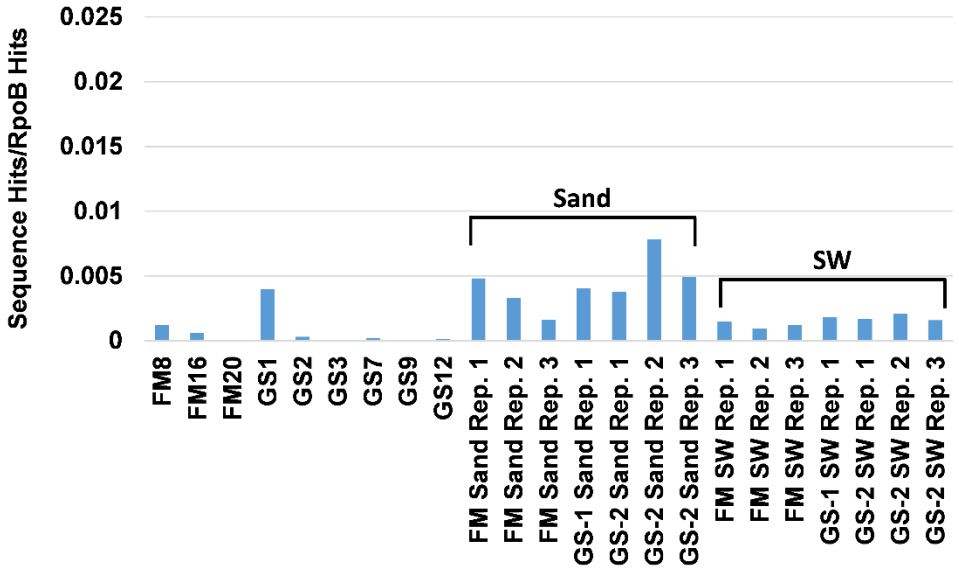
Sequence Hits/RpoB Hits
0.025
0.02
0.015
0.01
0.005
0
Sand
SW
FM8
FM16
FM20
GS1
GS2
GS3
GS7
GS9
GS12
FM Sand Rep. 1
FM Sand Rep. 2
FM Sand Rep. 3
GS-1 Sand Rep. 1
GS-2 Sand Rep. 1
GS-2 Sand Rep. 2
GS-2 Sand Rep. 3
FM SW Rep. 1
FM SW Rep. 2
FM SW Rep. 3
GS-1 SW Rep. 1
GS-2 SW Rep. 1
GS-2 SW Rep. 2
GS-2 SW Rep. 3

J.

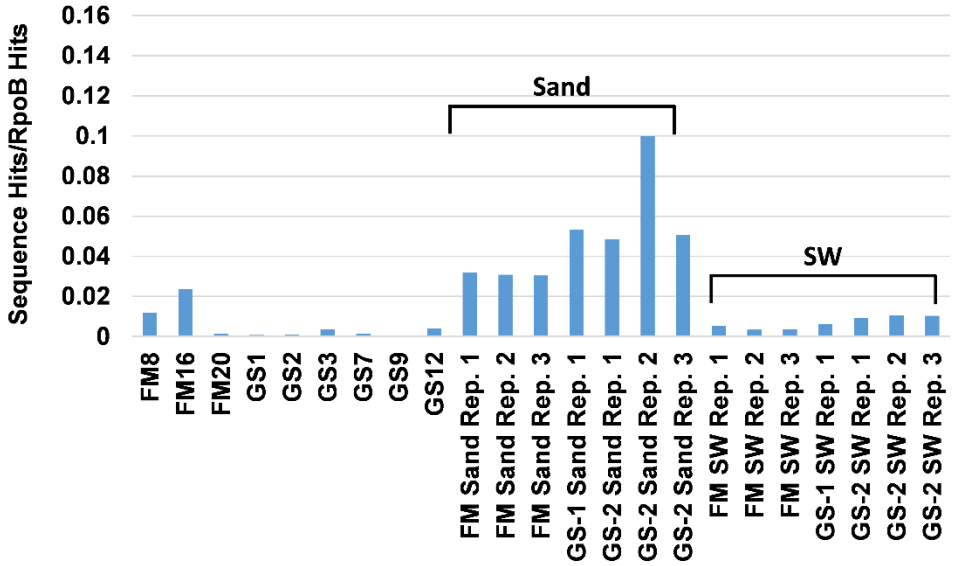
Sequence Hits/RpoB Hits
0.16
0.14
0.12
0.1
0.08
0.06
0.04
0.02
0
Sand
SW
FM8
FM16
FM20
GS1
GS2
GS3
GS7
GS9
GS12
FM Sand Rep. 1
FM Sand Rep. 2
FM Sand Rep. 3
GS-1 Sand Rep. 1
GS-2 Sand Rep. 1
GS-2 Sand Rep. 2
GS-2 Sand Rep. 3
FM SW Rep. 1
FM SW Rep. 2
FM SW Rep. 3
GS-1 SW Rep. 1
GS-2 SW Rep. 1
GS-2 SW Rep. 2
GS-2 SW Rep. 3

K.

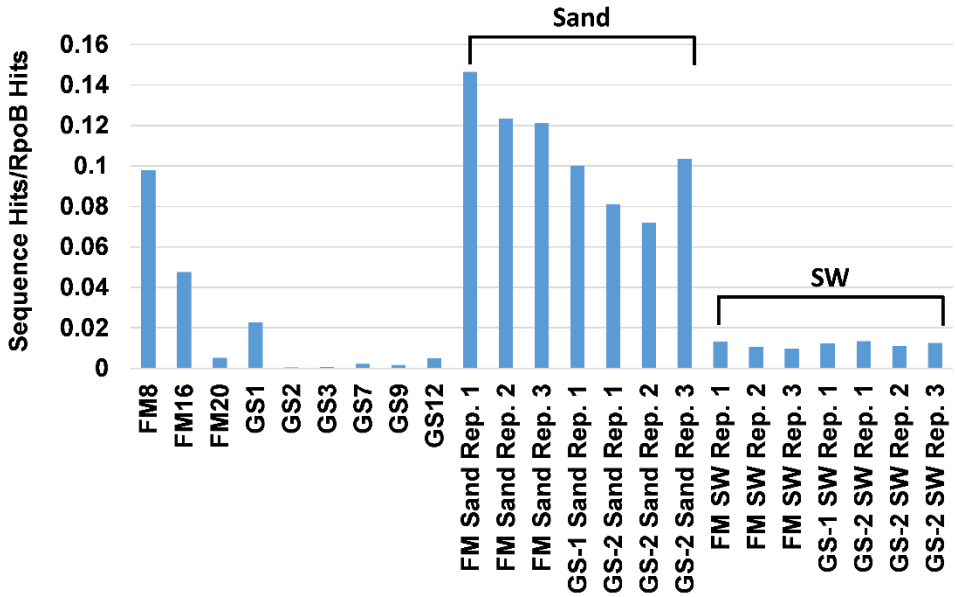
Sequence Hits/RpoB Hits
0.16
0.14
0.12
0.1
0.08
0.06
0.04
0.02
0
Sand
SW
FM8
FM16
FM20
GS1
GS2
GS3
GS7
GS9
GS12
FM Sand Rep. 1
FM Sand Rep. 2
FM Sand Rep. 3
GS-1 Sand Rep. 1
GS-2 Sand Rep. 1
GS-2 Sand Rep. 2
GS-2 Sand Rep. 3
FM SW Rep. 1
FM SW Rep. 2
FM SW Rep. 3
GS-1 SW Rep. 1
GS-2 SW Rep. 1
GS-2 SW Rep. 2
GS-2 SW Rep. 3

L.

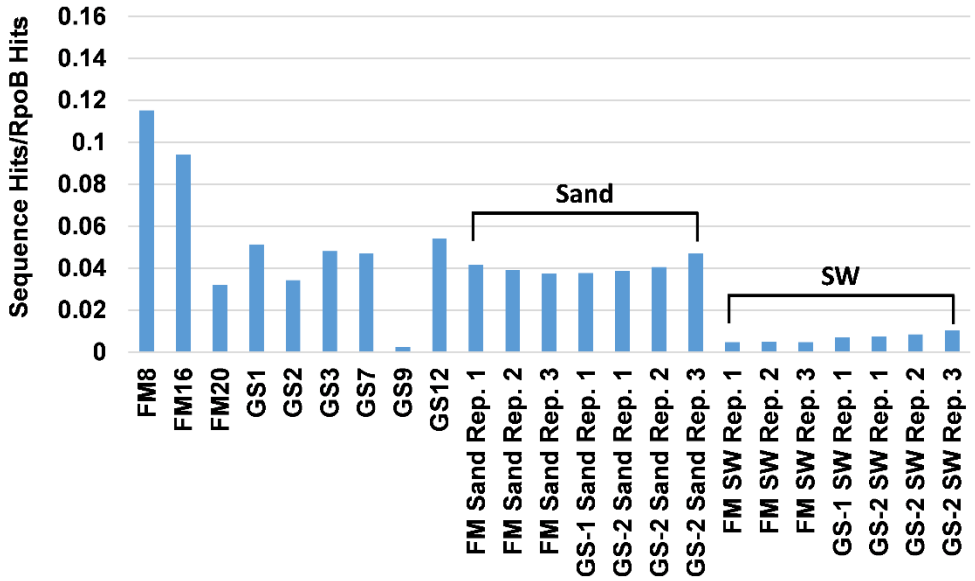
Sequence Hits/RpoB Hits
0.16
0.14
0.12
0.1
0.08
0.06
0.04
0.02
0
Sand
SW
FM8
FM16
FM20
GS1
GS2
GS3
GS7
GS9
GS12
FM Sand Rep. 1
FM Sand Rep. 2
FM Sand Rep. 3
GS-1 Sand Rep. 1
GS-2 Sand Rep. 1
GS-2 Sand Rep. 2
GS-2 Sand Rep. 3
FM SW Rep. 1
FM SW Rep. 2
FM SW Rep. 3
GS-1 SW Rep. 1
GS-2 SW Rep. 1
GS-2 SW Rep. 2
GS-2 SW Rep. 3

M.

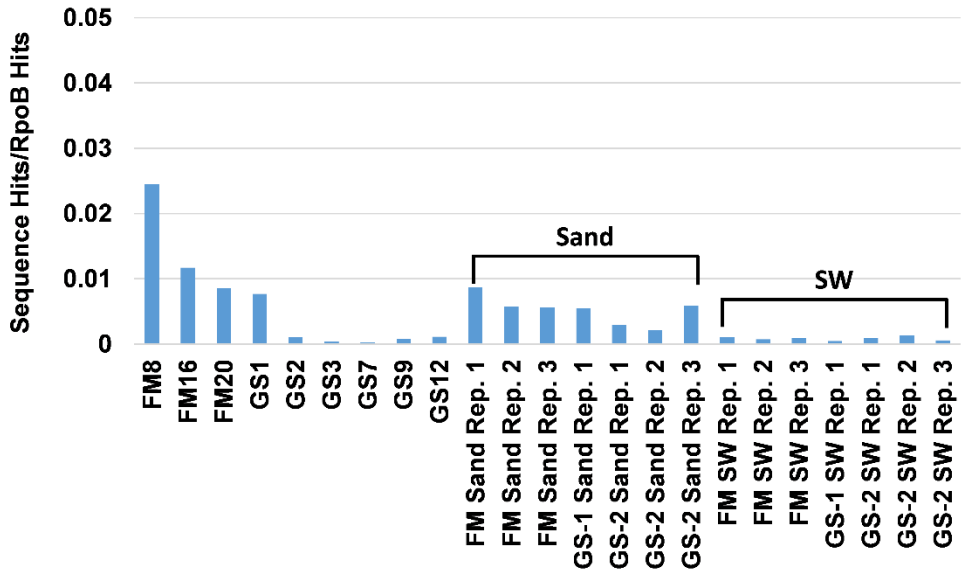
Sequence Hits/RpoB Hits
0.05
0.04
0.03
0.02
0.01
0
Sand
SW
FM8
FM16
FM20
GS1
GS2
GS3
GS7
GS9
GS12
FM Sand Rep. 1
FM Sand Rep. 2
FM Sand Rep. 3
GS-1 Sand Rep. 1
GS-2 Sand Rep. 1
GS-2 Sand Rep. 2
GS-2 Sand Rep. 3
FM SW Rep. 1
FM SW Rep. 2
FM SW Rep. 3
GS-1 SW Rep. 1
GS-2 SW Rep. 1
GS-2 SW Rep. 2
GS-2 SW Rep. 3

N.

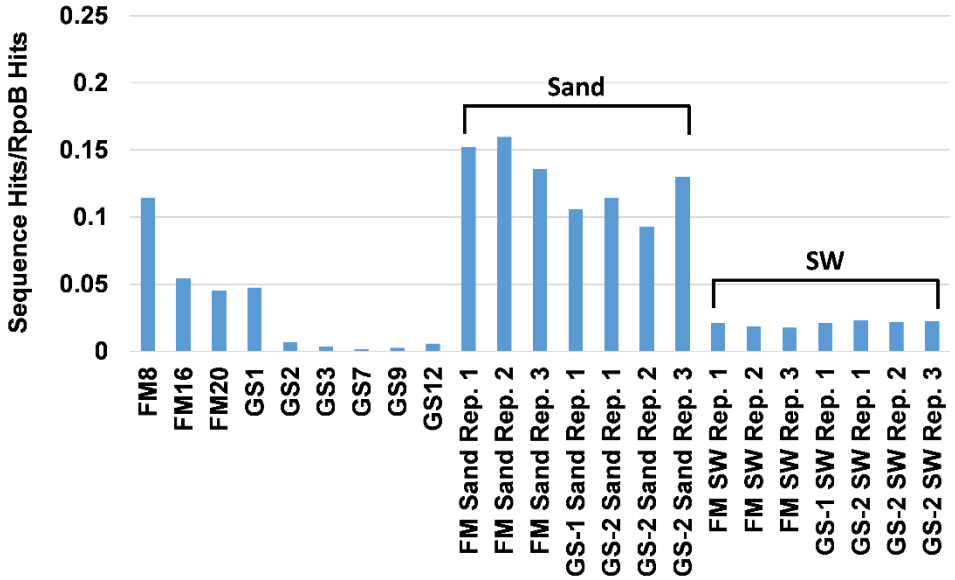
Sequence Hits/RpoB Hits
0.25
0.2
0.15
0.1
0.05
0
Sand
SW
FM8
FM16
FM20
GS1
GS2
GS3
GS7
GS9
GS12
FM Sand Rep. 1
FM Sand Rep. 2
FM Sand Rep. 3
GS-1 Sand Rep. 1
GS-2 Sand Rep. 1
GS-2 Sand Rep. 2
GS-2 Sand Rep. 3
FM SW Rep. 1
FM SW Rep. 2
FM SW Rep. 3
GS-1 SW Rep. 1
GS-2 SW Rep. 1
GS-2 SW Rep. 2
GS-2 SW Rep. 3

O.

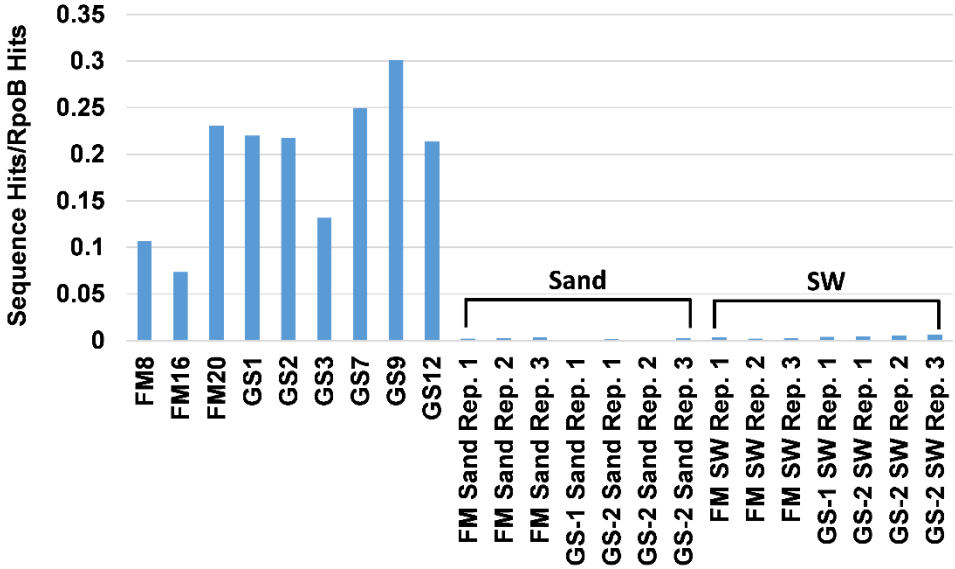
Sequence Hits/RpoB Hits
0.35
0.3
0.25
0.2
0.15
0.1
0.05
0
Sand
SW
FM8
FM16
FM20
GS1
GS2
GS3
GS7
GS9
GS12
FM Sand Rep. 1
FM Sand Rep. 2
FM Sand Rep. 3
GS-1 Sand Rep. 1
GS-2 Sand Rep. 1
GS-2 Sand Rep. 2
GS-2 Sand Rep. 3
FM SW Rep. 1
FM SW Rep. 2
FM SW Rep. 3
GS-1 SW Rep. 1
GS-2 SW Rep. 1
GS-2 SW Rep. 2
GS-2 SW Rep. 3

P.

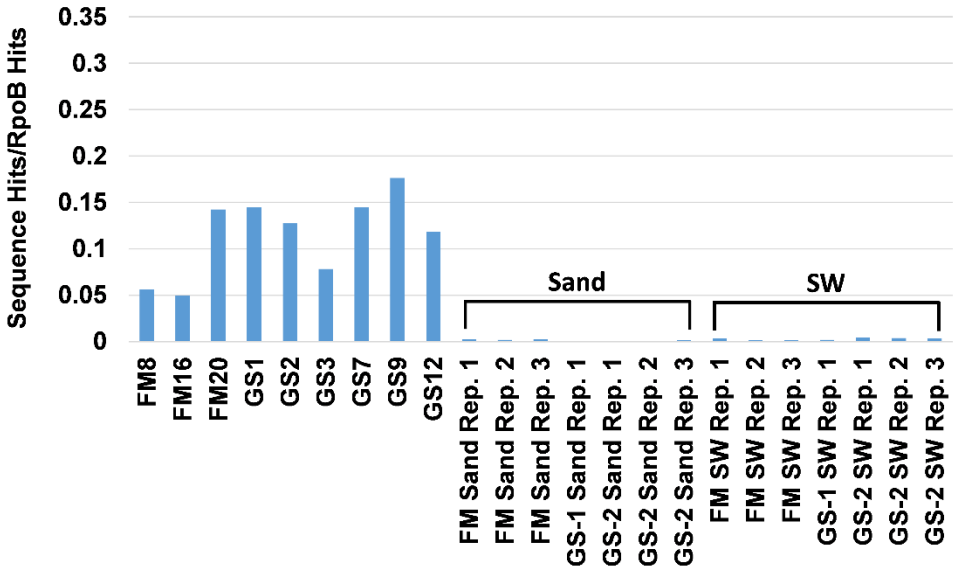
Sequence Hits/RpoB Hits
0.35
0.3
0.25
0.2
0.15
0.1
0.05
0
Sand
SW
FM8
FM16
FM20
GS1
GS2
GS3
GS7
GS9
GS12
FM Sand Rep. 1
FM Sand Rep. 2
FM Sand Rep. 3
GS-1 Sand Rep. 1
GS-2 Sand Rep. 1
GS-2 Sand Rep. 2
GS-2 Sand Rep. 3
FM SW Rep. 1
FM SW Rep. 2
FM SW Rep. 3
GS-1 SW Rep. 1
GS-2 SW Rep. 1
GS-2 SW Rep. 2
GS-2 SW Rep. 3

Q.

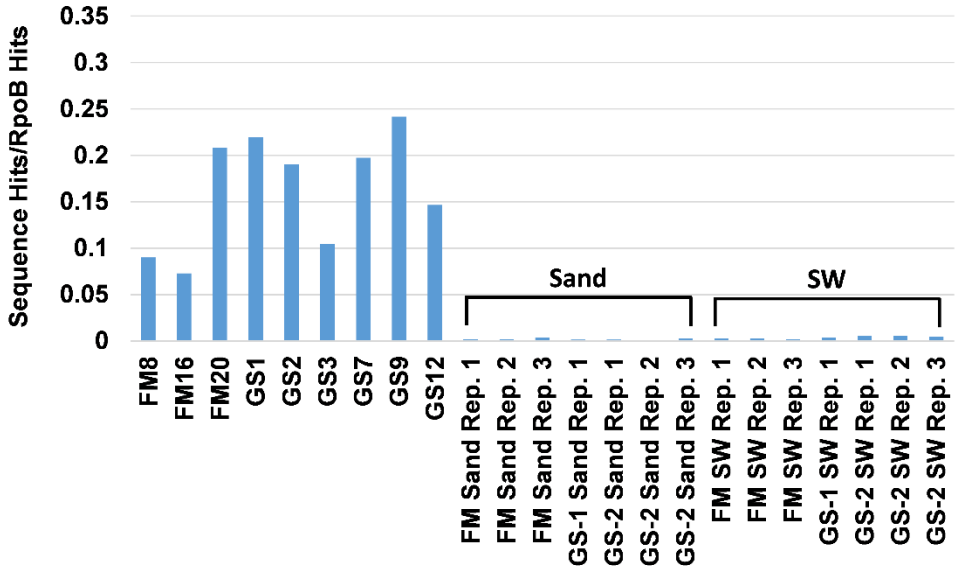
Sequence Hits/RpoB Hits
0.35
0.3
0.25
0.2
0.15
0.1
0.05
0
Sand
SW
FM8
FM16
FM20
GS1
GS2
GS3
GS7
GS9
GS12
FM Sand Rep. 1
FM Sand Rep. 2
FM Sand Rep. 3
GS-1 Sand Rep. 1
GS-2 Sand Rep. 1
GS-2 Sand Rep. 2
GS-2 Sand Rep. 3
FM SW Rep. 1
FM SW Rep. 2
FM SW Rep. 3
GS-1 SW Rep. 1
GS-2 SW Rep. 1
GS-2 SW Rep. 2
GS-2 SW Rep. 3

R.

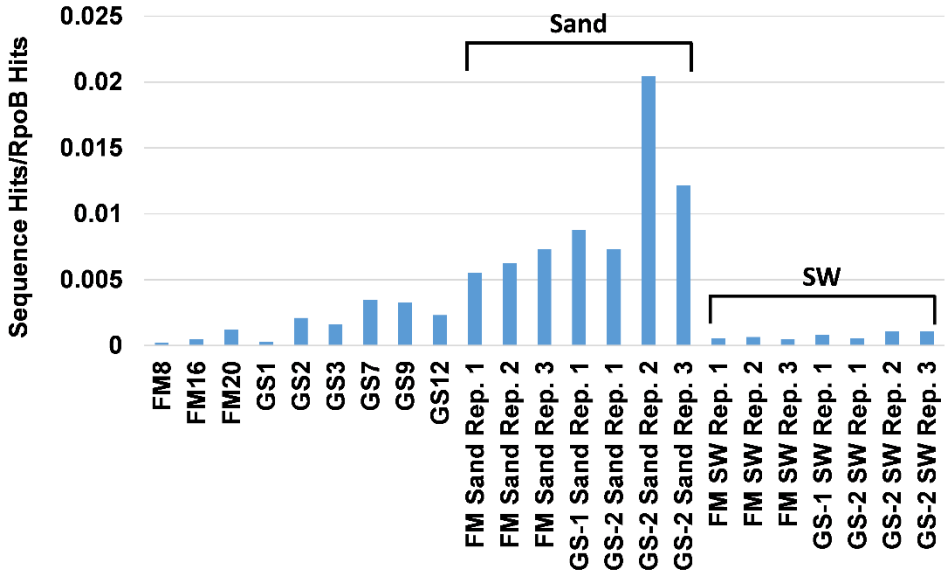
Sequence Hits/RpoB Hits
0.025
0.02
0.015
0.01
0.005
0
Sand
SW
FM8
FM16
FM20
GS1
GS2
GS3
GS7
GS9
GS12
FM Sand Rep. 1
FM Sand Rep. 2
FM Sand Rep. 3
GS-1 Sand Rep. 1
GS-2 Sand Rep. 1
GS-2 Sand Rep. 2
GS-2 Sand Rep. 3
FM SW Rep. 1
FM SW Rep. 2
FM SW Rep. 3
GS-1 SW Rep. 1
GS-2 SW Rep. 1
GS-2 SW Rep. 2
GS-2 SW Rep. 3

S.

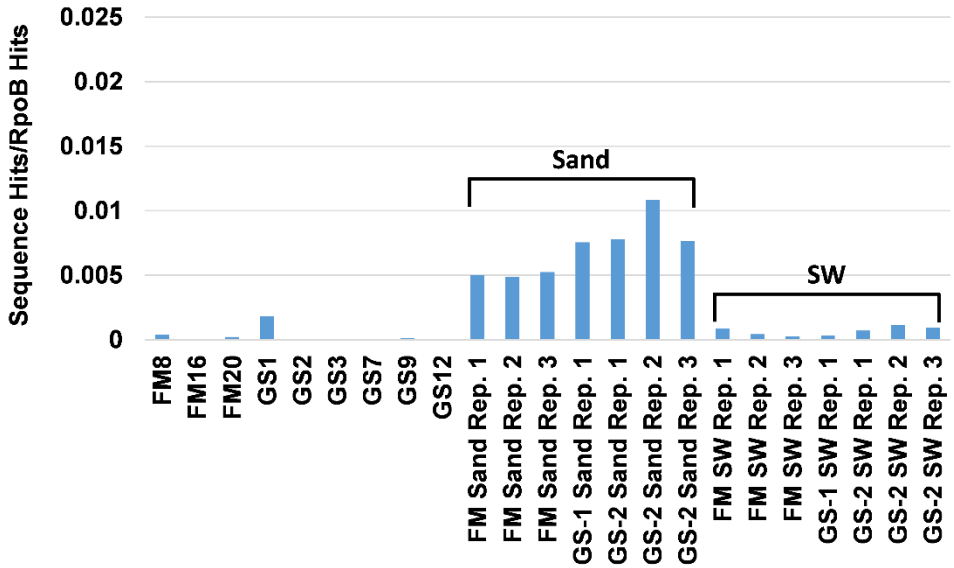
Sequence Hits/RpoB Hits
0.025
0.02
0.015
0.01
0.005
0
Sand
SW
FM8
FM16
FM20
GS1
GS2
GS3
GS7
GS9
GS12
FM Sand Rep. 1
FM Sand Rep. 2
FM Sand Rep. 3
GS-1 Sand Rep. 1
GS-2 Sand Rep. 1
GS-2 Sand Rep. 2
GS-2 Sand Rep. 3
FM SW Rep. 1
FM SW Rep. 2
FM SW Rep. 3
GS-1 SW Rep. 1
GS-2 SW Rep. 1
GS-2 SW Rep. 2
GS-2 SW Rep. 3

T.

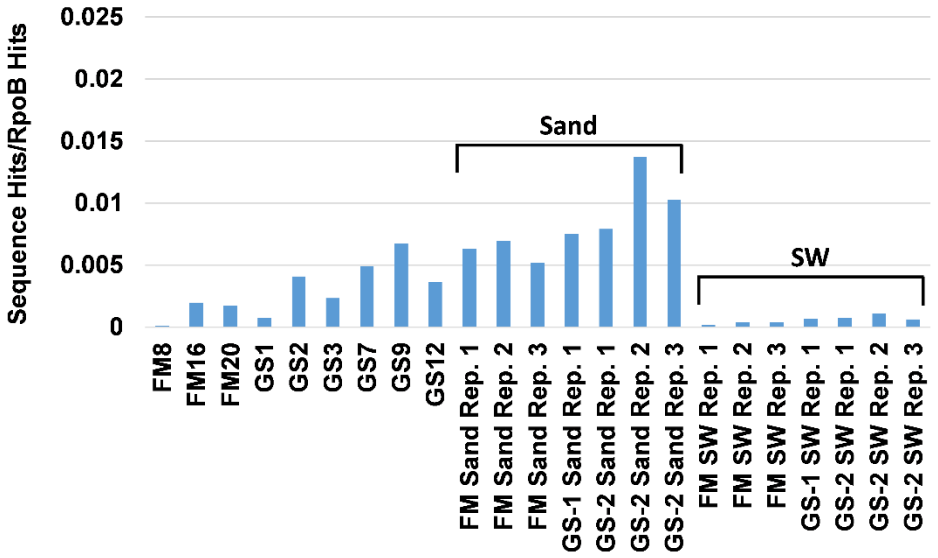
Sequence Hits/RpoB Hits
0.025
0.02
0.015
0.01
0.005
0
Sand
SW
FM8
FM16
FM20
GS1
GS2
GS3
GS7
GS9
GS12
FM Sand Rep. 1
FM Sand Rep. 2
FM Sand Rep. 3
GS-1 Sand Rep. 1
GS-2 Sand Rep. 1
GS-2 Sand Rep. 2
GS-2 Sand Rep. 3
FM SW Rep. 1
FM SW Rep. 2
FM SW Rep. 3
GS-1 SW Rep. 1
GS-2 SW Rep. 1
GS-2 SW Rep. 2
GS-2 SW Rep. 3

U.

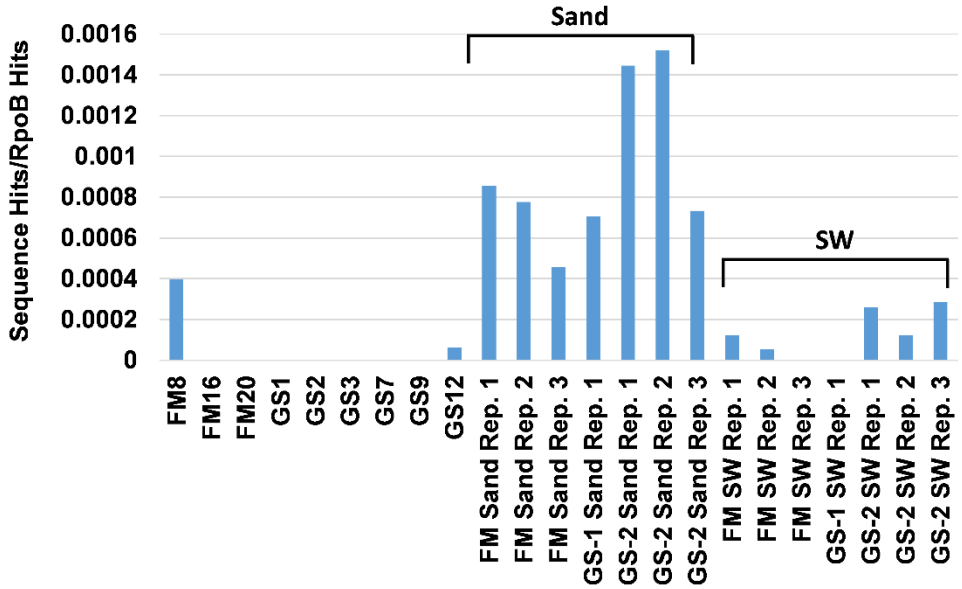
Sequence Hits/RpoB Hits
0.0016
0.0014
0.0012
0.001
0.0008
0.0006
0.0004
0.0002
0
Sand
SW
FM8
FM16
FM20
GS1
GS2
GS3
GS7
GS9
GS12
FM Sand Rep. 1
FM Sand Rep. 2
FM Sand Rep. 3
GS-1 Sand Rep. 1
GS-2 Sand Rep. 1
GS-2 Sand Rep. 2
GS-2 Sand Rep. 3
FM SW Rep. 1
FM SW Rep. 2
FM SW Rep. 3
GS-1 SW Rep. 1
GS-2 SW Rep. 1
GS-2 SW Rep. 2
GS-2 SW Rep. 3

Figure S6. Normalized ratios of functional gene markers associated with sulfur cycling processes. **(A)** Adenylylsulfate reductase subunit A, AprA, **(B)** adenylylsulfate reductase subunit B, AprB, **(C)** dissimilatory sulfite reductase subunit A, DsrA, **(D)** dissimilatory sulfite reductase subunit B, DsrB, **(E)** sulfur-oxidizing protein, SoxA, **(F)** sulfur-oxidizing protein, SoxB, **(G)** sulfane dehydrogenase subunit, SoxC, **(H)** cytochrome C, SoxD, **(I)** sulfur-oxidizing protein, SoxX, **(J)** sulfur-oxidizing protein, SoxY, **(K)** sulfur-oxidizing protein, SoxZ, **(L)** thiosulfate dehydrogenase large subunit, DoxD, **(M)** sulfide dehydrogenase cytochrome subunit, FccA, **(N)** sulfide dehydrogenase flavoprotein chain, FccB, **(O)** sulfur oxygenase/reductase, Sor, and **(P)** sulfide:quinone oxidoreductase, Sqr. Sequence hits normalized to either prokaryotic or bacterial RpoB hits based on whether genes have been previously detected in both Archaea and Bacteria or only in Bacteria.

A.

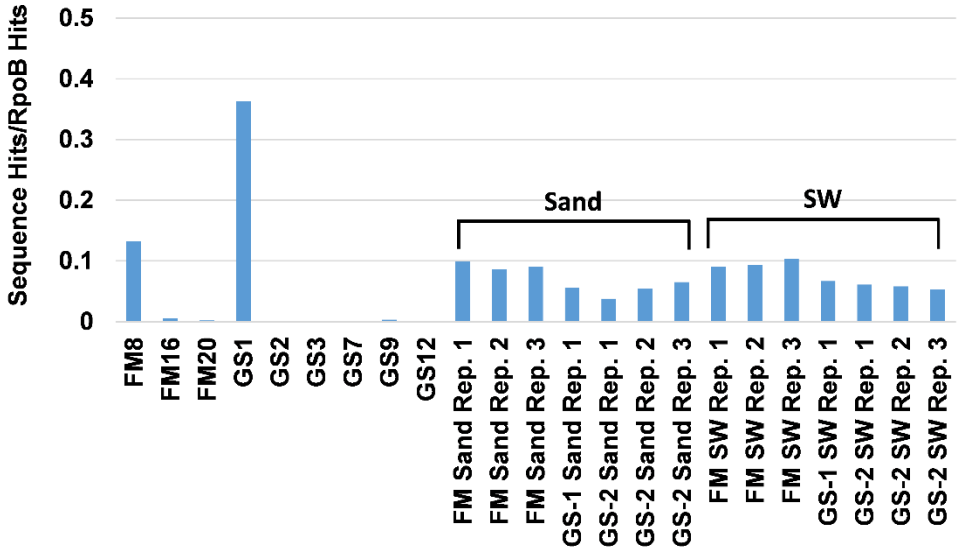

B.

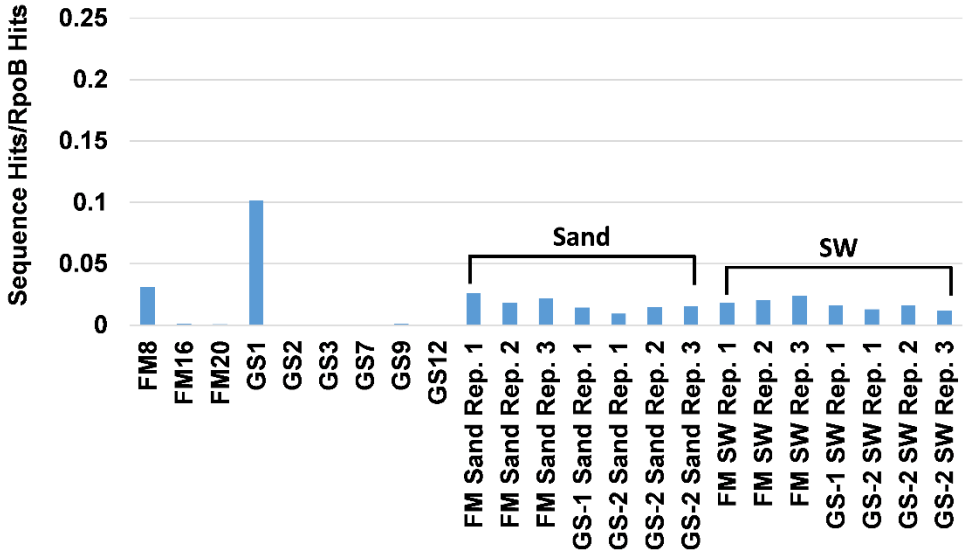
Sequence Hits/RpoB Hits
0.25
0.2
0.15
0.1
0.05
0
Sand
SW
FM8
FM16
FM20
GS1
GS2
GS3
GS7
GS9
GS12
FM Sand Rep. 1
FM Sand Rep. 2
FM Sand Rep. 3
GS-1 Sand Rep. 1
GS-2 Sand Rep. 1
GS-2 Sand Rep. 2
GS-2 Sand Rep. 3
FM SW Rep. 1
FM SW Rep. 2
FM SW Rep. 3
GS-1 SW Rep. 1
GS-2 SW Rep. 1
GS-2 SW Rep. 2
GS-2 SW Rep. 3

C.

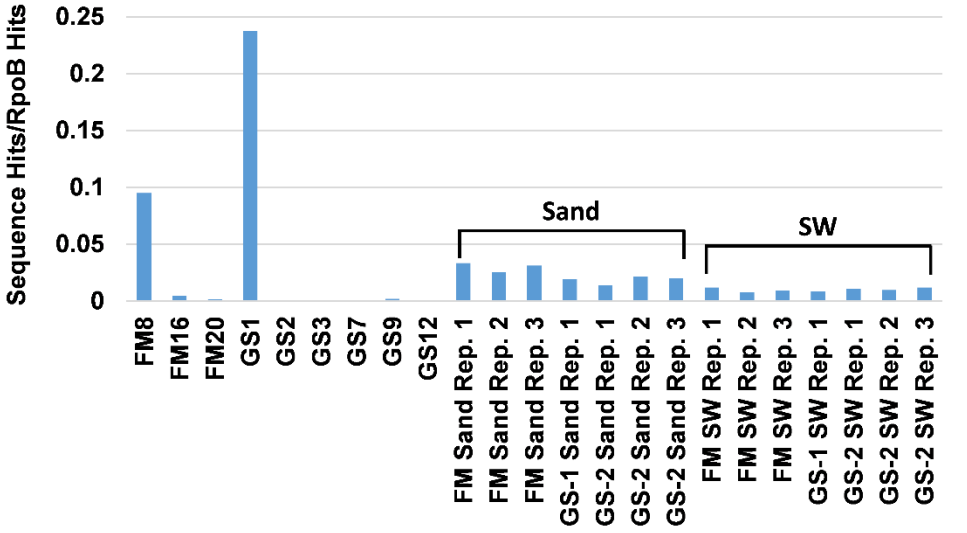
Sequence Hits/RpoB Hits
0.25
0.2
0.15
0.1
0.05
0
Sand
SW
FM8
FM16
FM20
GS1
GS2
GS3
GS7
GS9
GS12
FM Sand Rep. 1
FM Sand Rep. 2
FM Sand Rep. 3
GS-1 Sand Rep. 1
GS-2 Sand Rep. 1
GS-2 Sand Rep. 2
GS-2 Sand Rep. 3
FM SW Rep. 1
FM SW Rep. 2
FM SW Rep. 3
GS-1 SW Rep. 1
GS-2 SW Rep. 1
GS-2 SW Rep. 2
GS-2 SW Rep. 3

D.

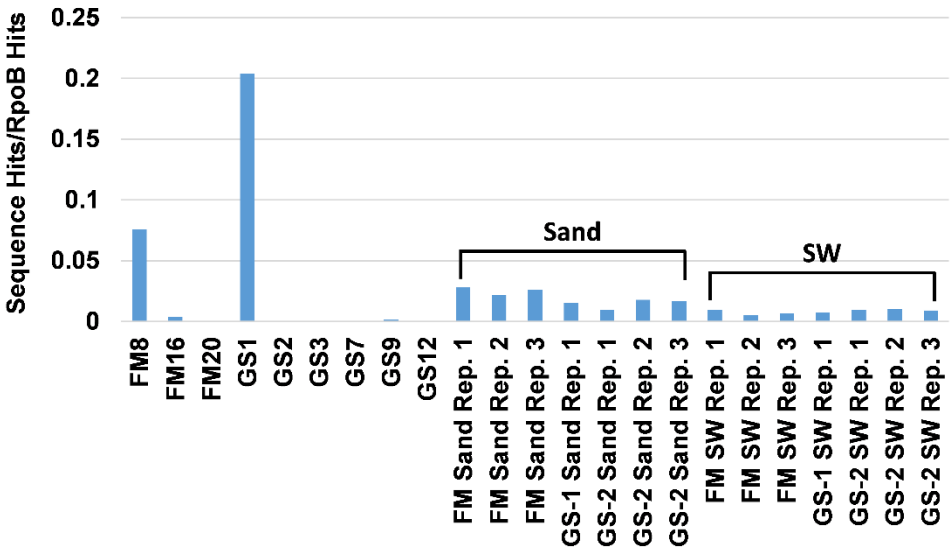
Sequence Hits/RpoB Hits
0.25
0.2
0.15
0.1
0.05
0
Sand
SW
FM8
FM16
FM20
GS1
GS2
GS3
GS7
GS9
GS12
FM Sand Rep. 1
FM Sand Rep. 2
FM Sand Rep. 3
GS-1 Sand Rep. 1
GS-2 Sand Rep. 1
GS-2 Sand Rep. 2
GS-2 Sand Rep. 3
FM SW Rep. 1
FM SW Rep. 2
FM SW Rep. 3
GS-1 SW Rep. 1
GS-2 SW Rep. 1
GS-2 SW Rep. 2
GS-2 SW Rep. 3

E.

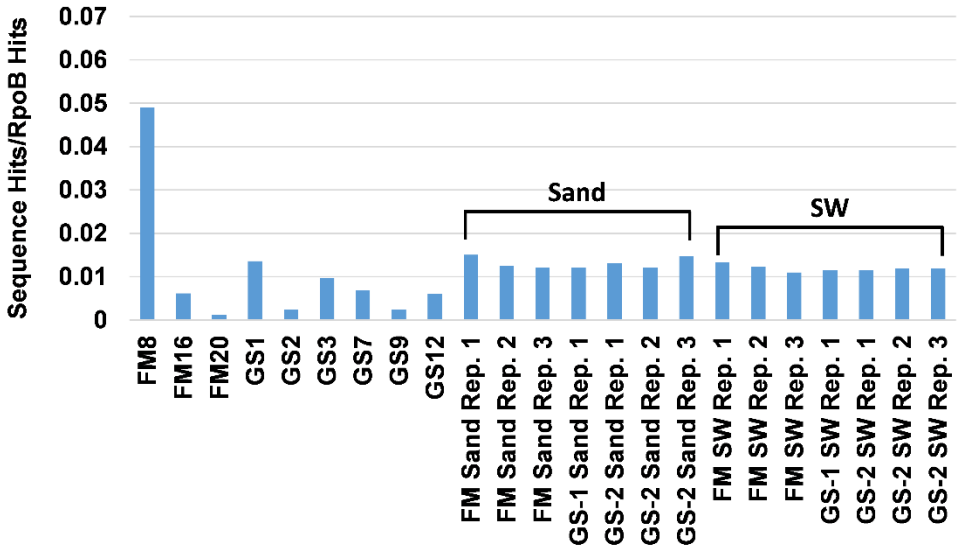
Sequence Hits/RpoB Hits
0.07
0.06
0.05
0.04
0.03
0.02
0.01
0
Sand
SW
FM8
FM16
FM20
GS1
GS2
GS3
GS7
GS9
GS12
FM Sand Rep. 1
FM Sand Rep. 2
FM Sand Rep. 3
GS-1 Sand Rep. 1
GS-2 Sand Rep. 1
GS-2 Sand Rep. 2
GS-2 Sand Rep. 3
FM SW Rep. 1
FM SW Rep. 2
FM SW Rep. 3
GS-1 SW Rep. 1
GS-2 SW Rep. 1
GS-2 SW Rep. 2
GS-2 SW Rep. 3

F.

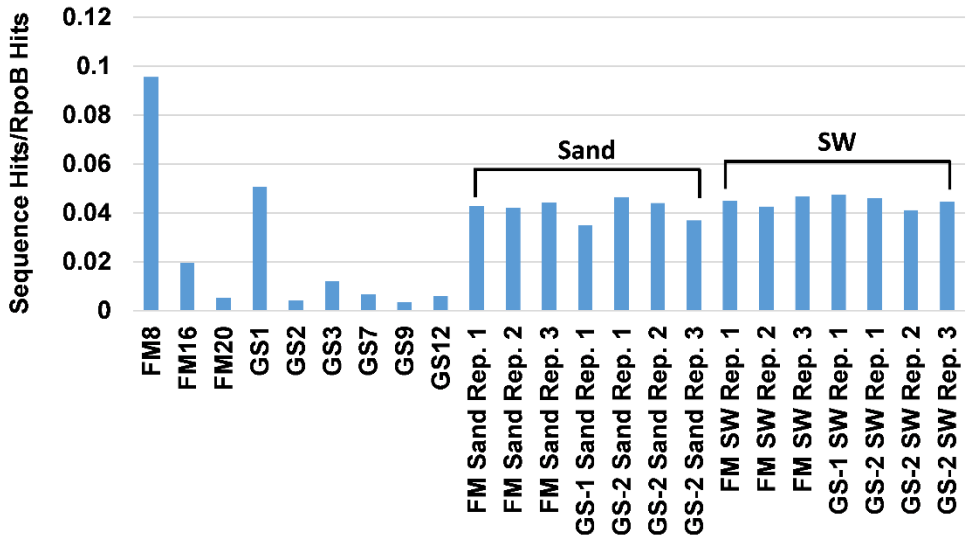
Sequence Hits/RpoB Hits
0.12
0.1
0.08
0.06
0.04
0.02
0
Sand
SW
FM8
FM16
FM20
GS1
GS2
GS3
GS7
GS9
GS12
FM Sand Rep. 1
FM Sand Rep. 2
FM Sand Rep. 3
GS-1 Sand Rep. 1
GS-2 Sand Rep. 1
GS-2 Sand Rep. 2
GS-2 Sand Rep. 3
FM SW Rep. 1
FM SW Rep. 2
FM SW Rep. 3
GS-1 SW Rep. 1
GS-2 SW Rep. 1
GS-2 SW Rep. 2
GS-2 SW Rep. 3

G.

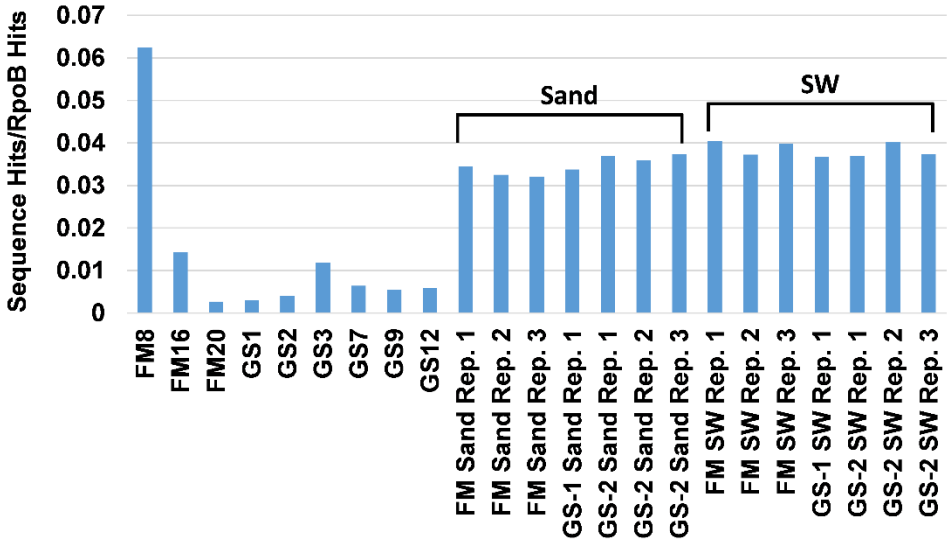
Sequence Hits/RpoB Hits
0.07
0.06
0.05
0.04
0.03
0.02
0.01
0
Sand
SW
FM8
FM16
FM20
GS1
GS2
GS3
GS7
GS9
GS12
FM Sand Rep. 1
FM Sand Rep. 2
FM Sand Rep. 3
GS-1 Sand Rep. 1
GS-2 Sand Rep. 1
GS-2 Sand Rep. 2
GS-2 Sand Rep. 3
FM SW Rep. 1
FM SW Rep. 2
FM SW Rep. 3
GS-1 SW Rep. 1
GS-2 SW Rep. 1
GS-2 SW Rep. 2
GS-2 SW Rep. 3

H.

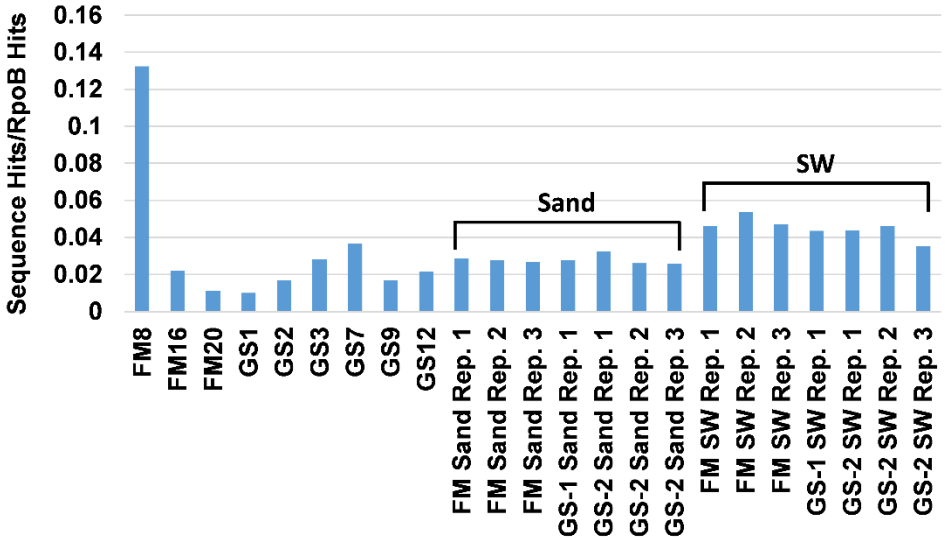
Sequence Hits/RpoB Hits
0.16
0.14
0.12
0.1
0.08
0.06
0.04
0.02
0
Sand
SW
FM8
FM16
FM20
GS1
GS2
GS3
GS7
GS9
GS12
FM Sand Rep. 1
FM Sand Rep. 2
FM Sand Rep. 3
GS-1 Sand Rep. 1
GS-2 Sand Rep. 1
GS-2 Sand Rep. 2
GS-2 Sand Rep. 3
FM SW Rep. 1
FM SW Rep. 2
FM SW Rep. 3
GS-1 SW Rep. 1
GS-2 SW Rep. 1
GS-2 SW Rep. 2
GS-2 SW Rep. 3

I.

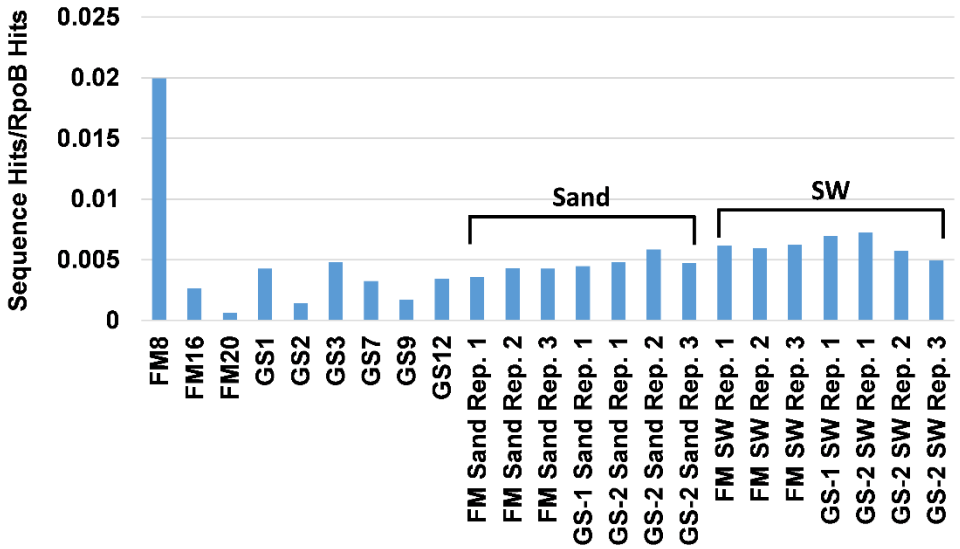
Sequence Hits/RpoB Hits
0.025
0.02
0.015
0.01
0.005
0
Sand
SW
FM8
FM16
FM20
GS1
GS2
GS3
GS7
GS9
GS12
FM Sand Rep. 1
FM Sand Rep. 2
FM Sand Rep. 3
GS-1 Sand Rep. 1
GS-2 Sand Rep. 1
GS-2 Sand Rep. 2
GS-2 Sand Rep. 3
FM SW Rep. 1
FM SW Rep. 2
FM SW Rep. 3
GS-1 SW Rep. 1
GS-2 SW Rep. 1
GS-2 SW Rep. 2
GS-2 SW Rep. 3

J.

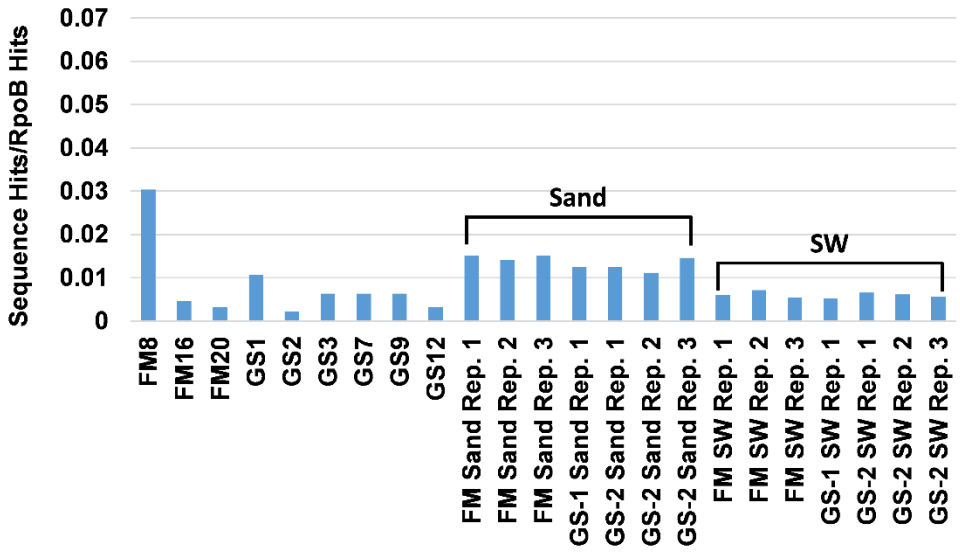
Sequence Hits/RpoB Hits
0.07
0.06
0.05
0.04
0.03
0.02
0.01
0
Sand
SW
FM8
FM16
FM20
GS1
GS2
GS3
GS7
GS9
GS12
FM Sand Rep. 1
FM Sand Rep. 2
FM Sand Rep. 3
GS-1 Sand Rep. 1
GS-2 Sand Rep. 1
GS-2 Sand Rep. 2
GS-2 Sand Rep. 3
FM SW Rep. 1
FM SW Rep. 2
FM SW Rep. 3
GS-1 SW Rep. 1
GS-2 SW Rep. 1
GS-2 SW Rep. 2
GS-2 SW Rep. 3

K.

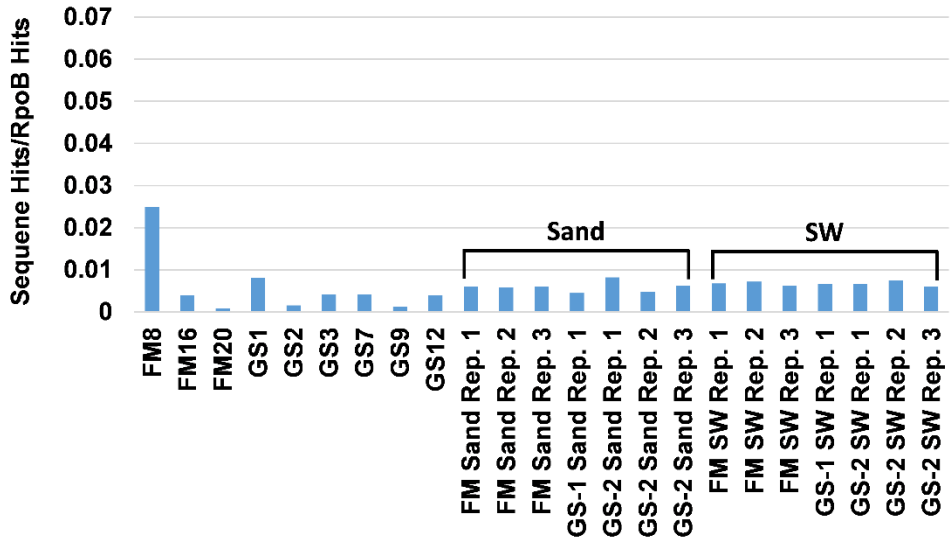
Sequene Hits/RpoB Hits
0.07
0.06
0.05
0.04
0.03
0.02
0.01
0
Sand
SW
FM8
FM16
FM20
GS1
GS2
GS3
GS7
GS9
GS12
FM Sand Rep. 1
FM Sand Rep. 2
FM Sand Rep. 3
GS-1 Sand Rep. 1
GS-2 Sand Rep. 1
GS-2 Sand Rep. 2
GS-2 Sand Rep. 3
FM SW Rep. 1
FM SW Rep. 2
FM SW Rep. 3
GS-1 SW Rep. 1
GS-2 SW Rep. 1
GS-2 SW Rep. 2
GS-2 SW Rep. 3

L.

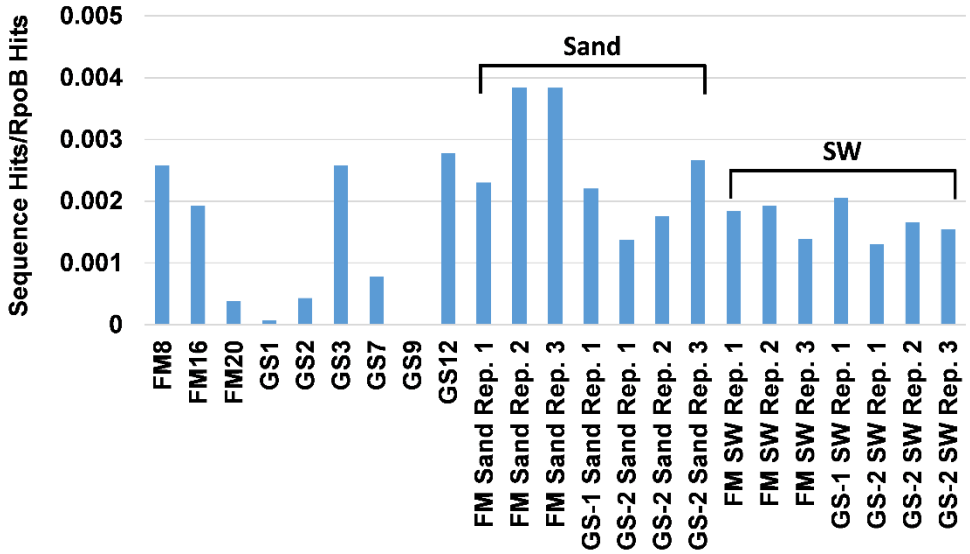
Sequence Hits/RpoB Hits
0.005
0.004
0.003
0.002
0.001
0
Sand
SW
FM8
FM16
FM20
GS1
GS2
GS3
GS7
GS9
GS12
FM Sand Rep. 1
FM Sand Rep. 2
FM Sand Rep. 3
GS-1 Sand Rep. 1
GS-2 Sand Rep. 1
GS-2 Sand Rep. 2
GS-2 Sand Rep. 3
FM SW Rep. 1
FM SW Rep. 2
FM SW Rep. 3
GS-1 SW Rep. 1
GS-2 SW Rep. 1
GS-2 SW Rep. 2
GS-2 SW Rep. 3

M.

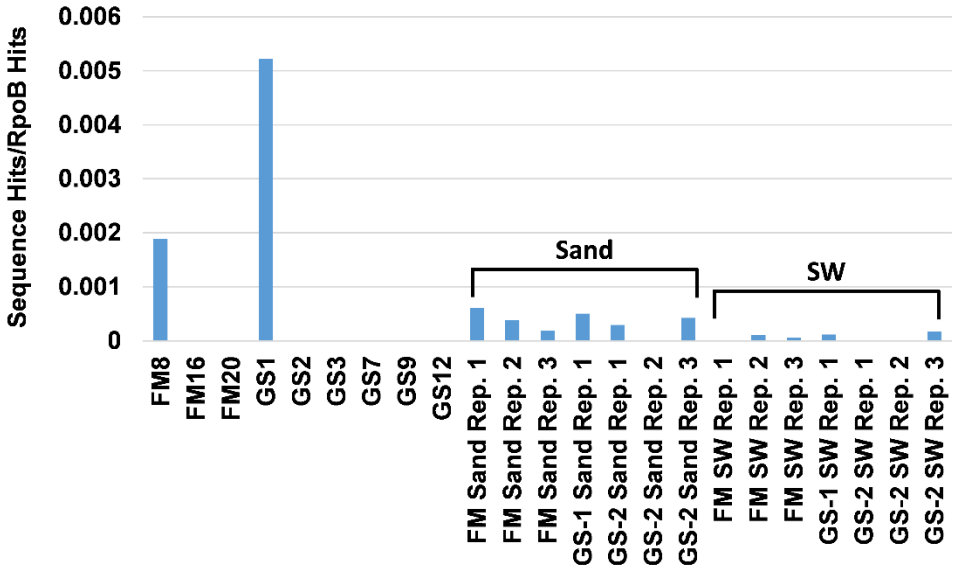
Sequence Hits/RpoB Hits
0.006
0.005
0.004
0.003
0.002
0.001
0
Sand
SW
FM8
FM16
FM20
GS1
GS2
GS3
GS7
GS9
GS12
FM Sand Rep. 1
FM Sand Rep. 2
FM Sand Rep. 3
GS-1 Sand Rep. 1
GS-2 Sand Rep. 1
GS-2 Sand Rep. 2
GS-2 Sand Rep. 3
FM SW Rep. 1
FM SW Rep. 2
FM SW Rep. 3
GS-1 SW Rep. 1
GS-2 SW Rep. 1
GS-2 SW Rep. 2
GS-2 SW Rep. 3

N.

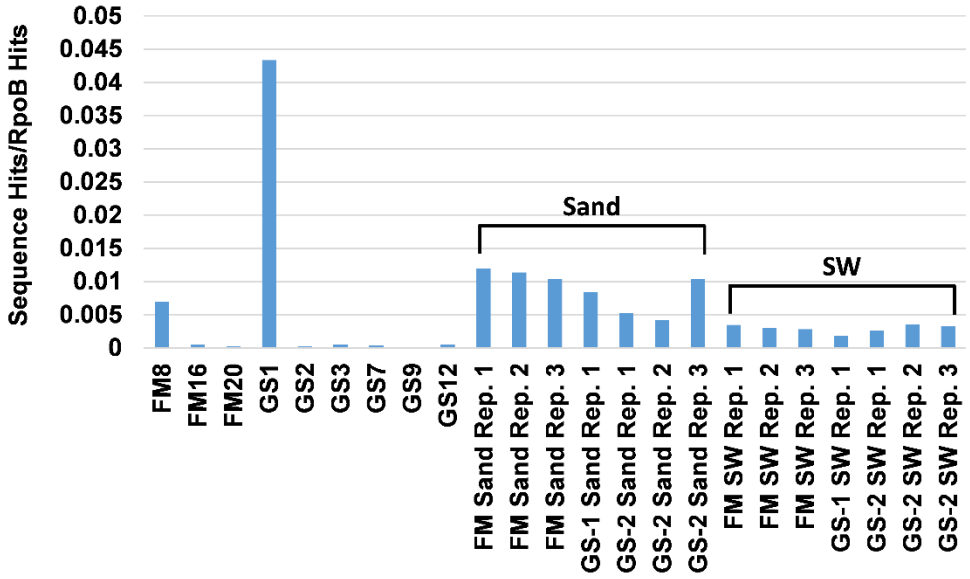
Sequence Hits/RpoB Hits
0.05
0.045
0.04
0.035
0.03
0.025
0.02
0.015
0.01
0.005
0
Sand
SW
FM8
FM16
FM20
GS1
GS2
GS3
GS7
GS9
GS12
FM Sand Rep. 1
FM Sand Rep. 2
FM Sand Rep. 3
GS-1 Sand Rep. 1
GS-2 Sand Rep. 1
GS-2 Sand Rep. 2
GS-2 Sand Rep. 3
FM SW Rep. 1
FM SW Rep. 2
FM SW Rep. 3
GS-1 SW Rep. 1
GS-2 SW Rep. 1
GS-2 SW Rep. 2
GS-2 SW Rep. 3

O.

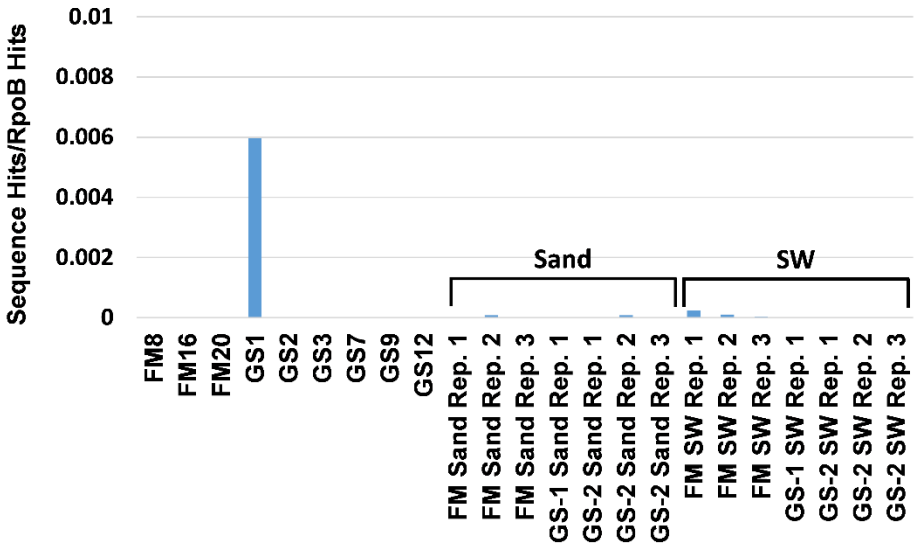
Sequence Hits/RpoB Hits
0.01
0.008
0.006
0.004
0.002
0
Sand
SW
FM8
FM16
FM20
GS1
GS2
GS3
GS7
GS9
GS12
FM Sand Rep. 1
FM Sand Rep. 2
FM Sand Rep. 3
GS-1 Sand Rep. 1
GS-2 Sand Rep. 1
GS-2 Sand Rep. 2
GS-2 Sand Rep. 3
FM SW Rep. 1
FM SW Rep. 2
FM SW Rep. 3
GS-1 SW Rep. 1
GS-2 SW Rep. 1
GS-2 SW Rep. 2
GS-2 SW Rep. 3

P.

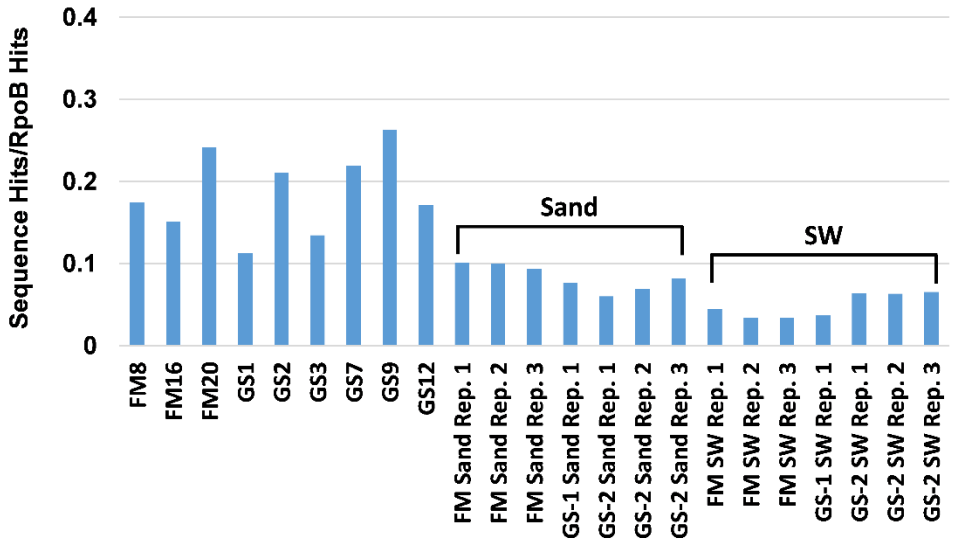
Sequence Hits/RpoB Hits
0.4
0.3
0.2
0.1
0
Sand
SW
FM8
FM16
FM20
GS1
GS2
GS3
GS7
GS9
GS12
FM Sand Rep. 1
FM Sand Rep. 2
FM Sand Rep. 3
GS-1 Sand Rep. 1
GS-2 Sand Rep. 1
GS-2 Sand Rep. 2
GS-2 Sand Rep. 3
FM SW Rep. 1
FM SW Rep. 2
FM SW Rep. 3
GS-1 SW Rep. 1
GS-2 SW Rep. 1
GS-2 SW Rep. 2
GS-2 SW Rep. 3

Figure S7. Normalized ratios of functional gene markers associated with methanogenesis. **(A)** Heterodisulfide reductase subunit A, HdrA, **(B)** heterodisulfide reductase subunit B, HdrB, **(C)** heterodisulfide reductase subunit C, HdrC, **(D)** methyl-coenzyme M reductase subunit alpha, McrA, **(E)** methyl-coenzyme M reductase subunit beta, McrB, and **(F)** methyl-coenzyme M reductase subunit gamma, McrG. Sequence hits normalized to archaeal RpoB hits.

A.

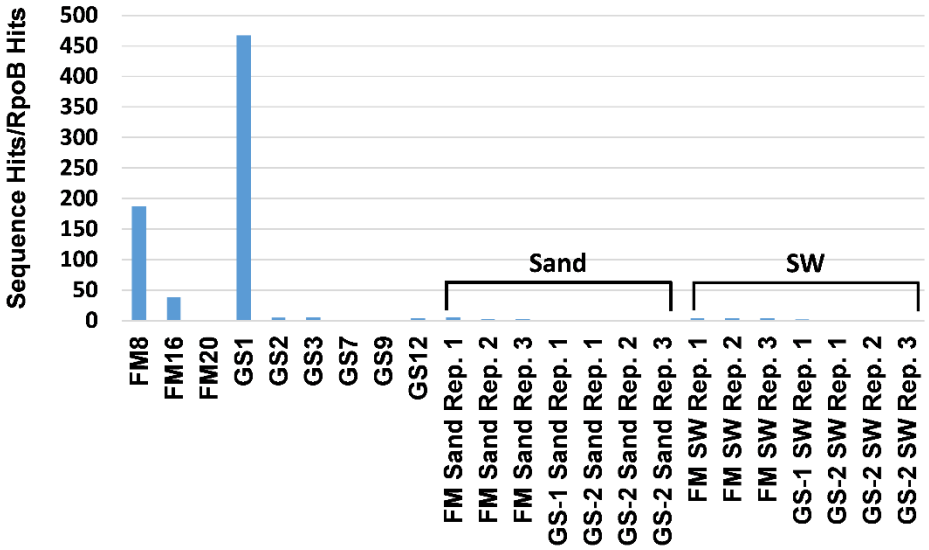

B.

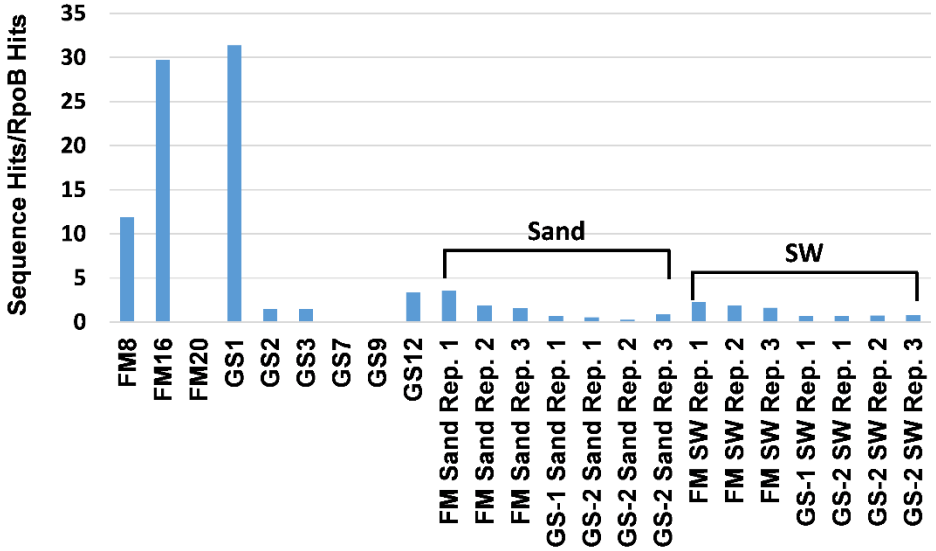

C.

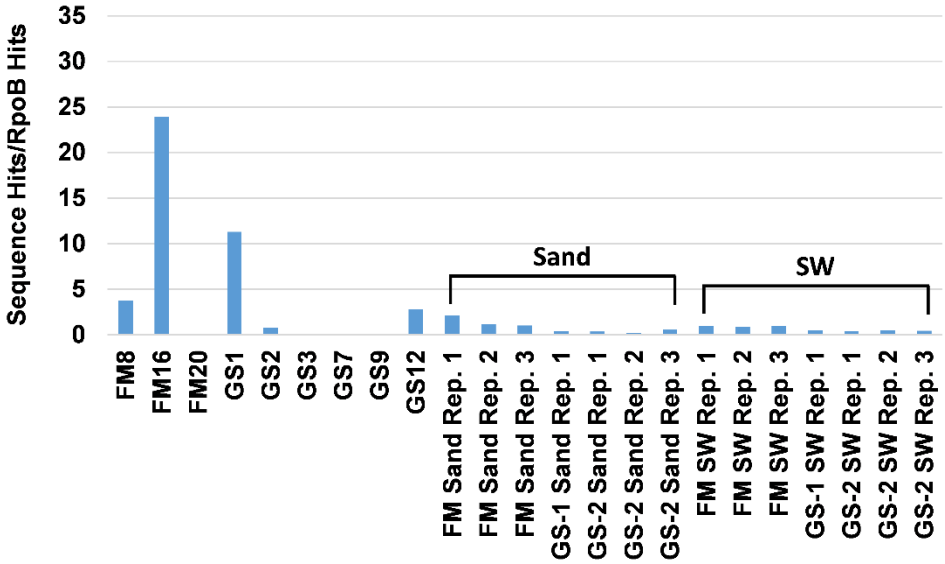
Sequence Hits/RpoB Hits
35
30
25
20
15
10
5
0
Sand
SW
FM8
FM16
FM20
GS1
GS2
GS3
GS7
GS9
GS12
FM Sand Rep. 1
FM Sand Rep. 2
FM Sand Rep. 3
GS-1 Sand Rep. 1
GS-2 Sand Rep. 1
GS-2 Sand Rep. 2
GS-2 Sand Rep. 3
FM SW Rep. 1
FM SW Rep. 2
FM SW Rep. 3
GS-1 SW Rep. 1
GS-2 SW Rep. 1
GS-2 SW Rep. 2
GS-2 SW Rep. 3

D.

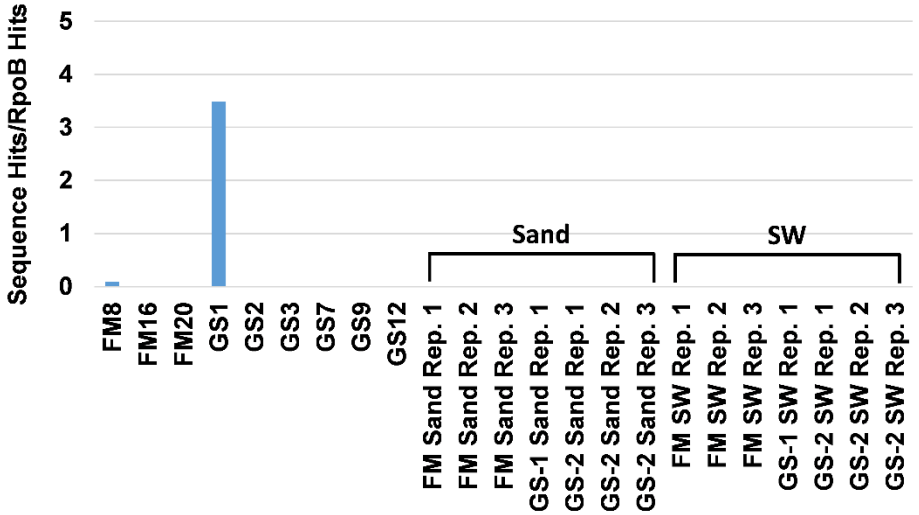
Sequence Hits/RpoB Hits
5
4
3
2
1
0
Sand
SW
FM8
FM16
FM20
GS1
GS2
GS3
GS7
GS9
GS12
FM Sand Rep. 1
FM Sand Rep. 2
FM Sand Rep. 3
GS-1 Sand Rep. 1
GS-2 Sand Rep. 1
GS-2 Sand Rep. 2
GS-2 Sand Rep. 3
FM SW Rep. 1
FM SW Rep. 2
FM SW Rep. 3
GS-1 SW Rep. 1
GS-2 SW Rep. 1
GS-2 SW Rep. 2
GS-2 SW Rep. 3

E.

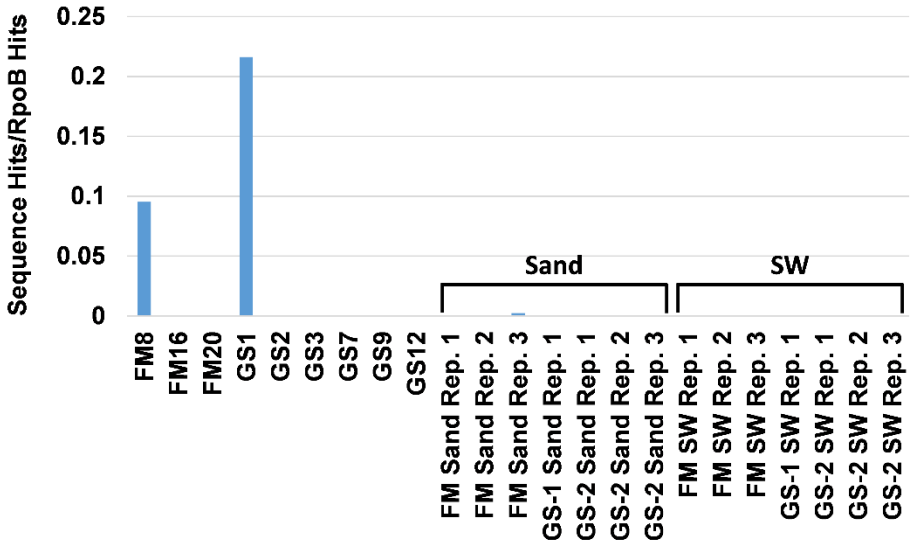
Sequence Hits/RpoB Hits
0.25
0.2
0.15
0.1
0.05
0
Sand
SW
FM8
FM16
FM20
GS1
GS2
GS3
GS7
GS9
GS12
FM Sand Rep. 1
FM Sand Rep. 2
FM Sand Rep. 3
GS-1 Sand Rep. 1
GS-2 Sand Rep. 1
GS-2 Sand Rep. 2
GS-2 Sand Rep. 3
FM SW Rep. 1
FM SW Rep. 2
FM SW Rep. 3
GS-1 SW Rep. 1
GS-2 SW Rep. 1
GS-2 SW Rep. 2
GS-2 SW Rep. 3

F.

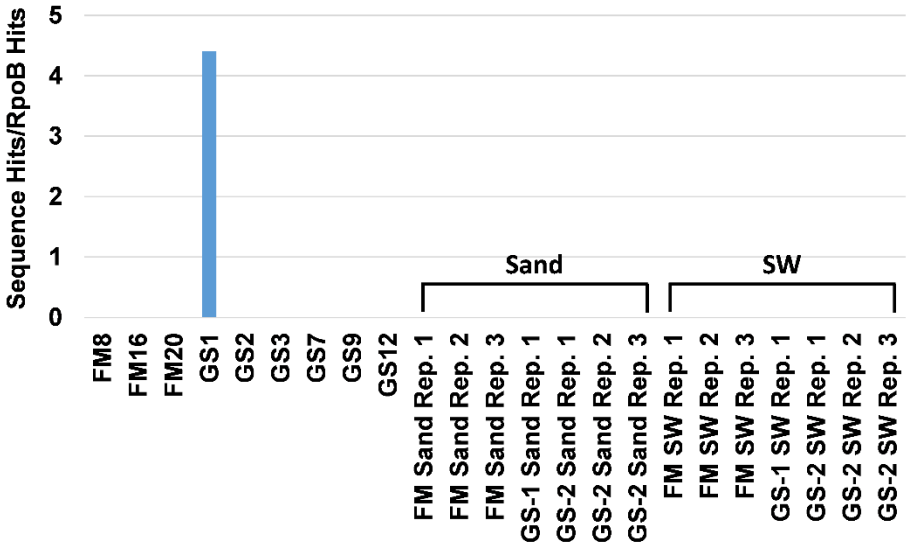
Sequence Hits/RpoB Hits
5
4
3
2
1
0
Sand
SW
FM8
FM16
FM20
GS1
GS2
GS3
GS7
GS9
GS12
FM Sand Rep. 1
FM Sand Rep. 2
FM Sand Rep. 3
GS-1 Sand Rep. 1
GS-2 Sand Rep. 1
GS-2 Sand Rep. 2
GS-2 Sand Rep. 3
FM SW Rep. 1
FM SW Rep. 2
FM SW Rep. 3
GS-1 SW Rep. 1
GS-2 SW Rep. 1
GS-2 SW Rep. 2
GS-2 SW Rep. 3

Figure S8. Normalized ratios of functional gene markers associated with carbon fixation. **(A)** Carbon-monoxide dehydrogenase iron sulfur subunit, CooF, **(B)** carbon-monoxide dehydrogenase catalytic subunit, CooS, and **(C)** ribulose-bisphosphate carboxylase large chain, RbcL. Sequence hits normalized to bacterial RpoB hits.

A.

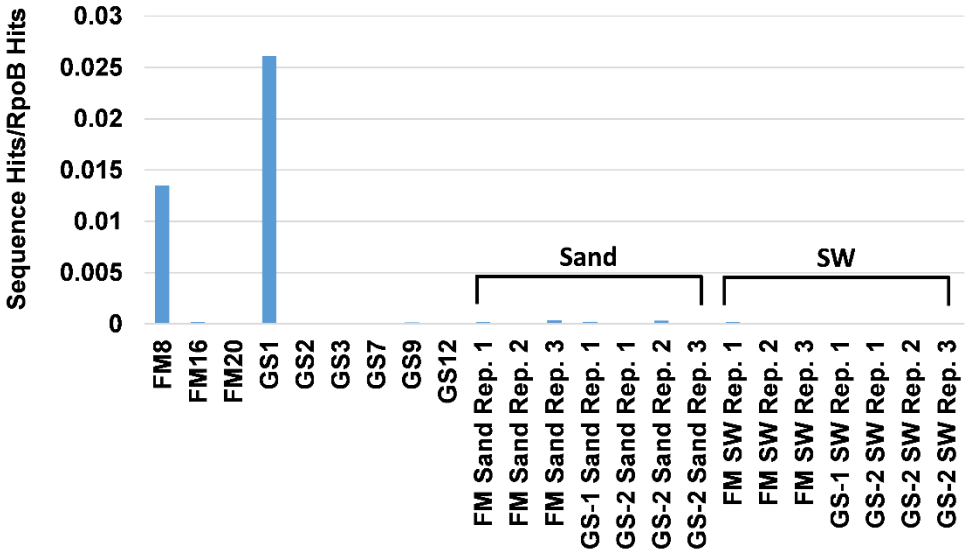

B.

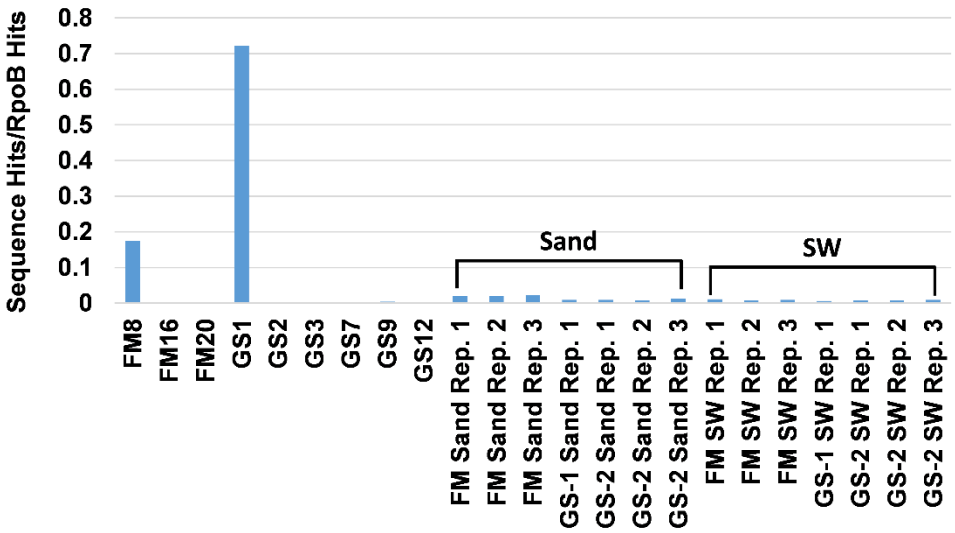

C.

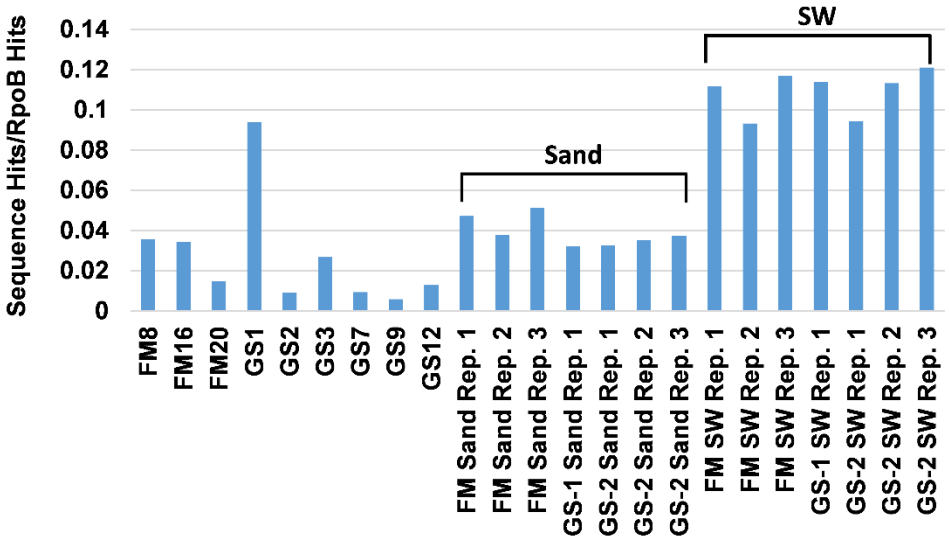
Sequence Hits/RpoB Hits
0.14
0.12
0.1
0.08
0.06
0.04
0.02
0
Sand
SW
FM8
FM16
FM20
GS1
GS2
GS3
GS7
GS9
GS12
FM Sand Rep. 1
FM Sand Rep. 2
FM Sand Rep. 3
GS-1 Sand Rep. 1
GS-2 Sand Rep. 1
GS-2 Sand Rep. 2
GS-2 Sand Rep. 3
FM SW Rep. 1
FM SW Rep. 2
FM SW Rep. 3
GS-1 SW Rep. 1
GS-2 SW Rep. 1
GS-2 SW Rep. 2
GS-2 SW Rep. 3

Figure S9. Normalized ratios of genes encoding enzymes involved in anaerobic hydrocarbon activation via the addition to fumarate pathway, including **(A)** catalytic subunits, **(B)** alkylsuccinate synthase (AssABCD) and (methyl)alkylsuccinate synthase (MasE), **(C)** benzylsuccinate synthase (BssABCD) and 2-napthylmethylsuccinate synthase (NmsA), **(D)** (4-isopropylbenzyl)succinate synthase (IbsABCD), and **(E)** hydroxybenzylsuccinate synthase (HbsABCD). Values represent normalized ratios calculated as the number of gene sequence hits/number of bacterial RpoB hits.

A.

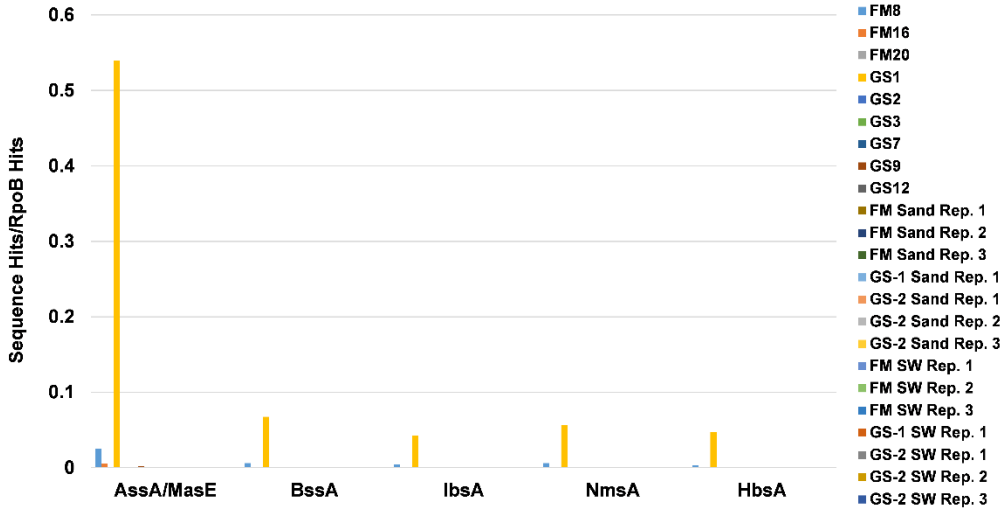

B.

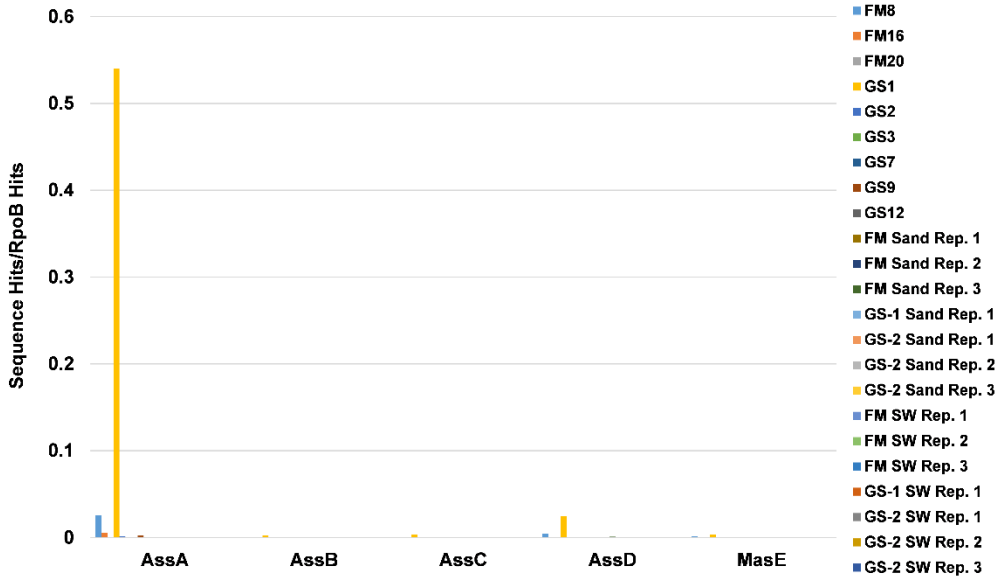

C.

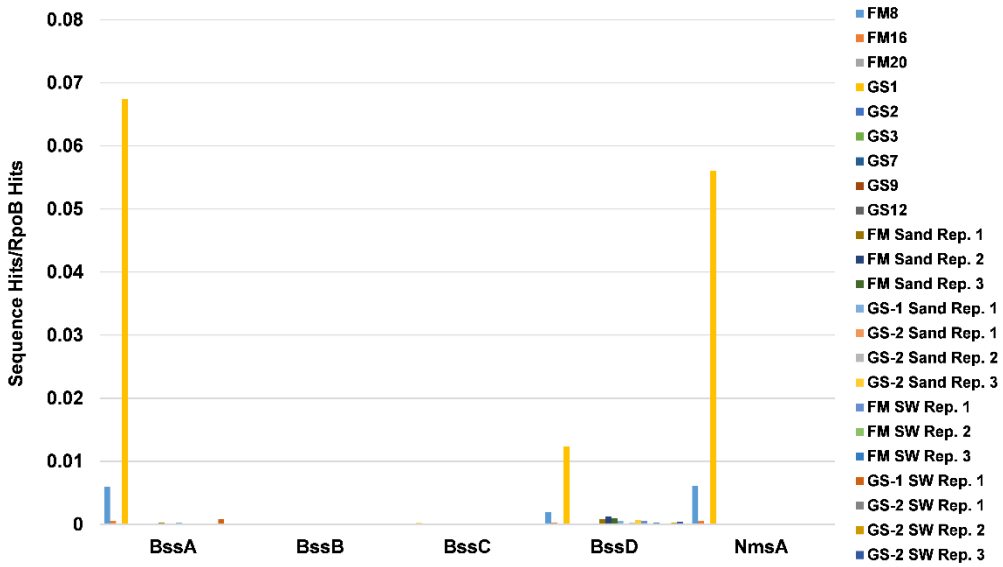
0.08
0.07
0.06
0.05
0.04
0.03
0.02
0.01
0
Sequence Hits/RpoB Hits
BssA
BssB
BssC
BssD
NmsA
FM8
FM16
FM20
GS1
GS2
GS3
GS7
GS9
GS12
FM Sand Rep. 1
FM Sand Rep. 2
FM Sand Rep. 3
GS-1 Sand Rep. 1
GS-2 Sand Rep. 1
GS-2 Sand Rep. 2
GS-2 Sand Rep. 3
FM SW Rep. 1
FM SW Rep. 2
FM SW Rep. 3
GS-1 SW Rep. 1
GS-2 SW Rep. 1
GS-2 SW Rep. 2
GS-2 SW Rep. 3

D.

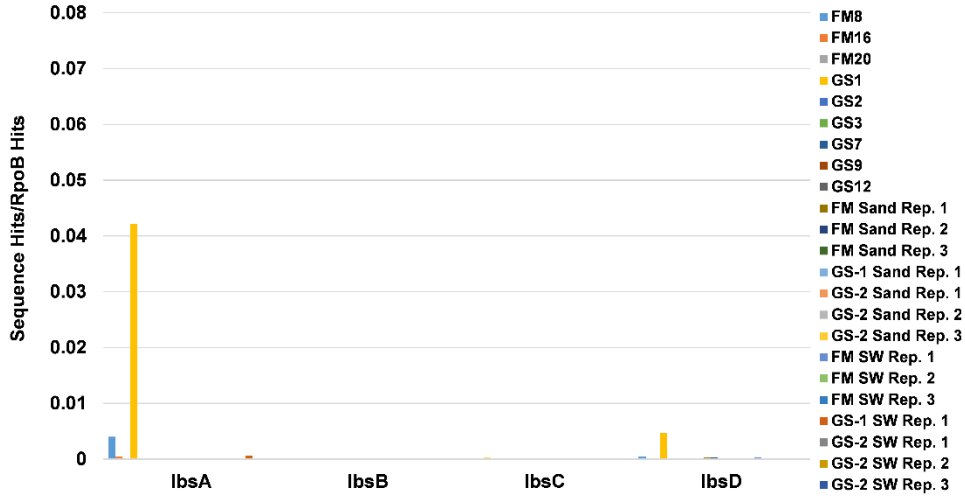
0.08
0.07
0.06
0.05
0.04
0.03
0.02
0.01
0
Sequence Hits/RpoB Hits
IbsA
IbsB
IbsC
IbsD
FM8
FM16
FM20
GS1
GS2
GS3
GS7
GS9
GS12
FM Sand Rep. 1
FM Sand Rep. 2
FM Sand Rep. 3
GS-1 Sand Rep. 1
GS-2 Sand Rep. 1
GS-2 Sand Rep. 2
GS-2 Sand Rep. 3
FM SW Rep. 1
FM SW Rep. 2
FM SW Rep. 3
GS-1 SW Rep. 1
GS-2 SW Rep. 1
GS-2 SW Rep. 2
GS-2 SW Rep. 3

E.

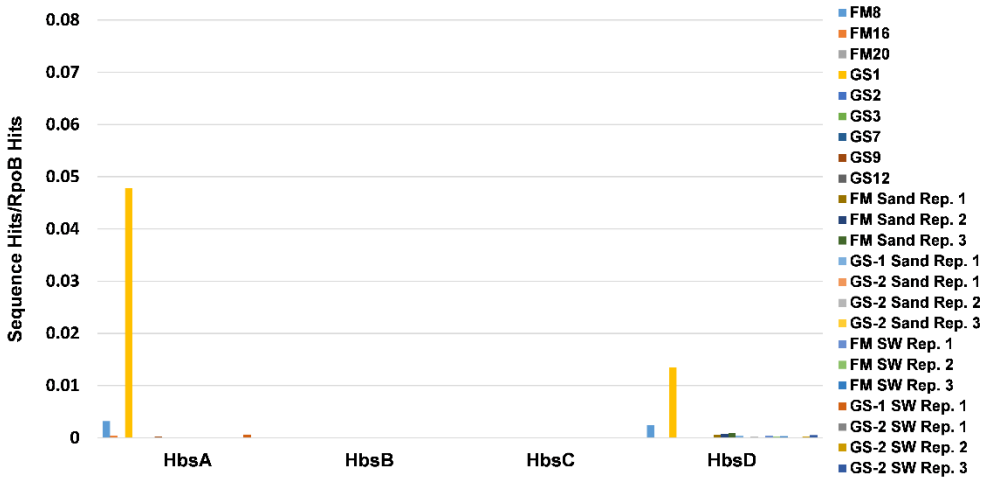

Figure S10. Normalized ratios of genes encoding enzymes involved in **(A)** anaerobic hydroxylation of ethylbenzene, including **(B)** ethylbenzene dehydrogenase (EbdABCD), **(C)** phenylethanol dehydrogenase (Ped), and **(D)** acetophenone carboxylase (ApcABCDE). Values represent normalized ratios calculated as the number of gene sequence hits/number of bacterial RpoB hits.

A.

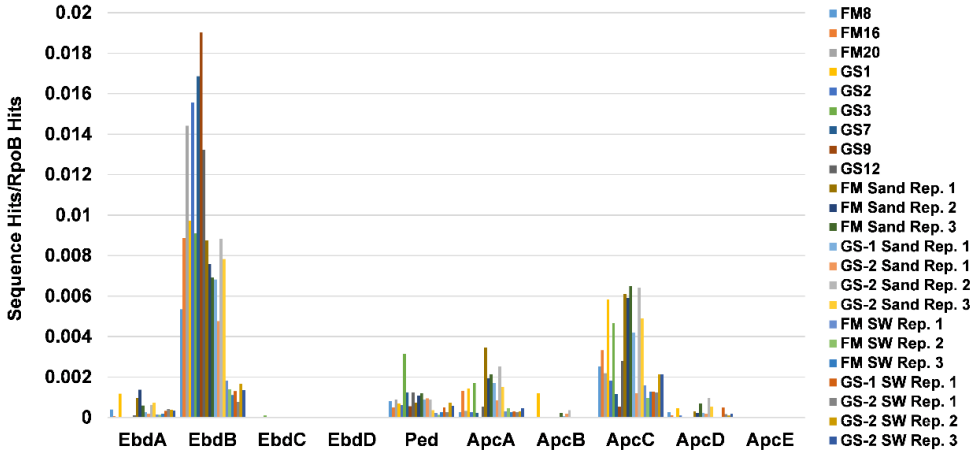

B.

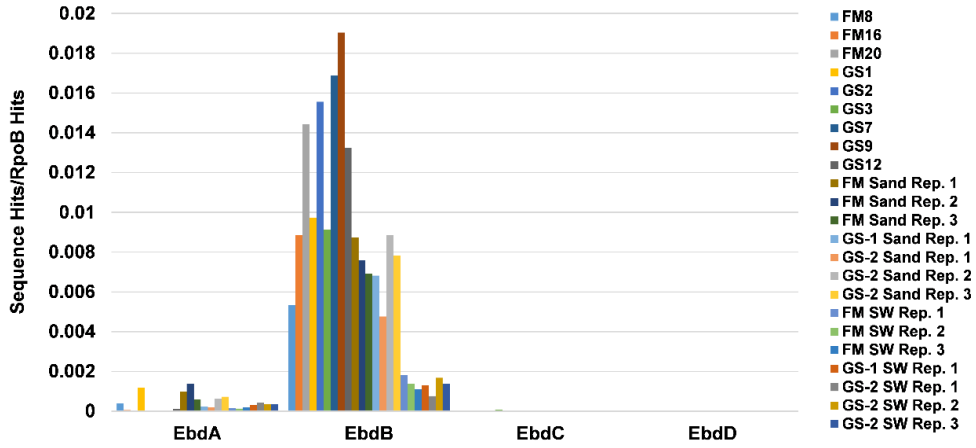
Sequence Hits/RpoB Hits
0.02
0.018
0.016
0.014
0.012
0.01
0.008
0.006
0.004
0.002
0
EbdA
EbdB
EbdC
EbdD
FM8
FM16
FM20
GS1
GS2
GS3
GS7
GS9
GS12
FM Sand Rep. 1
FM Sand Rep. 2
FM Sand Rep. 3
GS-1 Sand Rep. 1
GS-2 Sand Rep. 1
GS-2 Sand Rep. 2
GS-2 Sand Rep. 3
FM SW Rep. 1
FM SW Rep. 2
FM SW Rep. 3
GS-1 SW Rep. 1
GS-2 SW Rep. 1
GS-2 SW Rep. 2
GS-2 SW Rep. 3

C.

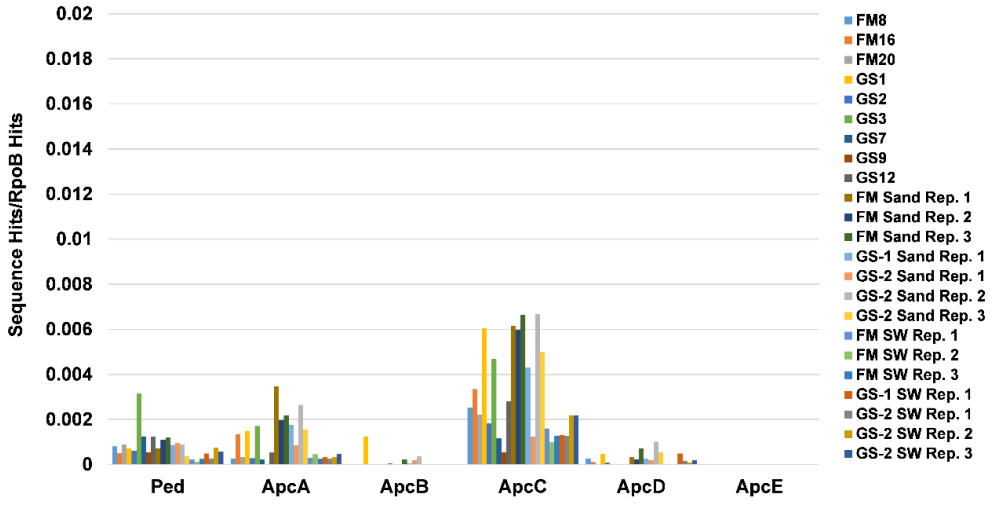
Sequence Hits/RpoB Hits
0.02
0.018
0.016
0.014
0.012
0.01
0.008
0.006
0.004
0.002
0
Ped
ApcA
ApcB
ApcC
ApcD
ApcE
FM8
FM16
FM20
GS1
GS2
GS3
GS7
GS9
GS12
FM Sand Rep. 1
FM Sand Rep. 2
FM Sand Rep. 3
GS-1 Sand Rep. 1
GS-2 Sand Rep. 1
GS-2 Sand Rep. 2
GS-2 Sand Rep. 3
FM SW Rep. 1
FM SW Rep. 2
FM SW Rep. 3
GS-1 SW Rep. 1
GS-2 SW Rep. 1
GS-2 SW Rep. 2
GS-2 SW Rep. 3

Figure S11. Normalized ratios of genes encoding enzymes involved in various anaerobic hydrocarbon transformation pathways including **(A)** a putative alkane C2 methylene hydroxylase (AhyABCD), **(B)** *p*-cymene dehydrogenase (CmdABCD), **(C)** anaerobic benzene carboxylase (AbcAD), and **(D)** phenylphosphate synthase (PpsAB) and phenylphosphate carboxylase (PpcABCD). Values represent normalized ratios calculated as the number of gene sequence hits/number of bacterial RpoB hits.

A.

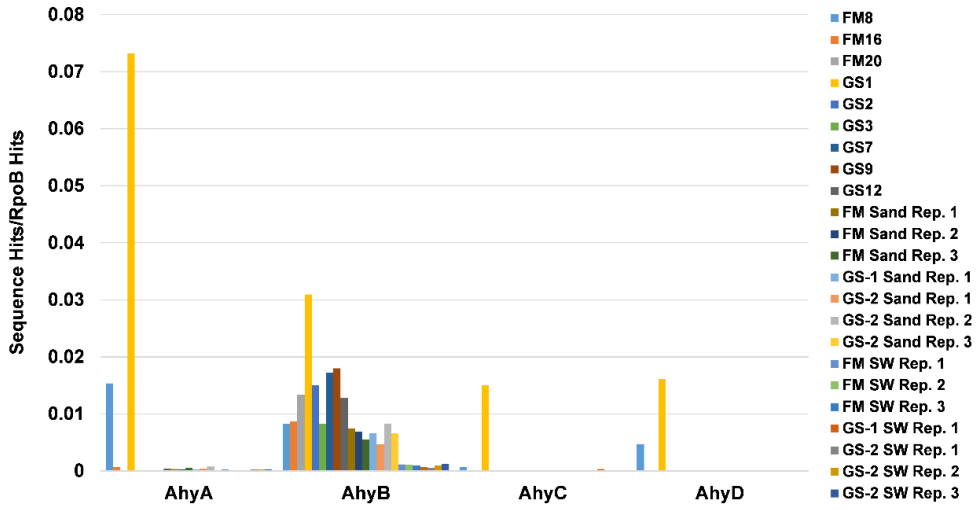

B.

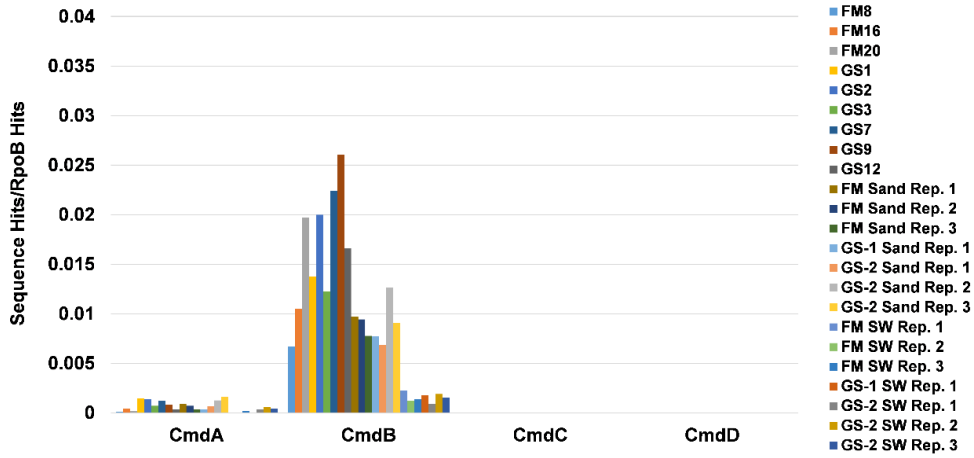

C.

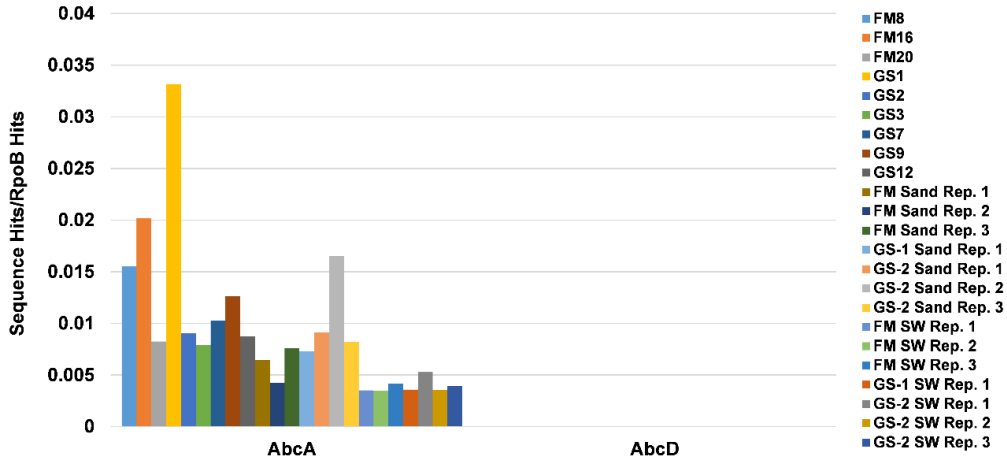
0.04
0.035
0.03
0.025
0.02
0.015
0.01
0.005
0
Sequence Hits/RpoB Hits
AbcA
AbcD
FM8
FM16
FM20
GS1
GS2
GS3
GS7
GS9
GS12
FM Sand Rep. 1
FM Sand Rep. 2
FM Sand Rep. 3
GS-1 Sand Rep. 1
GS-2 Sand Rep. 1
GS-2 Sand Rep. 2
GS-2 Sand Rep. 3
FM SW Rep. 1
FM SW Rep. 2
FM SW Rep. 3
GS-1 SW Rep. 1
GS-2 SW Rep. 1
GS-2 SW Rep. 2
GS-2 SW Rep. 3

D.

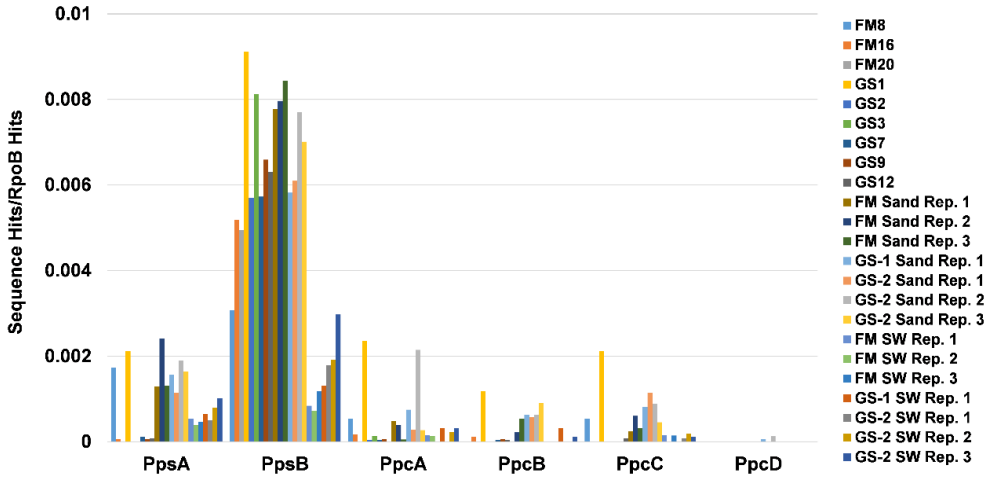
0.01
0.008
0.006
0.004
0.002
0
Sequence Hits/RpoB Hits
PpsA
PpsB
PpcA
PpcB
PpcC
PpcD
FM8
FM16
FM20
GS1
GS2
GS3
GS7
GS9
GS12
FM Sand Rep. 1
FM Sand Rep. 2
FM Sand Rep. 3
GS-1 Sand Rep. 1
GS-2 Sand Rep. 1
GS-2 Sand Rep. 2
GS-2 Sand Rep. 3
FM SW Rep. 1
FM SW Rep. 2
FM SW Rep. 3
GS-1 SW Rep. 1
GS-2 SW Rep. 1
GS-2 SW Rep. 2
GS-2 SW Rep. 3

Figure S12. Normalized ratios of genes involved in aerobic transformation of hydrocarbons including alkane monooxygenase (AlkB), cytochrome P450 alkane hydroxylase (CYP153), and protein sequences contained within the AromaDeg database (Duarte *et al*, 2014). Values represent normalized ratios calculated as the number of sequence hits/number of bacterial RpoB hits.

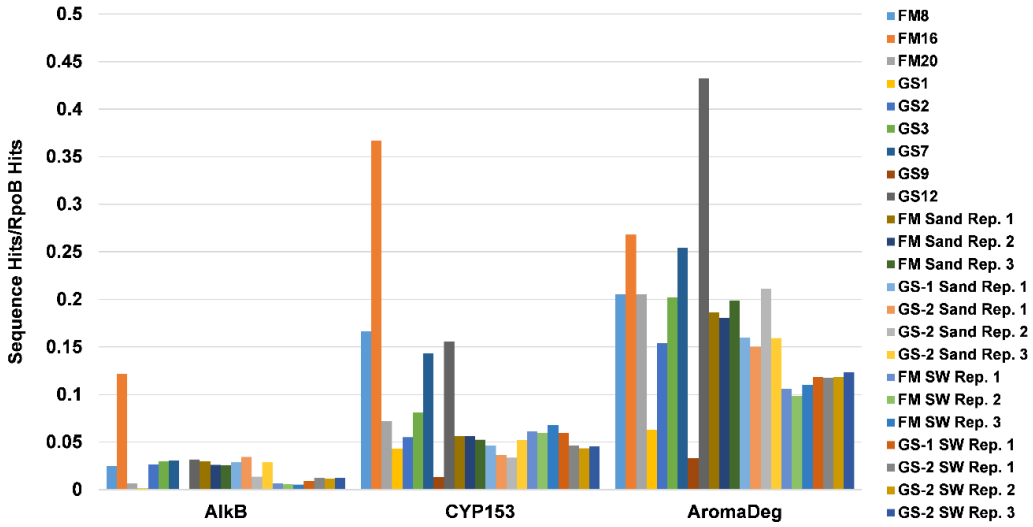

Figure S13. (A) Individual AromaDeg (Duarte *et al*, 2014) dioxygenase protein families containing **(B)** benzoate oxygenases, **(C)** biphenyl oxygenases, **(D)** phthalate oxygenases, **(E)** salicylate oxygenases, extradiol dioxygenases acting on **(F)** monocyclic substrates, **(G)** bicyclic substrates, and **(H)** miscellaneous substrates, **(I)** protocatechuate oxygenases, **(J)** homoprotocatechuate oxygenases, and **(K)** gentisate oxygenases. Values represent normalized ratios calculated as the number of protein sequence hits/number of bacterial RpoB hits.

A.

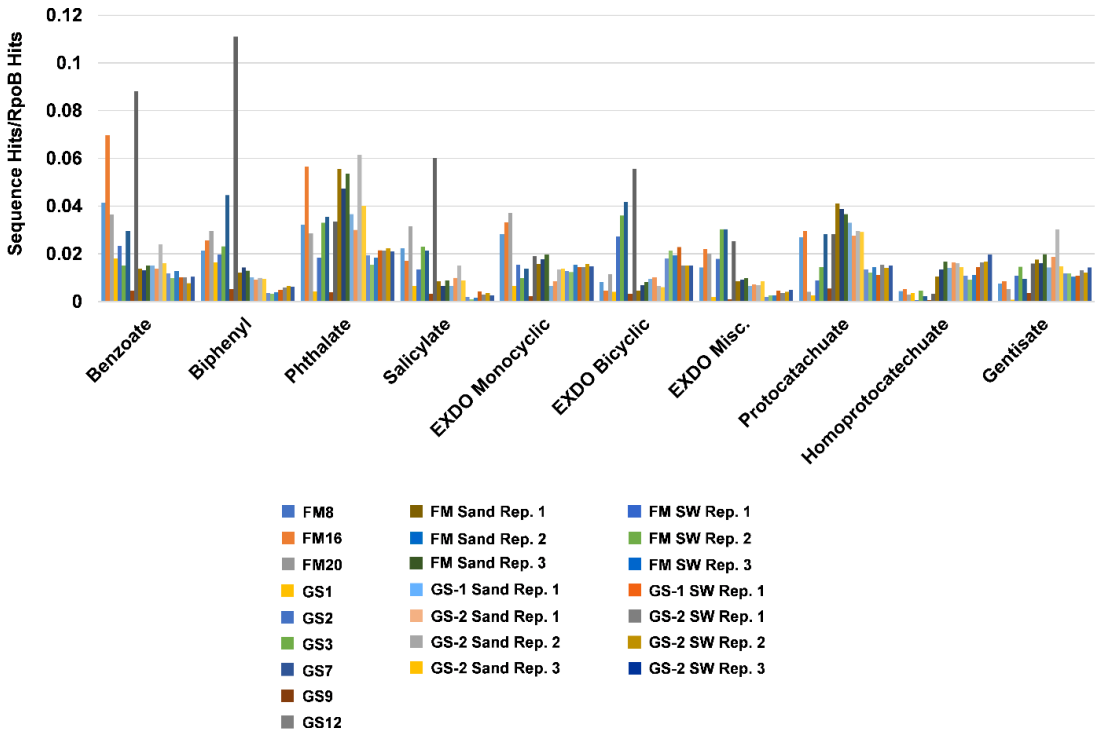

B.

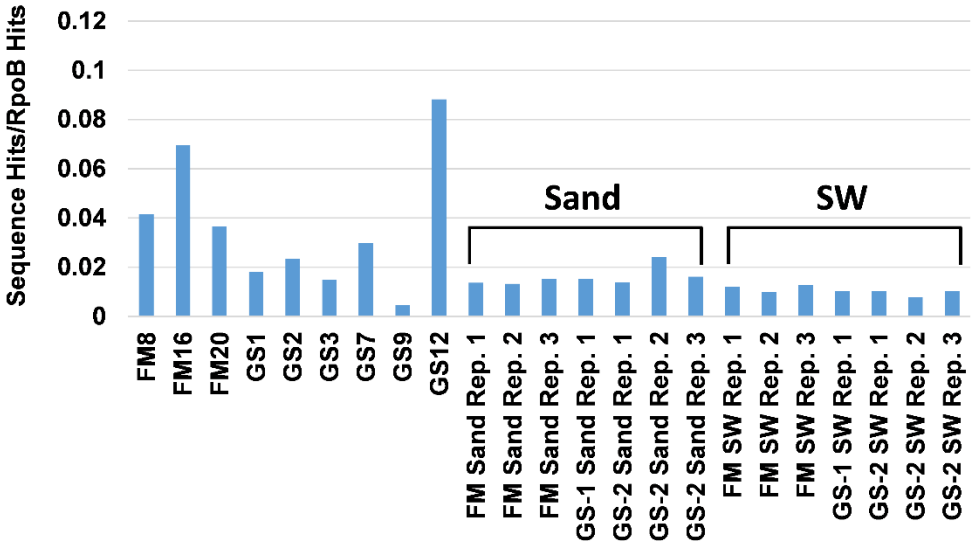
Sequence Hits/RpoB Hits
0.12
0.1
0.08
0.06
0.04
0.02
0
Sand
SW
FM8
FM16
FM20
GS1
GS2
GS3
GS7
GS9
GS12
FM Sand Rep. 1
FM Sand Rep. 2
FM Sand Rep. 3
GS-1 Sand Rep. 1
GS-2 Sand Rep. 1
GS-2 Sand Rep. 2
GS-2 Sand Rep. 3
FM SW Rep. 1
FM SW Rep. 2
FM SW Rep. 3
GS-1 SW Rep. 1
GS-2 SW Rep. 1
GS-2 SW Rep. 2
GS-2 SW Rep. 3

C.

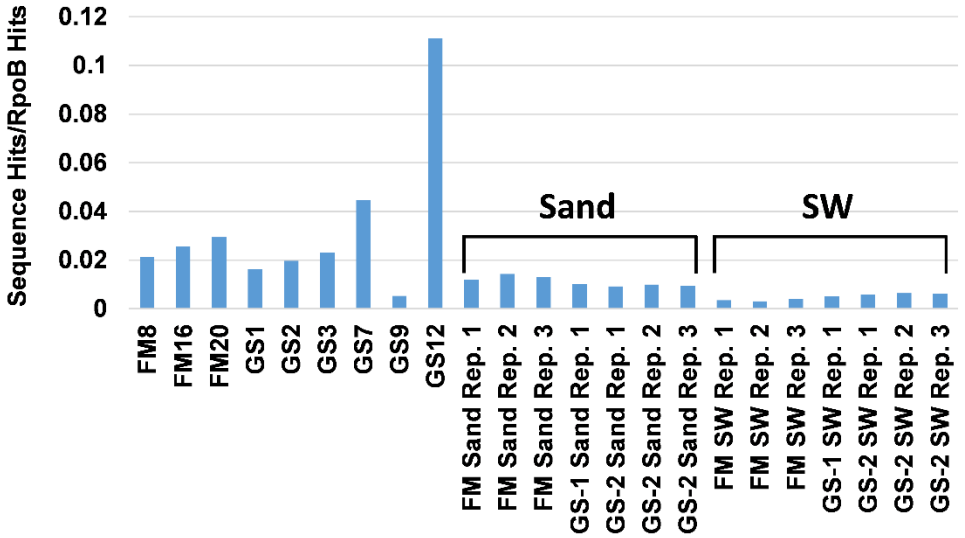
Sequence Hits/RpoB Hits
0.12
0.1
0.08
0.06
0.04
0.02
0
Sand
SW
FM8
FM16
FM20
GS1
GS2
GS3
GS7
GS9
GS12
FM Sand Rep. 1
FM Sand Rep. 2
FM Sand Rep. 3
GS-1 Sand Rep. 1
GS-2 Sand Rep. 1
GS-2 Sand Rep. 2
GS-2 Sand Rep. 3
FM SW Rep. 1
FM SW Rep. 2
FM SW Rep. 3
GS-1 SW Rep. 1
GS-2 SW Rep. 1
GS-2 SW Rep. 2
GS-2 SW Rep. 3

D.

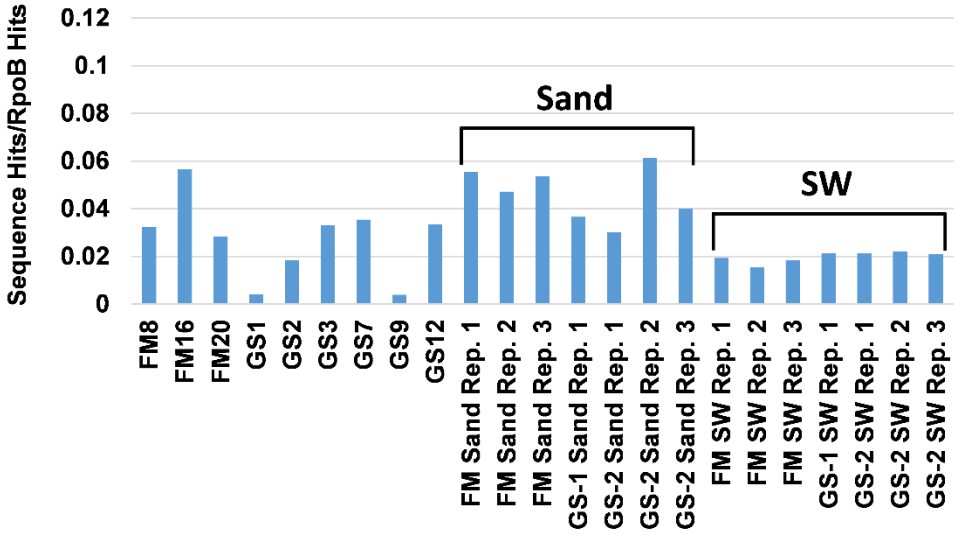
Sequence Hits/RpoB Hits
0.12
0.1
0.08
0.06
0.04
0.02
0
Sand
SW
FM8
FM16
FM20
GS1
GS2
GS3
GS7
GS9
GS12
FM Sand Rep. 1
FM Sand Rep. 2
FM Sand Rep. 3
GS-1 Sand Rep. 1
GS-2 Sand Rep. 1
GS-2 Sand Rep. 2
GS-2 Sand Rep. 3
FM SW Rep. 1
FM SW Rep. 2
FM SW Rep. 3
GS-1 SW Rep. 1
GS-2 SW Rep. 1
GS-2 SW Rep. 2
GS-2 SW Rep. 3

E.

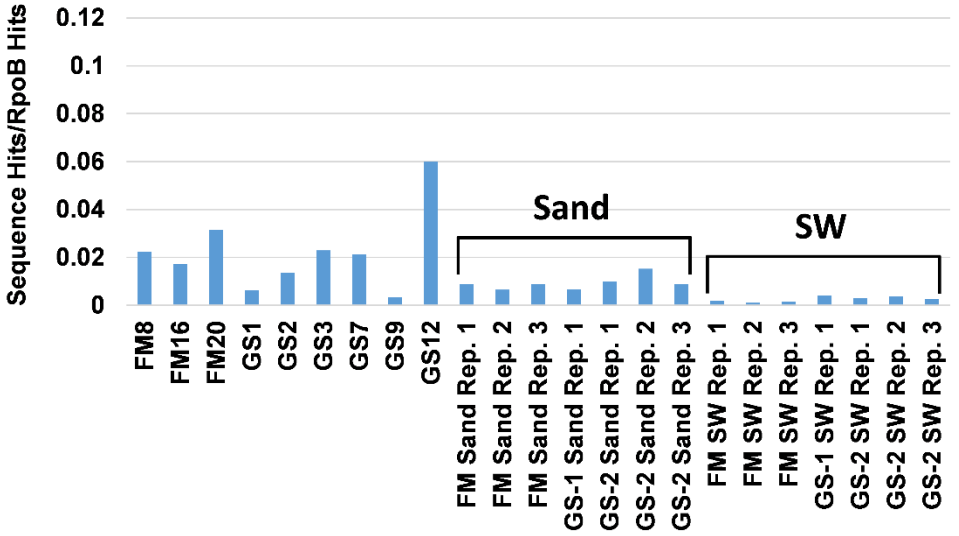
Sequence Hits/RpoB Hits
0.12
0.1
0.08
0.06
0.04
0.02
0
Sand
SW
FM8
FM16
FM20
GS1
GS2
GS3
GS7
GS9
GS12
FM Sand Rep. 1
FM Sand Rep. 2
FM Sand Rep. 3
GS-1 Sand Rep. 1
GS-2 Sand Rep. 1
GS-2 Sand Rep. 2
GS-2 Sand Rep. 3
FM SW Rep. 1
FM SW Rep. 2
FM SW Rep. 3
GS-1 SW Rep. 1
GS-2 SW Rep. 1
GS-2 SW Rep. 2
GS-2 SW Rep. 3

F.

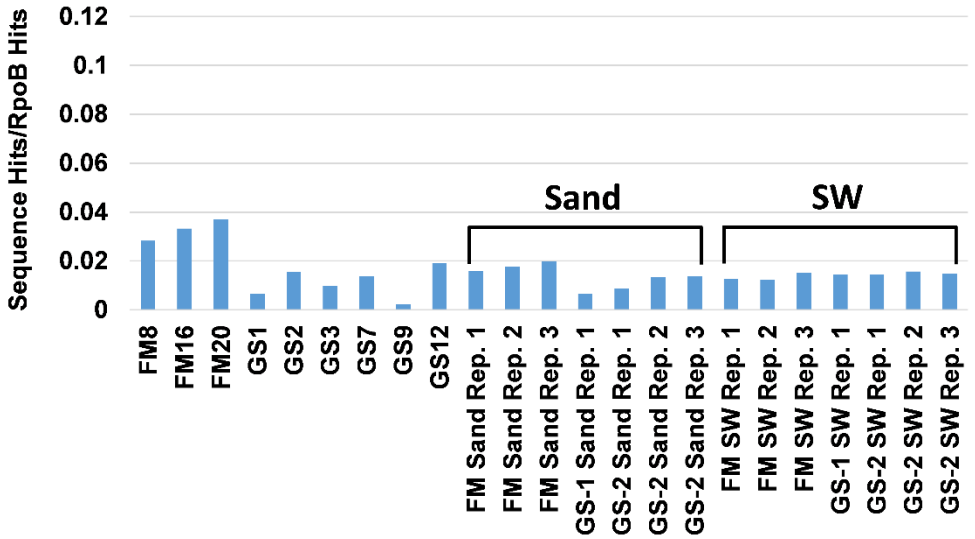
Sequence Hits/RpoB Hits
0.12
0.1
0.08
0.06
0.04
0.02
0
Sand
SW
FM8
FM16
FM20
GS1
GS2
GS3
GS7
GS9
GS12
FM Sand Rep. 1
FM Sand Rep. 2
FM Sand Rep. 3
GS-1 Sand Rep. 1
GS-2 Sand Rep. 1
GS-2 Sand Rep. 2
GS-2 Sand Rep. 3
FM SW Rep. 1
FM SW Rep. 2
FM SW Rep. 3
GS-1 SW Rep. 1
GS-2 SW Rep. 1
GS-2 SW Rep. 2
GS-2 SW Rep. 3

G.

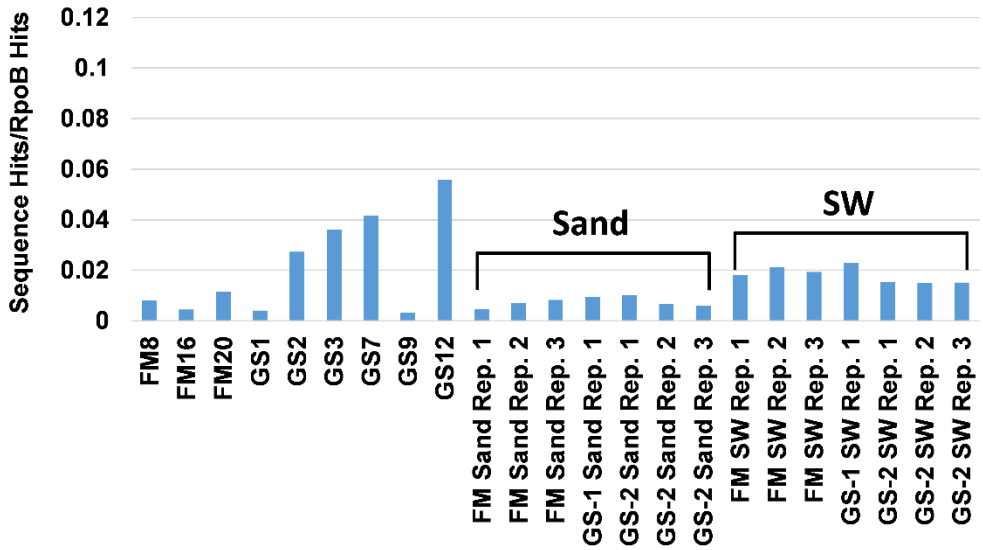
Sequence Hits/RpoB Hits
0.12
0.1
0.08
0.06
0.04
0.02
0
Sand
SW
FM8
FM16
FM20
GS1
GS2
GS3
GS7
GS9
GS12
FM Sand Rep. 1
FM Sand Rep. 2
FM Sand Rep. 3
GS-1 Sand Rep. 1
GS-2 Sand Rep. 1
GS-2 Sand Rep. 2
GS-2 Sand Rep. 3
FM SW Rep. 1
FM SW Rep. 2
FM SW Rep. 3
GS-1 SW Rep. 1
GS-2 SW Rep. 1
GS-2 SW Rep. 2
GS-2 SW Rep. 3

H.

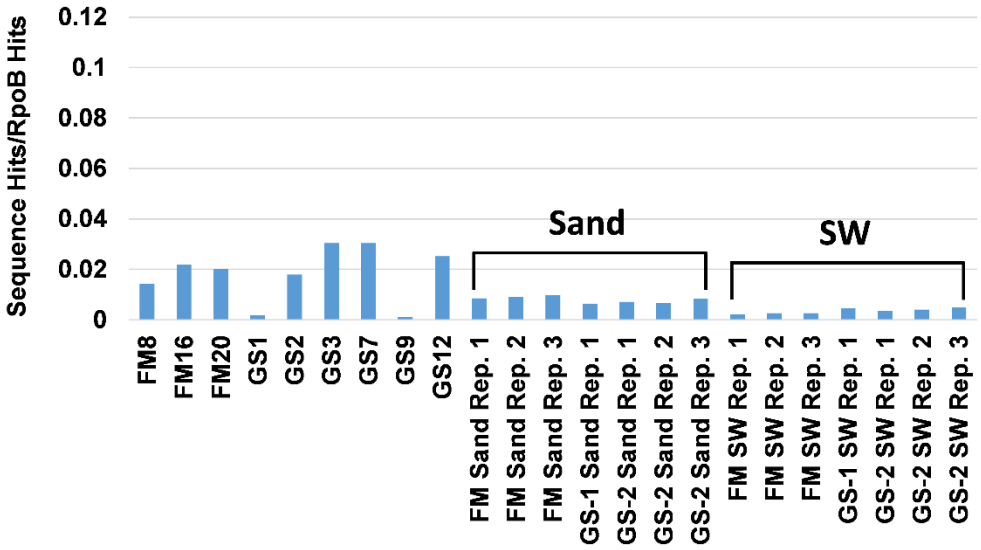
Sequence Hits/RpoB Hits
0.12
0.1
0.08
0.06
0.04
0.02
0
Sand
SW
FM8
FM16
FM20
GS1
GS2
GS3
GS7
GS9
GS12
FM Sand Rep. 1
FM Sand Rep. 2
FM Sand Rep. 3
GS-1 Sand Rep. 1
GS-2 Sand Rep. 1
GS-2 Sand Rep. 2
GS-2 Sand Rep. 3
FM SW Rep. 1
FM SW Rep. 2
FM SW Rep. 3
GS-1 SW Rep. 1
GS-2 SW Rep. 1
GS-2 SW Rep. 2
GS-2 SW Rep. 3

I.

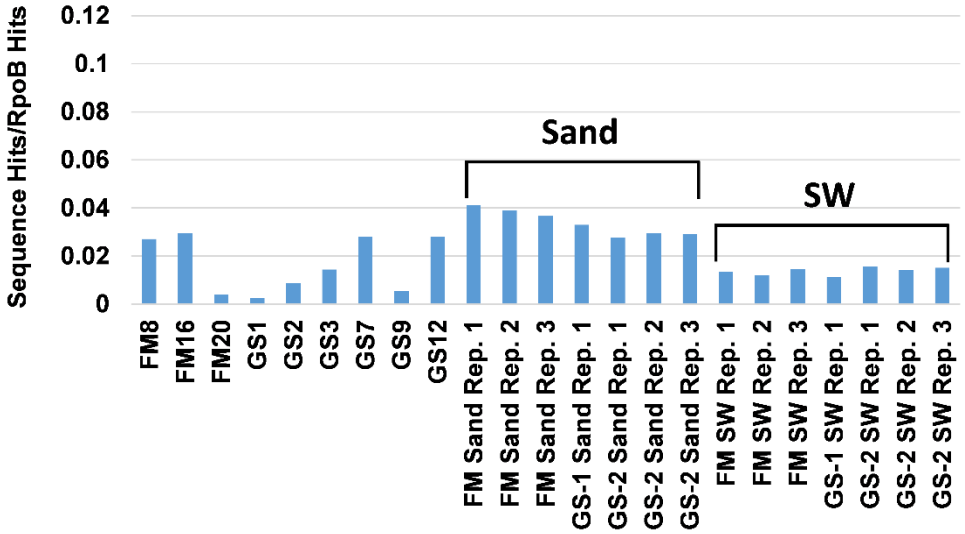
Sequence Hits/RpoB Hits
0.12
0.1
0.08
0.06
0.04
0.02
0
Sand
SW
FM8
FM16
FM20
GS1
GS2
GS3
GS7
GS9
GS12
FM Sand Rep. 1
FM Sand Rep. 2
FM Sand Rep. 3
GS-1 Sand Rep. 1
GS-2 Sand Rep. 1
GS-2 Sand Rep. 2
GS-2 Sand Rep. 3
FM SW Rep. 1
FM SW Rep. 2
FM SW Rep. 3
GS-1 SW Rep. 1
GS-2 SW Rep. 1
GS-2 SW Rep. 2
GS-2 SW Rep. 3

J.

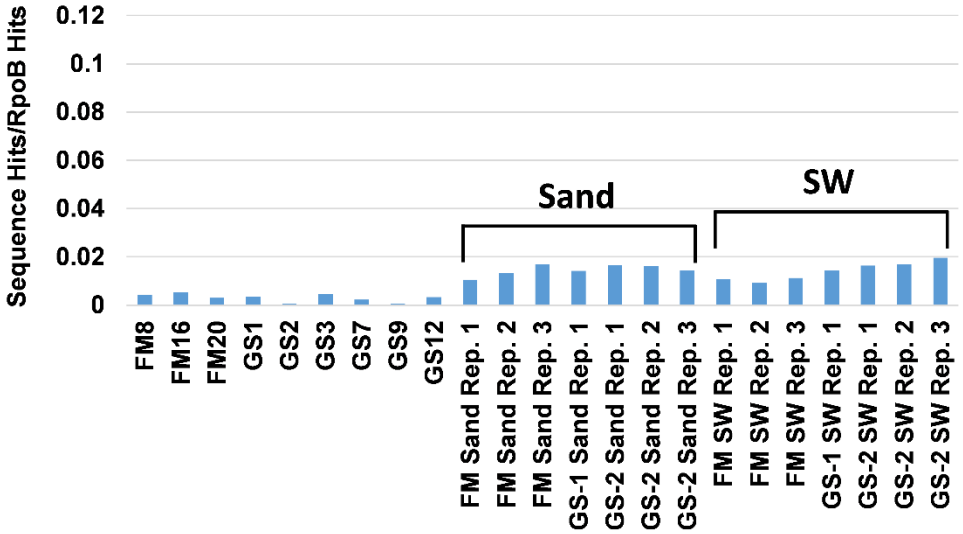
Sequence Hits/RpoB Hits
0.12
0.1
0.08
0.06
0.04
0.02
0
Sand
SW
FM8
FM16
FM20
GS1
GS2
GS3
GS7
GS9
GS12
FM Sand Rep. 1
FM Sand Rep. 2
FM Sand Rep. 3
GS-1 Sand Rep. 1
GS-2 Sand Rep. 1
GS-2 Sand Rep. 2
GS-2 Sand Rep. 3
FM SW Rep. 1
FM SW Rep. 2
FM SW Rep. 3
GS-1 SW Rep. 1
GS-2 SW Rep. 1
GS-2 SW Rep. 2
GS-2 SW Rep. 3

K.

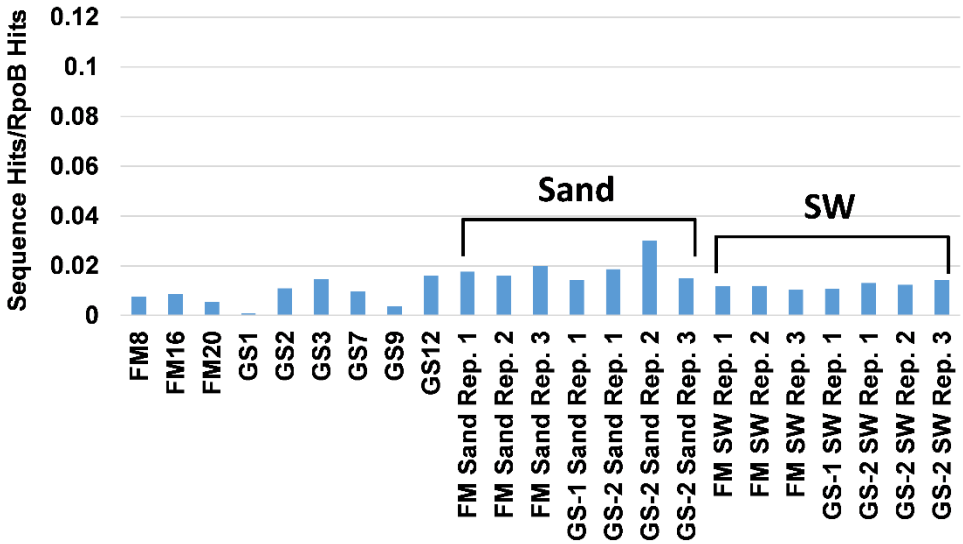
Sequence Hits/RpoB Hits
0.12
0.1
0.08
0.06
0.04
0.02
0
Sand
SW
FM8
FM16
FM20
GS1
GS2
GS3
GS7
GS9
GS12
FM Sand Rep. 1
FM Sand Rep. 2
FM Sand Rep. 3
GS-1 Sand Rep. 1
GS-2 Sand Rep. 1
GS-2 Sand Rep. 2
GS-2 Sand Rep. 3
FM SW Rep. 1
FM SW Rep. 2
FM SW Rep. 3
GS-1 SW Rep. 1
GS-2 SW Rep. 1
GS-2 SW Rep. 2
GS-2 SW Rep. 3